DISSERTATION

THE OCCURRENCE OF CWD PRIONS AND THEIR RISK TO HUMANS

Submitted by

Kristen Anne Davenport

Department of Microbiology, Immunology, and Pathology

In partial fulfillment of the requirements

For the Degree of Doctor of Philosophy

Colorado State University

Fort Collins, Colorado

Summer 2017

Doctoral Committee:

Advisor: Edward Hoover
Co-Advisor: Candace Mathiason

Eric Ross
Glenn Telling

Copyright by Kristen Anne Davenport 2017

All Rights Reserved

ABSTRACT

THE OCCURRENCE OF CWD PRIONS AND THEIR RISK TO HUMANS

Zoonotic diseases are often caused by viruses or bacteria, which adapt to new species with changes to their nucleic acid sequence. The etiologic agent of transmissible spongiform encephalopathies (TSEs), the prion, is a self-templating, abnormal isomer of a normal protein, PrP^C, and does not include nucleic acids. Despite its protein-only composition, prions are transmissible and can adapt to new species. We are particularly interested in chronic wasting disease (CWD), the TSE of cervids.

CWD is horizontally transmissible among cervids and has spread across much of North America and to Europe and Asia. It is apparent that excreta from CWD(+) deer is infectious, but the mechanism of horizontal transmission of CWD has not been explained. We hypothesized that deer accumulate prions in many tissues and that accumulation of prions is dictated by PrP^C expression. Next, we used a battery of *in vitro* systems to compare the biochemical characteristics and infectivity of prions in lymphoid tissues. Finally, we hypothesized that *in vitro* detection of prions in saliva is hampered by the presence of an inhibitor. We demonstrated that prions accumulate in many tissues in deer and that accumulation is determined by tissue type, not PrP^C expression. We confirmed that the prions in lymph nodes are infectious *in vitro.* Last, we confirmed the presence of an inhibitor in saliva which results in the underestimation of prion shedding in saliva.

The TSE of cattle, bovine spongiform encephalopathy (BSE), crossed the species barrier and infected humans, confirming that TSEs can infect new species. However, the zoonotic potential of CWD remains unclear. For a prion from one species to infect a new host, the invading prion and the PrP^C of the new host must be compatible. We hypothesized that prions are most compatible with their own species' PrP^C and that human PrP^C could not be induced to misfold by CWD prions. Upon infection of a new host, CWD adapted, but BSE did not. Curiously, CWD prions efficiently induced the misfolding of human PrP^C. We concluded that the species barrier between humans and CWD prions is not due to

incompatibility of human PrP^C and CWD prions. Finally, we tested a specific region of PrP^C, the amino-terminal domain (NTD), for its role in the species barrier. We demonstrated that the NTD of PrP^C hindered misfolding for most species, but that interactions of the NTD with the rest of molecule facilitated the misfolding of human PrP^C by CWD prions.

We propose that horizontal transmission among cervids is facilitated by the widespread propagation and deposition of prions in tissues. We hypothesize that prions in the periphery are infectious and that they are the source of excreted prions to which naïve cervids are exposed. We conclude that the species barrier preventing transmission of CWD to humans is not as robust as has been suggested. The species barrier is not due to incompatibility of human PrP^C and CWD prions. We suggest that CWD infection of humans would be difficult to identify because CWD adapts to new species. Our work to understand horizontal transmission and the risk of CWD prions to humans contributes to an understanding of the pathology and ecology of CWD and the prevention and identification of zoonotic events involving CWD.

ACKNOWLEDGEMENTS

The work in this dissertation was made possible by funding from NIH-5F30OD021442 and NIH-R01NS061902. I have enjoyed working in the Prion Research Center, where the answer to a burning question is never far away. Special thanks to Jifeng Bian, Julie Moreno, Yoshi Iwamaru and Hae-Eun Kang for their patience and willingness to help. The Hoover/Mathiason lab group provided lots of laughs and made work fun. In particular: Nate provided entertainment and institutional memory when I needed either; Davin (coach) got me out of troubleshooting disasters and always had a guffaw lurking just below the surface; Jeff had patience, insight and advice about my experiment, my career and my adventure du jour; Clare was my older sister – she paved the way for me in many ways and never hesitated to help, whether it was related to the science or not; Kassi was my therapist, tiny-office companion and friend. Her sense of humor, taste in comedy, and optimism made the first four years of graduate school much more pleasant. Amy and Sherry were always receptive to my newest, greatest joke, and made the work we did so much easier. Nikki Burhdorf did a lot of the grunt work that led to these. I appreciate her contributions, her patience and the opportunity to teach.

These years at Colorado State University have filled my mentor coffer. I am lucky to have bounced ideas and crises and excitement off Dr. Anne Avery, Dr. Randy Basaraba, Dr. Sandra Quackenbush, Dr. Nick Haley, Dr. Mark Zabel, Dr. Justin Lee and Dr. Sue VandeWoude. And thanks to those mentors from an earlier time, who answered emails and found time to visit Colorado and whose advice I cherish. Dr. Mitch McVey and Dr. Bob Chapin, you're in this for the long haul.

I am grateful for the time my graduate committee spent on me and my project. Dr. Glenn Telling and Dr. Eric Ross provided invaluable insight, helped me stay on track, and challenged me to think more deeply. Thank you to Dr. Candace Mathiason for the immense amount of time spent meeting and editing and advising me at each fork in the road. I appreciate your willingness to help and your contributions to the work in this dissertation. I am grateful for Dr. Edward Hoover's decision to take one more graduate student. It has been fascinating to work with someone who cares so much about mentoring and whose

track record demonstrates the effectiveness of his approach. Not only do I respect and strive to absorb your scientific and leadership abilities, but your willingness to listen, your taste in books, your excessive patience and your sense of humor made these five years truly special.

Outside the lab, I have found a thriving community in Fort Collins. Thank you to all the friends who have filled these years with *life*. Some of you are still here and some have moved on, but our relationships are here to stay. Thank you to the DVM/PhD students ahead of and behind me for your comradery, patience and mentoring. I feel lucky to be part of such a vivid, busy, happy, successful family. Aimee and Brittany, thank you for the adventures, the love and the support. You made Fort Collins home. Max, thank you for your love, energy, humor, patience and distraction. Finally, Mom, Dad, and Laura, thanks for making me who I am. The apple doesn't fall far from the tree and your example of hard work, humor and empathy is what to try to match.

DEDICATION

I humbly dedicate this dissertation to Dr. Edward Hoover, my mentor and primary advisor. Dr. Hoover has taught me how to be a scientist, but that's really only a fraction of what I've learned.

TABLE OF CONTENTS

INTRODUCTION

Zoonotic Disease

Zoonosis is defined by the Merriam Webster dictionary as an "infection or disease that is transmissible from animals to humans under natural conditions" (1). Etiologic agents of zoonoses include viruses, bacteria, fungi, parasites and prions, the protein-only infectious agents that are the subject of this dissertation (2). Experts estimate that 50-75% of human pathogens emerged from animals, and zoonotic disease causes one billion human cases and one million human deaths per year (2, 3). Evolution dictates that pathogens will exploit and adapt to new niches, like a new host. Some zoonotic pathogens are enzootic in their animal host populations and are rarely transmitted from human to human, while others have adapted and are very easily transmitted among humans (3). There are factors intrinsic and extrinsic to pathogens that affect their chances of leaping from animal to human hosts. Extrinsic factors include modifications to agricultural practices, human intrusion into animal habitat, human population growth, travel, and behavior, and breakdown of public health systems (3). To further complicate matters, climate change will alter the contact frequency between reservoir host and humans (as reservoir hosts' habitats change) (4). Intrinsic factors that affect zoonosis emergence include the basic reproduction number of the pathogen (R_0), which describes the ease with which the pathogen is transmitted, and adaptation to a new vaccine, treatment or host. Frameworks like the Bradford-Hill criteria make it possible to identify the causative agent in zoonotic outbreaks, but are only effective after the zoonotic event has occurred (5). The scientific community has never successfully predicted the emergence of a zoonotic pathogen in human populations, but improved understanding of the characteristics that facilitated past emergence has led to increased efforts toward outbreak prediction. A group of preeminent virologists established a list of criteria upon which the zoonotic potential of a virus may be assessed, and argue that these characteristics must be understood if outbreak prediction is to be realized (Table 1). Most of the efforts to study and to predict zoonotic disease have been centered on viral agents, but these principles can be applied to any disease-causing agent.

Table 1. Characteristics of animal pathogens related to the likelihood of infecting human hosts (6)
Relatedness and contact frequency of reservoir host and humans
Viral relatedness to human viruses
Host range and plasticity
Viral mutability
Host-receptor interactions
Routes of transmission
Prediction of virulence in humans
Host-virus coevolution

Prions as a causative agent

Though most zoonotic disease is caused by viruses, bacteria and other traditional pathogens, there is one notable exception. The bovine spongiform encephalopathy (BSE, mad cow disease) outbreak in the United Kingdom in the 1980s – 1990s not only resulted in the culling of nearly 5 million cattle, but also resulted in the infection of humans with variant Creutzfeldt-Jakob disease (vCJD) (7-11). However, the causative agent of BSE and vCJD is not a virus or bacterium and it does not rely on nucleic acids to transmit information. BSE and vCJD are classified as transmissible spongiform encephalopathies (TSEs) and are caused by prions (12). Prion diseases have been described for 250 years, but the causative agent was not identified until the 1980s, when Dr. Stanley Prusiner proposed the prion hypothesis. The prion hypothesis postulates that the etiologic agent of TSEs is a misfolded form of a normal protein, PrP^{C} (7, 13-19).

Robert Koch postulated that a disease-causing pathogen must (i) be present in all cases of the disease, but absent from healthy individuals; (ii) be isolated and grown in pure culture; (iii) cause the same disease when inoculated into healthy hosts; and (iv) be re-isolated from the new host. Koch's postulates were proposed in an age when the pathogens of interest were mostly bacteria that were solely pathogenic and easily cultured. For viruses, prions, and many bacteria, Koch's postulates do not sufficiently define the pathogen (20). For example, viruses cannot be cultured in isolation and many disease-causing bacteria can exist benignly in healthy individuals. Prion biologists have proposed a

modified set of postulates to define a protein as a disease-causing agent (21). To summarize the history and current state of prion disease research, I will discuss each of the protein-only pathogen postulates.

(1) The first postulate states that the protein must be *invariably present in the disease-specific form and arrangement in the diseased tissue* (21). This postulate is reminiscent of Koch's requirement that the causative organism must be present in all cases of the disease. It requires that the prion (PrP^{Sc})[1] be found in the tissue of diseased individuals in the expected pattern. PrP^{Sc} was identified as the principal component of the fibrils observed in the brains of humans, sheep, cattle and cervids with prion disease through early electron microscopy experiments (22-29). The "scrapie-associated fibrils" stained with Congo red, suggesting that they were comprised of amyloid, which was interpreted as a marker of the disease-specific form of the protein (29, 30). The fibrils were identified in extracellular plaques, and have slightly different phenotypes depending on the particular prion disease (30).

(2) The second postulate requires that the *structure and post-translational modifications that confer infectivity be characterized* (21). Before a discussion of the PrP^{Sc} structure, it is worthwhile to briefly review the structure of PrP^{C}. The mature peptide is comprised of 208 amino acids, with signaling peptides present in the unprocessed form. An amino-terminal signal peptide directs the molecule to the endoplasmic reticulum for post-translational modifications and a carboxyl-terminal signal is replaced by a glycosylphosphatidylinositol (GPI) anchor during processing. The mature protein has an amino-terminal unstructured domain from amino acids 23-120 (numbering based on human PrP^{C}) that contains a variable number of octapeptide repeats (PHGGGWGQ). The structured carboxy-terminal domain contains 3 alpha helices and a small beta-sheet region and extends from amino acids 121-231. A disulfide bond links alpha helices 2 and 3 via cysteines at positions 179 and 214 (Figs. 1-2) (31).

[1]A note about terminology: There are a variety of terms for the disease-causing form of the prion protein, including PrP^{Sc}, PrP^{res}, PrP^{D}, PrP^{CWD} and prion. For simplicity's sake, I will use the term **PrP^{Sc}** or **prion** for the disease-associated form. When I discuss protease resistance (the basis for the PrP^{res} term), I will describe the molecules as "protease-resistant PrP^{Sc}". The only exception will be when discussing real-time, quaking-induced conversion. The field has not coalesced around the hypothesis that the molecules detected by RT-QuIC are bona fide infectious PrP^{Sc} molecules, so I will describe the detection of "seeding activity," not PrP^{Sc}, by this method.

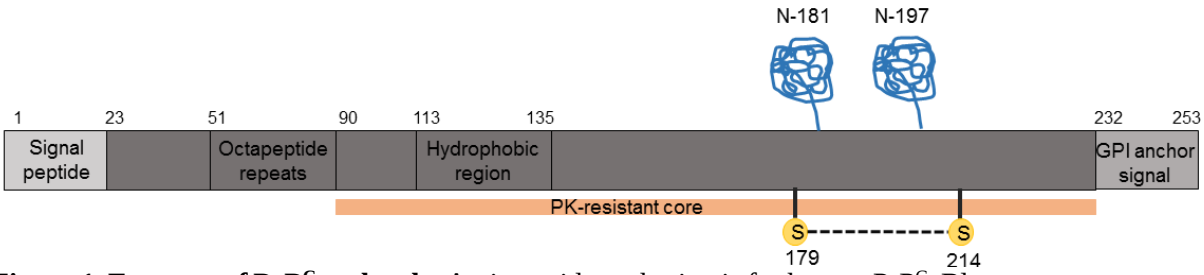

Figure 1. Features of PrP^{C} molecule. Amino acid numbering is for human PrP^{C}. Blue cartoons represent N-linked glycosylation and dotted line indicates the disulfide bond. Adapted from Acevedo-Morantes, et al., 2014 (31).

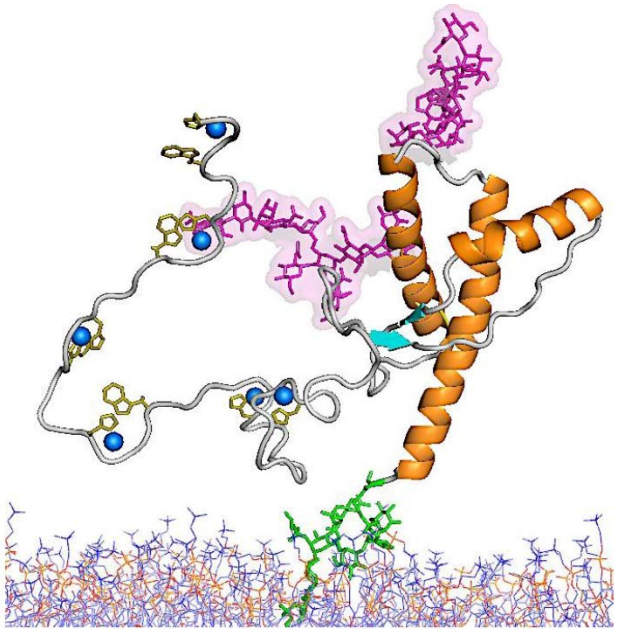

Figure 2. PrP^{C} tertiary structure. Image derived from Acevedo-Morantes, et al., 2014 (31). The GPI anchor is shown in green. Octapeptide repeats are shown in yellow and bind copper (blue). Carbohydrates are shown in pink and alpha helices are shown in orange.

PrP^{C} can undergo a conformational change to PrP^{Sc}, which is autocatalytic and facilitates the conversion of more PrP^{C} to PrP^{Sc} (32-34). The task of defining the structural characteristics of PrP^{Sc} is ongoing in the prion field, particularly efforts to characterize its tertiary and quaternary structure (35). The primary structure of PrP^{Sc}, which is encoded by the *PRNP* gene, has been defined for many species and does not differ between the healthy and diseased states for an individual (14, 15, 36-39). Instead, a change in secondary, tertiary and quaternary structure defines the transition from PrP^{C} to PrP^{Sc}. PrP^{C} is primarily alpha-helical, while PrP^{Sc} has a large beta-sheet component (40). This conversion to a beta-

sheet conformation likely affects the tertiary structure (which remains unclear), and PrP^{Sc} aggregates as amyloid, defined by its cross- β sheet construction (30, 34, 41). There have been many attempts to predict the tertiary and quaternary structure of PrP^{Sc}, but none of the models perfectly predict the experimental behavior of the molecule (42).

Finally, several post-translational modifications of PrP^{C} have been identified. First, a GPI anchor is added to the carboxy-terminal end of PrP^{C} in the endoplasmic reticulum (Figs. 1-2) (32). The GPI anchor tethers PrP^{C} to lipid rafts, where conversion to PrP^{Sc} is hypothesized to occur. Reengineering PrP^{C} to reside in a transmembrane configuration, but not in rafts, prevented conversion to PrP^{Sc} (43, 44). The carboxy-terminal domain of PrP^{Sc} is more protected (from hydrogen-deuterium exchange) in the presence of the GPI anchor (45). Transgenic mice that express PrP^{C} without a GPI anchor have a delayed clinical disease, though PrP^{Sc} still accumulates (46, 47). Second, up to two N-linked carbohydrates (glycans) are added to PrP^{C} in the ER (at Asn-181 and Asn-197) (Figs. 1-2) (33, 48). The effect of glycosylation depends on species and isolate, but glycosylation seems to play a role in the conversion of PrP^{C} to PrP^{Sc} (49, 50). And third, the glycans of PrP^{C} carry between zero and four sialic acid residues on their termini (51). Sialylation plays a role in conversion efficiency and infectivity of PrP^{Sc}; undersialylated PrP^{C} is less prone to conversion *in vitro* and undersialylated PrP^{Sc} is not infectious (51-53). Sialylation was also implicated in prions' ability to hijack the immune system; when PrP^{Sc} arrives in the spleen, it is sialylated further (54).

(3) The third postulate dictates that the *susceptibility of an organism* be defined, including cellular, genetic and other features. Most simply, this postulate highlights the importance of the prion's primary structure, which certainly governs susceptibility of a host to a prion (13, 14, 48, 55-58). Without *PRNP*, individuals are resistant to prion disease (59, 60). For many species, there are polymorphisms in the *PRNP* gene that influence susceptibility. In humans, the most common polymorphism is at amino acid 129. Methionine homozygosity results in earlier onset and more rapid progression of clinical signs, compared to heterozygosity or homozygosity for valine. Gerstmann-Sträussler-Scheinker syndrome (GSS, a genetic prion disease of humans) is associated with the following missense mutations: P102L,

P105L, A117V, F198S, D202N, Q212P, Q217R, or inserts into the octapeptide repeat region. Familial CJD (a genetic prion disease) is associated with the following mutations: D178N, V180I, T188A, E196K, E200K, V203I, R208H, V210I, E211Q, M232R, and inserts into the octarepeat region. Finally, fatal familial insomnia (FFI, another genetic prion disease) is caused by the mutation D178N (31). In white-tailed deer, increased susceptibility to prion disease is associated with the following polymorphisms: H95Q, S96G, and G116S. In elk, L132M is associated with increased susceptibility, and in mule deer, F225S is associated with susceptibility (61). In addition to the effects of *PRNP* on host susceptibility, it remains unclear whether some other "Protein X" (or non-protein cofactor) is required for prion conversion and whether that cofactor may vary with cell and tissue types (62-64). The majority of efforts to define cofactor requirements have involved attempts to create infectious prions *in vitro*, as I describe in the following section.

(4) The fourth postulate states that disease should be *induced in a susceptible organism by a purified or synthetic agent* (21). Similar to Koch's third postulate, this type of experiment ensures that the agent in question is indeed infectious. It has also been among the most elusive results in the prion field (65). In 2004, Legname, et al. inoculated aggregated, truncated, recombinant PrP^C ($rPrP^C$, amino acids 90-231) into transgenic mice that dramatically overexpressed PrP^C. Mice inoculated with aggregated PrP^C were euthanized due to clinical signs between 380-660 days post-inoculation, while controls remained healthy until 670 days post-inoculation (66-68). The Prusiner lab created synthetic amyloid from recombinant PrP^C and compared the stability *in vitro* to the incubation time *in vivo* (69). However, each of these experiments was performed in susceptible organisms that may have been *too* susceptible; both transgenic mouse lines were at risk of developing spontaneous disease, which clouds the interpretation of the results. The group led by Claudio Soto used PrP^C from healthy transgenic mouse brain homogenate as the substrate for a synthetic prion and used prions from sick mouse brains to catalyze the misfolding process. Amplification proceeded for so long that the original sick mouse brain was essentially diluted away, ensuring that the synthetic prions were the ones causing disease (70). The same group repeated the experiment with prions derived entirely *in vitro* in PMCA, without the use of infected brain homogenate

to catalyze the misfolding and still observed infectivity in transgenic mice (71). The team led by Jiyan Ma performed a similar experiment in a brand-new laboratory that had never been exposed to prions, which confirmed that the *de novo* prion generation was truly *de novo* and not a result of contamination (72). Ilya Baskakov's group denatured PrP^{C} to cause misfolding and aggregation, then inoculated hamsters, a non-transgenic host. Disease did not manifest in the first or second passage, though atypical, aggregated prions were detectable (73-75). They proposed that recombinant fibrils matured in the brain of inoculated hamsters, and that traditional PrP^{Sc} eventually evolved, a process they called deformed templating (76, 77). The group led by Surachai Supattapone created infectious fibrils by addition of phosphatidylethanolamine to recombinant PrP^{C}, and has investigated other cofactors that control the infectivity and properties of prion isolates (78-83). Finally, John Collinge's group observed prion formation from normal brain homogenate on the surface of metal wire in the absence of PrP^{Sc} seeds (84). The creation of *de novo* infectious prions, especially from recombinant PrP^{C}, are evidence that the etiologic agent is comprised only of protein.

(5) The fifth postulate requires that the infectious agent be recovered from an organism after infection with the purified agent (21). In the studies that included infection of susceptible organisms with infectious, recombinant prions, the investigators demonstrated the existence of PrP^{Sc} in the brains of the inoculated laboratory animals (73, 74, 82). Naturally-occurring prions can be recovered from the experimentally-inoculated individual and re-inoculated into a naïve individual, with remarkably similar disease presentation in subsequent passages. Observations about the similar disease caused by a given isolate over passages resulted in the definition of strains in prion disease. Prion strains have identical primary sequences, but have different biochemical characteristics *in vitro* and different phenotypic characteristics *in vivo* (12). Prototypical examples include the hyper and drowsy strains of transmissible mink encephalopathy and the Me7 and 22A strains of mouse-adapted scrapie (12, 85-90). Strains may result in different incubation periods, different clinical signs, different neuropathology, different protease-sensitivity or different conformational stability (85). Strains are common among viruses with rapidly mutating genomes, but differences in nucleic acid sequence cannot explain the existence of strains in

prion disease. Prion strains are hypothesized to be caused by different conformations of PrP^{Sc}, conformations that are propagated upon infection of a new host (87, 88). When a prion strain infects a new host, it will often stabilize and adapt to the new host after several passages, though there is evidence that not all strains adapt upon transmission to a new host (91-93). The experiments I summarized in this section provide compelling evidence to support the prion hypothesis, which states that the etiologic agent for TSEs is a protein-only pathogen.

Yeast prions and prion-like proteins

In the decades since the proposal of the prion hypothesis, similar mechanisms of information transfer have been identified in mammals and in other systems. Investigators studying *Saccharomyces cerevisiae* and other yeast species have identified a number of prions that can undergo a conformational change and catalyze the same conformational change in another molecule (94-96). Some yeast prions are considered detrimental, though they are not invariably lethal like PrP^{Sc} (95). Yeast prions are similar to mammalian prions in a number of ways, including shared structural features (i.e. β-sheet-rich amyloid), self-templated replication, and the existence of strains (97). One non-lethal yeast prion, Het-S, is a functional prion; in other words, it performs a cellular function in its amyloid state (98). Functional prions have also been described in insects, mammals, sea slugs, plants and bacteria. In *Drosophila*, Kausik Si's group has identified a synaptic protein involved in long-term memory that acts as a transcription repressor, but adopts the phenotype of a transcription activator upon conversion to the amyloid state (99, 100). In mammals, two proteins involved in immune signaling have been characterized as functional prions. MAVS and ACS are involved in the signal transduction that follows RIG-I activation during viral infection (101, 102). In aplysia (sea slugs), a functional prion similar to the translation regulator in Drosophila plays a role in memory potentiation (103, 104). Susan Lindquist's group identified a prion in plants, though its function (or not) remains unknown (105). Recently, Ann Hochschild's group identified a prion in bacteria that serves as a transcription terminator in its soluble form, but loses its function upon aggregation, enabling dramatic changes in the transcriptome (106).

In light of the discovery of functional prions, the lack of consensus about the physiological role of PrP^C is especially interesting. PrP^C is likely to have some function besides serving as the substrate for conversion to PrP^{Sc}. However, years of investigation have produced many incongruous hypotheses for the normal role of PrP^C, including neurotransmission, olfaction, neural cell development, myelin maintenance, metal ion transport and neuroprotection (107, 108). PrP^C interacts with several receptors, including G-protein-coupled receptors, glutamate receptors, and voltage-gated calcium channels (109-111). Mice devoid of PrP^C have few phenotypic differences from wild-type mice, which makes it difficult to confirm the hypothesized roles for the molecule (107, 112).

In addition to the aforementioned functional prions, a number of neurodegenerative diseases have features reminiscent of prion disease. Specifically, normal proteins adopt a new conformation, coerce other molecules to adopt the same conformation, and form aggregates, a process called prion-like propagation. Examples of neurodegenerative diseases with prion-like propagation through the brain are described in Table 2 (113). The mechanism that controls the propagation of misfolded proteins through the brain is likely similar in all cases, and offers an opportunity for the translation of findings from the prion field to the neurodegeneration field and for important scientific progress.

Table 2. Other neurodegenerative proteinopathies. Several neurodegenerative disorders that result in protein aggregation are described here.

Disease	**Misfolded protein**	**Aggregate name**
Alzheimer's disease	tau, amyloid beta	neurofibrillary tangles, neuropil threads
Parkinson's disease	alpha synuclein	Lewy bodies
Huntington's disease	huntingtin	
Spinocerebellar ataxia	poly-glutamine proteins	
frontotemporal dementias	tau, TDP43, FUS	
chronic traumatic encephalopathy	tau	
amyotropic lateral sclerosis	SOD1 and others	

Transmissible spongiform encephalopathies of animals

TSEs affect several animal species, including sheep and goats (scrapie), cattle (BSE), cervids (chronic wasting disease, CWD), felines (feline spongiform encephalopathy, FSE) and mink (transmissible mink encephalopathy, TME). TME and BSE spread among farmed mink and cattle through

the feeding of contaminated animal byproducts and FSE was the result of BSE infection in cats (114-118). Scrapie has been recognized in captive sheep flocks for many years (119). Because scrapie has a strong genetic component, breeding programs have effectively reduced the incidence of scrapie in captive flocks (120). CWD is the only TSE that is currently spreading among wild populations (as well as within and between captive populations); it has been identified in North America, South Korea and Norway (121, 122).

CWD is characterized by a variable, long incubation period, followed by clinical signs that begin with subtle changes in behavior and movement. More advanced clinical signs include weight loss (wasting), bruxism, altered posture and head carriage, head tremors, ataxia, polydipsia, polyphagia and excessive salivation (61, 123-126). CWD(+) deer are more likely than uninfected deer to be hit by vehicles or preyed upon by mountain lions (127, 128). Modeling of cervid population growth suggests that CWD does result in reduced (or, in some cases, negative) population growth, though estimates are variable (129-134). CWD spreads easily among individuals, as demonstrated by its prevalence and the degree to which exposure of deer to contaminated environments results in infection (135). Estimates of prevalence vary depending on the diagnostic technique, the specific population and the cervid species, and range from 2 or 3% and 79% (129-132, 134, 136-138). Anecdotal and experimental evidence suggest that CWD prions contaminate the environment and remain infectious for long periods (126).

The etiology of CWD was only beginning to be recognized in the 1980s – 1990s, when another TSE was sweeping through Europe and devastating the cattle industry. The first detection of BSE occurred in 1986, and researchers in the UK soon recognized the neurological disorder as a TSE (22, 23). Nearly 5 million cattle were slaughtered in an attempt to stem the spread of BSE (8, 139). The inclusion of prion-contaminated cattle or sheep meat and bone meal (MBM) in cattle feed was likely responsible for the origin and proliferation of BSE in cattle herds in the UK (7, 118, 139-141). Near the end of the BSE outbreak, physicians in the UK and France diagnosed atypical cases of the human prion disease, Creutfeldt-Jakob disease (CJD), in young adults, which they described as variant CJD (vCJD) (10, 142). These cases were unusual and concerning because CJD (now called sporadic CJD, sCJD) is generally

recognized when the patient is 60+ years old, while the average age of vCJD patients was in the late 20s (12, 143). The authors observed other differences: the median disease course of sCJD is 4 months, while the median vCJD course lasts over a year and though many symptoms occur in both diseases, their order of appearance is dramatically different (10, 143). In vCJD cases, the earliest symptoms are psychiatric, followed by neurological signs, while sCJD begins with neurological symptoms (143). Careful biochemical analyses and laboratory animal bioassays revealed the remarkable similarities between vCJD and BSE, essentially confirming that vCJD was the human form of BSE (7, 10, 11, 91, 144-147). Like any potential zoonotic disease, the connection between human and animal hosts was tested with both epidemiological and molecular assessment. Epidemiologists failed to find increased vCJD incidence among those who worked in the dairy cattle industry (farmers, butchers, etc.) and the only risk factors identified among vCJD patients were residence in the UK, homozygosity for methionine at amino acid 129 in the human PrP^{C} sequence and relatively young age (118, 141, 143). Microbiologists and molecular biologists were unable to use the nucleic acid-based techniques that are frequently used to identify the source of zoonotic pathogens, but focused on the biochemistry and biology of the isolates instead. Specifically, researchers identified similarities between BSE and vCJD in 1) the electrophoretic mobility pattern of proteinase K (PK)-resistant PrP^{Sc}, 2) the incubation period, clinical signs and neuropathological lesion characteristics in inoculated laboratory animals, and 3) the susceptibility of transgenic mice to vCJD and BSE vs. sCJD (11, 146, 147).

As a response to the BSE outbreak in the UK, legislation was drafted that prevented the feeding of MBM to cattle, which effectively ended the exposure of cattle to prions. Several protective measures were enacted to limit exposure of humans to BSE prions, including the exclusion of specified risk materials, tissues considered to contain particularly high BSE titers (including brain, spinal cord, spinal ganglia, retina and terminal small intestine), and the exclusion of cattle over 30 months old from the food chain (for human food and pet food) (141). Cases of BSE have essentially disappeared across the world (with the exception of the occasional case of atypical BSE) and vCJD incidence appears to have disappeared with it, though the possibility of asymptomatic vCJD carriers remains (148-153). Though the

BSE outbreak appears to have been resolved, the increasing incidence of CWD across the world is cause for concern. This relatively new TSE has attracted the attention of the prion field, and significant improvements have been made in the methods available for prion detection and analysis in the era of CWD.

Prion detection methods (Table 3)

Infectivity: bioassay and cell culture

Animal models are often used to study the infectivity and pathogenesis of prions. These include transgenic mice that express the *Prnp* gene of various species and at various levels of expression, gene-targeted mice that express the *Prnp* gene of another species under the control of the mouse *PRNP* promoter, and the natural hosts of prion disease (154-157). Due to the long incubation periods and high cost of bioassays, many alternative assays have been introduced for the detection of prions. Attempts to establish cell-based models for prion infectivity have been plentiful, but relatively few cell lines are susceptible to prions and accumulate PrP^{Sc}, and even fewer models have been developed into useful assays for prion detection or infection (reviewed in (158)). The first attempts at cell culture systems for prions used neuronal cultures (159), but prion susceptibility has been identified in other cell types since then (160). Susceptible cell types include neuroblastoma cells (161, 162), Schwann cells (163), glioblastoma cells (164), rabbit kidney epithelial cells (165, 166), neural stem cells and neurosphere cultures (167-171), fibroblasts (172), muscle cells (173) and cells derived from transgenic mice (174, 175). Others have subcloned cell lines and isolated both susceptible and resistant cells to investigate the factors that determine susceptibility (176-178). Applications of cell-based systems include testing the efficacy of antibody and small molecule prion inhibitors, investigating cell to cell prion propagation and identifying differences between strains (179-196). Several cell models are practical screening tools for the detection of infectious prions (165, 168, 169, 171, 197-199).

Direct detection: IHC, Western blot, ELISA

Several methods to identify prions directly detect PrP^{Sc}, almost always based upon the variable protease sensitivity between PrP^{C} and PrP^{Sc}. Western blots are useful for the detection of PK-resistant PrP^{Sc} and the analysis of glycosylation patterns in a given tissue, species or strain, and are used very commonly in the prion field (200). Immunohistochemistry makes it possible to detect PK-resistant PrP^{Sc} in its tissue microenvironment and to study its distribution within and among tissues (201). Enzyme-linked immunosorbent assays (ELISAs) rely on antibody capture of PrP^{Sc} in PK-treated samples (with one exception, which uses a PrP^{Sc}-specific antibody and does not require PK-digestion) (202-207). All three assays are limited by their direct detection of PrP^{Sc}, which lowers sensitivity.

Amplification: PMCA and RT-QuIC

The central tenant of the prion hypothesis is that PrP^{Sc} coerces PrP^{C} to misfold and adopt the abnormal conformation. This propagation makes it possible to amplify prions *in vitro* – if PrP^{C} encounters PrP^{Sc} under the proper conditions, it will be misfolded and the amount of PrP^{Sc} will increase dramatically, well above the limit of detection. Two amplification assays are used frequently in the prion field – protein misfolding cyclic amplification (PMCA) and real-time, quaking-induced conversion (RT-QuIC). PMCA uses brain homogenate for its source of PrP^{C} and sonication to fracture fibrils and provide more free ends for the growth of the amyloid fibrils. The accumulation of PrP^{Sc} is identified with PK-treatment and western blot (208, 209). In RT-QuIC, the PrP^{C} source is recombinant PrP (rPrP) instead of brain homogenate and shaking is used in place of sonication. The readout relies on the binding of thioflavin T (ThT), an amyloid-specific dye, to the amyloid fibrils that result from seeding (210-212). When ThT intercalates within amyloid, its fluorescence spectrum shifts and its fluorescence intensity increases (213). RT-QuIC experiments are carried out in fluorimeters that make it possible to detect fluorescent emission from ThT in real-time, enabling the analysis of kinetics, which is much more elusive with PMCA. Because there is no PK-treatment, RT-QuIC may also be better equipped for detection of PK-sensitive prions.

Table 3. Summary of prion detection techniques. The detection techniques described above are summarized here. Several advantages ("pros") and disadvantages ("cons") are listed for each.

Technique	Amplification	Characteristic of PrP^{Sc}	Pros	Cons
Bioassay, natural host	Yes	Infectivity	Gold standard for infectivity, natural history of disease	Expensive, time-consuming, small n, natural variation
Bioassay, rodent model	Yes	Infectivity	Gold standard for infectivity, transgenics possible	Expensive, time-consuming, small n
Cell culture	Yes	Infectivity, conversion ability	Surrogate for infectivity, cellular processes intact	Technically difficult, infectivity does not persist
IHC	No	PK-resistance	Fast, tissue distribution, specific	Relies on PK-resistance, low sensitivity
Western blot	No	PK-resistance	Fast, specific	Relies on PK-resistance, low sensitivity
ELISA	No	PK-resistance or underglycosylation	Fast, specific, high-throughput	Relies on PK-resistance or underglycosylation, low sensitivtiy
PMCA	Yes	Conversion ability	Makes infectious product, specific, sensitive, contains cellular factors	Requires animal tissue, slow western blot readout relies on PK-resistance
RT-QuIC	Yes	Conversion ability	Sensitive, high-throughput, kinetic data, mutable system	Imperfect specificity, infectivity of product unknown

Gaps in understanding CWD and its risk to humans

Unsurprisingly, the prion field has been very interested in the zoonotic potential of CWD. As I outlined in Table 1, there is much to learn if we are to predict a species-barrier-crossing event. In particular, this dissertation addresses: 1) the routes of transmission (and ability to spread, signified by R_0) of CWD, and 2) the host range and plasticity of CWD.

1) Routes of transmission and R_0 of CWD

For a CWD(+) deer to infect another susceptible host, CWD prions must be present in a substance that will be encountered by the naïve individual and must be present in an infectious form. Only with an understanding of the distribution of infectious prions in tissues and excreta from deer can we estimate the routes by which other individuals can be exposed and infected by CWD, information that is necessary to calculate the basic reproductive number (R_0) for CWD. Years of CWD research have confirmed that deer can be infected with CWD through several routes, including intracerebral, intravenous, per os (oral), intraperitoneal and inhalation (123, 214, 215). It is also clear that PrP^{Sc} accumulates in many tissues in CWD(+) cervids, including the central, enteric and peripheral nervous system, the lymphoreticular system, the upper and lower gastrointestinal tract, muscle, endocrine tissues, fat, reproductive and excretory tissues (138, 156, 157, 216-223). Perhaps more importantly for the calculation of R_0, PrP^{Sc} has also been identified in saliva, feces, urine and blood from CWD(+) deer (123, 124). Positive excreta likely explain the environmental contamination that seems to exist in endemic CWD regions (135).

The prion hypothesis states that PrP^{Sc} forms as a result of a conformational change in PrP^{C}, which implies that PrP^{C} must be present for PrP^{Sc} to develop. Despite this requirement, we know relatively little about the distribution of PrP^{C} in the natural host of CWD. And despite a fairly robust description of PrP^{Sc} deposition in the deer, there have been very few assessments of the infectivity of tissues outside the CNS. Lymph nodes accumulate prions particularly early and consistently in deer with CWD, but their infectivity has not been analyzed (156, 224). However, in sheep with scrapie, lymph nodes have been confirmed to be infectious by bioassay in several models (including sheep and bank voles) (225-228).

Finally, the development of ultra-sensitive detection methods, as described above, has vastly simplified the identification of PrP^{Sc} in a number of complex, low-titer samples. However, the interpretation of results from each of these detection methods must be made with an understanding that the tests are imperfect in their sensitivity and specificity, with the possibility of false negatives and false positives. Because we are particularly interested in the RT-QuIC assay, we have been mindful of its vulnerability to inhibitors and activators of amyloid formation (229-231). It is essential that we

investigate the limitations of our detection methods if we are to properly understand their results, which will ultimately inform the R_0 of CWD.

2) Host range and plasticity of CWD

The dreadful zoonotic outcomes of the BSE outbreak and the rapid, unchecked spread of CWD underlie the importance of understanding the host range of CWD. Experimental inoculations of squirrel monkeys (232, 233), cattle (234, 235), sheep (236), domestic cats (237) and ferrets (238) have caused disease in at least some of the inoculated individuals. Macaques appear to be refractory to CWD infection; 7 inoculated macaques failed to show any signs of TSE infection after >5.5 years (233). BSE, the prototype zoonotic TSE, infected sheep (239), pigs (240), macaques (144, 241, 242), and cervids (243, 244) upon experimental inoculation and felines (114, 115, 245, 246) and exotic ruminants (247) upon natural exposure. Therefore, both prion diseases have fairly plastic host ranges when the outcomes of experimental inoculations are compared. However, only BSE has definitively crossed a species barrier in a natural transmission event (248).

Of course, it is not possible to test the susceptibility of humans to CWD (or BSE) by experimental inoculation. To simulate the natural host when the natural host is unavailable or difficult to use in laboratory experiments, the prion field has relied heavily upon mice engineered to express the *PRNP* gene of another species. In particular, a number of transgenic mouse lines expressing one polymorphism or another of human PrP^C exist (TgHu). Upon intracerebral inoculation, BSE has approximately a 50% attack rate in TgHu mice (155, 249-252), while CWD inoculation has never resulted in disease (155, 253-255).

Epidemiologists monitor the prevalence of human prion disease, particularly sCJD, in populations that have increased exposure to CWD, but there has been no evidence that sCJD prevalence is increased among those exposed to venison (256-259). There were several cases of sCJD in American young adults who were much younger than the average sCJD patient and all three were exposed to venison, but there was no strong causal link between their disease and CWD (260). Of course, similar epidemiological approaches were used in the UK during the BSE outbreak to look for infection in humans, but there was

not an increased prevalence of vCJD among dairy farmers or those with occupations in the abattoir industry (141).

In vitro assays provide one more avenue for the investigation of CWD susceptibility in humans. The advantages of *in vitro* systems include their relative mutability, precise conditions and their ability to isolate specific features of PrP^{C} or PrP^{Sc}. The primary structure of PrP^{C} is undoubtedly important in prion disease species barriers, as are the tertiary and quaternary structures of PrP^{Sc} (56, 261-265). *In vitro* systems are particularly useful to study the effects of particular PrP^{C} regions on misfolding. Several investigators have used *in vitro* prion amplification systems to test the ability of CWD PrP^{Sc} to coerce PrP^{C} to misfold. Overall, the results suggested that misfolding of human PrP^{C} by CWD prions was unfavorable, but not impossible (266-270).

Conclusion

I intended to answer questions essential to understanding the R_0 and host range of CWD. The results of those inquiries are presented in this dissertation. In short, we asked:

1) Where is PrP^{C} expressed in the deer and is PrP^{C} expression correlated with the accumulation of prion seeding activity?
2) Are CWD prions from lymph nodes infectious?
3) How accurate are our attempts to measure prion shedding in excreta, particularly in saliva?
4) How do prions adapt to new species and is there a barrier to the misfolding of human recombinant PrP^{C} by CWD prions?
5) What is the role of the amino terminal domain of PrP^{C} in the susceptibility of human PrP^{C} to CWD?

I will demonstrate that PrP^{C} and CWD seeding activity are widespread in deer, though not clearly correlated, that CWD prions in lymph nodes are infectious in cell culture, and that prions are likely shed in saliva more frequently than we recognize. Despite the unique transmissibility of CWD, the risk to humans remains unclear. The apparent species barrier is not due to an impediment at the level of PrP^{C} /PrP^{Sc} interaction, as CWD prions can cause misfolding of human PrP^{C}. Finally, the amino-terminal

domain of human PrP^{C} appears to facilitate the conversion of PrP^{C} to PrP^{Sc} in the presence of CWD prions.

CHAPTER 1: PrP^C EXPRESSION AND PRION SEEDING ACTIVITY IN THE ALIMENTARY TRACT AND LYMPHOID TISSUE OF DEER

Summary

The agent responsible for prion diseases is a misfolded form of a normal protein (PrP^C). The prion hypothesis stipulates that PrP^C must be present for the disease to manifest. Cervid populations across the world are infected with chronic wasting disease, a horizontally-transmissible prion disease that likely spreads via oral exposure to infectious prions (PrP^{Sc}). Though PrP^{Sc} has been identified in many tissues, there has been little effort to characterize the overall PrP^C expression in cervids and its relationship to PrP^{Sc} accumulation. We used immunohistochemistry (IHC), western blot and enzyme-linked immunosorbent assay to describe PrP^C expression in CWD(-) white-tailed deer. We used real-time, quaking-induced conversion (RT-QuIC) to detect prion seeding activity in CWD(+) deer.

We assessed tissues comprising the alimentary tract, alimentary-associated lymphoid tissue and systemic lymphoid tissue from five naïve deer. PrP^C was expressed in all tissues, though expression was often very low compared to the level in the CNS. Specific cell types express high levels of PrP^C. To compare the distribution of PrP^C to PrP^{Sc}, we examined five deer with advanced CWD infection. We detected prion seeding activity in all 21 tissues using RT-QuIC. In three subclinical deer sacrificed four months post-inoculation, we detected PrP^{Sc} consistently in alimentary-associated lymphoid tissue, irregularly in alimentary tract tissues, and not at all in the brain. Contrary to our hypothesis that PrP^C levels dictate prion accumulation, PrP^C expression was higher in the lower gastrointestinal tissues than in the alimentary-associated lymphoid system and was higher in salivary glands than in the oropharyngeal lymphoid tissue. These data suggest that PrP^C expression is not the sole driver of prion accumulation and that alimentary tract tissues accumulate prions before centrifugal spread from the brain occurs.

Background

Chronic wasting disease (CWD) is spreading among deer, elk and other cervids in North America, the Republic of Korea, and, recently, Norway (61, 121, 122, 271). The etiologic agent, a prion, results from the templated conversion from a normal protein, PrP^{C}, to a primarily beta-sheet, misfolded form (PrP^{Sc}). The prion hypothesis stipulates that the normal prion protein, PrP^{C}, is necessary for the manifestation of PrP^{Sc} and the disease state (13). As deer are likely exposed via the oral route to prions in the natural environment and because there is evidence that prions accumulate in the lymphoid tissue of cervids, we were interested in the expression of PrP^{C} in the alimentary tract and lymphoid system of the natural host (white-tailed deer, *Odocoileus virginianus*) (156, 204, 216, 219, 220, 224, 272). The relationship between PrP^{C} expression and PrP^{Sc} accumulation in specific tissues has not been reported, though it is classically understood that the spread of prions involves centripetal spread from the peripheral nerves to the brain, followed by replication in the brain and centrifugal spread to the rest of the body (226, 227, 273, 274).

There is no literature describing the expression of PrP^{C} in cervids, the natural host of CWD. The expression of PrP^{C} has been described in cattle, the host of bovine spongiform encephalopathy, and sheep, the host of scrapie, and in common experimental models (hamsters and mice). In cattle, PrP^{C} is expressed in the brain, lymphoid tissue, gastrointestinal nervous and mucosal tissues, thymus, kidney, heart, lung, liver, muscle and pancreas (275-278). In sheep, PrP^{C} expression has been detected in the brain, intestine, lymphoid tissue, lung, heart, kidney, muscle, uterus, adrenal gland, salivary glands, stomachs and mammary glands (279, 280). Finally, PrP^{C} has been identified in the muscle, alimentary tract, skin and respiratory epithelium of mice (281, 282) and in the CNS, lymphoid tissue, heart, liver, lung, kidney, stomach and intestine of hamsters (283-285). We hypothesized that PrP^{C} would be widely distributed in white-tailed deer and that expression would be highest in lymphoid tissue, since lymphoid tissue plays a role in early CWD pathogenesis (156, 216, 224).

We were also interested in the accumulation of PrP^{Sc} in alimentary tissues, since the oral route of exposure is likely responsible for horizontal transmission of CWD (126, 135). We hypothesized that

tissues with the highest PrP^{C} expression would accumulate PrP^{Sc} earlier in disease, and that tissues with low PrP^{C} expression may never accumulate detectable PrP^{Sc} or only much later in disease. PrP^{Sc} has been detected in a number of deer tissues by a variety of methods, including western blot, immunohistochemistry (IHC) and enzyme-linked immunosorbent assay (ELISA). Tissues that have been identified as prion-positive in CWD(+) cervids include lymphoid tissues, brain, salivary glands, some parts of the intestinal tract, forestomachs, abomasum, pituitary, heart, adrenal gland, muscle, and fat (156, 157, 216-222).

We used ELISA and western blot to measure PrP^{C} expression and IHC to describe to the distribution of PrP^{C} in 21 alimentary tissues and alimentary-associated lymphoid tissues of CWD(-) deer. We used real-time, quaking-induced conversion (RT-QuIC) to detect prion-seeding activity in the same tissues from orally-inoculated, CWD(+) deer either in the symptomatic stages of disease or four months after oral inoculation with CWD (at least 12 months before we typically see clinical signs) (215). We observed that PrP^{C} expression is widespread, and that seeding activity does not accumulate first in the tissues with the highest PrP^{C} expression. Importantly, we conclude that prion replication occurs in alimentary tissues before centrifugal spread of PrP^{Sc} from the brain. These results are an important step toward understanding the pathogenesis of CWD and for understanding its facile horizontal transmission.

Methods

White-tailed deer husbandry, inoculation and necropsy

We obtained hand-raised, indoor-adapted, white-tailed deer fawns (*Odocoileus virginianus*) from collaborators Sally Dahmes (WASCO Inc.), David Osborn, Carl Miller, and Robert Warren (Warnell School of Forestry, University of Georgia). The deer were maintained in accordance with Colorado State University's Animal Care and Use Committee. The genotype of the deer at amino acid 96 was determined as previously described, and all deer were homozygous for glycine (Table 1.1) (38, 286). Deer that were sacrificed in symptomatic stages of disease (1031, 1078, 1079, 1081, 1082) were inoculated *per os* with 0.01g of 10% brain homogenate pooled from 6 CWD(+), white-tailed deer. Deer sacrificed in pre-clinical

stages of CWD (1171, 1201, 1205) were inoculated *per os* with 0.5g of the same brain homogenate. CWD(-) deer were inoculated with 0.5g of CWD(-) brain homogenate (deer 1140, 1169, 1211) or were uninoculated (deer 952, 955). Negative deer were housed in separate suites in the same indoor facility as the CWD-inoculated deer (214).

Table 1.1. White-tailed deer polymorphisms. The genotype at codons 13, 21, 96 and 226 for each deer is described below.

Deer Number	*Codon 13*	*Codon 21*	*Codon 96*	*Codon 226*
1031	LL	VV	GG	QQ
1078	LL	VV	GG	QQ
1079	LL	VV	GG	QQ
1081	LL	VV	GG	QQ
1082	LF	VV	GG	QQ
1171	LL	VV	GG	No data
1201	LL	VV	GG	No data
1205	LL	VV	GG	No data

Tissue collection and processing

We collected each tissue with new, prion-free, disposable instruments. We froze half of each tissue at -80ºC and fixed the other half in periodate-lysate-paraformaldehyde (PLP) for four days. After fixing, we stored the tissues in sterile PBS until trimming, followed by 70% ethanol for long-term storage. We trimmed tissues into cassettes and embedded them in paraffin blocks using routine histologic techniques.

We homogenized frozen tissue for western blots, RT-QuIC, and ELISA using the following protocol: we trimmed approximately 200mg of tissue on ice and added it to ice-cold 1X PBS with protease inhibitors (Roche Complete Mini protease inhibitor tablets; one tablet/10mL PBS) to create a 20% w/v homogenate. We homogenized the tissues (Bead Ruptor 24 Bead Mill Homogenizer, Omni International) for 30 seconds, followed by a 10 second pause, then another 30 second homogenization. We chilled the homogenates on ice for 5 minutes, then repeated the homogenization and chill protocol twice more. We diluted each sample to 1% for the bicinchoninic acid (BCA) assay (Pierce BCA Protein Assay Kit, Thermo Scientific), and froze the remaining 20% homogenates at -80ºC.

We performed BCA assays according to the manufacturer's instructions, with each sample and standard tested in triplicate. We recorded optical density with an Opsys MR microplate reader (Dynex technologies).

Western blot

We thawed frozen 20% tissue homogenates on ice and added 500µg of total protein to 2% N-lauroylsarcosine sodium salt in PBS for a final volume of 150µL. We thawed brain homogenates on ice and added 5.0ug of total protein to 2% sarkosyl in PBS for a final volume of 150µL. We added 25µL of 6X Laemmli sample buffer to each sample, then boiled for 5 minutes. Next, we loaded 20µL of each sample preparation (~57µg total protein for tissues and 0.57µg total protein for brain) to each well of an 18-well precast gel (12% Criterion™ XT Bis-Tris protein gels, Bio-Rad) and electrophoresed the gels for 90 minutes at 150V. We transferred the proteins to a PVDF membrane for 1 hour at 80V on ice (Criterion™ Blotter, Biorad), then blocked the membranes with 5% non-fat dry milk in TBST for 20 minutes at room temperature, then incubated the membrane with 0.2µg/mL antibody Bar224 (Cayman Chemicals, continuous epitope aa141-151) overnight at 4ºC. We followed the primary antibody with a horseradish-peroxidase-labeled goat anti-mouse IgG for one hour at room temperature and developed the western blots with Pierce ECL substrate (ThermoFisher Scientific) for five minutes. We captured images with the GE ImageQuant LS 400 imager; specifically, we exposed the membranes for 70 seconds and analyzed the western blots whose bands were uninterrupted by bubbles or other artifacts.

We used Image Studio Lite v4.0 (Li-Cor Biosciences) for densitometry. First, we drew a rectangle around the first lane and copied it onto each lane, then used the software's background subtraction tool, which subtracted the median background from the right and left of each rectangle for three border-widths. Next, we calculated the intensity of each lane relative to the brain sample that was included in every experiment. We plotted a frequency histogram of all lane intensities from every experiment and divided the data evenly into four quadrants. We used the borders of these quadrants as cutoffs for our final classification (very low, low, medium and high).

Histology and immunohistochemistry

We mounted 5μm sections of paraffin-embedded tissue on positively-charged glass slides. We heated the slides at 65˚C, then removed paraffin with xylene and rehydraded the tissues in graded alcohols (100%, 95%, 70%) and water. We treated the tissues with 88% formic acid for five minutes to expose epitopes. To quench peroxidases, we incubated the tissues with 3% hydrogen peroxide in methanol. We blocked tissues with 5% non-fat dry milk (in TNT [0.1M Tris-HCl, 150mM NaCl, 0.1% Tween]). We incubated tissues overnight at 4˚C in a bath of 2μg/mL anti-PrP^C antibody Bar224 (Cayman Chemicals) or mouse IgG_{2A} as a negative control (RD Systems). We incubated the tissues with secondary anti-mouse IgG conjugated to horseradish peroxidase (Envision+™, Dako) at room temperature. Finally, we detected the immunoreactivity with AEC chromagen (Dako). We counterstained with Mayer's hematoxylin (Dako), followed by 0.1% sodium bicarbonate bluing reagent, then added coverslips with aqueous mounting media (Dako) and allowed to dry completely. For hematoxylin and eosin staining, we used the same deparaffinization protocol. We stained the tissues with Mayer's hematoxylin, then eosin (NovaUltra™ H&E Stain Kit, IHC World). We cleared the slides in xylene, then added coverslips with xylene-based mounting media and allowed to dry. We visualized staining with light microscopy.

Enzyme-linked immunosorbent assay

We coated 96-well plates (Maxisorp plates, Nunc) with 20μg/mL capture antibody D18 (287) (Telling laboratory, Colorado State University Prion Research Center) in carbonate/bicarbonate buffer, sealed and stored for 1-4 days at 4ºC. We blocked the plates with 3% bovine serum albumin (BSA) in PBS at 37ºC. We thawed tissue homogenates on ice and added 250-2000μg/mL total protein to 0.23% BSA, 0.035% Triton X100 and PBS. We added 100μL of each sample to three wells and incubated overnight at 4ºC. We added PRC5 (1:5000, Prion Research Center, Colorado State University (202)) in 1% BSA in PBS to the plates at 37ºC, then washed and added anti-mouse IgG2s-HRP conjugate (Alpha Diagnostic International Inc) at a 1:5000 dilution at 37ºC. We developed the plates with ABTS peroxidase substrate (Thermo Fisher Scientific), then stopped the reaction. We read the absorbance at 405nm on an

ELx808 Ultra Microplate Reader (Bio-Tek Instruments, Inc.). In addition to the samples of interest, we included blank wells and standard wells. The blanks were missing only the tissue homogenates and the standards included recombinant white-tailed deer rPrP instead of tissue homogenate. We used concentrations of 0.1-1250ng/mL rPrP for the standard curve.

We assessed each sample for its linearity. Samples that did not exhibit a linear response to dilution were repeated at higher total protein concentrations. Samples that did not cross the threshold (3 standard deviations above the mean absorbance of the blanks) were also repeated with higher total protein concentrations. If samples exhibited a linear response of absorbance to dilution and had at least two dilutions above the threshold, we proceeded with analysis. We were able to proceed with analysis of all tissues except the following: 1/3 rumen samples (below threshold), 1/3 spleen samples (nonlinear dose response), 2/3 prescapular lymph node samples (nonlinear dose response), 1/3 omasum samples (below threshold), and 1/3 ileocecocolic LN (nonlinear dose response). We computed the linear regression for the standard curves (within the linear range) and extrapolated the ng/mL PrP^C for each sample (choosing the dilution in the center of the linear range). We divided the ng/mL PrP^C by the μg/mL total protein added to the ELISA to calculate a ratio of PrP^C/total protein for each sample. We plotted a frequency histogram of the ng PrP^C/mg total protein for every replicate and divided the data into quartiles. We assigned a score of 4 to replicates that fell within the highest quartile, 3 for the 50-75% quartile, 2 for the 25-50% quartile and 1 for the lowest quartile. We averaged the scores of each replicate (n=3) and each deer (n=3) in Figure 1.4. A score of 1 represents less than 1.36 ng PrP^C/mg total protein, a score of 2 represents 1.37-2.51ng PrP^C/mg total protein, a score of 3 represents 2.52 – 4.77ng PrP^C/mg total protein and a score of 4 represents greater than 4.78ng PrP^C/mg total protein. We compared sample types or groups of samples with a one-way ANOVA, followed by Tukey's multiple comparison post-test.

Expression and purification of recombinant PrP

We expressed full-length white-tailed deer (WTD) PrP^C for standard curves in ELISA as previously reported (93) and truncated Syrian hamster (SH) PrP^C for RT-QuIC as previously reported

(288). Briefly, the cDNA sequence for the WTD *PRNP* gene was cloned into the pet100D expression system (Life Technologies). The plasmid for expression of amino acids 90-231 of SH PrP^C was kindly provided by Dr. Byron Caughey. We stored the plasmids in *E. coli* BL21 Star cells (Life Technologies). To express PrP^C, we added BL21 cells from frozen glycerol stocks to 5mL LB media, grew the cultures overnight, then added the bacteria to 1L LB media with auto-induction reagents (final concentration: 0.5M $(NH_4)_2SO_4$, 1M KH_2PO_4, 1M Na_2HPO_4, 0.5% glycerol, 0.05% glucose, 0.2% α-lactose and .001M $MgSO_4$.) We harvested bacteria when the OD_{600} reached approximately 3.0 for WTD and 1.7 for SH PrP^C. We lysed the cells and purified inclusion bodies according to the manufacturer's protocol with BugBuster™ and Lysonase™ (EMD-Millipore).

To purify recombinant PrP (rPrP), we solubilized the inclusion bodies in 8M guanidine hydrochloride (GdnHCl) and 100mM Na_2HPO_4 at room temperature, overnight, in an end-over-end rotator. We mixed the denatured rPrP slurry with Superflow™ nickel resin (Qiagen) and refolded the rPrP on the column and eluted as previously reported (93).

Real-time quaking-induced conversion (RT-QuIC) with NaPTA precipitation

We thawed aliquots of frozen tissue homogenates on ice and diluted the homogenate to 0.1% in 0.1% SDS/PBS. We added sodium phosphotungstic acid (NaPTA) (final concentration 0.33% NaPTA, 0.28% $MgCl_2$) to 100µL 0.1% tissue homogenate. We shook the mixture at 1400rpm for 1 hour at 37ºC, then pelleted precipitated proteins at 14,000g for 30 minutes. We resuspended NaPTA pellets in 10µL 0.1% SDS/PBS and added 2µL to each well of the RT-QuIC plate. We did not subject brain samples to NaPTA precipitation; we diluted 10% brain homogenates in 0.1% SDS/PBS and tested the 10^{-3} and 10^{-4} dilutions.

We performed RT-QuIC experiments in black, optical-bottom 96-well plates (Nunc). Each RT-QuIC reaction was comprised of 0.1mg/mL SH rPrP, 320mM NaCl, 1.0mM EDTA, 20mM NaH_2PO_4 and 10µM thioflavin T. An RT-QuIC experiment consisted of 250 cycles (62.5 hours) of shaking (1 minute,

double orbital shaking at 700rpm) and rest (1 minute) at 40°C. Microplate readers (Fluostar, BMG) recorded the fluorescence (450nm excitation and 480nm emission) every 15 minutes using a gain of 1700.

We included matched negative control tissues (i.e. the same tissue from a CWD(-) deer) on every plate and samples were run in quadruplicate twice (8 total replicates). We calculated a threshold at 5 standard deviations above baseline fluorescence to determine which replicates were positive. We used Omega software (BMG Labtech) to determine the lag phase – the time at which the fluorescence in a given well exceeded the threshold. If the fluorescence for a sample never crossed the threshold during the experiment, we estimated a value of 70 hours. We analyzed the lag phase data using non-parametric, rank-based tests (Wilcoxon-Mann-Whitney (WMW) and Wilcoxon signed-rank tests). If all values for one sample were equal, WMW tests are invalid, so we used Wilcoxon signed-rank tests instead. We chose these tests for several reasons: 1) our data was often non-normal (right skewed due to replicate wells that don't cross the threshold in the course of the experiment); 2) our n was relatively small (8); and 3) we had to choose values to substitute for the replicate wells that did not cross the threshold. The choice of that value would affect the mean (and the results of any statistical tests that relies on means, like t-tests), but will not affect rank-based statistical analysis, since those values will have the longest lag phase regardless of which value we choose. We described a tissue as positive when it was statistically different from the same tissue from a negative control deer ($p<0.05$).

Results

PrP^C expression is widespread, but low, in many tissues of the alimentary tract and alimentary-associated lymphoid tissue.

We used western blots and ELISA to detect PrP^C in frozen tissue samples from captive, CWD(-), white-tailed deer. We examined 21 tissues of the alimentary tract, alimentary-associated lymphoid tissues, and peripheral lymphoid tissues. We classified PrP^C expression in each tissue into quartiles and assigned expression scores based on the quartile where the tissue fell. We detected PrP^C expression in all tissues by western blot, although expression was often near the limit of detection (representative western blots in Fig

1.1). We were able to detect PrP^C expression by ELISA in nearly all tissues (select raw ELISA data in Fig 1.2.) Overall, the assays detected similar expression in a given tissue. When expression levels varied between assays, the ELISA detected higher PrP^C expression than did western blot (ileum and cecum), with the exception of the mesenteric LN (Fig 1.3). For the statistical analysis, we used the ELISA data, since it is inherently the more quantitative assay (281).

We were interested in a comparison of alimentary-associated lymphoid tissue (which is assumed to play a major role in CWD pathogenesis) and tissues of the alimentary tract. Tissues of the lower alimentary tract (small and large intestines and rectum) had higher PrP^C expression than did the group comprised of all the alimentary-associated lymphoid tissue (ANOVA, Tukey post-test, $p<0.05$) (Fig 1.4) Earliest CWD prion replication has been detected in oropharyngeal lymphoid tissue (224), so we compared PrP^C expression in these tissues (mandibular LN, parotid LN, tonsil, retropharyngeal LN) to the salivary glands, which are also proximate to the oral cavity and are likely involved in the contamination of saliva with prions (218, 224, 231, 288). The salivary glands had higher PrP^C expression than did the oropharyngeal lymph nodes (ANOVA, Tukey post-test, $p<0.05$) (Fig 1.4). However, there was no difference in the PrP^C expression of the oropharyngeal lymph nodes and the lymph nodes of the lower GI (ANOVA, Tukey post-test, $p>0.05$) (Fig 1.4). Finally, we were interested in the PrP^C expression level in the spleen, which had lower expression than the lower alimentary tract tissues, the salivary glands and the ruminant stomachs (ANOVA, Tukey post-test, $p<0.05$). The spleen also had (statistically insignificantly) lower PrP^C expression than all lymph nodes combined (Fig 1.4).

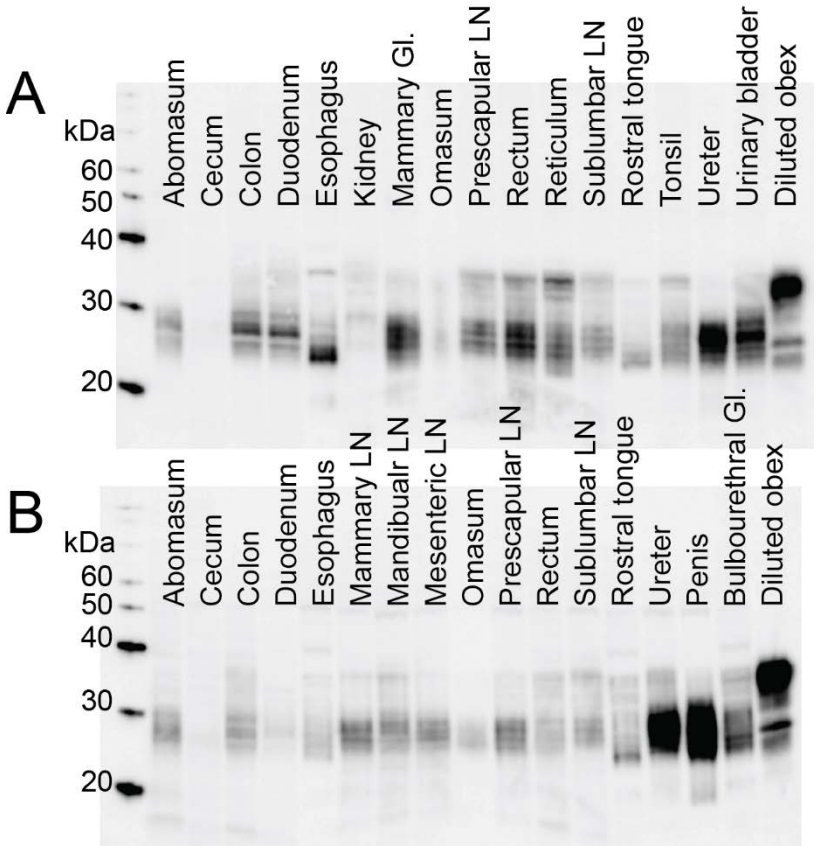

Figure 1.1 Representative western blots. We performed western blots for PrP^C expression on tissue homogenates from five CWD(-) deer. We used a diluted obex homogenate (1% of total protein added for other samples) to normalize each western blot (lane 18) and performed densitometry on each lane. A) Representative western blot from deer 952. B) Representative western blot from deer 955. Expression of PrP^C was variable among tissues and, to some degree, between deer. However, we detected PrP^C in every tissue in at least one of the deer. α-PrP antibody BAR224 recognizes a continuous epitope from aa141-151, and is expected to recognize the C1 fragment of PrP^C.

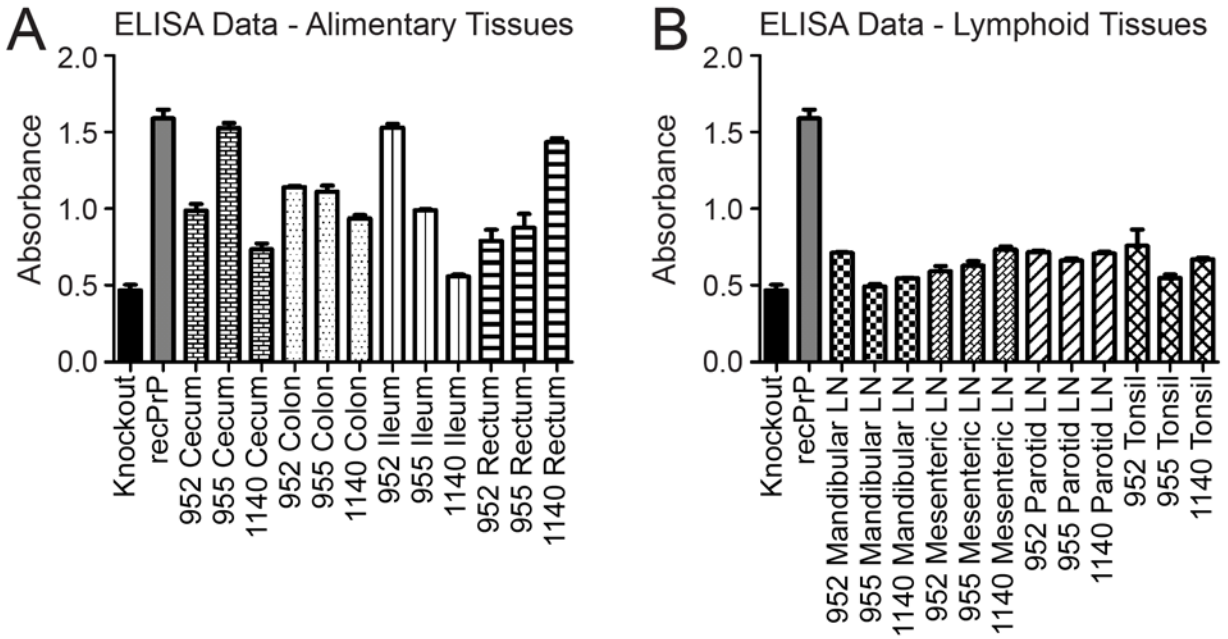

Figure 1.2. Representative ELISA results. We performed sandwich ELISA assays for PrP^{C} expression for three CWD(-) deer. We used $PrP^{0/0}$ mouse tissues as negative controls and five dilutions of recombinant white-tailed deer PrP^{C} ($rPrP^{C}$) to generate a standard curve, one dilution of which is shown here. Bars represent the mean absorbance of three technical replicates and error bars represent standard error of the mean. A. We compared several alimentary tissues from all three deer. B. We compared several alimentary-associated lymphoid tissues from all three deer. Replicate samples from individual deer were very consistent (error bars), but there was some variability between deer for a given tissue (note differences in bars of the same pattern). Overall, expression was higher in the alimentary tissues than in the alimentary-associated lymphoid tissues.

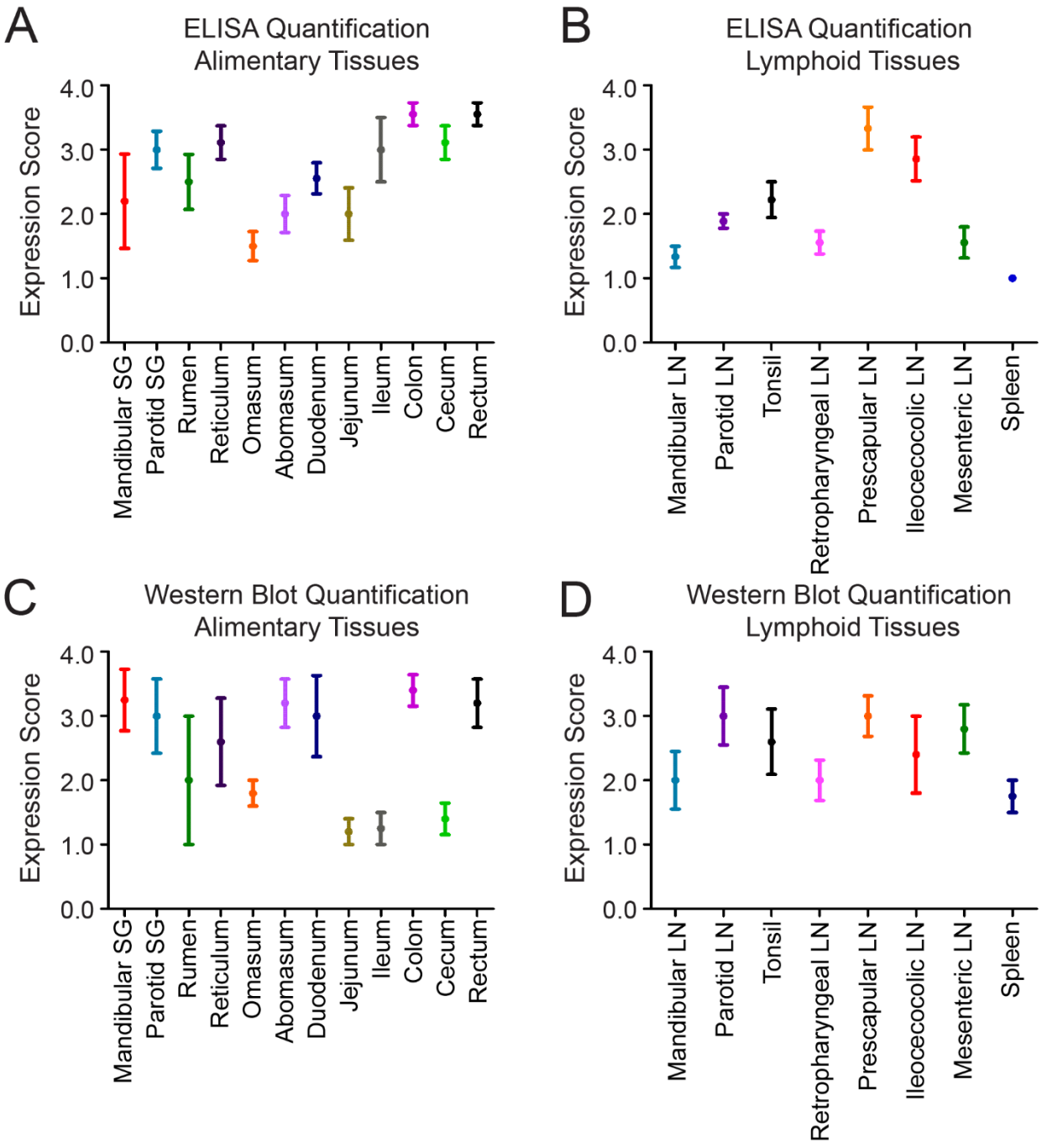

Figure 1.3. Quantification of PrP^C expression. A-B. We converted ELISA absorbance values to expression scores using the approach detailed in the methods section. Briefly, we divided each replicate into quartiles based on their absorbance and assigned the top quartile a score of 4 and the lowest quartile a score of 1. For every tissue, the mean score for three replicates for each of three deer is plotted with the standard error of the mean. We divided the tissues we tested into alimentary (A) and lymphoid (B) tissues. C-D. We converted western blot densitometry data to expression scores using the technique described in the methods. Briefly, we normalized each lane to the diluted obex on the same blot, then divided all normalized densitometry data into quartiles. The top quartile received a score of 4 and the lowest received a score of 1. We plotted the mean score for five deer with the standard error of the mean. We divided the

tissues into alimentary (including glandular) (C) and lymphoid (D) tissues. The error bars indicate that the alimentary tissues were more variable than the lymphoid tissues and that the western blot results were more variable than the ELISA results.

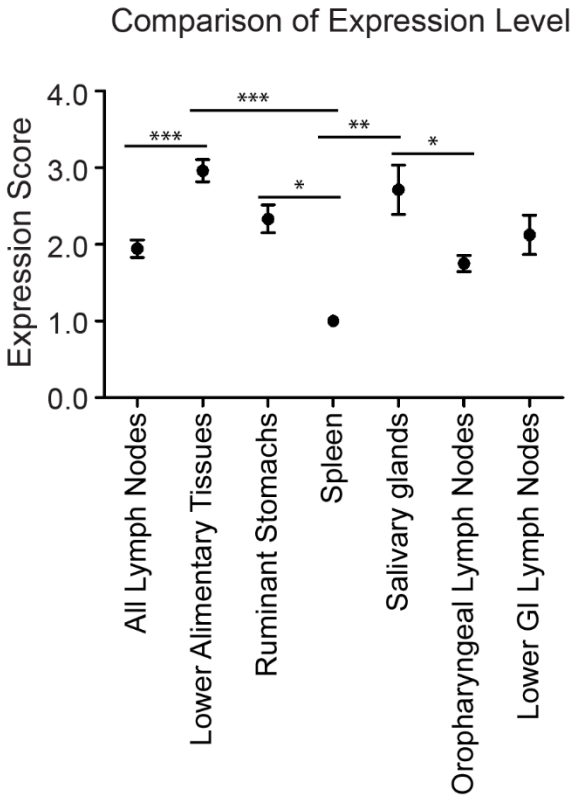

Figure 1.4. Comparison of PrP^C expression among tissue types. We used one-way ANOVA and Tukey's multiple comparison post-test to analyze differences between PrP^C expression levels in types of tissue (based on ELISA results.) * indicates $p<0.05$, ** $p<0.01$, *** $p<0.0001$. *Lower alimentary tissues* include: duodenum, jejunum, ileum, cecum, colon and rectum. *Ruminant stomachs* include: rumen, reticulum, omasum and abomasum. *Oropharyngeal lymph nodes* include: tonsil, retropharyngeal lymph node, mandibular lymph node and parotid lymph node. *Lower GI lymph nodes* includes ileocecocolic lymph node and mesenteric lymph node. As indicated by the asterisks, there are statistically significant differences between the following groups: lower alimentary tissues > all lymph nodes; lower alimentary tissues > spleen; ruminant stomachs > spleen; salivary glands > spleen; salivary glands > oropharyngeal lymph nodes. We plotted means and standard error of the mean.

PrP^C is expressed in the epithelium and nervous tissue components of many alimentary tissues.

We observed PrP^C immunoreactivity in mucosal stratum spinosum and stratum granulosum epithelial cells of the rumen, reticulum, and omasum forestomachs (Fig 1.5, Table 1.2, Table 1.3). In the abomasum, we detected PrP^C immunoreactivity in individual cells in the gastric pits with a phenotype consistent with peptic chief cells (Fig 1.5, Table 1.2, Table 1.3). We observed immunoreactivity in the

apical region of the small intestinal mucosal villi, with the greatest intensity toward the villar tips, which is consistent with increased expression as the cells mature (Fig 1.5, Table 1.2, Table 1.3). Occasionally, we detected PrP^C immunoreactivity in mucosal enterocytes of the cecal and colonic crypts; however, we observed the majority of PrP^C in histiocytic cells residing in the mucosal lamina propria. The greatest and most consistent PrP^C immunoreactivity was in myenteric plexi throughout the entire alimentary tract. For every tissue, we treated a matching slide with an isotype control antibody, which consistently failed to result in staining.

Table 1.2. Summary of PrP^C expression patterns. We evaluated the distribution of PrP^C in all the tissues investigated in this manuscript. The histologic descriptions of the staining patterns are summarized in this table. Gray boxes represent the presence of staining in the cell types or structures (rows) of a given tissue (column). In alimentary tissues, staining of mucosal epithelium was common, as was staining of histiocytes and myenteric plexi. In lymphoid tissues, staining was common in germinal centers.

Alimentary tissues Staining present in:	Rumen	Reticulum	Omasum	Abomasum	Duodenum	Jejunum	Ileum	Cecum	Colon	Rectum	Mandibular SG	Parotid SG
Mucosal epithelial cells	■	■	■	■	■	■	■	■	■			
stratum spinosum and granulosum	■	■	■									
gastric pits				■								
apical villi					■	■	■					
crypt enterocytes								■	■			
Mucosal histiocytic cells	■	■	■	■	■	■	■	■	■	■		
Myenteric plexi	■	■	■	■	■	■	■	■	■	■		
Ductular epithelial cells											■	■

Lymphoid tissues Staining present in:	Tonsil	Retropharyngeal LN	Mandibular LN	Parotid LN	Mesenteric LN	Ileocecocolic LN	Prescapular LN	Spleen
Germinal centers	■	■	■	■	■	■	■	■
Mantle zone	■		■			■		■
Individual histiocytic cells	■	■	■				■	

Table 1.3. Description of PrP^C expression patterns. We described the PrP^C distribution in the alimentary and alimentary-associated lymphoid tissues of interest. This table contains the histologic descriptions of the staining patterns for each tissue. Patterns were conserved among deer and every tissue type was compared to a specimen stained with an isotype-control antibody, which were consistently unstained.

Tissue	**PrP^C pattern**
Alimentary tissues	
Rumen	Marked granular cytoplasmic staining diffusely in stratum granulosum and spinosum of mucosal stratified squamous epithelium; lesser staining in basal epithelium. No staining of superficial keratin.
Reticulum	Similar to rumen. Marked granular cytoplasmic staining diffusely in stratum granulosum, similar pattern but lesser staining in stratum spinosum, of mucosal stratified squamous epithelium. No staining of superficial keratin.
Omasum	Individual epithelial cells in stratum granulosum display diffuse cytoplasmic staining and occasionally perinuclear granular staining. Diffuse faint staining of mural smooth muscle.
Abomasum	Individual cells in the gastric pits consistent with peptic chief cells display cytoplasmic staining. Minimal staining is observed in the superficial mucosa. Diffuse faint staining of mural smooth muscle.
Duodenum	Cytoplasmic staining in mucosal epithelial cells diffusely affecting the apical 2/3 of villi. No immunoreactivity observed in villar crypts or Bruner's glands.
Jejunum	Cytoplasmic staining in apical mucosal epithelial cells. Cytoplasmic staining in a mild to moderate number of individual histiocytic-like cells in mucosal lamina propria. No staining in crypts. In Peyer's patches, diffuse staining in germinal center of lymphoid follicle and intense cytoplasmic staining in individual histiocytic-like cells. Cytoplasmic staining in follicular-associated epithelium overlying Peyer's patches. Diffuse immunoreactivity in smooth muscle of tunica muscularis and myenteric plexi.
Ileum	Cytoplasmic staining in apical mucosal epithelial cells with greatest intensity in villar tips. In Peyer's patches, diffuse staining in germinal centers of lymphoid follicles. Cytoplasmic staining in individual histiocytic-like cells and occasionally membranous staining in lymphocytes. Intense diffuse staining of myenteric plexi.
Cecum	Diffuse mild cytoplasmic staining of epithelial cells in the base of mucosal crypts. Cytoplasmic staining of individual histiocytic-like cells in the mucosal lamina propria.
Colon	Minimal staining in the colonic mucosa. A mild number of individual histiocytic cells in the mucosal lamina propria displayed cytoplasmic staining. Intense staining in myenteric plexi. Faint diffuse staining in the tunica muscularis.
Rectum	No staining in mucosa. Faint diffuse staining in the tunica muscularis. Intense staining in myenteric plexi.
Lymphoid tissues	
Tonsil	Cytoplasmic staining of surface mucosal epithelial cells. Diffuse staining in germinal centers of lymphoid follicles that extends to the mantle zone when present. Occasional cytoplasmic staining of histiocytic-like cells in medulla.
Retropharyngeal LN	Diffuse staining in germinal centers which occasionally extends to the interfollicular lymphoid tissues. Individual blast and histiocytic cells germinal centers display nuclear membrane staining. Individual cells in the subcapsular sinus display cytoplasmic staining.
Mandibular LN	Diffuse staining in germinal centers of lymphoid follicles that occasionally extends into the mantle zone with greater intensity observed in outer cortical

	follicles compared with deeper cortical follicles. Individual blast or dendritic cells in germinal centers display nuclear membrane staining. A mild number of individual histiocytic-like cells in the medulla display cytoplasmic staining.
Parotid LN	Diffuse staining in germinal centers of lymphoid follicles.
Mesenteric LN	Diffuse staining in germinal centers of lymphoid follicles. Occasional parafollicular cortical staining. Mild number individual cells display cytoplasmic staining. Diffuse mild staining of connective tissue in capsule and trabecular stroma. Intense staining of peripheral nerves in adjacent mesentery.
Ileocecocolic LN	Diffuse staining in germinal centers of lymphoid follicles that extends to the mantle zone when present. Greatest follicular staining intensity in outer cortical follicles compared with deeper follicles. Individual blast or dendritic cells in germinal centers display cytoplasmic staining. Connective tissues of lymphoid capsule, trabeculae, and vessel walls have diffuse staining.
Prescapular LN	Diffuse staining in germinal centers of lymphoid follicles. Greatest staining intensity in outer cortical follicles compared with deeper follicles. A mild number of blast cells or histiocytic cells in germinal centers display cytoplasmic staining.
RAMALT*	Diffuse cytoplasmic staining of the stratum spinosum and stratum granulosum of anal mucosa. Diffuse intense staining of the rectal myenteric plexi. Diffuse faint staining of the tunica muscularis. *recto-anal associated lymphoid tissue
Spleen	Diffuse staining in germinal centers that occasionally extends to mantle zone when present. Intense staining of peripheral nerves in trabeculae.
Nervous system	
Obex	Diffuse neuropil staining with greater intensity of grey matter compared with white matter. In grey matter, mild punctate and linear staining of neuronal cell processes.
Secretory tissues	
Mandibular salivary gland	Faint cytoplasmic staining in ductular epithelial cells. No immunoreactivity in acinar cells.
Parotid salivary gland	Faint cytoplasmic staining in ductular epithelial cells. No immunoreactivity in acinar cells.

PrP^C is expressed in germinal centers of lymphoid tissue

We observed diffuse immunoreactivity in germinal centers of lymphoid follicles that extended to the mantle zone when present (Fig 1.5, Table 1.2, Table 1.3). The more superficial cortical follicles typically had more intense staining when compared to secondary follicles deeper in the cortex. Individual cells in the germinal centers, with a blast or dendritic cell appearance, displayed cytoplasmic or nuclear membrane immunoreactivity. In lymph nodes, we observed occasional staining in connective tissues of the capsule, trabeculae, and vascular walls (Table 1.2, Table 1.3).

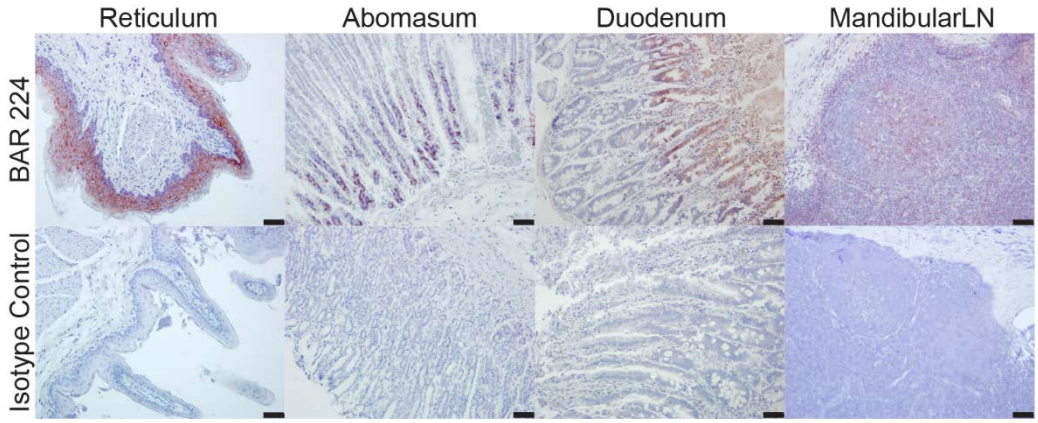

Figure 1.5. Representative IHC results. These tissues represent the most common PrP^C staining patterns. Tissues were stained with the anti-PrP antibody (BAR 224, top row) or with an isotype control antibody (mouse IgG_{2A}, bottom row). Scale bar represents 50μm. Descriptions of the staining patterns are in Table 1.2 and Table 1.3.

Prion seeding activity is widespread in alimentary tissues and alimentary-associated lymphoid tissue.

Our observation that PrP^C expression was widespread, albeit low, prompted us to investigate the distribution of PrP^{Sc} seeding activity in these same tissues in CWD(+) deer. We examined all 21 tissues (plus the obex region of the brain stem) by RT-QuIC with NaPTA precipitation to eliminate spontaneous conversion. In deer sacrificed after clinical signs developed, every tissue we tested was positive (lag phase was statistically different from the paired negative control) in all five deer (Table 1.4). The time required for detectable amyloid to form (the lag phase) for all tissues was very similar, and very fast (Fig. 1.6 – 1.7).

Other work in our laboratory demonstrated that by four months after oral inoculation with CWD, deer have substantial prion seeding activity in many lymphoid tissues, but not in brain (224). We were curious to test the alimentary tract tissues from these subclinical deer to learn which tissues are involved before prion amplification is detectable in the brain. Indeed, some of the alimentary tissues were positive (statistically different from the negative control deer) in some deer four months post inoculation (Table 1.4, Fig. 1.8). Involvement of the ileum was not surprising, given the extent of lymphoid tissue and Peyer's patches in the ileum, but the omasum, abomasum, colon and salivary glands have little

appreciable lymphoid tissue and demonstrated significant prion seeding activity. In these deer, there was more variability in RT-QuIC lag phase between tissues (Fig. 1.6-1.7).

Table 1.4. Distribution of prion seeding activity in CWD-infected white-tailed deer. We performed RT-QuIC with NaPTA pre-treatment on homogenates of the same tissues in CWD-inoculated white-tailed deer. We included five deer that were euthanized in symptomatic stages of disease and three deer that were euthanized four months after oral inoculation with CWD-positive brain tissue (4mpi, no signs of CWD). We compared inoculated deer to negative control deer; for a tissue to be designated as positive, its lag phase must have been significantly different from the negative control tissue tested in the same experiment (Wilcoxon-Mann-Whitney or Wilcoxon Signed Rank tests, $p<0.05$). The number of positive deer/ number of total deer is in this table. The darker shades indicate tissues where a greater proportion of deer were positive. Clear wells had no positive results. We classified tissues into lymphoid or alimentary categories. Finally, we tested the obex region of the brainstem to assess whether the deer had reached the neuroinvasion stage.

Prion seeding activity in mucosal tissues		
Tissue	Terminal Deer	4mpi Deer
Mandibular SG	5/5	0/3
Parotid SG	5/5	2/3
Rumen	5/5	0/3
Reticulum	5/5	0/3
Omasum	5/5	1/3
Abomasum	5/5	1/3
Duodenum	5/5	0/3
Jejunum	5/5	0/3
Ileum	5/5	3/3
Colon	5/5	1/3
Cecum	5/5	0/3
Rectum	5/5	0/3
Prion seeding activity in lymphoid tissues		
Tissue	Terminal Deer	4mpi Deer
Mandibular LN	5/5	3/3
Parotid LN	5/5	3/3
Tonsil	5/5	3/3
Retropharyngeal LN	5/5	3/3
Prescapular LN	5/5	3/3
Ileocecolic LN	5/5	3/3
Mesenteric LN	5/5	2/3
Spleen	5/5	3/3
Prion seeding activity in the CNS		
Obex	5/5	**0/3**

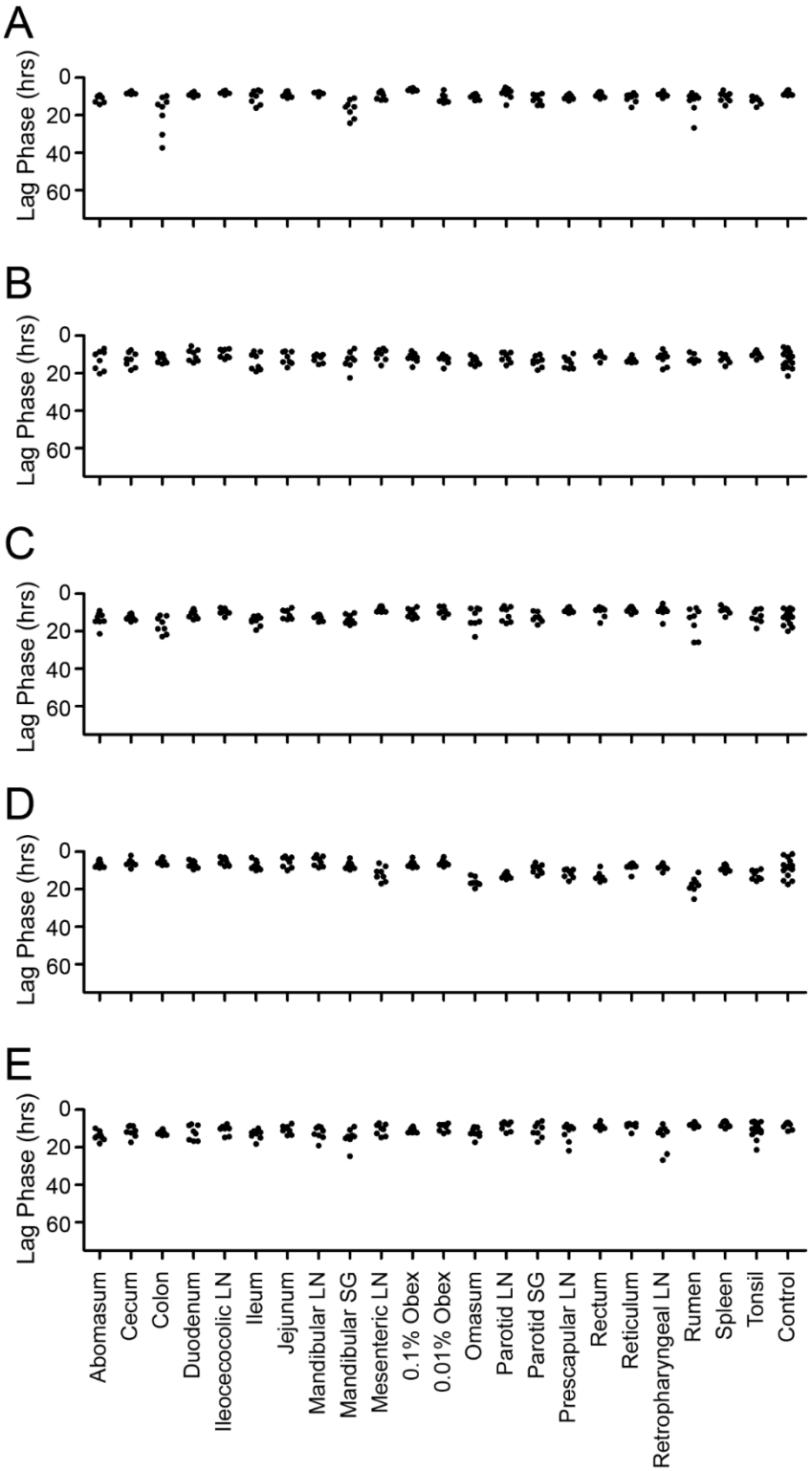

Figure 1.6. Terminal deer have seeding activity in all tissues. We performed 8 replicates of NaPTA RT-QuIC on each tissue from five deer in the clinical stages of CWD. The lag phase (in hours) is indicated on the y-axis and each point indicates one replicate. A. Deer 1031. B. Deer 1078. C. Deer 1079. D. Deer 1081. E. Deer 1082.

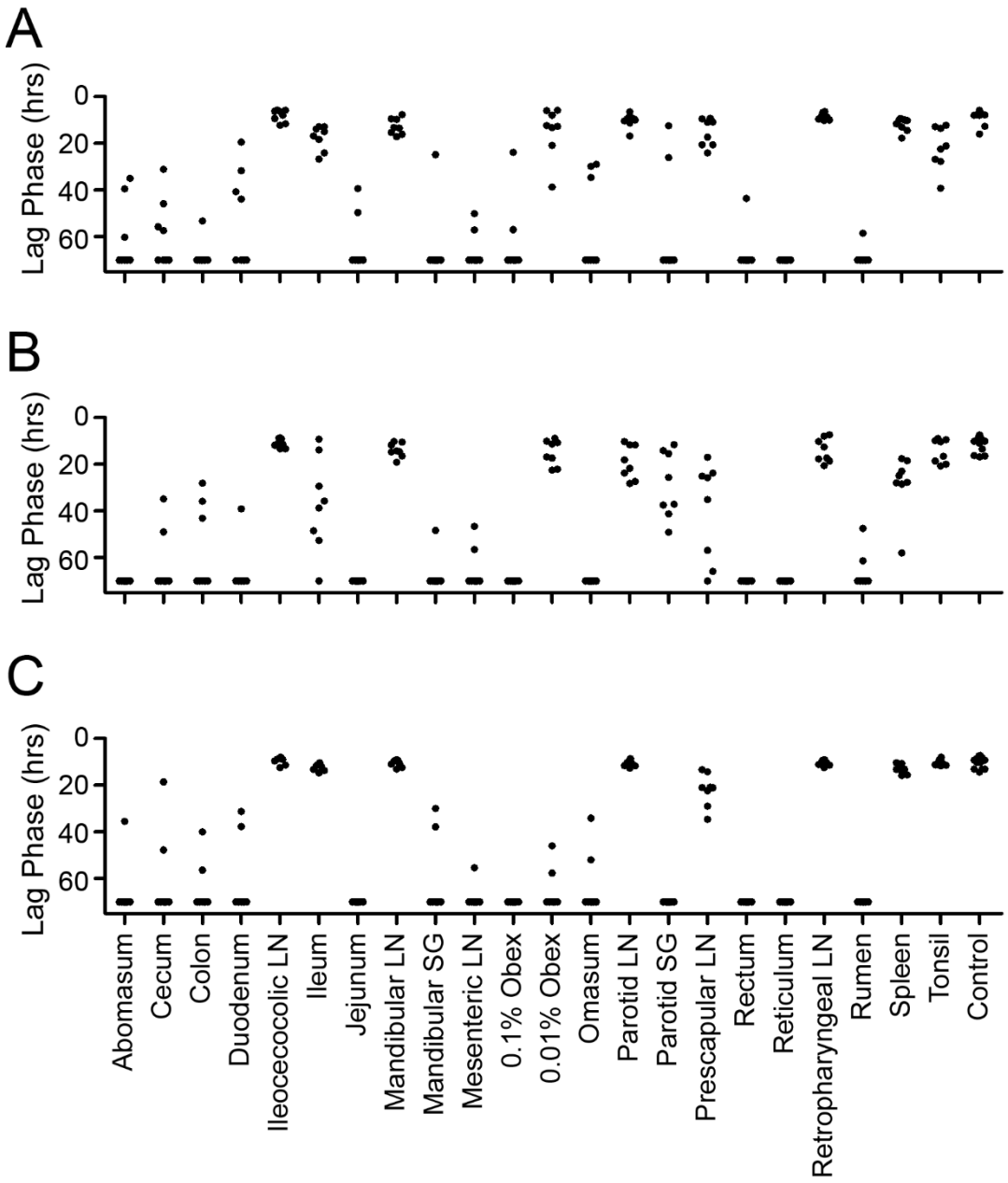

Figure 1.7. Deer sacrificed 4mpi have seeding activity in some tissues. We performed 8 replicates of NaPTA RT-QuIC on each tissue from three deer four months after oral inoculation with CWD. The lag phase (in hours) is indicated on the y-axis and each point indicates one replicate. A. Deer 1171. B. Deer 1201. C. Deer 1215.

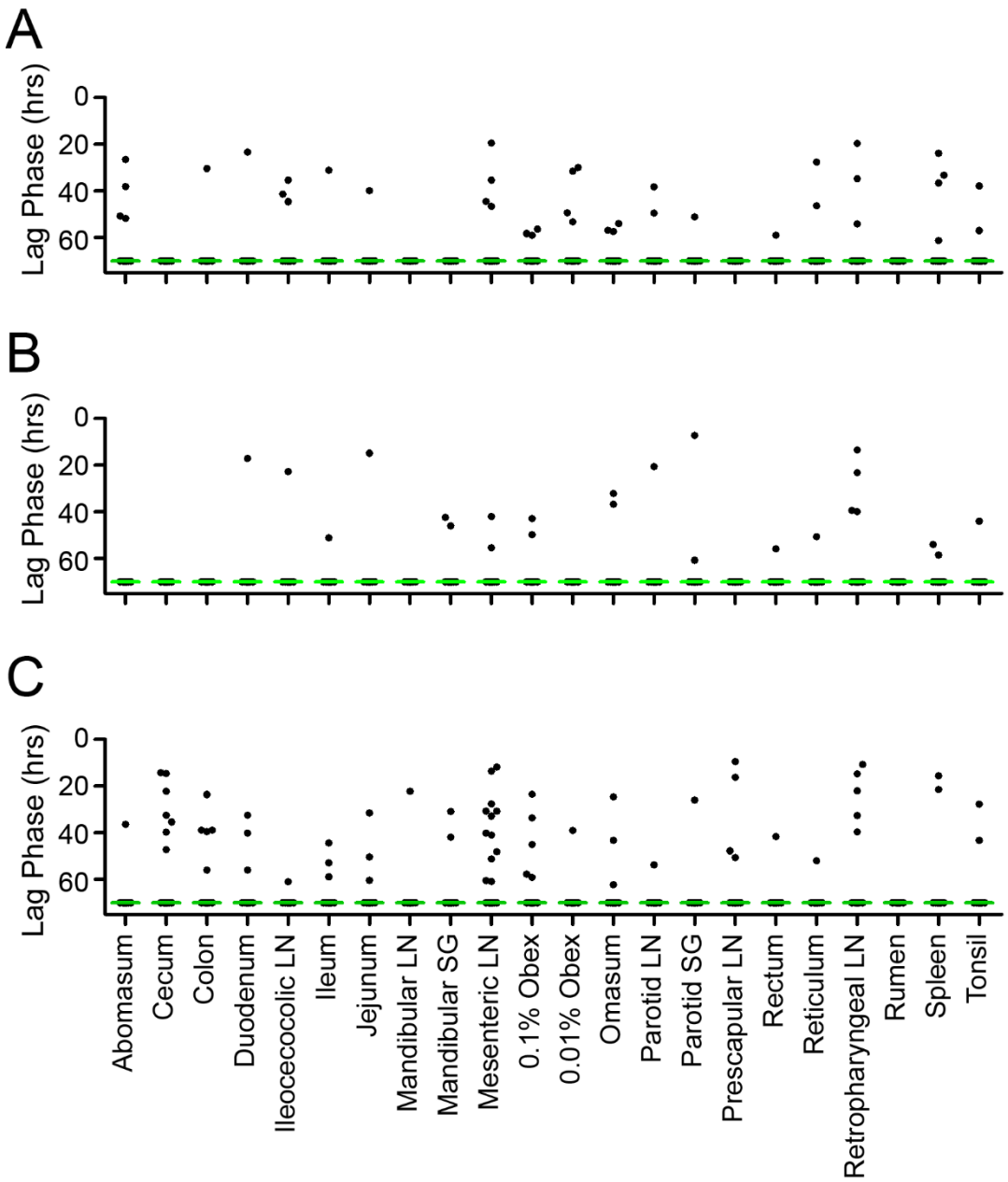

Figure 1.8. Negative deer have little seeding activity. We performed at least 20 replicates of NaPTA RT-QuIC on each tissue from 3 CWD(-) deer. The lag phase (in hours) is indicated on the y-axis and each point indicates one replicate. The green lines indicate the median seeding activity. Replicates that never crossed the threshold were assigned a value of 70 hours. A. Deer 952, 44 replicates/tissue. B. Deer 955, 36 replicates/tissue. C. Deer 1140, 24 replicates/tissue, except mesenteric lymph node, which includes 48 replicates.

Discussion

The prion hypothesis postulates that the normal prion protein, PrP^{C}, must be present in an individual for the disease to manifest, since it is the essential component of pathogenic prions (59, 60). Though the presence of PrP^{Sc} has been demonstrated in many tissues in CWD-infected cervids, there has been no comprehensive description of PrP^{C} expression in the natural host (156, 157, 216-222). Several questions about the pathogenesis of CWD and the mechanism by which prions spread through the host remain unanswered: (1) is PrP^{C} substrate available for conversion to PrP^{Sc} in the tissues of deer where prions are detected? And (2) do prions accumulate earliest in the tissues with the highest PrP^{C} expression? We began these studies with the hypothesis that prions accumulate early in disease in tissues where PrP^{C} expression is highest. We found that PrP^{C} expression was widespread and was not highest in the tissues where prions first accumulate. Specifically, PrP^{C} expression was higher in the lower GI tissues than in the alimentary-associated lymphoid system and higher in salivary glands than in the oropharyngeal lymphoid tissue. However, we detected seeding activity more consistently in oropharyngeal lymphoid tissues than in the salivary glands or lower GI tissues of subclinical deer. The difference in consistency among deer suggests that seeding activity accumulates in the lymphoid tissues before lower GI tissues or salivary glands (Table 1.4).

We were interested in the tissues of the alimentary tract because, in nature, cervids are most likely exposed to CWD prions via the oral route. We found that PrP^{C} expression was widespread in the alimentary tract, albeit at variable levels (Fig 1.3A, C). We describe PrP^{C} expression in the myenteric plexi of the GI tract (where PrP^{Sc} has been demonstrated (157, 219, 220)) (Table 1.2). PrP^{C} was also present in the intestinal mucosal stratum spinosum and granulosm layers and in follicle-associated epithelium of Peyer's patches (Table 1.2). The follicle-associated epithelium contains M cells, whose role in prion uptake has been demonstrated in mice with scrapie (289-291). While the function of PrP^{C} in alimentary epithelia is unclear, Morel, et al. demonstrated a role for PrP^{C} in the maintenance of cell-cell junctions and cellular division (292, 293).

We hypothesized that lymph nodes would have high PrP^C expression compared to non-lymphoid, alimentary tissues, since they play a role in early CWD pathogenesis and are prion-positive by many methods in symptomatic disease (156, 204, 216, 219, 220, 224, 272). However, expression of PrP^C in lymph nodes was fairly low overall (Fig 1.4), but was more consistent among deer than were PrP^C expression levels in the other tissues (error bars in Fig 1.3). The importance of lymph nodes early (and throughout) CWD progression may not be because they have the highest pool of available PrP^C substrate, but rather because of their specific immunosurveillance role in the alimentary tract, transporting and presenting antigens. This hypothesis is supported by PrP^C staining in lymphoid follicle germinal centers, consistent with B cells and follicular dendritic cells, and mantle zones, consistent with resting B cells (156). B cells have been implicated in the uptake and trafficking of prions and in the transfer of prions to follicular dendritic cells (294). B cells from CWD(+) deer are infectious to naïve deer, supporting the hypothesis that lymphoid cells play a specific role in CWD pathogenesis that does not rely on high PrP^C expression (214). In sheep, PrP^C is expressed in the spleen (280), and the spleen is a site of prion accumulation (295-297) and a source of infectious prions (228). The spleen has been identified as an early, but not required, site of prion replication in mouse-adapted scrapie (227, 273, 298, 299), but similar to Syrian hamsters, PrP^C expression in the deer spleen is relatively low compared to other tissues (285) (Fig 1.3, Fig. 1.4).

A potential caveat of the present study is the duration of storage for the CWD(-) deer tissues. All tissue samples were either frozen at -80°C or paraformaldehyde-fixed, thereby preventing assays that require preserved mRNA (RT-PCR) or fresh, unfixed tissues (flow cytometry). It is also plausible that tissue sections from different deer vary in their relative connective tissue, fat, stroma, etc. content. Our IHC data indicate that PrP^C expression is specific to particular cell types, so a difference in the proportion of that cell type in the tissue homogenate could cause the expression level to vary by western blot or ELISA. We do not suspect falsely elevated expression levels in deer tissue due to components other than PrP^C because the knockout mouse tissues used as negative controls in western blot and ELISA produced

no signal above background (Fig. 1.2). We would also expect the tissue milieu to be similar among individual deer.

Several authors have proposed a centrifugal spread of prions, in which amplification occurs in the brain, and prions spread through the body along peripheral nerves (61, 226, 274, 300). Prions have been hypothesized to reach the brain via peripheral nerves, including those in the GI tract (226, 273, 301), and it is clear that prion inoculum can cross the mucosal barrier of the alimentary tract very soon after exposure (302). We tested alimentary and alimentary-associated lymphoid tissues of deer in the symptomatic stages of CWD and at 4mpi for the presence of prion seeding activity by RT-QuIC. In symptomatic animals, all examined tissues were positive, including the obex region of the brainstem, and all tissues had similarly short RT-QuIC lag phases (Table 1.4, Fig. 1.6). We hypothesize that the very fast, consistent lag phases are a result of the NaPTA pre-treatment, which concentrates prions. The lag phases for terminal deer tissues are among the fastest we've observed in RT-QuIC, suggesting that these samples are at the upper limit of the linear range.

At 4mpi, prions were widespread in alimentary-associated lymphoid tissues, and were detectable in a few alimentary tissues (Table 1.4). At 4mpi, the obex was still negative, which suggests that the positive alimentary tissues were not positive due to the centrifugal spread of prions from the CNS to the myenteric plexi of the peripheral nervous system. We propose that prions replicate in GI tissues, and are not all derived from the CNS. The fact that individual 4mpi deer had different combinations of positive alimentary tissues, and that the lag phases were not so consistently high, suggests that this early timepoint falls in the midst of progression from lymphoid involvement to involvement of other tissues (Fig. 1.6) (224, 303).

Our data demonstrate that PrP^C expression is widespread in white-tailed deer and confirms that symptomatic, CWD-positive, white-tailed deer have widespread prion seeding activity. Several questions arise from this work: 1) What is the role of local, cellular PrP^C in the generation of prions that are excreted by infected cervids? CWD prions have been detected in a number of excreta from cervids (124, 218, 231, 288, 304-306) and in the organs that generate those excreta (218), but we are left to wonder

whether the misfolding event that produced those prions occurred in the excretory organ, or whether the prions were transported there. 2) Can many organs be used for CWD diagnosis in deer? Our data suggest that RT-QuIC may permit the testing of a broad array of tissues and that many tissues have detectable prion seeding activity later in disease progression. 3) What mechanism explains the presence of prion seeding activity in alimentary tissues before neuroinvasion? Our data suggest that prions replicate in tissues of the alimentary tract before they reach the brain. This work contributes to the growing body of evidence that CWD prions are widespread within cervids and that PrP^{C} expression alone does not dictate the kinetics of prion spread in the body.

CHAPTER 2: CWD PRIONS IN THE LYMPHOID SYSTEM DIFFER BIOCHEMICALLY FROM THOSE IN THE BRAIN

Summary

The lymphoid system plays a critical role in the early propagation of PrP^{Sc} in cervids, but the infectivity of lymph nodes from CWD(+) deer has not been examined. This topic is pertinent because peripheral lymph nodes could be the source of the infectious prions secreted and excreted by CWD(+) deer. Prions shed by infected deer likely fuel the facile horizontal transmission that results in the spread of CWD within and between cervid populations.

Methods for identification of PrP^{Sc} usually do not assess its infectivity directly. However, the development of cell-based assays makes *in vitro* assessment of infectivity possible. To explore whether differences exist between brain and lymph node prions from CWD(+) cervids, we coupled the cervid prion cell assay (CPCA) with real-time, quaking-induced conversion (RT-QuIC), enzyme-linked immunosorbent assay (ELISA), and western blotting. While each assay produced different patterns of results, the consensus clearly confirmed that substantial infectious PrP^{Sc} is present in lymph nodes of CWD(+) cervids, often at levels approaching those found in the brain of the same animal. We propose that infectious prions are formed *in situ* in tissues outside the brain, and are the source of the PrP^{Sc} responsible for the horizontal transmission of CWD.

Background

Prion diseases are fatal neurodegenerative diseases caused by the misfolding of a normal protein, PrP^{C}, and propagation of the pathogenic isoform, PrP^{Sc}. Neurodegeneration results when the accumulation of PrP^{Sc} causes neuronal death. Prion diseases include scrapie in sheep and goats, CWD in cervids, bovine spongiform encephalopathy (BSE) in cattle and Creutzfeldt Jakob disease (CJD) in humans. Infectivity has been tested with brain tissue in most experimental inoculations (119). It is clear that prions accumulate to infectious levels in the central nervous system of scrapie, CWD, BSE and CJD (307).

However, PrP^{Sc} also accumulates outside the CNS. In sheep with scrapie, PrP^{Sc} has been identified in spleen, lymph nodes, adrenal glands, the enteric nervous system and placenta (228, 295-297, 308-310). In laboratory animals with scrapie, PrP^{Sc} has also been identified in muscle, skin, tongue, fat, plasma and intestines (300, 311, 312). In cervids with CWD, PrP^{Sc} has been identified in lymph nodes, spleen, salivary gland, bladder, intestines, heart, adrenal gland, pituitary gland, stomachs, ganglia, pancreas, fat, reproductive tissue and muscle (138, 156, 157, 216-223, 272). Most of the CWD studies identified PrP^{Sc} by western blot or immunohistochemistry and a few used amplification assays, but none have tested the infectivity of non-CNS tissues.

Research confirming the infectious nature of prion diseases was completed largely in the scrapie model, wherein several studies have tested the infectivity of non-CNS tissues. In 1959, Stamp et al. inoculated sheep with lymph nodes or spleen from scrapie(+) sheep and observed disease in 2/10 or 3/10 sheep after 12 months of incubation, respectively (225). In the late 1980s, Kimberlin and Walker inoculated lymph nodes from scrapie(+) sheep into mice and observed clinical disease in the inoculated mice (226, 227). In 1998, the infectivity of scrapie(+) lymph nodes was confirmed by mouse bioassay and, in 2006, by bank vole bioassay (228, 313, 314). To our knowledge, the infectivity of lymph nodes from CWD(+) deer has not been determined.

Infectivity of tissue from prion-infected individuals is classically tested by bioassay in a susceptible animal, either the natural host, wild-type mice, or transgenic mice expressing PrP^{C} homologous to the donor species' PrP^{C} (156, 315, 316). However, bioassays require long incubation periods, are costly, and have limited statistical power due to the low feasibility of large experimental groups. A number of assays have been developed for disease diagnosis, analysis of the biochemical features of prions, and investigation of the infectivity of many sample types (61). Direct detection assays include western blot for the detection of protease-resistant PrP^{Sc}, immunohistochemistry and ELISA (30, 200, 201, 203-207). Amplification assays include protein misfolding cyclic amplification (PMCA) and RT-QuIC. Both are anchored in the prion hypothesis, which states that PrP^{Sc} will coerce the misfolding of PrP^{C}, which propagates and results in the production of amyloid fibrils. PMCA uses brain homogenate as

the source for PrP^{C}, sonication to increase free ends available for conversion, and the detection of PK-resistant PrP^{Sc} by western blot, while RT-QuIC uses recombinant PrP^{C} ($rPrP^{C}$) as the substrate for conversion, shaking to provide free ends, and thioflavin T (ThT) binding of amyloid fibrils to enable detection (70, 208-212, 317).

Cell-based assays for prion detection are based on years of effort to establish prion-susceptible cells (160-162, 166, 175, 176, 318-321). Several groups have used neurosphere cultures as an *in vitro* alternative to bioassay (168, 169, 171). The scrapie cell assay (SCA) was developed for the detection of mouse-adapted scrapie and enabled immunodetection of prion replication in cell lysates (197). The SCA was expanded to permit infection with other prions (165, 198). For the cervid prion cell assay (CPCA), rabbit kidney epithelial cells were engineered to produce deer or elk PrP^{C}, which propagated prions. Prions were detected by cell blotting with PK-treatment and immunodetection on ELISPOT plates (165). The infected cells were positive in transgenic mouse bioassay, which suggests that they amplify infectious prions (165).

As described in the previous chapter and elsewhere, we have tested a number of tissues from CWD(+) deer in RT-QuIC (204, 218, 224, 322, 323). We have attempted to correlate the seeding efficiency in RT-QuIC to the lethal dose in bioassay, but we only have access to bioassay data for CWD(+) brain samples (229, 231, 305). Ideally, we would be able to correlate RT-QuIC seeding activity for each tissue type to an assay of infectivity, like CPCA. We are particularly interested in the lymph nodes of CWD(+) deer, since they are involved early in the disease course (156, 224). We hypothesized that lymph nodes and brains of cervids in the terminal stages of CWD would have infectious PrP^{Sc}, but that there would be more in the brain. We designed the following study to test the *in vitro* behavior of 5 paired brain and retropharyngeal lymph node (RPLN) samples and to test their infectivity in CPCA. We expected to corroborate the outcome of a transgenic mouse bioassay (324).

Methods

Sample preparation

We received 20% homogenates of terminally-ill, CWD(+) red deer, elk and white-tailed deer brain and RPLN samples from our collaborator, Dr. Aru Balanchandran. We made 10% weight/volume homogenates of brain and 20% weight/volume homogenates of RPLN from white-tailed deer 814 (negative), 816 (terminal disease), 817 (terminal disease), 1201 (four months post inoculation) and 1215 (four months post inoculation). 1X PBS and protease inhibitors (Halt Protease Inhibitor Cocktail, Roche) comprised the diluent and we homogenized the tissue for 3x 30-second cycles in an Omni Bead Ruptor (Omni International). Homogenates were stored at -80°C.

Western blot – Figure 2.3A-B

To determine the concentration of total protein, we performed bicinchoninic acid (BCA) assays on our homogenates according to the manufacturer's protocol (Pierce BCA Protein Assay, ThermoScientific). For brain samples treated with proteinase K (PK), we added 240ug total protein to 2% N-lauroylsarcosine sodium (sarkosyl) and added PK for a final concentration of 80μg/mL (Proteinase K, Roche). We treated lymph node samples the same, except that we added 1500μg total protein. We incubated the samples in a 45° waterbath for one hour, then added 6.25mM phenylmethylsulfonyl fluoride (PMSF), 6X Laemmli sample buffer (LSB) and boiled for 5 minutes.

For the non-PK treated samples, we added 80μg total protein for brain samples and 500μg total protein for lymph nodes to 2% sarkosyl and 6X LSB and boiled for 5 minutes. We added 22μL to each lane of a 10-well NuPage 12% Bis-Tris precast gel. The samples migrated for 2 hours at 100V, then proteins transferred to polyvinylidene fluoride (PVDF) membranes overnight at 20V. We blocked the membranes with 5% nonfat dry milk in TBS, then incubated with 1:5000 BAR224 in TBST (Cayman Chemicals) for one hour at room temperature. We washed the membrane with TBST for three 5 minute washes and incubated with goat anti-mouse IgG_2 labeled with peroxidase (SeraCare). We washed and

developed for 5 minutes with ECL developing reagent (Pierce ECL 2 Substrate, ThermoScientific). We captured images with an ImageQuant LAS 4000 Imager.

Western blot – Figure 2.3C-D

Western blots and images in Figure 2.3C-D were provided by Dr. Jifeng Bian. We determined the total protein content of brain and RPLN homogenates by BCA assay. We digested 500µg total protein from each brain homogenate and 2000µg total protein from each RPLN homogenate with PK at 37°C. After PK digestion, we spun the samples at 100,000g to pellet the PrP^{Sc}, and resuspended the whole pellet and added it to the gel. For non-PK treated samples, we added 200µg total protein for RPLN samples and 50µg for brain samples to sample buffer and loaded the whole volume on the gel. We resolved the samples by sodium dodecyl sulfate polyacrylamide gel electrophoresis (SDS-PAGE) before transfer to PVDF membranes. We probed the western blots with anti-PrP antibody PRC5 and detected signal with infrared fluorescent-conjugated secondary antibodies (202). We scanned the membranes and captured images using an Odyssey CLx Infrared Imager (Li-Cor Biosciences, Inc.).

RT-QuIC

We purified recombinant, truncated Syrian hamster PrP as previously described (325). Briefly, we expressed the construct in *E. coli* BL21-Star cells with overnight induction under the following conditions: LB media, kanamycin and chloramphenicol, 20X NPS [0.5M $(NH_4)_2SO_4$, 1M KH_2PO_4, 1M Na_2HPO_4], 50X 5052 [0.5% glycerol, 0.05% glucose, 0.2% lactose], 1mM $MgSO_4$. We harvested inclusion bodies with lysozyme (0.25mg/mL), DNase (1µg/mL) and $MgCl_2$ (5mM) in 1X Bugbuster (Novagen). We solubilized inclusion body pellets in 8M guanidine hydrochloride (GdnHCl) overnight, then batch-bound the solubilized protein to Ni-agarose resin (GE Healthcare Life Sciences). We renatured the protein with a gradient from 6M GdnHCl in 100mM Na_2HPO_4 and 10mM Tris to an identical buffer with no GdnHCl on a GE FPLC (AktaPure, GE Healthcare Life Sciences). We eluted the protein with a

gradient to 0.5M imidazole and dialyzed in two changes of 20mM NaH_2PO_4 overnight. We stored recombinant PrP (rPrP) at 4°C.

For RT-QuIC on the tissue homogenates, we added 10μg rPrP to 10μM thioflavin T, 320mM NaCl, 1mM EDTA and 1X PBS in one well of a 96-well plate (Nunc black, optical-bottom, 96-well plates, ThermoScientific). We added 2μL diluted tissue in 0.1% SDS to each well and used a BMG Fluostar Omega microplate reader to shake the plates for one minute (double orbital shaking at 700RPM), followed by one minute of rest, for 62.5 hours at 42°C. The fluorescence was recorded every 15 minutes with a 450nm excitation wavelength and a 480nm emission wavelength and a gain of 1700.

For RT-QuIC of the cell pellets, we resuspended pellets in 100μL of a cell lysis buffer containing 1X PBS, 1% Triton-X 100, 150mM NaCl, 5mM EDTA (pH 7.2). We performed two freeze-thaw cycles, then spun the suspension in a microcentrifuge at 13,000RPM for 5 minutes. We carefully removed the supernatant and diluted it 1000-fold in 0.1% SDS/ 1X PBS. We added 2uL of the 10^{-3} dilution to a 96-well plate containing the reaction mixture described above, then mixed the plate and divided each well into 4 wells of a 384-well plate (Nunc black, optical-bottom, 384-well plates) and performed the RT-QuIC assay as described above.

To analyze the data, we calculated a threshold that was 5 standard deviations above the mean baseline fluorescence. The time required to cross that threshold is the lag phase. If a sample never crossed the threshold, it was assigned an arbitrary value of 70 hours. We compared lag phases using a non-parametric Wilcoxon-Mann-Whitney test.

7-5 ELISA

We used PRC5 and PRC7 (a conformational antibody) to quantify PrP^{Sc} in our homogenates (202). We incubated equivalent volumes of each sample with 10% Triton-X100 in 1X PBS, then added 0.5M GdnHCl for 15 minutes at 37°C to denature the PrP^{Sc}. We diluted the samples in 1% BSA and added to Nunc Maxisorb ELISA plates that were coated with 20μg/mL PRC7 in carbonate/bicarbonate buffer and blocked with 3% BSA in PBS. We incubated samples overnight at 4°C on the plate, then

washed and added PRC5 (0.27μg/mL), then anti-mouse $IgG2_a$-HRP (Alpha Diagnostic International, Inc.) and developed with peroxidase substrate (ABTS). We stopped the development and read the absorbance at 405nm with an ELx808 Microplate Reader (Bio-Tek Instruments, Inc.) We report the absorbance for triplicate wells.

CPCA

We diluted brain homogenate to 0.1% weight/volume in PBS and lymph nodes to 1.0% weight/volume, then extruded each homogenate through a 28ga needle five times. We coated the first row of a 96-well plate (for the first and third CPCA experiments (Fig. 2.4, Fig. 2.7, Fig. 2.8)) with 200μL or coated 10-cm plates (for the second CPCA experiment (Fig. 2.5, Fig. 2.6)) with 1mL of the homogenate. For the 96-well plates, we serially diluted the homogenate 3-fold into 1X PBS in the remaining rows. We covered the plates and allowed the prions to bind for one hour at room temperature. We removed the homogenates and washed the plates, then dried and stored the plates at 4°C. We added one of the following RK-13 cell types to each well: sensitive (Deer 5E9 or Elk 21 cells, which express deer or elk PrP^C and HIV Gag precursor protein) or resistant (RKV, not transfected). For the 96-well plates, we added $2x10^4$ cells to each well and for the 10cm plates, we added 10^6 cells to each plate. We incubated the cells on the coated plates for 12 hours – 6 weeks, depending on the experiment, and replaced the media every 5 days.

At the end of the incubation, we harvested the cells from the tissue culture plates and added 20,000 cells from a single well of the 96-well plate (or from the 10cm plate) to a single well of a 96-well ELISPOT plate (EMD Millipore) that was first activated with ethanol and washed. We dried the plates, then added cell lysis buffer (50mM TrisHCl, 150mM NaCl, 0.5% v/v octylphenoxypolyethanol (IGEPAL), 0.5% w/v deoxycholic acid) and 5μg/mL PK to each well and rocked at 37°C for 90 minutes. We terminated digestion with PMSF, then exposed the epitopes with 3M guanidine thiocyanate for 10 minutes. We washed the plates and blocked with 5% Pierce superblock (ThermoFisher), then added PRC5 (0.27μg/mL) overnight at 4°C. We washed the plates and added AP-anti-mouse-IgG_2 (Southern

Biotechnology Associates) for one hour at room temperature. We washed the plates again and removed the rubber bottoms, rinsed the plates with deionized water and dried overnight. Finally, we developed the plates with alkaline phosphatase conjugate (Roche), stopped the reaction, and dried again. We captured plate images and counted spots with the ImmunoSpot S6-V analyzer. We set the sensitivity and spot size based on our positive and negative controls and used the same settings for every plate. To confirm the accuracy of the automatic spot counting, we manually counted random wells and confirmed the automatic count. We centrifuged the remaining cells from each well and froze the cell pellets at -80°C.

To calculate the CPCA titer, we plotted the spots/well vs. the grams of tissue added to the well. We fit a four-parameter sigmoidal curve in GraphPad Prism. We calculated the midpoint of the spots/well by subtracting the bottom plateau from the top, then interpolated the X value in grams (equivalent to the LD_{50}) that would yield the median spot number. We divided the number of spots at the midpoint by the grams at the midpoint, then took the $\log_{10}$ for the CPCA titer.

Results

Lymph node and brain homogenates from CWD(+) cervids have similar seeding activity in RT-QuIC.

RT-QuIC detects minute amounts of amyloid seed by converting $rPrP^{C}$ to amyloid. Like RT-PCR, the time required to form detectable amyloid (lag phase) is related to the amount of initial seed present in the sample. Therefore, RT-QuIC can be used to estimate the seeding activity of a sample. We used RT-QuIC to test our hypothesis that the RPLN accumulates less PrP^{Sc} than the brain by the terminal stages of CWD.

We tested two white-tailed deer, 817 and 816, which were inoculated via the aerosol route and maintained in a laboratory setting until euthanasia due to clinical signs of CWD (215). In both deer, the brain had consistently higher seeding activity, but the RPLN was also positive (Fig. 2.1A-B). We analyzed three more paired brains and RPLNs from CWD(+) cervids that were euthanized in the terminal stages of disease. The white-tailed deer and elk (Fig. 2.1C-D) were naturally infected with CWD and the red deer (Fig. 2.1E) was experimentally infected via the oral route (219). In all three individuals, the

RPLN had seeding activity that was statistically indistinguishable from the brain (with the exception of one dilution of the red deer samples.) We interpret these data to indicate that the RPLNs of several species of cervids have the ability to accumulate PrP^{Sc}, in some cases to the degree that the brain accumulates PrP^{Sc}, by the terminal stages of CWD.

We were also interested in CWD progression, so we tested the seeding activity of two RPLN samples collected at four months post-inoculation (4mpi). At this stage, the brain is negative (Table 1.2) (224). The RPLNs had seeding activity similar to other samples we tested (Fig. 2.1F). Finally, we confirmed the seeding activity of our laboratory's positive control brain pool (Fig. 2.1G). Overall, RPLN samples had substantial seeding activity in RT-QuIC, albeit lower than brain tissue in some animals. However, it remains unclear whether the RT-QuIC assay is specific for particular strains of CWD or for particular characteristics of the seed (infectivity). Therefore, two equally positive samples in RT-QuIC may not be identical in other assays.

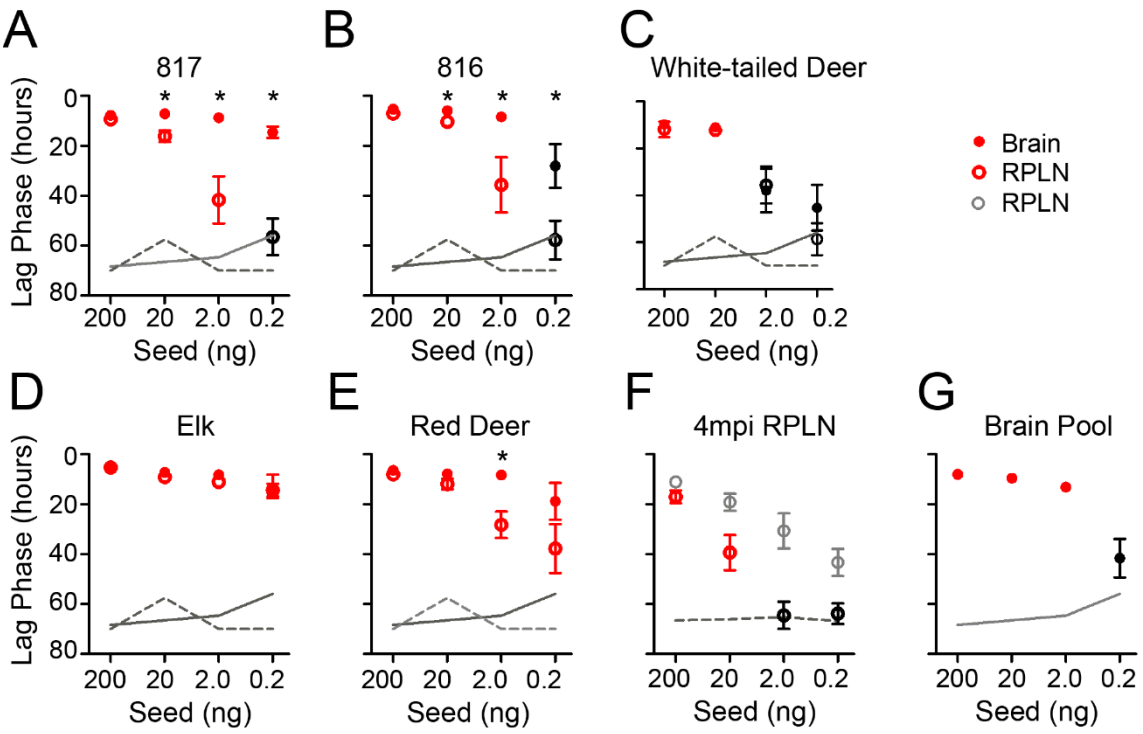

Figure 2.1. Similar amyloid seeding activity is present in lymph node and brain samples. We used brain or RPLN homogenate to seed the RT-QuIC assay. Points indicate the mean and error bars represent standard error of the mean. * indicates a statistically significant difference between the lag phases for brain and RPLN samples at the same dilution ($p<0.05$, Wilcoxon Mann Whitney test). The mean lag phase for the negative controls is indicated by the gray lines. The solid line represents negative brain samples and the dotted line represents negative RPLN samples. Negative controls from every experiment are combined for the means displayed in these graphs. Red points are statistically different from the negative control and black points are not ($p<0.05$, Wilcoxon Mann Whitney test)

Overall, lymph nodes have less PrP^{Sc} content than brain by 7-5 ELISA.

The capture antibody, PRC7, is selective for underglycosylated PrP^{C}. Underglycosylated PrP^{C} is overrepresented in PrP^{Sc}, so the 7-5 ELISA is specific for the disease form. After confirming similar RT-QuIC seeding activity in the brain and RPLN for many individuals (Fig. 2.1), we tested whether the tissues had PrP^{Sc} that was detectable by 7-5 ELISA. We added both a high volume of sample (indicated by the H) and a low volume (L, 2.5 fold less than H). The brain homogenates from 817, 816, elk and red deer had detectable PrP^{Sc}, but the WTD brain homogenate did not (Fig. 2.2). The PrP^{Sc} content was variable among deer, but each individual deer had very consistent replicates (Fig. 2.2, error bars).

However, only the elk had detectable PrP^{Sc} in the RPLN; the PrP^{Sc} content was higher in the RPLN than the brain at both dilutions (Fig. 2.2).

These data suggest that the 7-5 ELISA detects something different than RT-QuIC or is less sensitive, which are not mutually exclusive. It is clear that a 2.5 fold reduction in sample reduced the ELISA absorbance for the brain samples to near the limit of detection (Fig. 2.2, see 817, 816, RD, elk brain). For some samples, RT-QuIC data suggests that there may be a 10-fold difference between brain and RPLN seeding activity. For example, the seeding activity of 817 RPLN was roughly 10-fold less than 817 brain in RT-QuIC (0.2ng brain is detectable, but 0.2ng RPLN is not). Therefore, it's possible that a ten-fold difference in PrP^{Sc} content would result in no signal above background for the RPLN in 7-5 ELISA.

The red deer RPLN and brain samples were not statistically different in RT-QuIC, but it is possible that there was still a ten-fold difference in seeding activity (20ng brain has a very similar QuIC rate to 200ng RPLN). Therefore, it seems plausible that we did not add enough red deer RPLN to exceed the limit of detection in 7-5 ELISA. Regardless of whether we missed the limit of detection in 7-5 ELISA or whether the 7-5 ELISA and RT-QuIC detect different characteristics of prions, the 7-5 ELISA indicates lower PrP^{Sc} in RPLN than in brain, except in the elk sample (Fig. 2.2).

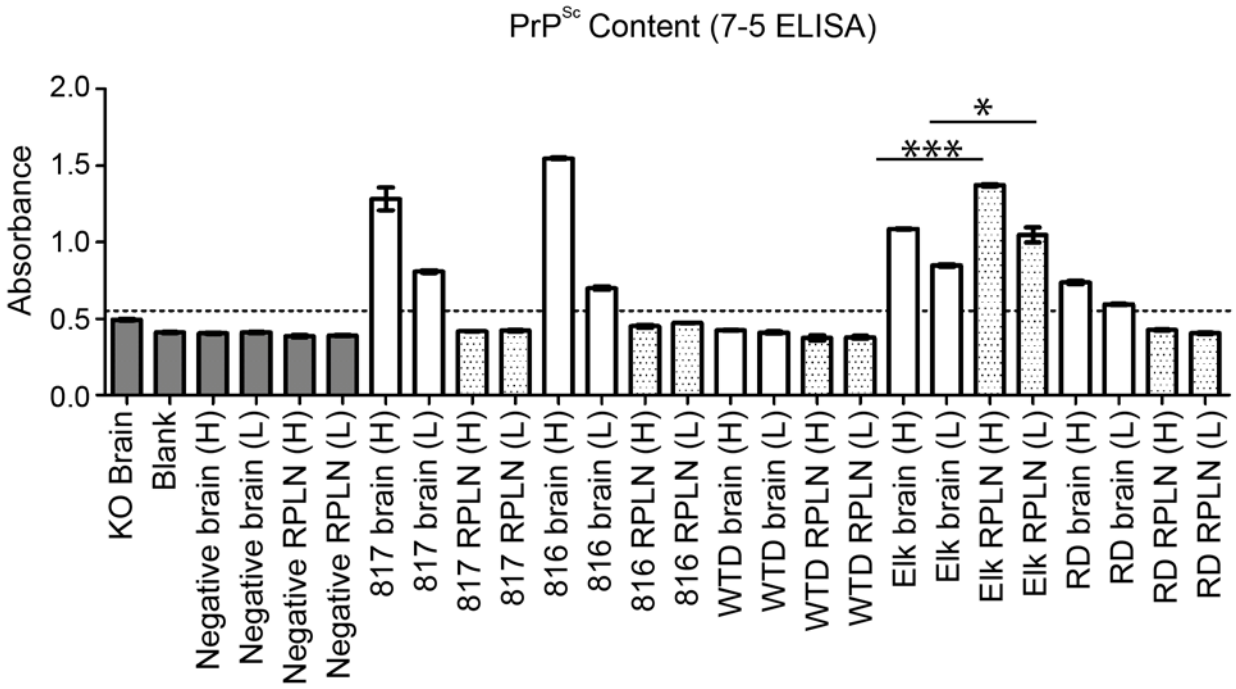

Figure 2.2. 7-5 ELISA detects different PrP^{Sc} levels in RPLN and brain samples. We added two volumes of brain or RPLN homogenate to the 7-5 ELISA (high (H) was 2.5 fold more homogenate than low (L)). We used brain from a *PRNP* knockout mouse, blank (no homogenate), two negative brains and two negative RPLNs as negative controls (gray bars). The dotted line is the cutoff for background and was calculated by adding three standard deviations to the mean absorbance for the negative control samples. Bars indicate mean absorbance and error bars indicate SEM for three replicates.

PrP^{Sc} is detectable by western blot in almost all brain and RPLN samples.

Western blot for proteinase-K (PK)-resistant PrP^{Sc} has been the gold standard for prion detection since the early days of prion research (200). After assessing the seeding activity (RT-QuIC) and the PrP^{Sc} content (7-5 ELISA), we compared the protease-resistant PrP^{Sc} by PK-treatment and western blot. We observed PK-resistant PrP^{Sc} in the brain and RPLN of the elk, red deer, 816 and 817 (Fig. 2.3). In the WTD sample, there was a faint signal for PK-resistant material in the brain and no signal in the RPLN (Fig. 2.3A, E). However, the non-PK treated sample had very low signal for the WTD RPLN, so it is possible that the sample was degraded and the PK-resistant material was below the limit of detection (Fig. 2.3B, E). A similar explanation is likely appropriate for the 817 RPLN sample, which had faint PK-resistant bands, and also has faint non-PK treated bands (Fig. 2.3D, F).

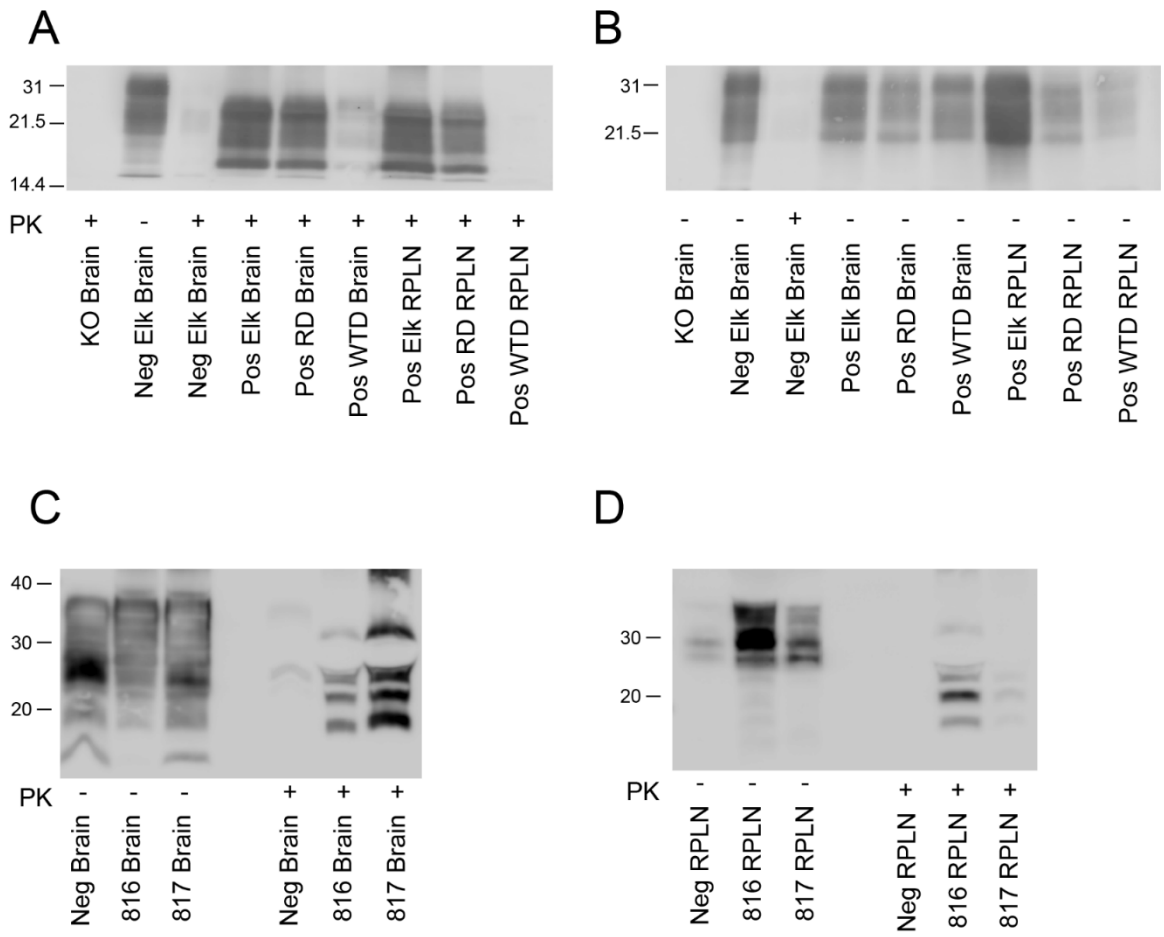

Figure 2.3. There is PK-resistant PrP^{Sc} in almost all samples. A. We treated 2000µg total protein for RPLN samples and 500µg total protein for brain samples with PK, then spun the samples at 100,000g and added the whole pellet. We probed with PRC5. B. We added 200µg total protein for RPLN samples and 50µg total protein for brain samples and probed with PRC5. The western blots in panels A and B are courtesy of Dr. Jifeng Bian. C. We PK-treated 30µg total protein or we added 40µg untreated sample to the gel, then probed with BAR224. D. We PK-treated 200µg total protein or we added 250µg untreated sample to the gel, then probed with BAR224. All protein markers are indicated with dashes on the left, in kDa.

Lymph node prions are less infectious than brain prions after four weeks in cell culture.

After we assessed the RPLNs and brains by RT-QuIC, ELISA and western blot, we tested their infectivity. Because CPCA had never been tested with lymph node samples, we performed a pilot study to ensure that lymph node prions would infect the cells. After 4 weeks of infection, we were surprised to observe that only the positive brain pool caused substantial infection (Fig. 2.4A). We calculated the titer for the brain pool (Fig. 2.4B), but were unable to calculate titers for lymph nodes due to the apparent lack

of infection. However, we noticed that the wells of the ELISPOT plate that contained lymph node-infected cells had a smattering of spots, while the negative controls were almost completely blank. We confirmed that there were time-dependent increases in spots in the lymph node-infected cells, but that the increase was considerably lower than the increase in for the CWD(+) brain pool (Fig 2.4C).

We had four hypotheses for the very limited infection of cells by lymph node samples. 1) The RPLN PrP^{Sc} detected in RT-QuIC and western blot is not a form that is particularly infectious to cells, 2) CPCA can replicate PrP^{Sc} from lymph nodes, but the products are PK-sensitive, 3) the lymph node PrP^{Sc} failed to adhere to the CPCA plates, effectively eliminating exposure of the cells to PrP^{Sc}, or 4) the PrP^{Sc} titer in the lymph node samples was too low to infect the cells. We designed an experiment to test these possibilities, wherein we collected samples of cells much earlier in the procedure (to assess whether PrP^{Sc} adhered to the plate), let the infection proceed for longer (five weeks vs. four weeks) and tested the cells at the end of the experiment by RT-QuIC (which does not involve a PK step).

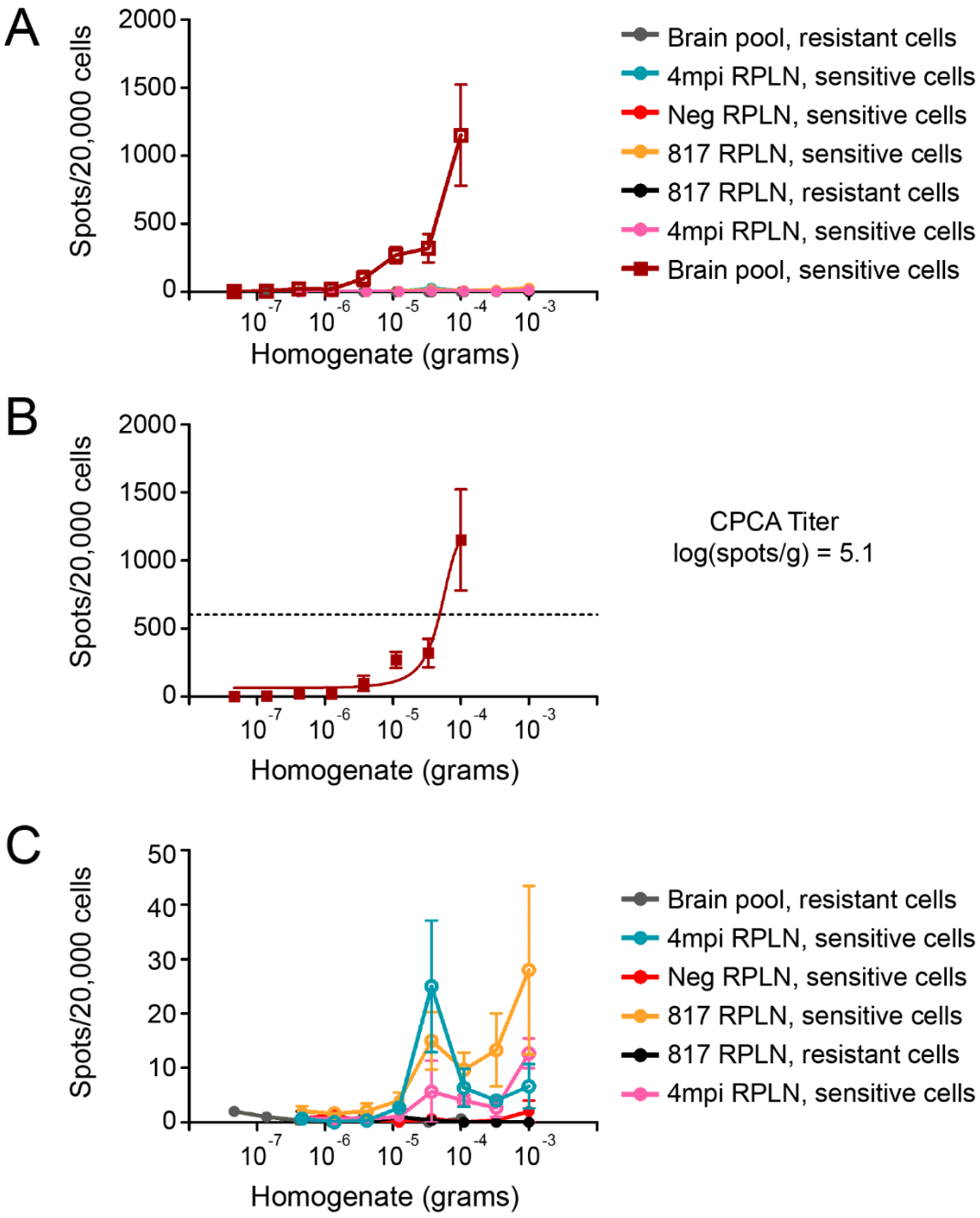

Figure 2.4. Brain pool is more infectious than lymph nodes. The number of spots/20,000 cells is indicated on the Y axis and the grams of homogenate added to the well is on the X axis. Open symbols indicate that the spot count in sensitive cells is statistically different from the same inoculum in resistant cells ($p<0.05$, unpaired t-test). A) The positive control brain pool produced significant PK-resistant material after 4 weeks. B) We fit a four-parameter sigmoidal curve to the brain pool data and determined the CPCA titer, which is the log-transformed spots/g at the midpoint of the curve's range. C) Adjusting the Y axis permitted our observation that the lymph node-infected cells have increased spot numbers compared to the negative controls (negative tissue or resistant cells).

Infection by RPLN prions is delayed and less severe compared to brain.

When we tested the kinetics of cell infection, we observed that the brain sample caused a more rapid increase in spots (and more total spots, indicating a more severe infection) than the RPLN sample (Fig. 2.5). The positive RPLN did infect sensitive cells, but the infection was delayed until three weeks and there was no substantial increase in spots until the fifth week post-inoculation, while resistant cells have very few or no spots at later time points. However, the RPLN sample did successfully infect the cells and result in PK-resistant spots in this experiment, which confirms that the cells can propagate lymph node prions, that lymph node prions adhered to the plate and that at least some of the propagated prions are PK-resistant.

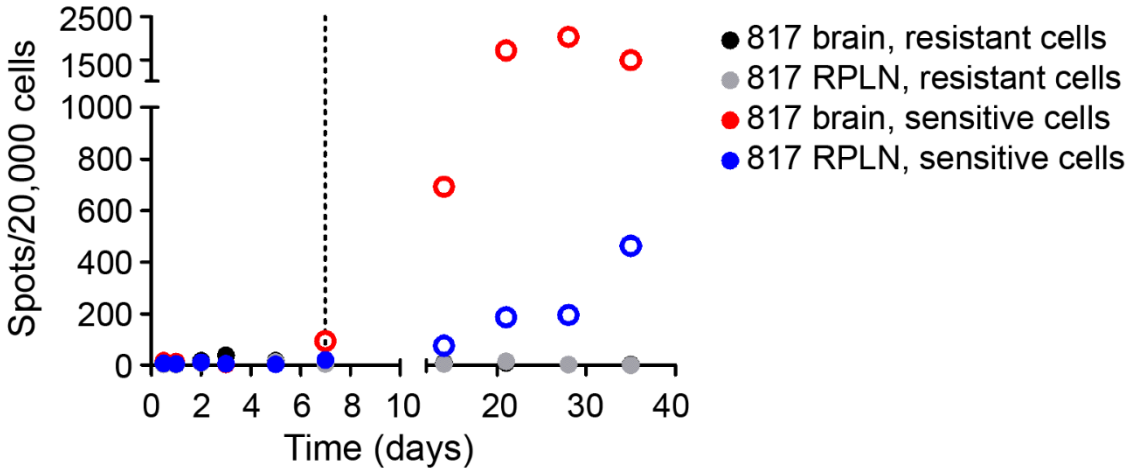

Figure 2.5. RPLN prions infect cells in culture, but infection is delayed compared to brain. The positive brain sample infected the sensitive cells and had detectable spots around 2 weeks post-infection (dilution is the same as the highest is Fig. 2.4). The RPLN also infected sensitive cells, and the increase in spots was more dramatic from weeks 4-5. Open circles indicate that the sensitive cells are statistically different from the resistant cells inoculated with the same sample (brain or RPLN) ($p<0.05$, unpaired t-test).

To test whether RPLN prions are propagated earlier in the course infection, but yield PK-sensitive prions, we tested the cell lysates in RT-QuIC as well as by cell blotting (Fig. 2.6). The RT-QuIC data matches the cell blotting data; infection with the brain sample caused a significant increase in positive cells by the second week post-inoculation, but infection with the RPLN did not result in positive

cells until the fifth week post-inoculation. We hypothesized that the delayed propagation from RPLN prions was irrespective of dilution and that the delay indicated a difference in the PrP^{Sc} strain in brain and RPLN. Therefore, we designed an experiment to include multiple dilutions and multiple time-points (Fig. 2.7, Fig. 2.8, Fig. 2.9).

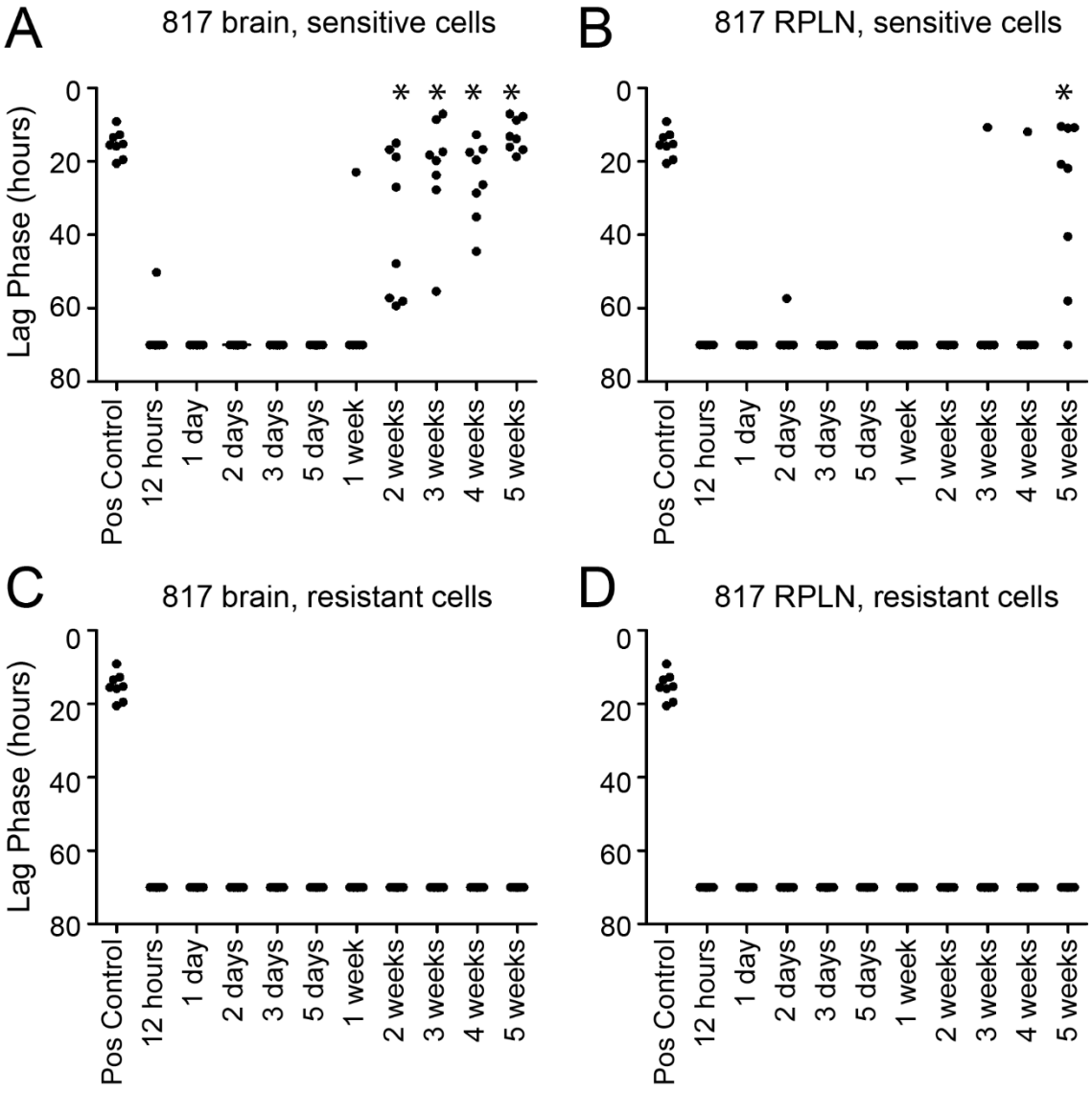

Figure 2.6. RPLN prions infect cells in culture, but infection is delayed compared to brain. We tested the cells from the experiment in Fig. 2.5 in RT-QuIC to determine whether there were PK-sensitive prions in samples that were cell blot-negative. * indicates a significant difference between the brain or RPLN sample in sensitive and resistant cells at a given time-point ($p<0.05$, Wilcoxon Signed Rank). The positive control is a CWD(+) transgenic mouse brain in sensitive cells.

RPLN prions consistently infect cells, with no consistent differences from brain in kinetics or titer.

We hypothesized that, regardless of dilution, the RPLN infection would be delayed compared to brain, and that spots and RT-QuIC seeding would be detectable only in later collections (5 weeks – 6 weeks). Similarly, we hypothesized that infection with brain prions would result in spots and RT-QuIC seeding as early as 2 weeks and that dilution would not affect the kinetics of infection.

However, we found no consistent difference in kinetics of PrP^{Sc} propagation between brain and RPLN, either by PK-resistant spots (Fig. 2.7) or RT-QuIC activity of the cells (Fig. 2.9). In the highest dilution, the spot formation was delayed in the lymph node samples compared to the brain samples, which is similar to our previous experiment (Fig. 2.5). Specifically, spots increased in the brain-infected cells from week 2-3, while the RPLN-infected cells experienced an increase from weeks 3-4 (Fig. 2.7). However, this pattern was not apparent in RT-QuIC or in subsequent dilutions (Fig. 2.7, Fig. 2.9).

Because RPLN prions robustly infected sensitive cells, we calculated titers for each inoculum. The elk RPLN had a higher titer than the brain, but the red deer, 816 and 817 had higher titers in their brains (Fig. 2.8). Interestingly, the white-tailed deer brain caused essentially no prion propagation in the cells, either by cell blotting or by RT-QuIC. The white-tailed deer RPLN-infected cells had very, very few spots and a lower titer than the other samples (Fig. 2.7, Fig. 2.8).

We tested the cells by RT-QuIC, which is able to detect PK-sensitive prions. However, there was no consistent delay in PrP^{Sc} propagation in cells infected with RPLN prions, nor was the seeding from RPLN-infected cells consistently slower than brain-infected cells (Fig. 2.9). We confirmed that the crests and troughs in lag phase were not artifacts of variability in the RT-QuIC assay – there was no relationship between faster samples and the RT-QuIC plate on which the cells were tested.

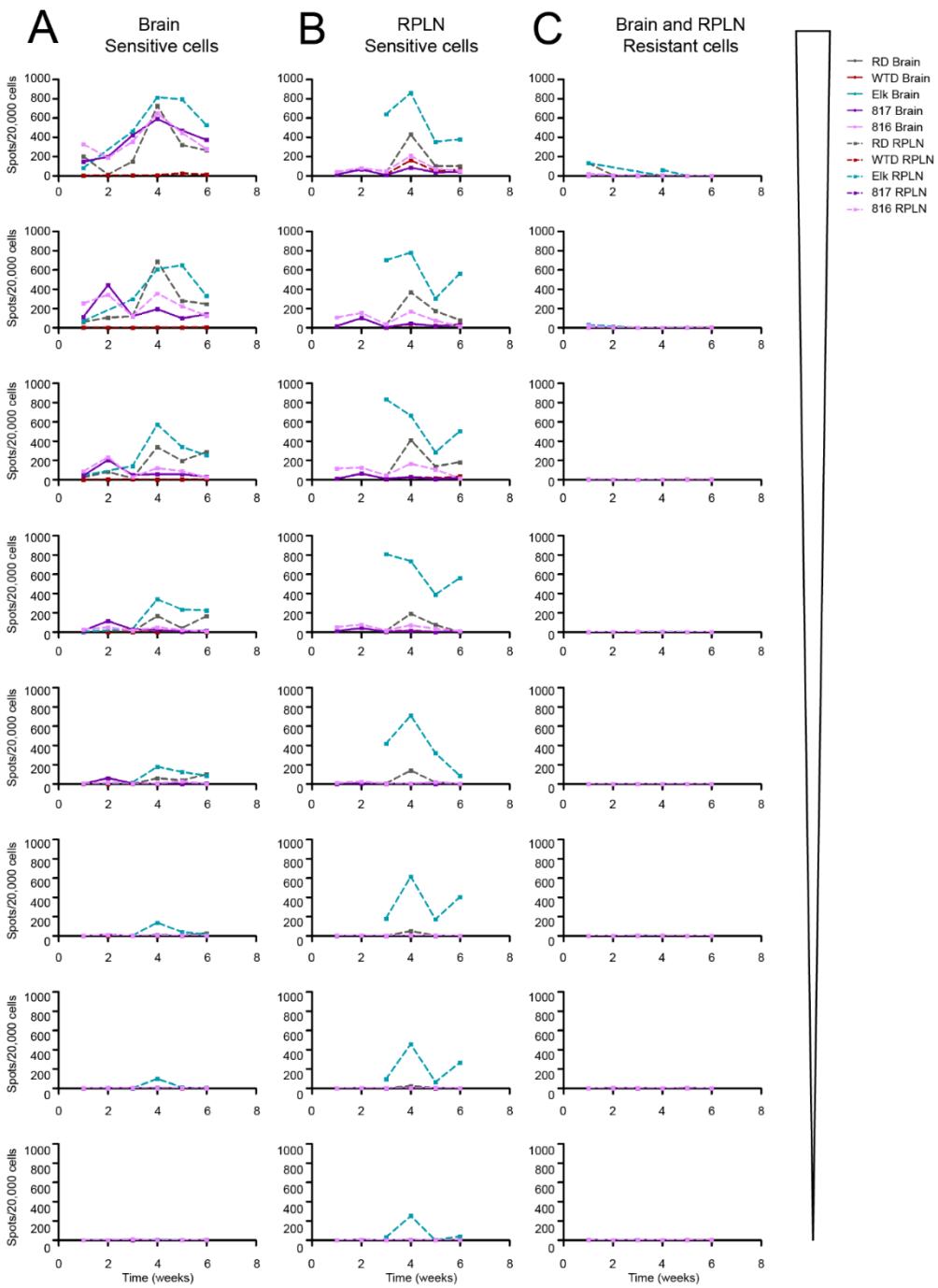

Figure 2.7. RPLN prions infect cells in culture, without consistent differences in infection kinetics. We collected cells at each week from 1-6 for each combination of homogenate (brain or RPLN), dilution (8 total) and cell type (resistant or susceptible). The mean number of PK-resistant spots is indicated on the y-axis and the most dilute homogenate is at the bottom of each column, as indicated by the arrow on the right (A, B, C). We are missing some data during early collection points due to insufficient homogenate volume for all the experiments.

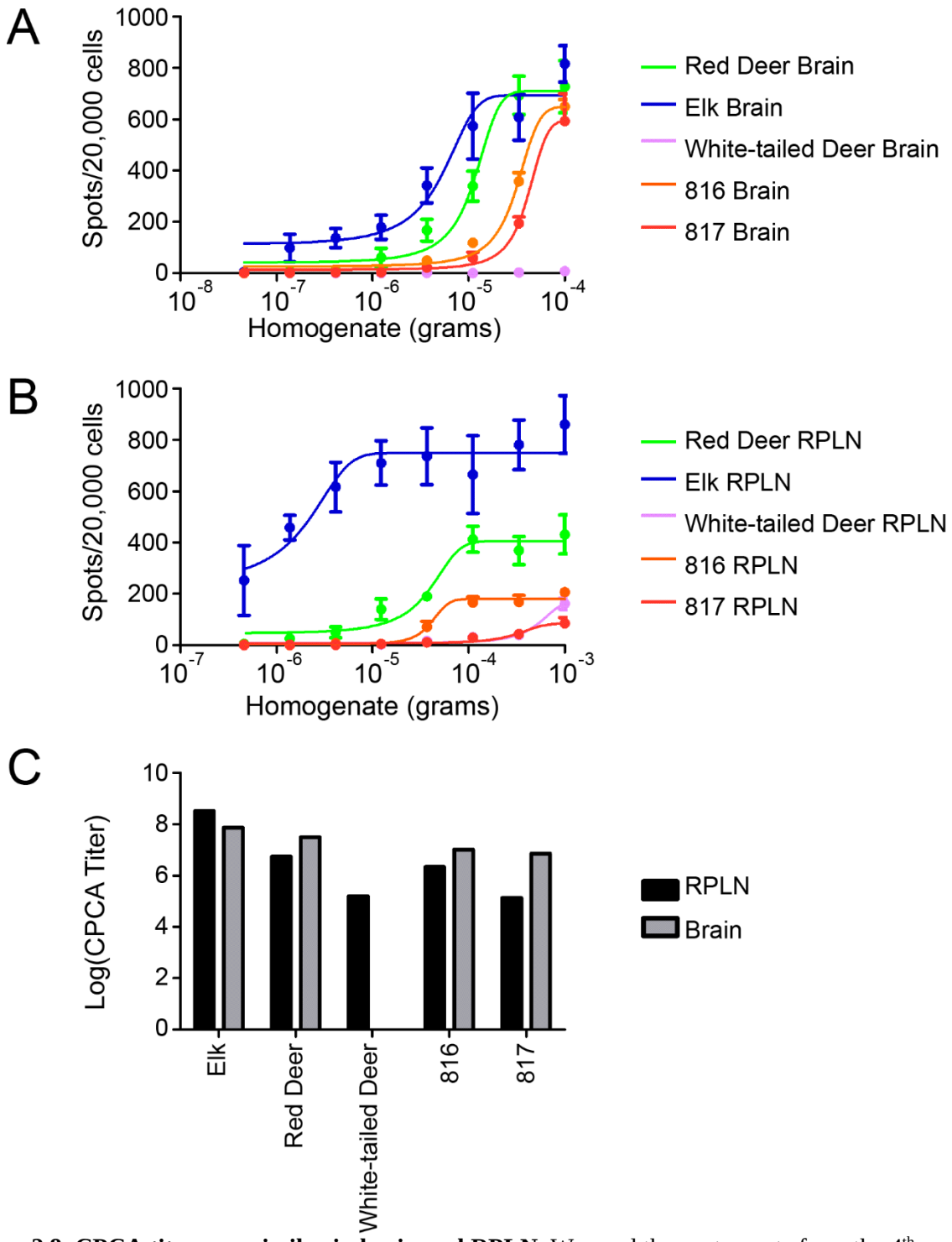

Figure 2.8. CPCA titers are similar in brain and RPLN. We used the spot counts from the 4th week of cell infection to calculate the CPCA titer for each sample. A-B. The points indicate the mean spot counts for each brain or RPLN sample and the error bars indicate the SEM for each dilution that was tested in CPCA. The lines are 4-parameter sigmoidal curves of best fit. C. We plotted the titer that was calculated from each of the curves in A-B. The titer is the log of the number of spots/wet gram tissue homogenate at the midpoint of the sigmoidal curve.

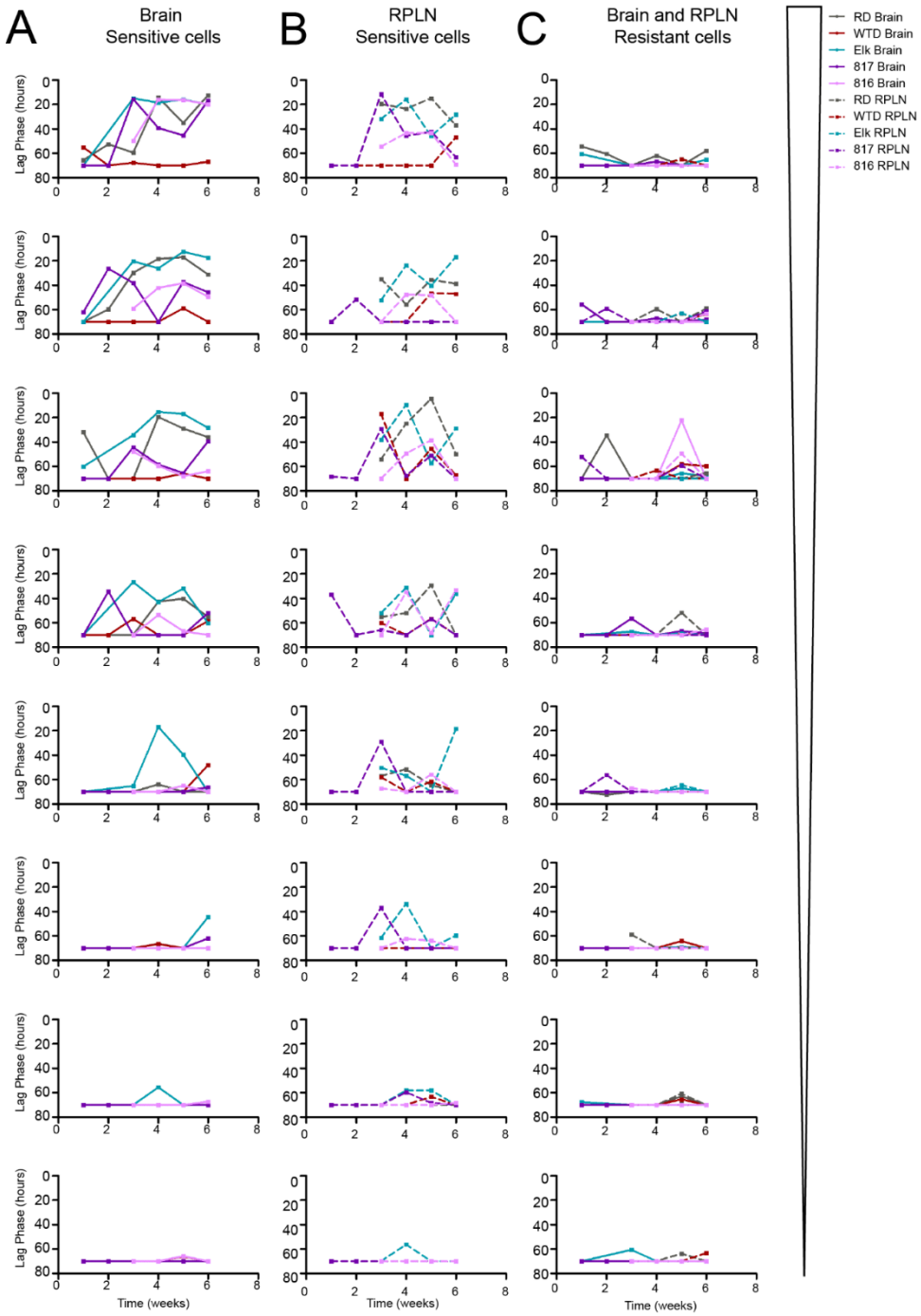

Figure 2.9. RPLN prions infect cells and cells seed RT-QuIC. We collected cells at each week from 1-6 for each combination of homogenate (brain or RPLN), dilution (8 total) and cell type (resistant or susceptible). The mean lag phase for cell lysates in RT-QuIC is indicated on the y-axis and the most dilute homogenate is at the bottom of each column, as indicated by the arrow on the right (A, B, C). We are missing some data during early collection points due to insufficient homogenate volume for all the experiments.

Discussion

Though PrP^{Sc} accumulates in many tissues of CWD(+) deer, differences between PrP^{Sc} in the brain vs. the peripheral tissues remain unknown. We were particularly interested in the *in vitro* characteristics and the infectivity of PrP^{Sc} in lymph nodes. We hypothesized that lymph node PrP^{Sc} would be similar to brain PrP^{Sc} in its *in vitro* characteristics and that lymph node prions would be infectious, but that there would be less PrP^{Sc} in lymph nodes than in brain. We observed similar RT-QuIC seeding activity for brain and RPLN, though the brain occasionally had higher seeding activity (Fig. 2.1). We observed PK-resistant PrP^{Sc} by western blot in most brain and RPLN samples, without dramatic differences between tissue types (Fig. 2.3). In 7-5 ELISA, we detected PrP^{Sc} in brain samples fairly consistently (4/5), but only in one RPLN sample (1/5) (Fig. 2.2). Finally, 5/5 RPLN samples and 4/5 brain samples were infectious by CPCA (Fig. 2.8). Results are summarized in Table 2.1.

Table 2.1. Comparison of lymph node and brain samples by various assays. We summarized the findings from each assay to enable comparison of the outcomes. In some cases (gray), the brain was indistinguishable from the RPLN. In other cases, brain had a higher titer (blue) or RPLN had a higher titer (yellow).

Sample	*Method*	*Comparison of RPLN and brain*
Red Deer	RT-QuIC	Brain = RPLN
Red Deer	CPCA	Brain > RPLN
Red Deer	7-5 ELISA	Brain > RPLN
WTD	RT-QuIC	Brain = RPLN
WTD	CPCA	RPLN > Brain
WTD	7-5 ELISA	*No signal*
Elk	RT-QuIC	Brain = RPLN
Elk	CPCA	RPLN > Brain
Elk	7-5 ELISA	RPLN > Brain
816 (WTD)	RT-QuIC	Brain > RPLN
816 (WTD)	CPCA	Brain > RPLN
816 (WTD)	7-5 ELISA	Brain > RPLN
817 (WTD)	RT-QuIC	Brain > RPLN
817 (WTD)	CPCA	Brain > RPLN
817 (WTD)	7-5 ELISA	Brain > RPLN

Because different assays gave slightly different results, it is important to discuss the differences among the assays we used. The 7-5 ELISA is specific for underglycosylated PrP^{C}, which has been

demonstrated to be characteristic of PrP^{Sc} in the brain (202). However, little is known about the recruitment of underglycosylated PrP^{C} to PrP^{Sc} in non-brain tissues. It is possible that lymph nodes do not experience the same enrichment of underglycosylated PrP^{Sc} in the disease state, which would render the 7-5 ELISA insufficiently sensitive to detect CWD in lymph nodes, even though the PrP^{Sc} could still be infectious. Western blots for PrP^{Sc} require the PrP^{Sc} to be PK-resistant. There is anecdotal evidence in our group that lymph node PrP^{Sc} is more PK-sensitive than brain PrP^{Sc}. If there is a difference in the PK sensitivity of PrP^{Sc} in brain vs. lymph node, we would expect western blot to differentiate the tissues, even though the infectivity may not be different. In fact, there is some evidence that the most infectious species of PrP^{Sc} are the small, PK-sensitive oligomers (326). Even if PK-sensitivity is similar, it is clear that PrP^{C} expression is much lower in the RPLN than the brain, which makes detection by western blot more difficult. Finally, RT-QuIC is presumed to amplify PrP^{Sc} amyloid and our statistical comparisons to negative tissue ensure that we are detecting bona fide amyloid formation. However, it is less clear whether RT-QuIC is specific for infectious prions, specific strains, or specific PrP^{Sc} molecules (i.e. large amyloid aggregates, oligomers, PK-sensitive PrP^{Sc}, etc.). The unknown specificity of RT-QuIC for certain characteristics of the prion agent led us to CPCA to attempt to calculate the LD_{50} for our lymph node samples (Fig. 2.4).

The first CPCA experiment yielded very low, albeit statistically significant, infection from lymph node PrP^{Sc} in RK-13 cells expressing deer PrP^{C} (Deer5E9 cells) (Fig. 2.4). When we prolonged the incubation from 4 weeks to 5 weeks, also in the Deer5E9 cells, we saw many more cells infected with RPLN PrP^{Sc} (Fig. 2.5). In the second experiment, we observed a delay in infection of cells with RPLN PrP^{Sc} vs. brain PrP^{Sc} (Fig. 2.5, 2.6). We replicated that delay in the third experiment, but it was only apparent in the cells infected with the highest dilution (Fig. 2.7). The delay was not apparent in the lower dilutions and was less apparent in the RT-QuIC analysis of the cell lysates, perhaps because there was more variation in the RT-QuIC data (Fig. 2.9). It seems that the delay is an artifact of the specific dilution, which may be due to inhibition by non-PrP^{Sc} RPLN components since the RPLN homogenates were applied to the plate at a 10-fold higher concentration than the brain.

It is also interesting that the WTD brain sample failed to infect the cells, produce a PK-resistant PrP^{Sc} signal, or be detected in ELISA. The failure of infection in CPCA cannot be blamed on the Deer5E9 cells, as the experiment was repeated twice and the accompanying CWD(+) sample, 817 brain, was positive in Deer5E9 cells in both cases. There is some evidence that CPCA is specific for particular CWD strains; in the original CPCA publication, one of the CWD isolates failed to infect cells, despite being infectious *in vivo*. The authors confirmed that the isolate was infectious *in vivo* and suggested the CPCA may be specific for some CWD strains (165). If the failure of CPCA to detect PrP^{Sc} in the WTD brain sample is due to a strain difference, these data suggest that RT-QuIC may be less sensitive than CPCA to differences in strain.

Of course, it is possible that RT-QuIC detects something other than infectious PrP^{Sc} and that the CPCA and ELISA correctly identified the *lack* of infectious PrP^{Sc} for the WTD brain sample. The best test of the infectivity is a bioassay. The Telling group performed a bioassay for the WTD brain and RPLN, in addition to the elk and red deer brain and RPLN samples, and all 6 were positive in transgenic mouse bioassay (324). In other words, the WTD brain and RPLN samples were both infectious *in vivo,* which agrees with the RT-QuIC result, the CPCA result (for RPLN, but not brain) and disagrees with the 7-5 ELISA and western blot, at least with the volume of homogenate we tested.

We used a number of assays to analyze the presence of PrP^{Sc} in brain and RPLN tissue from CWD(+) cervids and found substantial signal (seeding activity, PK-resistant PrP^{Sc} and cell infectivity) in both tissue types. It seems likely that PrP^{Sc} not only accumulates to high levels outside the CNS, but is in an infectious form. The prion field has largely focused its efforts on understanding neurodegeneration and its relationship to PrP^{Sc}, but the question of accumulation, replication, and dissemination of PrP^{Sc} by the lymphoid system has been lingering for decades. It is clear that CWD and scrapie are both lymphotropic and include an early stage during which prions replicate in the lymphoid system (156, 224, 303). Conversely, BSE is restricted almost exclusively to the nervous system, with a few reports of PrP^{Sc} detection in the distal ileum and the tonsil (327-330). Interestingly, when cattle were IC-inoculated with scrapie, PrP^{Sc} was not detected in the mesenteric lymph node or spleen (331). When cattle were IC-

inoculated with CWD, there was essentially no PrP^{Sc} detected outside the CNS (332). However, IC inoculation of CWD in deer results in robust PrP^{Sc} accumulation in the lymph node (218, 332). However, when red deer were inoculated IC with BSE, prions were detectable only in the CNS. It is likely that these deer had a very early infection, and that prion spread to the periphery had not yet occurred. Together, these results suggest that lymphotropism is dictated by the host, and that deer and sheep permit lymphotropism, while cattle do not.

The presence of infectious prions outside the CNS in CWD is important for several reasons: first, it offers clues into the mechanism of rapid spread of CWD from its initial description in mule deer in Northern Colorado in 1982 to its current (detectable) presence in 23 states, 3 Canadian provinces, Korea, and Norway (61, 122, 271). We hypothesize the highly contagious nature of CWD is related to the presence of infectious prions in the periphery, which leads to shedding of CWD in excreta. Prions in the periphery are far more likely to be encountered by naïve animals than prions from the CNS. Second, the lymphoid system and the CNS have different tolerances for cross-species prion transmission (333). When transgenic mice were inoculated with prion strains to which they were typically resistant, significant PrP^{Sc} (and infectivity) was detectable in their spleens (333). Therefore, it is possible that CWD prions from the spleen may have different risk to humans than prions present in the brain. There is already evidence that CWD strains have variable lymphotropic behavior, which supports the hypothesis that the CNS and lymphoid system provide different environments for prion replication (334). These results beg the question: are the peripheral tissues of CWD(+) cervids more infectious to humans than the CNS tissues that have been tested widely?

In conclusion, we demonstrated the infectivity of PrP^{Sc} from lymph nodes and we compared several prion detection assays to compare brain and RPLN samples from CWD(+) cervids. We observed differences among prion detection assays that should be considered for future analysis. Finally, this work prompts the question: is all the PrP^{Sc} identified in the periphery infectious?

CHAPTER 3: INSIGHTS INTO CWD AND BSE SPECIES BARRIERS USING REAL-TIME CONVERSION[2]

Summary

The propensity for trans-species prion transmission is related to the structural characteristics of the prions in the enciphering and new host, although the exact mechanism remains incompletely understood. The effects of variability in prion protein structure on cross-species prion transmission have been studied with animal bioassays, but the influence of prion protein structure vs. host co-factors (e.g. cellular constituents, trafficking, and innate immune interactions) remains difficult to dissect. To isolate the effects of protein-protein interactions on trans-species conversion, we used recombinant PrP^C ($rPrP^C$) and real-time, quaking-induced conversion (RT-QuIC) and compared chronic wasting disease (CWD) and classical bovine spongiform encephalopathy (cBSE) prions. To assess the impact of transmission to a new species, we studied feline CWD (fCWD) and feline BSE (i.e. feline spongiform encephalopathy, FSE). We cross-seeded fCWD and FSE into each species' full-length $rPrP^C$ and measured the time required for conversion to the amyloid form, the rate of amyloid conversion. These studies revealed that: (1) CWD and BSE seeded their homologous species' $rPrP^C$ best; (2) fCWD was a more efficient seed for feline $rPrP^C$ than for white-tailed deer $rPrP^C$; (3) conversely, FSE converted bovine $rPrP^C$ more efficiently than feline $rPrP^C$; (4) and CWD, fCWD, BSE, and FSE all converted human rPrP, though not as efficiently as homologous sCJD prions. These results suggest that: (1) at the level of protein-protein interactions, CWD adapts to a new species more readily than does BSE, and (2) the barrier preventing transmission of CWD to humans may be less robust than estimated.

[2] Copyright © American Society for Microbiology, [Journal of Virology, Volume 89, 2015, 9524-9531, 10.1128/jvi.01439-15]

Background

Prion diseases are characterized by the seeded misfolding and aggregation of the cellular prion protein, PrP^{C}, to a pathogenic state, PrP^{Sc}. All mammals express PrP^{C}, with only minor polymorphisms within and between species (335). Prion disease has been identified in humans (Creutzfeldt Jakob disease, CJD), cattle (BSE), cervids (CWD), felines (feline spongiform encephalopathy, FSE) and sheep and goats (scrapie), as well as other mammals (336). The transmissibility of prion diseases makes them unique among other protein misfolding diseases, including Alzheimer's and Parkinson's diseases. Though prion diseases vary in their proclivity to transmit to new species, the cBSE epidemic and subsequent transmission to humans (as variant CJD, vCJD), felines (FSE) and several ungulate species illustrate the importance of understanding zoonotic transmission (10, 114, 115, 146, 245, 247, 336).

The trans-species transmissibility of cBSE and CWD has been studied in natural hosts, conventional and transgenic rodents, and *in vitro* models. CWD has been transmitted experimentally to sheep, felines, cattle and squirrel monkeys (232, 233, 235-237, 337). BSE has been transmitted experimentally to sheep, European red deer and macaques (241-243). Transgenic mice were developed to explore the potential transmissibility of cBSE and CWD to humans. In four studies with mice expressing the human prion protein (TgHu), cBSE inoculation produced mixed results, with attack rates ranging from 0 to ~50% (155, 250-252). Inoculation of TgHu mice with CWD has yielded no infections (155, 255, 338, 339). Additionally, three distinct *in vitro* amyloid amplification methods have also shown that BSE is better able to induce the misfolding of human PrP^{C} than is CWD (266, 268, 269, 340-343).

That prion characteristics are not solely defined by primary structure can be inferred by the existence of prion strains (268). Indeed, several studies have noted the similarity that cBSE prions passaged in other species (FSE, vCJD, and sheep BSE) have to the original cBSE agent, despite the variable primary structure of the passaged prions (147, 252, 343, 344). Therefore, it is logical to conclude that variability in prion conformation and the interactions of PrP^{Sc} and PrP^{C} are essential to prion species barriers. We used RT-QuIC to assess the complementarity of seed-substrate pairing and the possibility of trans-species conversion of two prions pertinent to human health, CWD and cBSE.

We hypothesized that in RT-QuIC, cBSE and passaged forms of cBSE would have similar trans-species seeding characteristics and would readily convert human $rPrP^C$, whereas passaged forms of CWD would be less like CWD and would convert human $rPrP^C$ poorly.

Methods

Recombinant PrP (rPrP) Production

The coding regions for full-length (aa23-231) recombinant prion protein (rPrP) from each species (bank vole, bovine, feline, human M129 and white-tailed deer) were kindly provided by Dr. Glenn Telling. We cloned full-length constructs (bovine, feline, human M129 and white-tailed deer) into the pET100D expression system (Life Technologies). The truncated Syrian hamster construct in BL21 *E. coli* was kindly provided by Dr. Byron Caughey. We truncated the bank vole *PRNP* coding region using specific primers to isolate the sequence for amino acids 90-231, then cloned the sequence into the vector that contained the Syrian hamster construct. We used *E. coli* BL21 Star cells (Life Technologies) to express rPrP. Briefly, we spiked BL21 cells from a glycerol stock into 5mL LB media and 5μg/mL ampicillin and grew the cultures overnight, shaking at 37º. We inoculated 1L LB media with the 5mL culture, plus 5μg/mL ampicillin and auto-induction reagents (final concentration 0.5M $(NH_4)_2SO_4$, 1M KH_2PO_4, 1M Na_2HPO_4, 0.5% glycerol, 0.05% glucose, 0.2% α-lactose, .001M $MgSO_4$). When the OD_{600} reached approximately 3.0, we harvested and lysed bacteria, then isolated inclusion bodies according to the manufacturer's protocol with Bug Buster™ and Lysonase™ (EMD-Millipore). We solubilized inclusion bodies and rotated the solution in 8M guanidine hydrochloride (GdnHCl) and 100mM Na_2HPO_4 for at least one hour at room temperature. We bound the denatured rPrP to Superflow™ nickel resin (Qiagen) and refolded at a rate of 0.75mL/min on the column with a gradient from 6.0M GdnHCl, 100mM Na_2HPO_4, 10mM Tris (pH 8.0) to the same buffer with no GdnHCl. We used a gradient to 0.5M imidazole, 100mM NaH_2PO_4, 10mM Tris (pH 5.5) with a flow rate of 2.0mL/min to elute the $rPrP^C$. We filtered the eluted $rPrP^C$ and dialyzed at a concentration of ~.4mg/mL in two changes of 4.0L 20mM NaH_2PO_4 (pH 5.5). After dialysis, we filtered the $rPrP^C$ again and stored at 4ºC, having determined its

concentration by A_{280}. We tested the purity of the $rPrP^C$ samples was tested by performing gel electrophoresis (12% bis-tris gels with 1X MOPS [Bio-Rad], 190V, 55min) and staining with Coomassie Brilliant Blue (Bio-Rad).

Circular dichroism (CD) spectroscopy

We purged a Jasco 810 CD spectrometer (Jasco, Inc.) with N_2 for 15 minutes, then filled a clean, glass cuvette (2mM path length) with the diluent in which $rPrP^C$ is stored (20mM Na_2HPO_4) or an $rPrP^C$ sample. We measured the HT voltage and ellipticity (Θ) from 200-250nm, then calculated the molar ellipticity (Θ*molecular weight/(10* concentration (mg/mL)* path length) and plotted it against the wavelength.

Real-time quaking-induced conversion (RT-QuIC)

We combined 0.1mg/mL $rPrP^C$ with 400mM NaCl, 1mM EDTA, 20mM NaH_2PO_4 and freshly-made thioflavin T (ThT; final concentration 10μM) for a final volume of 95μL per well in a 96 well plate. We homogenized brain samples (see Table 3.1) in 1X PBS as a 10% solution with a bead beater (Next Advance), then aliquoted the homogenate in single-use tubes and froze the samples at -80°C. We thawed homogenate aliquots and diluted the samples into 1X PBS plus 0.05% SDS (Conditions 1) or 0.1% SDS (Conditions 2). We added 2μL diluted brain seed to 95μL reaction buffer in the well of an optical bottom 96 well plate. An RT-QuIC experiment consisted of 400 cycles (100 hours) of shaking and incubation at 45°C; specifically, plates were shaken for 1 minute (700rpm, double orbital), followed by 1 minute of rest. Fluorescence (450nm excitation and 480nm emission, 20 flashes/well) was recorded every 15 minutes using a gain of 1700 (96 well plate).

Table 3.1. Sources of the prion seeds used in these experiments.						
	Species (n)	**±**	**Tissue**	**Inoculum**	**Inoculation**	**Sample**
CWD	WTD (1)	+	Caudal brain sections	CO Dep't of Wildlife positive deer LA01	oral	104
Exper. CWD	WTD (6)	+	Whole brain	CSU CWD-positive deer 700, 800 series	oral/aerosol	CBP6
negative deer	WTD (1)	-	Caudal brain sections	CSU CWD-negative deer UGA 1/2	oral	123
Feline CWD	Feline (2)	+	Multiple brain sections	CSU CWD-positive deer	IC	4137/ 4152
negative cat	Feline (1)	-	Obex	CSU CWD-negative deer UGA 1/2	oral	4141
FSE (345)	Feline (1)	+	Medulla	*natural infection*	-	FSE
BSE	Bovine (1)	+	Obex	*natural infection*	-	BSE
negative cow	Bovine (1)	-	Brainstem	*not inoculated*	-	Negative bovine
Field CWD 1 (217)	WTD	+	Obex	Field Isolate	-	H92
Field CWD 2 (217)	WTD	+	Obex	Field Isolate	-	98-933968

To ensure that the results observed in our RT-QuIC experiments were not a result of specific experimental conditions, we completely repeated all the experiments in this study in two sets of conditions. For Condition 1, we used one or two batches of each rPrP species (bovine, feline, white-tailed deer, human) and an SDS concentration SDS of 0.05% for the homogenate diluent. For Condition 2, we used new batches (one or two) of each species of rPrP, with an SDS concentration of 0.1% in the sample dilution step. In both Condition 1 and Condition 2, we used were 6-8 replicates (on 3-4 plates) of every reaction. Because the reaction conditions resulted in different kinetics (kinetics using 0.1% SDS were faster than 0.05% SDS), we could not compare the rates of amyloid conversion between experiments. Data shown here is from Condition 2, but patterns were maintained in Condition 1.

Artificial Seeds

In order to assess each species' inherent propensity to convert from $rPrP^{C}$ to $rPrP^{Sc}$ (amyloidogenicity), we created synthetic $rPrP^{ThT+}$ seeds from truncated Syrian hamster $rPrP^{C}$ (SH, amino

acids 90-231) or truncated bank vole rPrP^{C} (BV, amino acids 90-231). For the SH artificial seeds, we shook 0.5mg/mL SH rPrP^{C} with 2M GdnHCl at 37ºC overnight. We made BV artificial seeds by shaking 0.3mg/mL BV rPrP^{C} at 37º without GdnHCl. In both cases, we added 2µL artificial seed (or ten-fold dilutions thereof) to the RT-QuIC reaction in place of a brain-derived seed.

Western Blot and Quantification

We added 5µL, 9µL or 13µL of a 5% homogenate of BSE or CWD (sample 104) to 1µL of Proteinase K (100µg/mL, Invitrogen), 1µL of 2% SDS and brought the volume to 15µL with water. We incubated the samples at 37ºC for 30 minutes, then 45ºC for 10 minutes. We added 5µL of a 4X sample loading buffer/reducing agent (Life Technologies) to the samples and incubated at 93º for 3 minutes. We added 18µL to each well of a 12-well, 12% bis-tris gel, then electrophoresed for 10 minutes at 115V followed by one hour at 150V. We transferred the protein to polyvinylidene fluoride (PVDF) membranes in cold transfer buffer (20% MeOH, 192mM glycine, 25mM tris base) for 1.5 hours at 115V, then blocked overnight at 4ºC in tris-buffered saline plus tween (TBST, 0.1% Tween) and non-fat dry milk. We bound anti-PrP antibody 6H4 to the membrane in TBST+milk for one hour at a concentration of 1:5000, then washed the membrane with TBST for one hour. We applied the secondary antibody, a near-infrared-tagged goat anti-mouse antibody, in TBST plus milk for one hour at a concentration of 1:20,000. We washed the membrane with TSBT for one hour. We collected images on the Odyssey CLx Infrared Imager (Li-Cor Biosciences, Inc.) and analyzed them using Image Studio Lite Version 4.0 (Li-Cor Biosciences, Inc.). We calculated the intensity for each lane of the western blot, then divided by the number of microliters of 5% brain homogenate added to the well. Finally, we divided the intensity/µL for each PK+ lane by the intensity of the PK- lane to determine the relative quantity of PK resistant material.

Quantitative Analysis

We determined the lag phases of positive and negative samples in MARS (BMG Labtech) by calculating the time required to meet a threshold for positive samples (305). We defined the threshold as

the average baseline fluorescence plus five standard deviations for each experiment. The rate is the inverse of the lag phase for each sample (1/lag phase), with units of hours^{-1}. We use the rate of amyloid conversion here instead of lag phase in order to account for the samples that never cross the threshold (the rate can be conservatively assigned a value of 0 hours^{-1}). Despite their similar purity, conformation and functionality, the rPrP^{C} substrates were not equally sensitive. In order to compare one seed's behavior across multiple substrates without confounding by the inherent amyloidogenicity differences between the substrates, we calculated relative rates and used them for analysis. Specifically, we divided all rates for a given substrate by the highest rate in that substrate; the fastest sample has a rate of 1.0. Average relative rates of amyloid conversion from 6-12 replicates are displayed as the mean with error bars indicating the standard error of the mean. We tested the difference between rates at each dilution with the non-parametric Mann-Whitney U (MWU) test (when both samples had a non-zero median) in Prism 5.0 (Graphpad), or the non-parametric one-sample Wilcoxon signed-rank (WSR) test (when one of the samples had a median of zero) in R. We defined a statistically significant difference by a p-value <0.05. Significant differences by the MWU test were indicated by *, while significant differences by the WSR test were indicated by #.

Results

Recombinant bovine, feline, human and white-tailed deer PrP^{C} have similar purity.

To compare the behavior of a given prion seed across multiple rPrP^{C} substrates, it was necessary to ensure that every batch of every substrate had similar purity, structure and functionality. We analyzed each rPrP^{C} preparation by gel electrophoresis and total protein staining to show that the substrates were of comparable purity (Fig. 3.1A). To ensure that the secondary structure of each preparation was comparable, we used CD spectroscopy (Fig. 3.1B-E). All substrates had minima at 208nm and 222nm, indicating a predominance of α-helical secondary structure, as expected.

We analyzed each preparation of recombinant protein with the homologous species' prion seed in RT-QuIC to verify its ability to form amyloid upon addition of seed. We used homologous seeds (e.g.

CWD brain samples in full-length white-tailed deer substrate) as positive controls and negative brain samples (deer, bovine and feline) as negative controls. We considered a batch of $rPrP^C$ to be functional if the fluorescence in wells containing positive control seeds crossed the threshold within 20 hours (rate ≥ 1/20, 0.05 $hours^{-1}$) and the negative controls had an average rate less than .015 $hours^{-1}$. By these metrics, we determined that all batches of $rPrP^C$ were comparable and that seed behavior could consequently be compared among substrates.

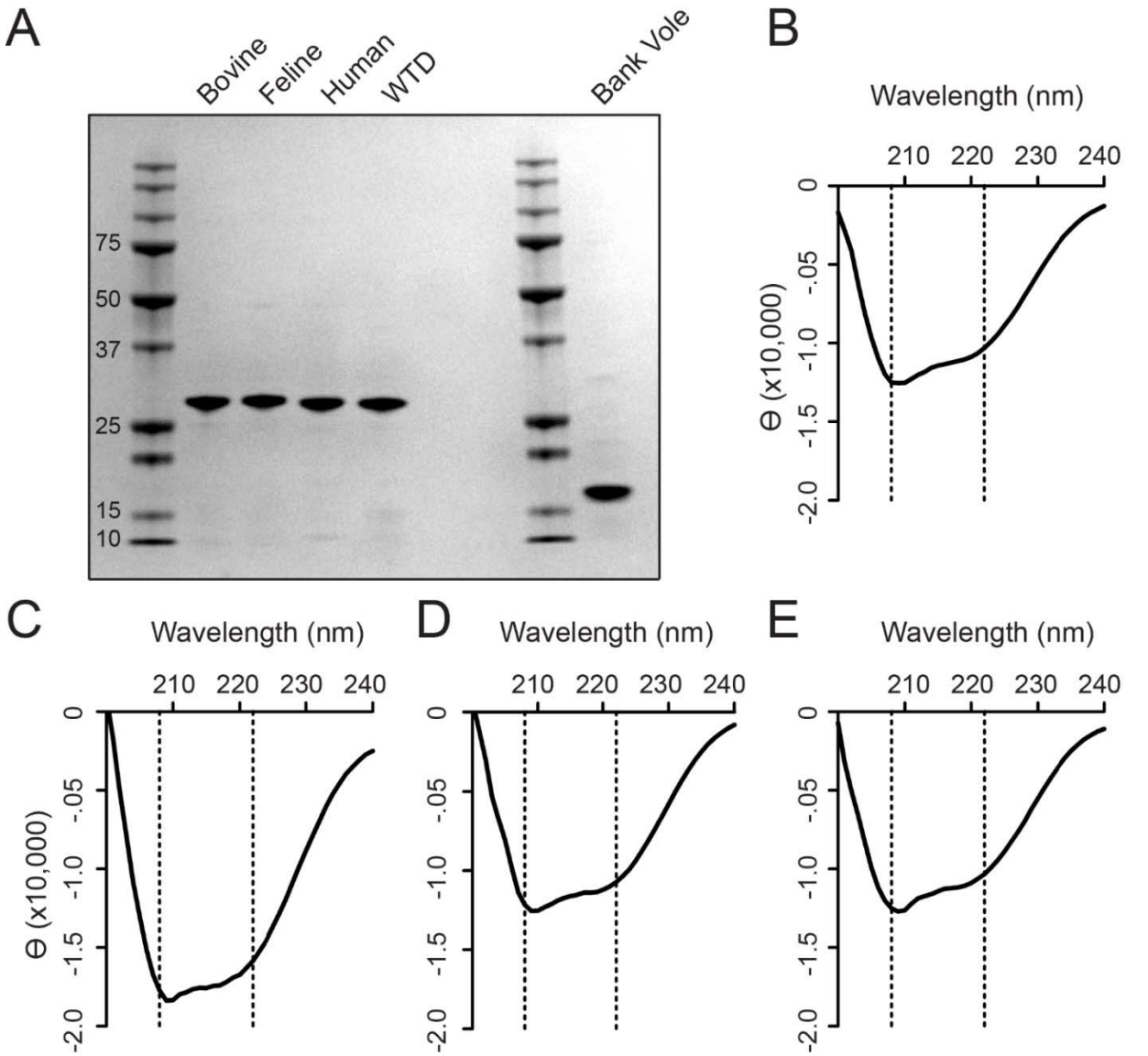

Figure 3.1. rPrP^{C} substrates are of comparable quality. A. Coomassie Blue visualization of 1.5µg rPrP^{C} substrate indicates the purity of each rPrP^{C}. Bands represent, from left-right, ladder; bovine (amino acids 23-231), feline (23-231), human M129 (23-231) and white-tailed deer (23-231) rPrP^{C}; ladder, bank vole (90-231) rPrP. B. CD spectrum for bovine rPrP^{C}. C. CD spectrum for feline rPrP^{C}. D. CD spectrum for human M129 rPrP^{C}. E. CD spectrum for white-tailed deer rPrP^{C}. The dotted lines indicate the anticipated minima for α-helical structure (B-F).

rPrP^{C} species differ in inherent propensity for conversion, as reflected by the rate of amyloid conversion.

Despite their similar purity, conformation and functionality, the rPrP^{C} substrates did not have an equal propensity to form amyloid (amyloidogenicity), which may reflect inherent features from each species, as multiple purified batches of rPrP^{C} of the same species had the same behavior. With a variety of

prion seeds (CWD, BSE, fCWD, FSE), the fastest rate of amyloid conversion for full-length white-tailed deer rPrP (0.27 $hours^{-1}$) was nearly twice the fastest rate in full-length bovine (0.13 $hours^{-1}$) or feline rPrP (0.17 $hours^{-1}$).

To verify the amyloidogenicity differences, we used artificial seeds ($rPrP^{ThT+}$ created by shaking $rPrP^{C}$ with guanidine hydrochloride at 37°) and compared the rates of amyloid conversion. Mimicking our observation with brain-derived prion seeds, white-tailed deer rPrP formed amyloid fastest with the addition of truncated bank vole $rPrP^{ThT+}$, with a rate approximately twice the rate of bovine and feline rPrP conversion (Fig 3.2A). We observed the same pattern when the seed was prepared from truncated Syrian hamster rPrP (Fig. 3.2B). The same trends are visualized with representative raw data (Fig. 3.2C-D). The use of artificial seeds confirmed the different propensities for amyloid conversion in divergent species. To compare the behavior of a given seed among species with variable amyloidogenicity, we normalized the rates by considering the maximum rate in each substrate to be 1.0 $hour^{-1}$.

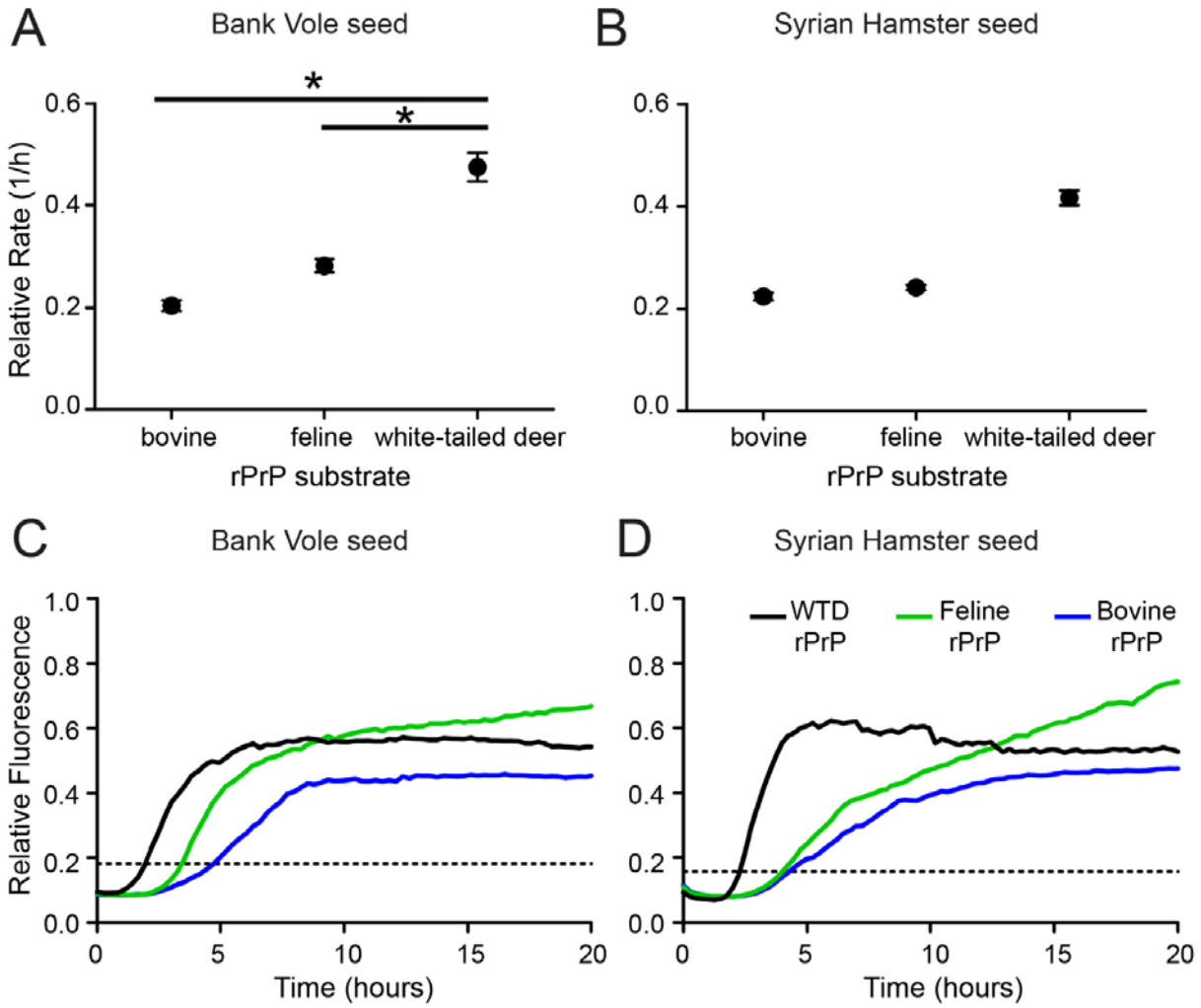

Figure 3.2. WTD rPrP^{C} is more amyloidogenic than bovine or feline rPrP^{C}. A. Points indicate the average rate of amyloid conversion for each substrate (bovine, feline and white-tailed deer) upon addition of artificial truncated bank vole rPrP^{ThT+}. B. Points indicate the rate of amyloid conversion for each substrate upon the addition of artificial truncated Syrian hamster rPrP^{ThT+}. Error bars represent the standard error of the mean (SEM) (A-B). C and D. Each line represents the average ThT fluorescence for 4 replicates for each seed-substrate combination and the dotted line indicates the threshold for determination of the lag phase.

RT-QuIC with full-length rPrP^{C} recapitulates BSE and CWD species barriers in vitro.

We hypothesized that RT-QuIC would reflect *in vivo* species barriers, as defined by preferential seeding of the native host species rPrP^{C}. We found the native prion of a given species to be most compatible (the fastest conversion to amyloid) with its host substrate. To demonstrate an *in vitro* species barrier, we added cBSE or CWD PrP^{Sc} to the non-homologous rPrP^{C} substrate. As anticipated, CWD converted full-length white-tailed deer rPrP^{C} faster than it did full-length bovine rPrP^{C} (Fig. 3.3A,C).

Likewise, cBSE seeded full-length bovine rPrP^{C} relatively faster than full-length white-tailed deer rPrP^{C} (Fig. 3.3B,D). Thus, RT-QuIC recapitulated the *in vivo* species-seeding proclivities of CWD and cBSE prions.

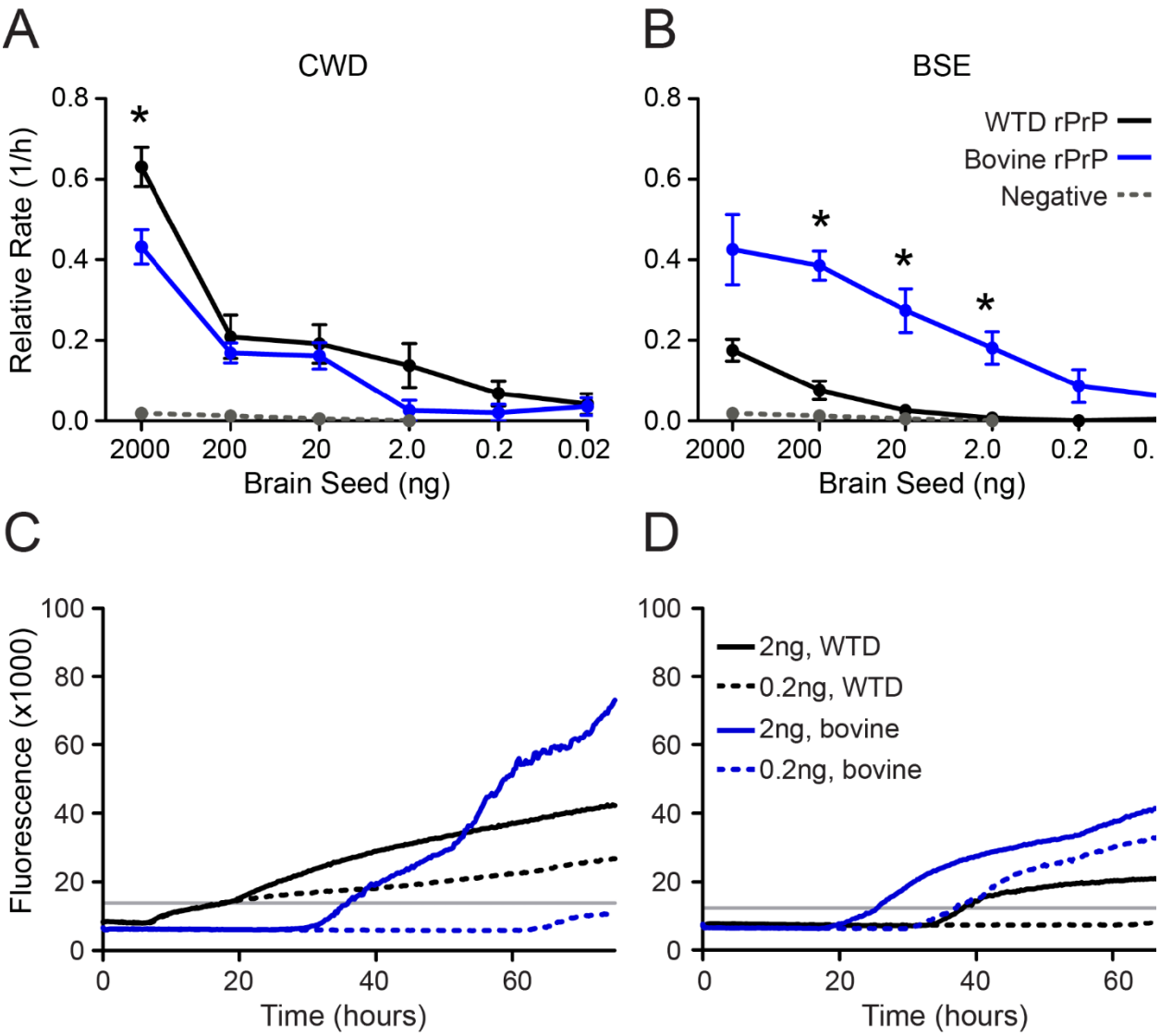

Figure 3.3. Preference for intra-species conversion by BSE and CWD prions was recapitulated in RT-QuIC. A. CWD was seeded into white-tailed deer rPrP^{C} (black line), or bovine rPrP^{C} (blue line). B. BSE was seeded into white-tailed deer rPrP^{C} (black line) or bovine rPrP^{C} (blue line). Each point represents the relative rate of amyloid conversion for each seed concentration (ng) and the error bars represent SEM. The rate of spontaneous amyloid conversion is designated by the dotted gray line in A and B. Significant differences between substrates were tested by the MWU test ($p<0.05$ indicated by *) or the WSR test ($p<0.05$ indicated by #). C and D. Each line represents the average ThT trace for 6 replicates of 3 dilutions of each seed/substrate combination and the gray line indicates the threshold for determination of the lag phase.

Characteristics of cBSE and cBSE-derived prions are conserved after trans-species transmission.

cBSE and CWD are prion diseases that have been naturally passaged in their respective species (cattle and deer), whereas FSE and fCWD are first-passage infections in a new host species. To investigate the biochemical properties of cBSE and CWD after trans-species transmission to felines, we compared the amyloidogenicity of fCWD and FSE in the original host and in feline substrate. We found fCWD to be a more efficient seed for its new (feline) host, suggesting that adaptation to the new host had occurred (Fig. 3.4A). By contrast, FSE remained a more efficient seed for its enciphering (bovine) host, despite its derivation from feline brain PrP^{C} (Fig. 3.4B). These cross-species seeding experiments in RT-QuIC suggest that cBSE may retain its ability to cross species barriers even after transmission to a new host species and that CWD may change substantially upon trans-species transmission.

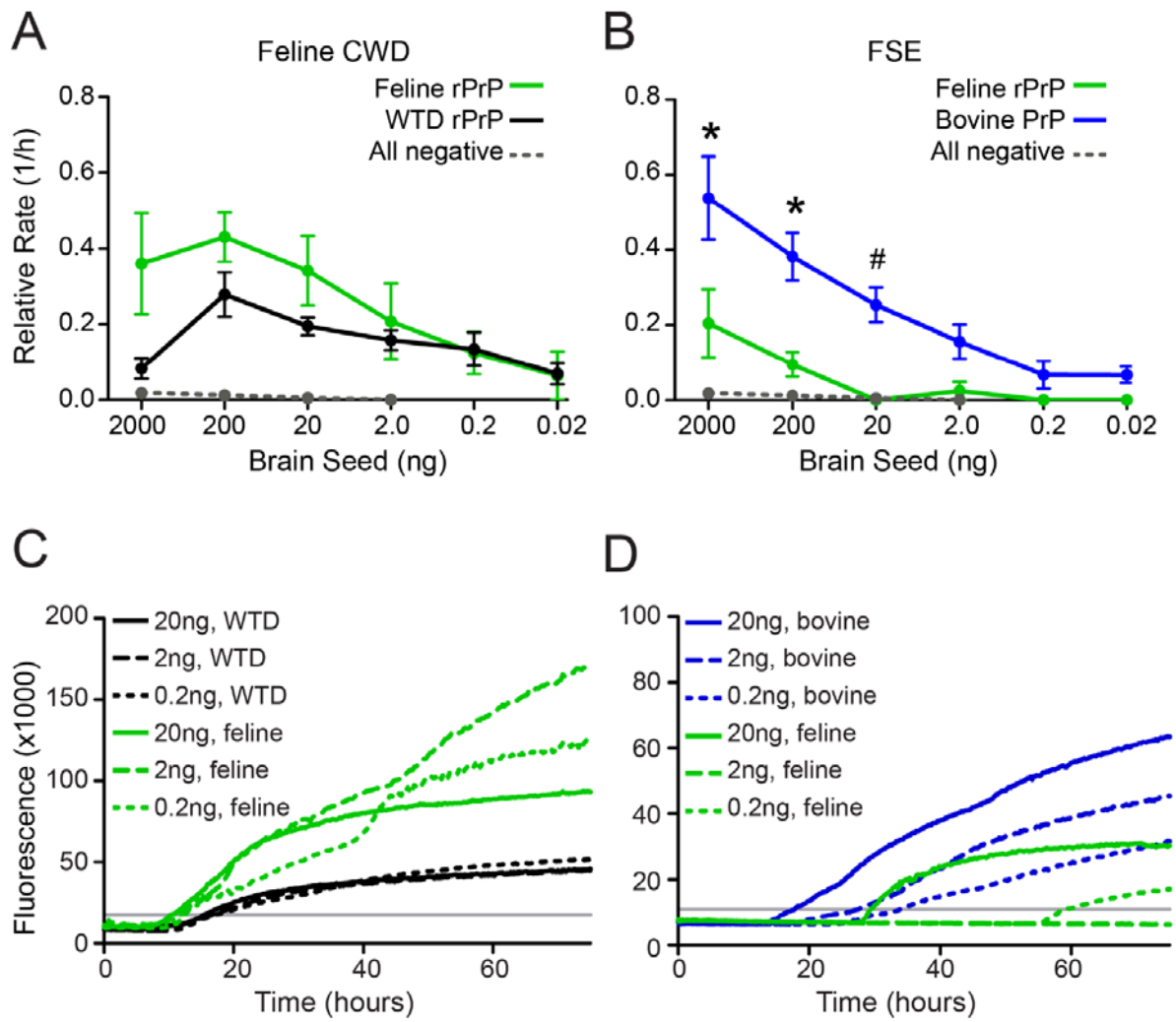

Figure 3.4. Prions from felines infected with BSE maintain original species characteristics, while prions from felines infected with CWD are adapted to the new species. A. Points indicate the average rate of amyloid conversion for white-tailed deer $rPrP^C$ (black line), or feline $rPrP^C$ (green line) upon seeding with an fCWD seed. B. Points indicate the rate of amyloid conversion for bovine $rPrP^C$ (blue line) or feline $rPrP^C$ (green line) upon addition of an FSE seed. The rate of spontaneous amyloid conversion is designated by the dotted gray line and error bars represent SEM. Significant differences between substrates were tested by the MWU test ($p<0.05$ indicated by *) or the WSR test ($p<0.05$ indicated by #). C-D. Each line represents the average ThT trace for 6 replicates of 3 dilutions of each seed/substrate combination and the gray line indicates the threshold for determination of the lag phase.

Human $rPrP^C$ can be converted by bovine, feline and cervid prions.

The threat of zoonotic transmission of prion disease is evident and well-documented, yet uncommonly observed and incompletely understood. We thereby explored the propensity of heterologous prions to convert human $rPrP^C$. We used sporadic CJD (sCJD) brain as a positive control, and normal bovine, white-tailed deer and feline brain as negative controls. sCJD, as expected, seeded human $rPrP^C$

most efficiently, so all other seeds were normalized to the rate of conversion of sCJD. We found human $rPrP^{C}$ to be a competent substrate in RT-QuIC for CWD, fCWD, cBSE and FSE (Fig. 3.5A). Interestingly, CWD and fCWD converted human $rPrP^{C}$ more efficiently than did cBSE and FSE. These data suggest that at the level of PrP^{C}-PrP^{Sc} interaction, CWD has the ability to template the conversion of human $rPrP^{C}$ to amyloid. To assess whether CWD was faster than cBSE due to an increased concentration of PrP^{Sc}, we performed western blots on the inocula. Western blots indicated that the cBSE sample had more PrP^{Sc} than the CWD sample, indicating that CWD did not appear to be a better seed than cBSE due to PrP^{Sc} titer (Fig. 3.5B). Finally, we assessed the behavior of 8 CWD field isolates, brain samples from white-tailed deer infected naturally and verified to be positive using full-length white-tailed deer PrP^{C} in RT-QuIC (Fig. 3.5C). All 8 of the isolates induced amyloid formation in human $rPrP^{C}$, confirming that our observations were not due to the use of experimental CWD (Fig. 3.5D). In all, these experiments suggest that the CWD prions naturally circulating in the western USA have the capacity to convert human $rPrP^{C}$ in this assay of protein-protein interactions.

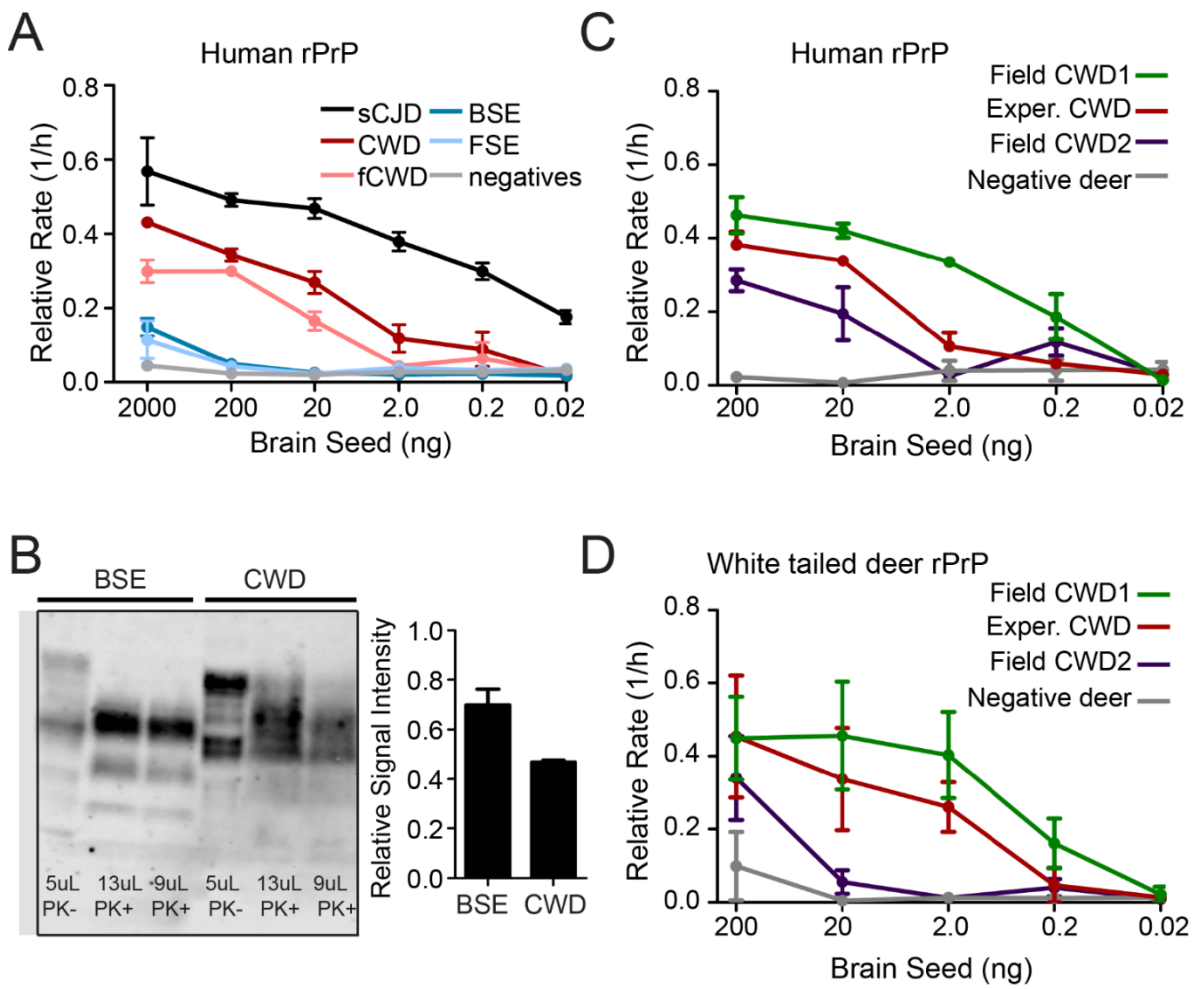

Figure 3.5. CWD is capable of efficiently seeding the conversion of human rPrP^{C}. A. Points represent the average rate of conversion of full-length human M129 rPrP^{C} by sporadic CJD (black line), CWD (red line), fCWD (pink line), BSE (dark blue line) and FSE (light blue line). Error bars indicated SEM. The rate of spontaneous amyloid conversion is indicated by the gray line. B. Western blot of BSE and CWD. PK-digested lanes indicate the presence of more PrP^{Sc} in the BSE sample than in the CWD sample. Densitometry indicates that BSE has more PrP^{Sc}/µL relative to total undigested PrP/µL than does CWD. C. Points indicate the average rate of amyloid conversion for multiple field isolates of CWD in full length human M129 rPrP^{C}. The gray line indicates the rate of spontaneous amyloid conversion. D. Points indicate the average rate of amyloid conversion for multiple field isolates of CWD in full length white-tailed deer rPrP^{C}. The gray line indicates the rate of spontaneous amyloid conversion.

Discussion

Despite decades of investigation, complete characterization of barriers to trans-species transmission of prion diseases remains elusive. Many animals, including multiple lines of transgenic mice, have been inoculated with various prions to define prion disease species barriers and to understand the effects of passage into a new host. Likewise, *in vitro* assays have been used to model propensities for

trans-species conversion of PrP^C to amyloid. We chose RT-QuIC because it permits observation of amyloid conversion in real-time and, consequently, comparison of the conversion efficiency of seed (PrP^{Sc}): substrate ($rPrP^C$) combinations.

We report that cBSE, after passage to felids in the form of FSE, remained a more efficient seed for the prion protein of the enciphering (bovine) host than for the new (feline) host (Fig. 3.4). This pattern has been observed in other contexts as well: cBSE-derived prions maintain many of their characteristics upon experimental or natural transmission to a new species (147, 344). We show that the features of cBSE are maintained as a result of the prion conformation and not solely due to cellular cofactors. Conversely, fCWD was a more efficient seed for the new (feline) host than for the enciphering (white-tailed deer) host (Fig 3.4). This result suggests that when felids are infected with CWD, the resulting fCWD has adapted to the new host. This appears to be an example of the difference between prions that adapt to new hosts upon passage and amplification that occurs without adaptation (92). It would be interesting to test other passaged BSE and CWD samples, particularly in light of the evidence for prion strains. The behavior of the fCWD and FSE in this paper may be dependent on the particular CWD and BSE samples that infected the cats, but examples of trans-species transmission of prions are rare and samples are not plentiful.

We also assessed the seeded conversion of human $rPrP^C$ by BSE, CWD, FSE and fCWD. Previous *in vitro* work using PMCA and two seeded fibrillization assays found human (polymorphism M129) PrP^C to be a weakly competent substrate for conversion by CWD and cBSE (268, 269, 342). We demonstrate that both FSE and fCWD have the ability to seed human $rPrP^C$ as well. Our finding that cBSE was a poor, if not ineffective, seed for human $rPrP^C$ in RT-QuIC was also observed by Orrú, et al. (346). By contrast, our finding that CWD is an efficient seed for human $rPrP^C$ (albeit not as efficient as human sCJD) differs from previous results using PMCA or other seeded fibrillization assays (268, 269, 342). Perhaps the disparities between these *in vitro* assays reflect the fact that RT-QuIC measures the rate of amyloid conversion (indicating the initial trans-species seeding) vs. total PrP^{Sc} after conversion (266, 268, 269, 342, 343). We understand the rate of amyloid conversion to depend on both the quantity of

prion in the seed and the competence of the seed to convert the substrate (305). Because our cBSE brain seed had a higher concentration of PrP^{Sc} relative to the total PrP than did our CWD brain sample, we interpreted the increased rate of amyloid conversion in human $rPrP^{C}$ to reflect the relative compatibility of seed with substrate, not a difference in PrP^{Sc} content. Indeed, our analysis supports the notion that human $rPrP^{C}$ is a competent substrate for several non-human prions. Of course, we also understand that any *in vitro* estimation of prion species barriers carries the innate caveats of a reductionist model of complex *in vivo* processes.

In summary, recapitulation of the species barrier phenomenon in RT-QuIC demonstrates that CWD and BSE prions differ in their tendency to adapt. These experiments also demonstrate that human $rPrP^{C}$ can be converted to amyloid by both cBSE and CWD prions. These data point to the importance of the mechanisms by which prions infect a new species, and prompt continued vigilance for transspecies prion transmission.

CHAPTER 4: ASSESSMENT OF THE AMINO-TERMINAL DOMAIN IN PRION SPECIES BARRIERS[3]

Summary

Chronic wasting disease (CWD) in cervids and bovine spongiform encephalopathy (BSE) in cattle are prion diseases that are caused by the same protein-misfolding mechanism, but appear to pose different risks to humans. We are interested in understanding the differences between the species barriers of CWD and BSE. We used real-time, quaking-induced conversion (RT-QuIC) to model the central molecular event in prion disease, the templated misfolding of the normal prion protein, PrP^{C}, to a pathogenic, amyloid isoform, PrP^{Sc}. We examined the role of the PrP^{C} amino-terminal domain (NTD, aa23-90) in cross-species misfolding by comparing the conversion efficiency of various prion seeds in either full-length (aa23-231) or truncated (aa90-231) PrP^{C}. We demonstrate that the presence of white-tailed deer and bovine NTDs hindered seeded conversion of PrP^{C}, but human and bank vole NTDs did the opposite. Additionally, full-length human and bank vole PrP^{C} were more likely to be converted to amyloid by CWD prions than were their truncated forms. A chimera made with replacement of the human NTD by the bovine NTD resembled human PrP^{C}. The requirement for an NTD, but not for the specific human sequence, suggests that the NTD interacts with other regions of the human PrP^{C} to increase promiscuity. These data contribute to the evidence that prion species barriers are controlled by interactions of the substrate NTD with the rest of the substrate PrP^{C} molecule, in addition to compatibility of primary sequence.

Background

CWD, BSE and Creutzfeldt-Jakob disease (CJD) are prion diseases of cervids, cattle, and humans, respectively. These neurodegenerative diseases are caused by the pathogenic misfolding of the

[3] Copyright © American Society for Microbiology, [Journal of Virology, Volume 90, 2016, 10752-10761, 10.1128/jvi.01121-16]

normal prion protein (PrP^{C}) to an amyloid conformation (PrP^{Sc}), the accumulation of which causes neuronal death (15, 16). CWD was first identified in the western United States in the 1980s in captive mule deer (*Odocoileus hemionus*) (271) and has since spread into free-ranging and farmed cervid populations in 24 US states, Norway, the Republic of Korea and two Canadian provinces (61). BSE was identified in the United Kingdom in the 1980s and is hypothesized to have been spread as a result of feeding animal by-products to cattle (8, 347). The BSE epidemic led to the culling of nearly 5 million cattle and over 200 people died from variant CJD, a form of CJD acquired from consumption of BSE-tainted beef (10, 11, 91, 145-147). So far, there is no evidence of transmission of CWD to humans, but the BSE epidemic indicates that prions have zoonotic potential.

Efforts to define the host range of both BSE and CWD have included experimental infections of non-host species. CWD inoculations have resulted in prion propagation in cattle, sheep, hamsters, voles, felines, ferrets, and some non-human primates (233, 234, 236-238, 337, 348, 349). BSE inoculations have resulted in prion propagation in deer, sheep and some non-human primates (144, 241-244, 350). Moreover, natural BSE infections occurred in felines and several species of zoo ungulates, in addition to humans (10, 11, 146). Transgenic mice expressing human PrP^{C} (TgHu) have been used to model human susceptibility to animal prion diseases. Published reports of CWD inoculation of TgHu mice have reported no prion propagation, although studies employing protein misfolding cyclic amplification (PMCA) have yielded more ambiguous results (267). Prion propagation has been reported in approximately 50% of TgHu mice inoculated with BSE (155, 249-255). Despite these reports, prion species barriers remain mostly empirical. While the most important known factor in trans-species transmission is the compatibility of the PrP^{C} amino acid sequences, there is evidence that the tertiary and quaternary structure of PrP^{Sc} also influence prion transmission (56, 93, 261, 263).

Multiple studies have identified specific PrP^{C} regions that may control susceptibility or resistance to conversion by non-homologous prions, but the role of the amino-terminal domain (NTD, we define as amino acids 23-90, following mouse numbering) in species barrier maintenance has not been tested (264, 265). Transgenic mice with an amino-terminal PrP^{C} truncation that resulted in expression of only amino

acids (aa) 90-231 had no overt changes in phenotype compared to wild-type mice, while larger truncations caused spontaneous neurodegenerative disease (351). A transgenic mouse expressing chimeric mouse-hamster PrP^{C} (aa90-231) had reduced susceptibility to prion infection compared to mice that expressed full-length chimeric PrP^{C}, and susceptibility varied with the strain of mouse-adapted scrapie used for infection (352). Mice that expressed mouse aa90-231 propagated prions upon inoculation, but had delayed disease onset and lower PrP^{Sc} titers compared to mice that expressed full-length PrP^{C} (353). Mice expressing mouse aa88-231 had reduced susceptibility to infection compared with mice expressing full-length PrP^{C}, but disease onset was accelerated when the inoculum consisted of PrP^{Sc} with the same truncation (354, 355). Finally, mice expressing Δ34-124 had prions with different protease-resistant bands, which were similar to bands observed when the mouse-hamster prion species barrier was crossed (356). Overall, these results suggest that amino acids 23-90 are involved in prion propagation and disease progression.

Evidence from *in vitro* studies indicates that the amino-terminal fragment of the prion protein (amino acids 23-144) misfolds easily without addition of a prion seed, and that the human fragment converted faster than did the hamster or mouse fragment (357). Other investigators determined that the aggregation mechanism and resulting aggregate morphology were heavily dependent on pH and truncation of the protein (90-231 vs. full-length) (358, 359). The NTD interacts with the cell adhesion molecule NCAM, suggesting that the NTD is involved in the physiological role for PrP^{C} (360). Finally, melanin has been shown to inhibit PrP^{C} misfolding in cell culture, and to be associated with the NTD (361). These *in vitro* data indicate that the absence of aa23-90 has dramatic effects on the mechanism and likelihood of misfolding. We were interested in the role of aa23-90 not only for its effect on amyloidogenicity, but for its role in preventing (or facilitating) templated misfolding between species.

We chose to compare full-length $rPrP^{C}$ (aa23-231) to truncated $rPrP^{C}$ comprised of aa90-231 for several reasons: (1) the PrP27-30 fragment, an important molecule identified early in prion disease research, is comprised of amino acids 90-231 (362); (2) amino acids 23-90 comprise the N2 cleavage product in the disease state (363); and (3) the aa90-231 fragment is commonly used as the substrate for

prion detection in RT-QuIC (364). Specifically, we hypothesized that the NTD decreases an $rPrP^C$ molecule's propensity to form amyloid and that it plays a role in defining *in vitro* species barriers. We have assessed species barriers using RT-QuIC because: (1) it makes possible assessment of conversion efficiency (by detection of amyloid formation in real time); and (2) we can study the effects of changes to the $rPrP^C$ primary structure without the complexity of a transgenic mouse or cell culture system.

Methods

Recombinant PrP^C ($rPrP^C$) cloning and expression

The coding regions for the bank vole and bovine prion protein (*PRNP*) were kindly provided by Drs. Glenn Telling and Jifeng Bian and we obtained cDNA for the white-tailed deer, human and chimeric *PRNP* from Genewiz, Inc. We cloned the sequences for the full-length PrP (amino acids 23-231) into the pet100D expression system (Life Technologies). We cloned the sequences for the truncated PrP (amino acids 90-231) into a vector kindly provided by Dr. Byron Caughey. We transformed and amplified the plasmids in *E. coli* Top 10 cells (Life Technologies), then stored the plasmids in *E. coli* BL21 Star cells (Life Technologies) in glycerol stocks at -80C. To express $rPrP^C$, we added BL21 cells from the glycerol stock to 5mL LB media and antibiotics (5μg/mL ampicillin for full-length constructs and 25μg/mL kanamycin for truncated constructs) and grew the culture overnight, shaking at 37°. We used the 5mL culture to inoculate 1L LB media plus antibiotics as described above. We added auto-induction reagents for a final concentration of 0.5M $(NH_4)_2SO_4$, 1M KH_2PO_4, 1M Na_2HPO_4, 0.5% glycerol, 0.05% glucose, 0.2% α-lactose and .001M $MgSO_4$. We harvested the bacteria when the OD_{600} reached approximately 3.0 for full-length constructs and 1.7 for truncated constructs. We either froze the cell pellets at -80C for up to 5 days or immediately lysed the cells and harvested inclusion bodies, which we isolated according to manufacturer's protocol with Bug Buster™ and Lysonase™ (EMD-Millipore).

Recombinant PrP purification

We solubilized inclusion bodies in 8M guanidine hydrochloride (GdnHCl) and 100mM Na_2HPO_4 and rotated the solution overnight at room temperature. We bound the denatured $rPrP^C$ to Superflow™ nickel resin (Qiagen) and refolded the $rPrP^C$ at a rate of 0.75mL/min on the column with a gradient from 6.0M GdnHCl, 100mM Na_2HPO_4, 10mM Tris (pH 8.0) to the same buffer with no GdnHCl (wash buffer). We used a gradient from the wash buffer to 1.0M imidazole, 100mM NaH_2PO_4, 10mM Tris (pH 5.5) with a flow rate of 2.0mL/min to elute full-length $rPrP^C$. For truncated $rPrP^C$, the final gradient ended with 0.5M imidazole. We filtered and dialyzed the eluted $rPrP^C$ at a concentration of ~.4mg/mL in two changes of 4.0L 20mM NaH_2PO_4 (pH 5.5). After dialysis, we filtered and stored the $rPrP^C$ at 4°C, its concentration having been determined by A_{280} and Beer's Law. We confirmed the purity of the $rPrP^C$ samples by gel electrophoresis (12% bis-tris gels with 1X MOPS [Bio-Rad], 190V, 55min) and staining with Coomassie Brilliant Blue (Bio-Rad).

Preparation of prion seed material

We homogenized brain tissue from deer, cattle or humans at 10% weight/volume in 1X PBS using a FastPrep bead beater (MB Biomedicals). Single-use aliquots of 10% homogenate were stored at -80°C. Both prion-positive and prion-negative brain material were prepared. Prion-positive brain material was used for the experiments, while prion-negative brain was used for the unseeded controls. The BSE sample is classical BSE (cBSE) and the sporadic CJD sample is MM1 (Type 1).

Real-time, quaking-induced conversion (RT-QuIC) for full-length rPrP

We combined 0.1mg/mL $rPrP^C$ with a pre-mixed reaction solution that contained a final concentration of 400mM NaCl, 1mM EDTA, 20mM NaH_2PO_4. Then, we added freshly-made thioflavin T (ThT; final concentration 10μM) for a final volume of 98μL per well in a 96 well plate. We thawed aliquots of 10% brain homogenate and serially diluted the samples into 1X PBS plus 0.1% SDS. We

added 2μL diluted brain seed to 98μL protein substrate mix in the well of an optical-bottom, 96-well plate. An RT-QuIC experiment consisted of 400 cycles (100 hours) of shaking and incubation at 45°C; specifically, plates were shaken for 1 minute (700rpm, double orbital) and 1 minute of rest. Fluorescence (450nm excitation and 480nm emission, 20 flashes/well) was recorded every 15 minutes using a gain of 1700 in a Fluostar microplate reader (BMG Labtech). To compare full-length PrP directly to truncated PrP with the same molarity (0.6nM), we increased the concentration of full-length $rPrP^C$ to 0.14mg/mL and the truncated rPrP to 0.10mg/mL (Fig 2). These conditions were optimized for use with full-length $rPrP^C$. For Figure 4, conditions were as follows: 0.6nM $rPrP^C$, 320mM NaCl, 0.1% SDS, 42ºC.

RT-QuIC for truncated PrP

We combined 0.07mg/mL $rPrP^C$ with a pre-mixed reaction solution that contained a final concentration of 320mM NaCl, 1mM EDTA, 20mM NaH_2PO_4. We added freshly-made thioflavin T (ThT; final concentration 10μM) for a final volume of 98μL per well in a 96 well plate. We thawed and serially diluted aliquots of 10% brain homogenate into 1X PBS plus 0.05% SDS. We added 2μL diluted brain seed to 98μL protein substrate mix in the well of an optical-bottom, 96-well plate. An RT-QuIC experiment consisted of at least 250 cycles (62.5 hours) of shaking and incubation at 42°C; specifically, plates were shaken for 1 minute (700rpm, double orbital), followed by 1 minute of rest. Fluorescence (450nm excitation and 480nm emission, 20 flashes/well) was recorded every 15 minutes using a gain of 1700 in a Fluostar microplate reader (BMG Labtech). These conditions were optimized for use with truncated rPrP.

Data analysis and statistics

The RT-QuIC read-out is fluorescence, which is recorded at 15 minute intervals (Fig. 4.1A). To assess the efficiency of reactions, we compared the lag phase for amyloid formation. First, we calculated a fluorescence threshold by averaging the baseline fluorescence for every well in the plate, then adding 5

standard deviations. We used Omega software (BMG Labtech) to determine the lag phase – the time at which the fluorescence in a given well exceeded the threshold (Fig. 4.1B). If the fluorescence for a sample never crossed the threshold during the experiment, we estimated a value of 105 hours (example is marked by an X symbol in Fig. 4.1B). Raw lag phase data are displayed as scatterplots with lines to indicate the median. We analyzed the lag phase data using non-parametric, rank-based tests (Wilcoxon-Mann-Whitney (WMW) and Wilcoxon signed-rank tests). If all values for one sample were equal, WMW tests are invalid, so we used Wilcoxon signed-rank tests instead. We chose these tests for several reasons: 1) our data was often non-normal (right skewed due to replicate wells that don't cross the threshold in the course of the experiment); 2) our n was relatively small (8-12); and 3) we had to choose values to substitute for the replicate wells that do not cross the threshold. The choice of that value would affect the mean (and the results of any statistical tests that relies on means, like t-tests), but will not affect rank-based statistical analysis, since those values will have the longest lag phase regardless of which value we choose. We chose to represent the median instead of mean for the same reason – the median is not affected by our choice of a value for wells that do not cross the threshold. We described differences as statistically significant when $p<0.05$, which is indicated by * or by brackets (Fig. 4.6).

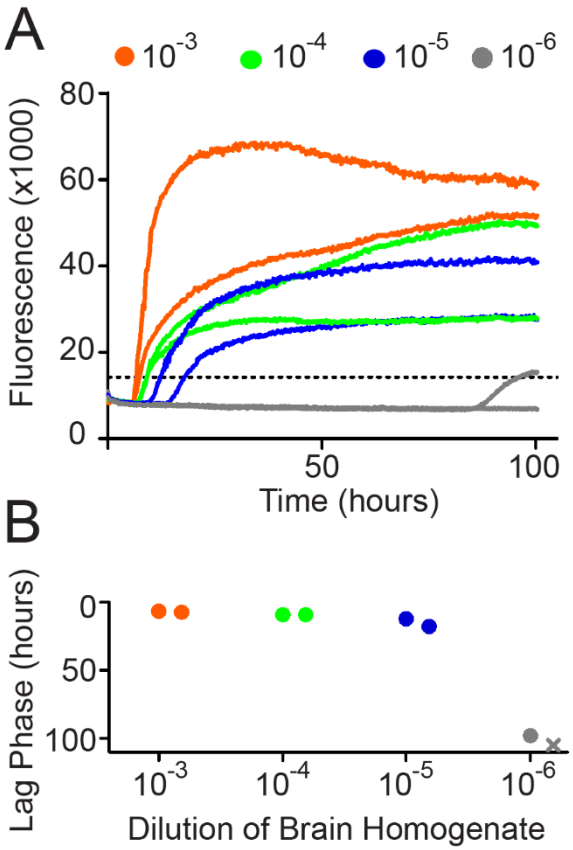

Figure 4.1. Data Analysis Workflow. A. Raw data was recorded as fluorescence every 15 minutes. We show two technical replicates for this example. B. We plotted the time required to reach the threshold (5SD above the mean background) vs. the dilution of 10% brain homogenate added to the reaction. The X indicates an estimated value for a sample that did not cross the threshold during the experiment. We have reversed the Y axis.

Results

Removal of the amino terminal domain affects efficiency of seeded conversion and increases spontaneous conversion of rPrP^C.

To investigate the effect of the NTD on the propensity of rPrP^C to form amyloid, we added the homologous prion seed (or negative brain material) to each species' rPrP^C, either truncated or full-length (e.g. CWD to deer PrP). To ensure that any differences in the median amyloid formation lag phase would be due to differences in the rPrP^C/seed compatibility, not other reaction conditions, we performed the RT-QuIC reactions with 0.6nM rPrP^C, salt, SDS, EDTA and at the same temperatures (the full-length conditions described in the Methods).

For all species, truncated rPrP^{C} was more prone to spontaneous conversion (after addition of negative brain material) than was the full-length substrate (Fig. 4.2A,C,E,G). The addition of cBSE brain to truncated bovine rPrP^{C} resulted in faster amyloid conversion than did addition of the same seed to full-length bovine rPrP^{C} (Fig. 4.2B). Likewise, the addition of CWD seed to truncated white-tailed deer rPrP^{C} resulted in faster amyloid conversion than addition of the same CWD material to full-length white-tailed deer rPrP^{c} (Fig. 4.2D).

The addition of sporadic CJD MM1 (sCJD) seed to truncated or full-length human rPrP^{C} (methionine at position 129) resulted in very fast amyloid conversion. However, conversion of the truncated human rPrP^{C} was significantly slower than the full-length human rPrP^{C} (Fig. 4.2F). Because the bank vole and human *PRNP* NTD sequences are very similar (Fig 4.3), we compared truncated to full-length bank vole rPrP^{C} as well. Like human rPrP^{C}, both the truncated and full-length bank vole rPrP^{C} formed amyloid very quickly upon addition of sCJD prions (which have been demonstrated to convert bank vole PrP effectively (53, 54)). Also like human rPrP^{C}, conversion of the full-length bank vole rPrP^{C} was statistically faster than truncated rPrP^{c} (365, 366)) (Fig. 4.2H). Because the conversion of human and bank vole rPrP^{C} was so fast, the data are also shown on a smaller scale (Fig. 4.4A,B).

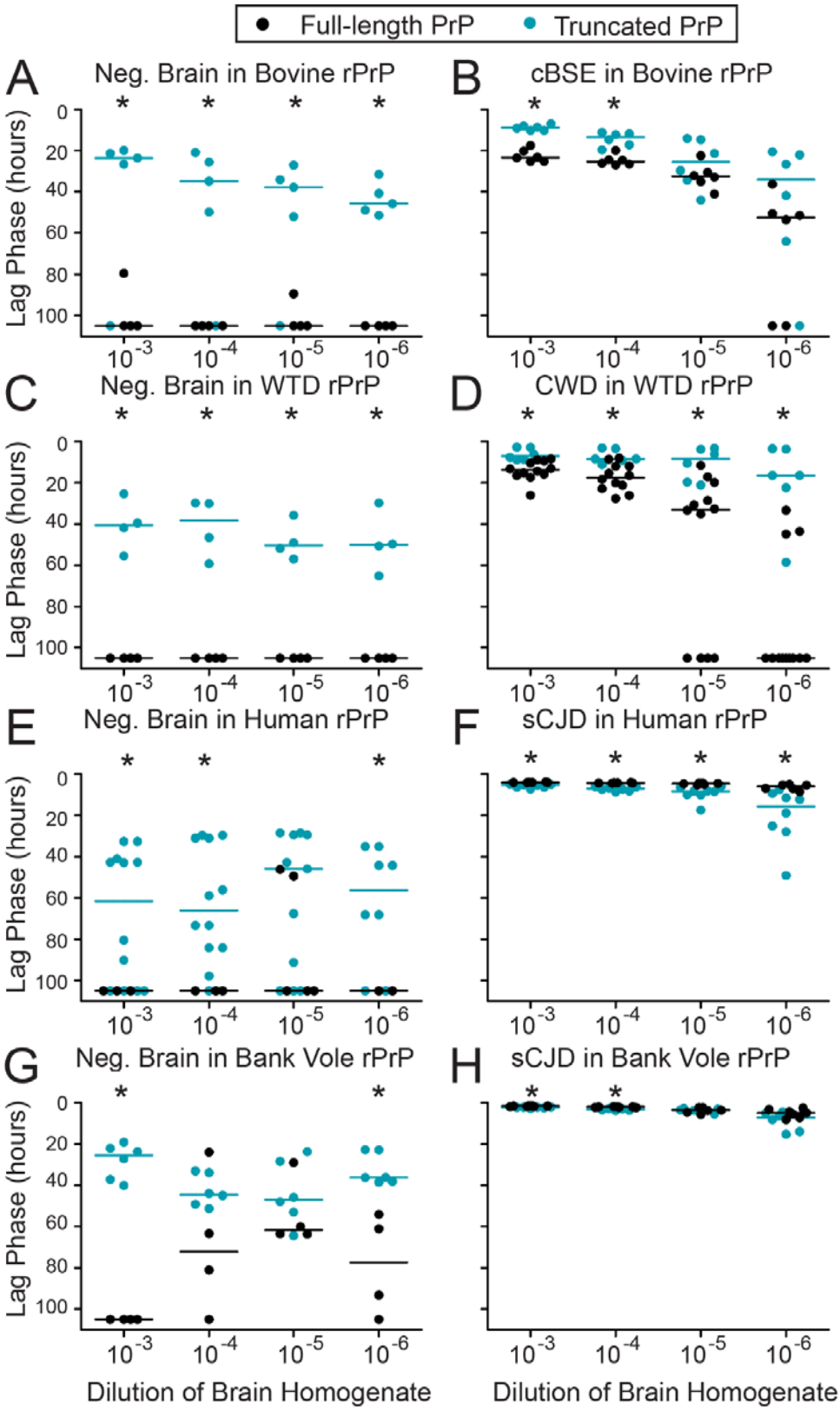

Figure 4.2. Removal of the amino terminal domain affects rate of seeded conversion and increases spontaneous conversion of rPrP. We added brain homogenate (prion-positive or negative) to the homologous substrate, in either its full-length or truncated version. Reaction

conditions were designed for increased amyloidogenicity and were the same for all experiments in this figure (RT-QuIC conditions for full-length PrP, as described in the methods). Scatterplots represent raw data and lines indicate the median. * indicates a difference between the lag phase for full-length and truncated substrates ($p<0.05$, WMW test). A. Truncated bovine rPrP spontaneously formed amyloid faster than full-length bovine rPrP (in the presence of normal brain homogenate). B. cBSE seeded truncated bovine rPrP faster than full-length. C. Truncated white-tailed deer rPrP spontaneously formed amyloid faster than full-length white-tailed deer rPrP (in the presence of normal brain homogenate). D. CWD seeded truncated white-tailed deer rPrP faster than full-length. E. Truncated human rPrP spontaneously formed amyloid faster than full-length human deer rPrP (in the presence of normal brain homogenate). F. sCJD seeded full-length human rPrP faster than truncated. G. Truncated bank vole deer rPrP spontaneously formed amyloid faster than full-length bank vole rPrP (in the presence of normal brain homogenate). H. sCJD seeded full-length bank vole rPrP faster than truncated.

```
N-Bo-Hu-C Chimera      KKRPKPGGGWNTGGSRYPGQGSPGGNRYPPQGGGGWGQPHGGGWGQPHGGGWGQPHGGGW
Bovine                 KKRPKPGGGWNTGGSRYPGQGSPGGNRYPPQGGGGWGQPHGGGWGQPHGGGWGQPHGGGW
N-Hu-Bo-C Chimera      KKRPKP-GGWNTGGSRYPGQGSPGGNRYPPQGGGGWGQPHGGGWGQPHGGGWGQPHGGGW
Bank Vole              KKRPKP-GGWNTGGSRYPGQGSPGGNRYPPQGGGTWGQPHGGGWGQPHGGGWGQPHGGGW
Human                  KKRPKP-GGWNTGGSRYPGQGSPGGNRYPPQGGGGWGQPHGGGWGQPHGGGWGQPHGGGW
                       ****** *************************** ************************

N-Bo-Hu-C Chimera      GQPHGGGWGQPHGGGGWGQGGTHSQWNKPSKPKTNMKHMAGAAAAGAVVGGLGGYMLGSA
Bovine                 GQPHGGGWGQPHGGGGWGQGGTHGQWNKPSKPKTNMKHVAGAAAAGAVVGGLGGYMLGSA
N-Hu-Bo-C Chimera      GQPHGGGWGQPHGGGGWGQGGTHGQWNKPSKPKTNMKHVAGAAAAGAVVGGLGGYMLGSA
Bank Vole              GQPHGGGWGQG--------GGTHNQWNKPSKPKTNIKHVAGAAAAGAVVGGLGGYMLGSA
Human                  GQPHGGGWGQG--------GGTHSQWNKPSKPKTNMKHMAGAAAAGAVVGGLGGYVLGSA
                       **********         **** ***********:**:****************:****

N-Bo-Hu-C Chimera      MSRPIIHFGSDYEDRYYRENMHRYPNQVYYRPMDEYSNQNNFVHDCVNITIKQHTVTTTT
Bovine                 MSRPLIHFGSDYEDRYYRENMHRYPNQVYYRPVDQYSNQNNFVHDCVNITVKEHTVTTTT
N-Hu-Bo-C Chimera      MSRPLIHFGSDYEDRYYRENMHRYPNQVYYRPVDQYSNQNNFVHDCVNITVKEHTVTTTT
Bank Vole              MSRPMIHFGNDWEDRYYRENMNRYPNQVYYRPVDQYNNQNNFVHDCVNITIKQHTVTTTT
Human                  MSRPIIHFGSDYEDRYYRENMHRYPNQVYYRPMDEYSNQNNFVHDCVNITIKQHTVTTTT
                       ****:****.*:*********.**********:*:*.*************:*:*******

N-Bo-Hu-C Chimera      KGENFTETDVKMMERVVEQMCITQYERESQAYYQRGS
Bovine                 KGENFTETDIKMMERVVEQMCITQYQRESQAYYQRGA
N-Hu-Bo-C Chimera      KGENFTETDIKMMERVVEQMCITQYQRESQAYYQRGA
Bank Vole              KGENFTETDVKMMERVVEQMCVTQYQKESQAYYEGRS
Human                  KGENFTETDVKMMERVVEQMCITQYERESQAYYQRGS
                       *********:***********:***::******:  :
```

Figure 4.3. Primary sequence alignment. The amino acid sequences of bovine, human, bank vole and the N-Hu-Bo-C and N-Bo-Hu-C chimeras are aligned. Green letters indicate differences between human and bovine NTD sequence and red letters indicate differences between bank vole and human PrP^c NTD sequence. The red bars indicate the junctions where human and bovine meet in the chimeras.

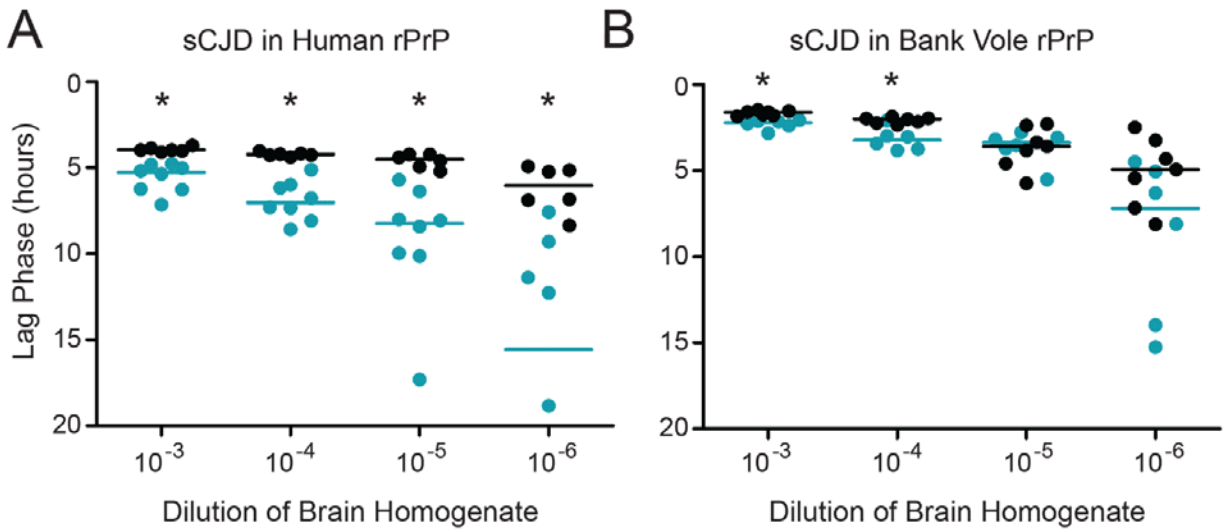

Figure 4.4. CWD converts human and bank vole rPrP very efficiently. This data is also displayed in Fig. 4.2, but is shown here on a smaller y-axis, which makes it easier to visualize the differences between the points. As described in Fig. 4.2, we added prion-positive human brain homogenate to A) human $rPrP^{c}$ substrate, in either its full-length or truncated version. B) We added prion-positive human brain homogenate to bank vole $rPrP^{c}$, in either its full-length or truncated form. Reaction conditions were designed for increased amyloidogenicity and were the same for all experiments in this figure (RT-QuIC conditions for full-length PrP, as described in the methods). Scatterplots represent raw data and lines indicate the median. * indicates a difference between the lag phase for full-length and truncated substrates ($p<0.05$, WMW test).

The amino terminal domain is not essential for preferential seeding of $rPrP^{C}$ species by native prions.

Once we completed the direct comparisons of truncated $rPrP^{C}$ to full-length $rPrP^{C}$, we modified the reaction conditions used for the truncated $rPrP^{C}$ to improve specificity. We decreased the salt, SDS, PrP concentration and temperature to reduce the amyloidogenicity of the reaction. Experiments in subsequent figures were performed with these more specific conditions (details in Methods).

We hypothesized that the NTD may play a role in defining an $rPrP^{C}$ molecule as bovine or human or white-tailed deer. For the RT-QuIC assay, we expect a prion seed to cause the most efficient conversion in its host substrate (93), but we hypothesized that this may no longer be the case upon removal of the NTD. Therefore, we added each prion of interest (cBSE, CWD, sCJD) to its homologous substrate and to a non-homologous substrate. For cBSE, CWD and sCJD, there was no indication that the NTD is necessary for the prion to preferentially seed its host $rPrP^{C}$. cBSE prions caused amyloid conversion faster in bovine $rPrP^{C}$ than non-host $rPrP^{C}$ (white-tailed deer), whether the $rPrP^{C}$ was amino-terminally-truncated or full-length (Fig. 4.5A-B). CWD prions converted white-tailed deer $rPrP^{C}$ faster

than non-host rPrP^{C} (bovine), whether the rPrP^{C} was truncated or full-length (Fig. 4.5C-D). sCJD prions caused amyloid conversion faster in human rPrP^{C} than in non-host (bovine), whether or not the rPrP^{C} was truncated (Fig. 4.5E-F). Therefore, the NTD was not essential for prion seeds to most efficiently seed their host rPrP^{C}. The amyloid formation in unseeded controls is indicated by the dotted lines in Fig. 4.5 and the distribution of those data is displayed in Fig. 4.6. Additionally, each data set in Fig. 4.5 was compared to unseeded controls and the results are shown in Table 4.1.

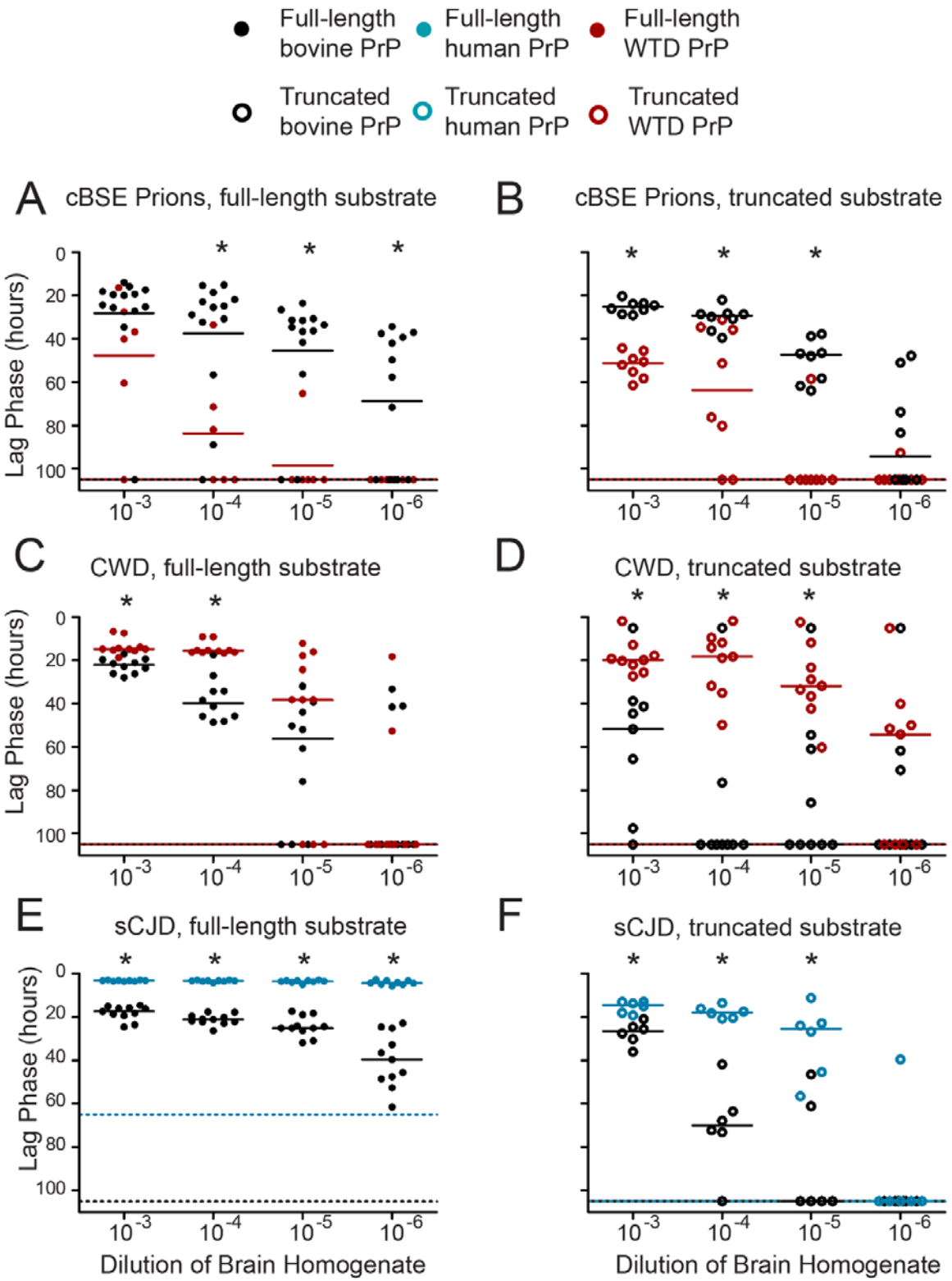

Figure 4.5. The amino terminal domain is not essential for preferential seeding of rPrP species by their native prions. We added prion-positive or prion-negative brain homogenate to both a homologous rPrP^{c} substrate and a non-host substrate, either truncated or full-length. We performed full-length rPrP experiments with RT-QuIC conditions for full-length PrP, as described in the methods. We performed truncated rPrP experiments with RT-QuIC conditions for truncated PrP, as described in the methods, and

unlike the conditions used in Fig. 4.2. Scatterplots represent raw data and lines indicate the median. Dotted lines indicate the median lag phase for unseeded misfolding for truncated substrates (colors indicate which species the line represents). * indicates a difference between the lag phase for the host and non-host substrate ($p<0.05$, MWM test). A. cBSE prions converted full-length bovine $rPrP^c$ faster than white-tailed deer $rPrP^c$. B. cBSE prions also converted bovine $rPrP^c$ faster than white-tailed deer $rPrP^c$ when the substrates were truncated. C. CWD prions converted white-tailed deer $rPrP^c$ faster than bovine $rPrP^c$ when the substrates were full-length. D. CWD prions converted white-tailed deer $rPrP^c$ faster than bovine $rPrP^c$ when the substrates were truncated. E. sCJD prions converted human $rPrP^c$ faster than bovine $rPrP^c$ when the substrates were full-length. F. sCJD prions converted human $rPrP^c$ faster than bovine $rPrP^c$ when the substrates were truncated.

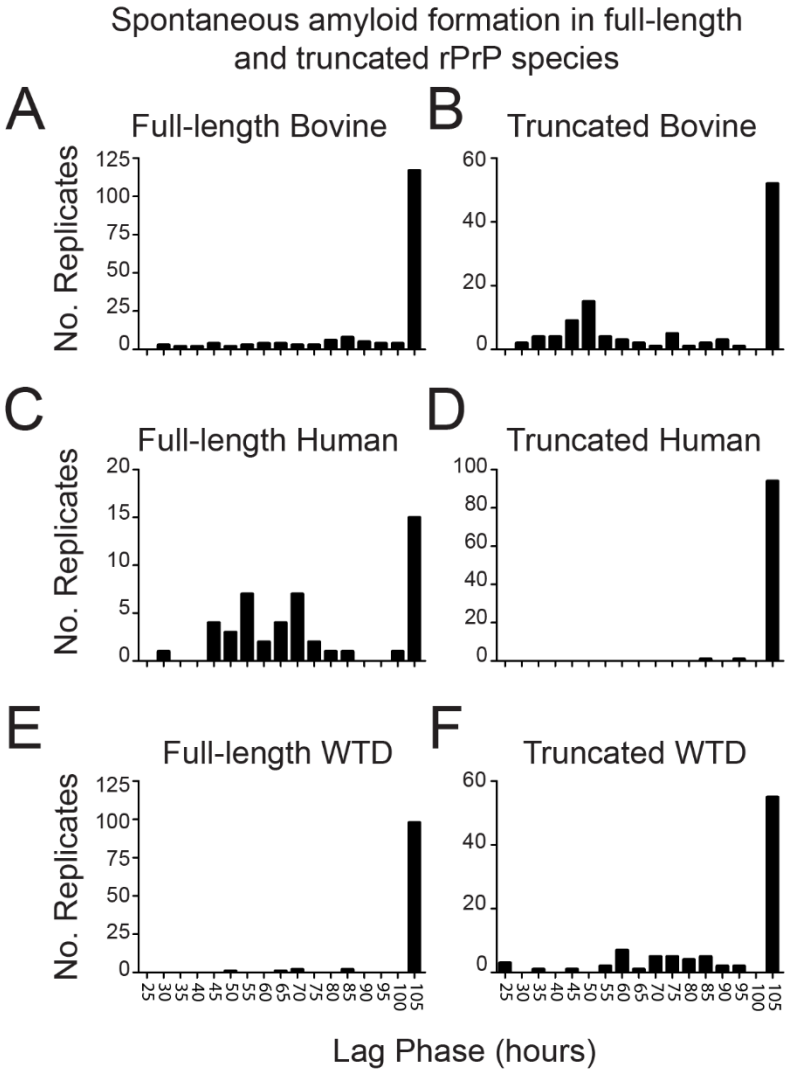

Figure 4.6. Distribution of unseeded controls. Frequency histogram of the negative controls (negative brain material) are displayed for A. full-length bovine substrate, B. truncated bovine substrate, C. full-length human substrate, D. truncated human substrate, E. full-length white-tailed deer (WTD) substrate, and F. truncated WTD substrate. The frequency of unseeded controls crossing the threshold is indicated by bar graphs for each lag phase.

Table 4.1. Statistical analysis of data in figure 4.5. Compare unseeded negative controls to seeded experiments.				
Figure	Prion Seed	Substrate	Dilution	Different from Unseeded Controls?
5A	BSE	FL Bovine	10^{-3}	P<0.05
5A	BSE	FL Bovine	10^{-4}	P<0.05
5A	BSE	FL Bovine	10^{-5}	P<0.05
5A	BSE	FL Bovine	10^{-6}	P<0.05
5A	BSE	FL WTD	10^{-3}	P<0.05
5A	BSE	FL WTD	10^{-4}	P<0.05
5A	BSE	FL WTD	10^{-5}	Not significant
5A	BSE	FL WTD	10^{-6}	Not significant
5B	BSE	Truncated Bovine	10^{-3}	P<0.05
5B	BSE	Truncated Bovine	10^{-4}	P<0.05
5B	BSE	Truncated Bovine	10^{-5}	P<0.05
5B	BSE	Truncated Bovine	10^{-6}	Not significant
5B	BSE	Truncated WTD	10^{-3}	P<0.05
5B	BSE	Truncated WTD	10^{-4}	P<0.05
5B	BSE	Truncated WTD	10^{-5}	Not significant
5B	BSE	Truncated WTD	10^{-6}	P<0.05
5C	CWD	FL WTD	10^{-3}	P<0.05
5C	CWD	FL WTD	10^{-4}	P<0.05
5C	CWD	FL WTD	10^{-5}	P<0.05
5C	CWD	FL WTD	10^{-6}	Not significant
5C	CWD	FL Bovine	10^{-3}	P<0.05
5C	CWD	FL Bovine	10^{-4}	P<0.05
5C	CWD	FL Bovine	10^{-5}	P<0.05
5C	CWD	FL Bovine	10^{-6}	Not significant
5D	CWD	Truncated WTD	10^{-3}	P<0.05
5D	CWD	Truncated WTD	10^{-4}	P<0.05
5D	CWD	Truncated WTD	10^{-5}	P<0.05
5D	CWD	Truncated WTD	10^{-6}	Not significant
5D	CWD	Truncated Bovine	10^{-3}	Not significant
5D	CWD	Truncated Bovine	10^{-4}	Not significant
5D	CWD	Truncated Bovine	10^{-5}	Not significant
5D	CWD	Truncated Bovine	10^{-6}	Not significant
5E	sCJD	FL Human	10^{-3}	P<0.05
5E	sCJD	FL Human	10^{-4}	P<0.05
5E	sCJD	FL Human	10^{-5}	P<0.05
5E	sCJD	FL Human	10^{-6}	P<0.05
5E	sCJD	FL Bovine	10^{-3}	P<0.05
5E	sCJD	FL Bovine	10^{-4}	P<0.05
5E	sCJD	FL Bovine	10^{-5}	P<0.05
5E	sCJD	FL Bovine	10^{-6}	P<0.05
5F	sCJD	Truncated Human	10^{-3}	P<0.05
5F	sCJD	Truncated Human	10^{-4}	P<0.05
5F	sCJD	Truncated Human	10^{-5}	P<0.05
5F	sCJD	Truncated Human	10^{-6}	P<0.05
5F	sCJD	Truncated Bovine	10^{-3}	P<0.05
5F	sCJD	Truncated Bovine	10^{-4}	Not significant

5F	sCJD	Truncated Bovine	10^{-5}	Not significant
5F	sCJD	Truncated Bovine	10^{-6}	Not significant

The amino terminal domain enables CWD conversion of human rPrP^{C} in vitro.

Above, we show that homologous prions are better seeds for their native rPrP^{C}, despite truncation (Fig. 4.5). However, when we assessed the behavior of *non-homologous* prions in human rPrP^{C}, we observed that the truncated human rPrP^{c} is less permissive to CWD prions than is the full-length human rPrP^{C} (Fig. 4.7A).

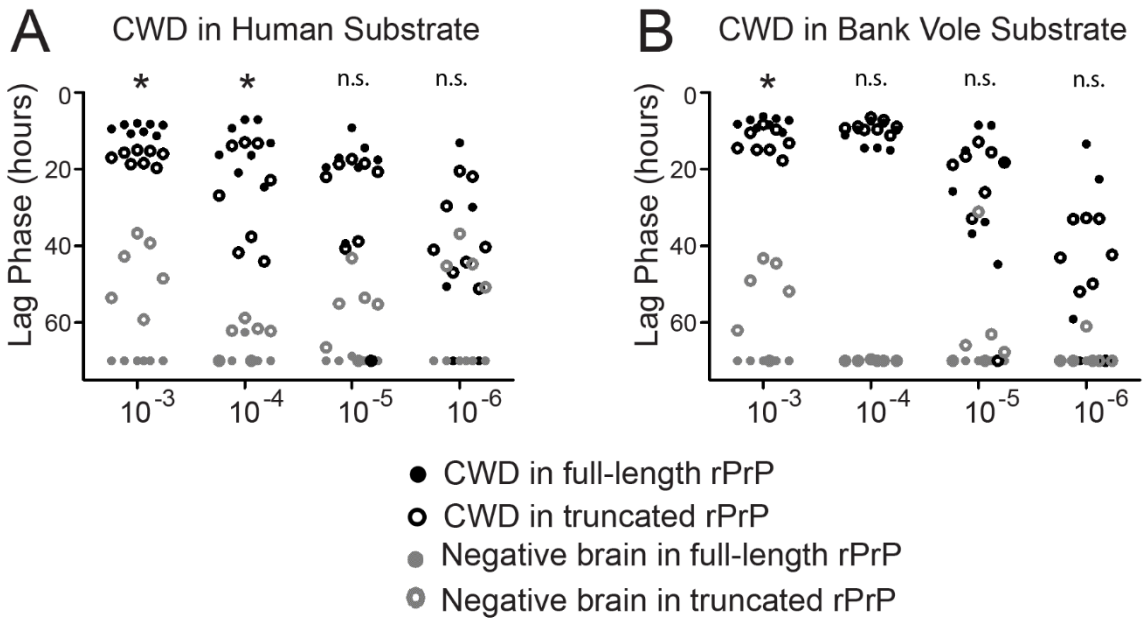

Figure 4.7. The amino terminal domain enables CWD conversion of human rPrP^{c}. A. We added prion-positive or prion-negative brain homogenate from white-tailed deer to truncated or full-length human rPrP^{C}. Experiments were under the same conditions, which are described in the methods. B. We added prion-positive or negative brain homogenate from white-tailed deer to truncated or full-length bank vole rPrP^{C}. Scatterplots represent raw data. * indicates that the differences in CWD susceptibilities are different between full length and truncated substrates ($p<0.05$, MWM test).

The amino terminal domain improves CWD conversion of bank vole rPrP^{C} in vitro.

Because bank vole and human PrP^{C} have only one amino acid difference in the NTD (Fig. 4.3), we hypothesized that the full-length bank vole rPrP^{C} may also be more susceptible to conversion by CWD prions than the truncated bank vole rPrP^{C}. We tested the effect of amino-terminal truncation on the

promiscuity of the bank vole rPrP^C (Fig. 4.7B). Again, CWD caused conversion slightly more efficiently in full-length bank vole rPrP^C than in truncated bank vole rPrP^C.

The human amino terminal domain does not increase susceptibility when substituted into another rPrP^C

Since the human NTD behaved differently than bovine or white-tailed deer in its effect on amyloidogenicity, we hypothesized that the human NTD may confer increased promiscuity to the molecule and that the substitution of the human NTD into bovine rPrP^C would increase the susceptibility of the chimeric rPrP^C to CWD prions. To test this hypothesis, we developed a chimera containing the human NTD and bovine carboxy-terminal domain (N-Hu-Bo-C). cBSE caused rPrP^C conversion with indistinguishable lag phases in the N-Hu-B-C chimera and bovine rPrP^C, which suggests that the NTD substitution does not reduce the homologous seeding of bovine rPrP^C with cBSE (Fig. 4.8A). sCJD prions converted the human rPrP^C faster than the N-Hu-Bo-C chimera, indicating that the human NTD alone was not sufficient to define the rPrP^C substrate as human (Fig. 4.8C). Finally, seeding efficiency with CWD was equivalent in the N-Hu-Bo-C chimera and in bovine rPrP^C, suggesting that the substitution of the human amino terminal domain did not increase the propensity of bovine rPrP^C to be converted by CWD prions (Fig. 4.8E).

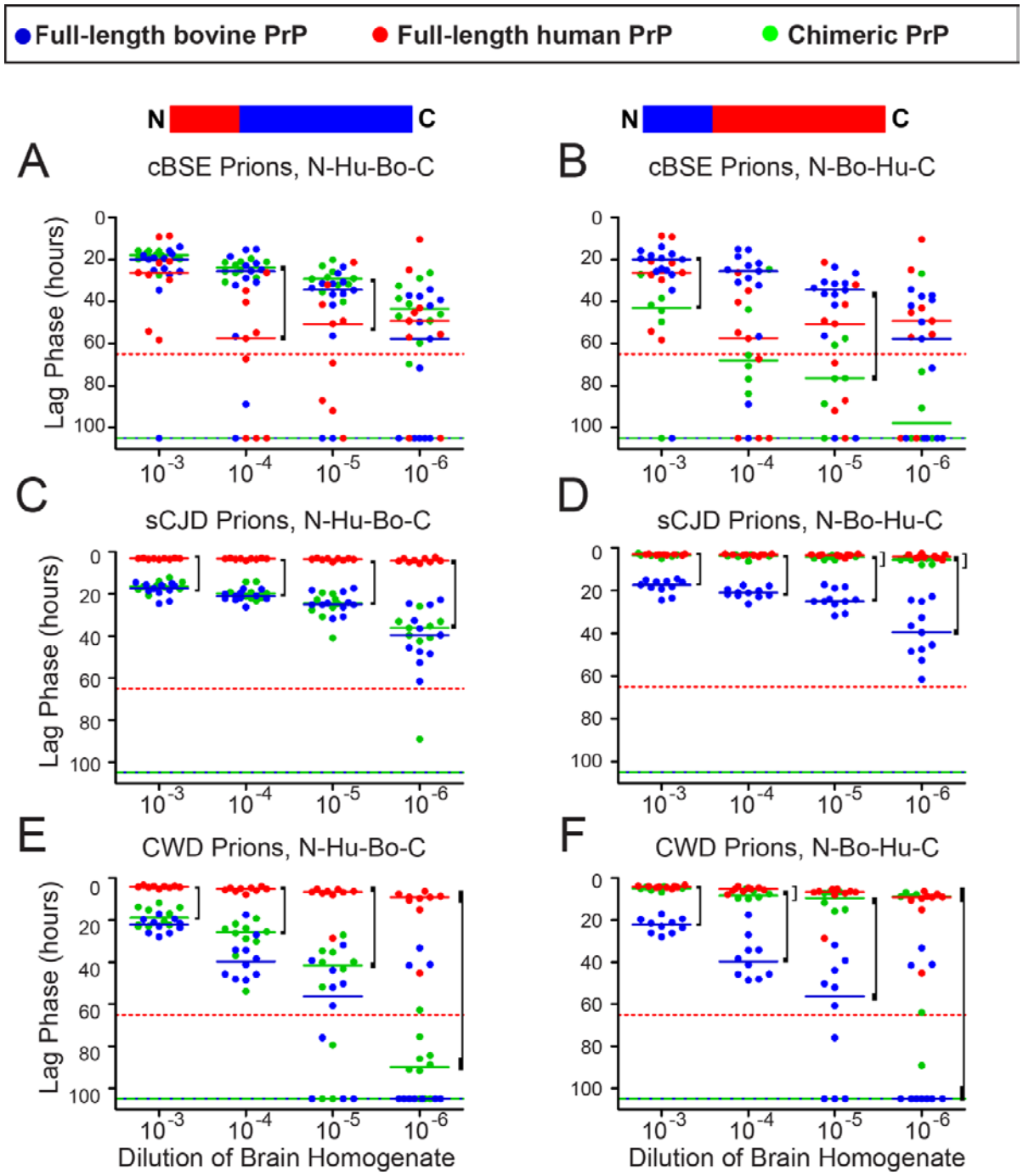

Figure 4.8. The human rPrP^{C} is susceptible to conversion by CWD prions regardless of its amino terminal domain sequence. However, the human amino terminal domain does not confer increased susceptibility to other species' rPrP^{C}. We added prion-positive or prion-negative brain homogenate from white-tailed deer (CWD), cattle (cBSE) or humans (sCJD) to full-length human, bovine or chimeric rPrP^{C}. These experiments used RT-QuIC conditions for full-length PrP, as described in the methods. Scatterplots represent raw data and lines indicate the median. Dotted lines indicate the median lag phase for unseeded misfolding for truncated substrates (colors indicate which species the line represents). Brackets indicate a significant difference between either full-length bovine or human and the chimera ($p<0.05$, WMW). A. cBSE prions convert bovine and N-Hu-Bo-C chimeric rPrP^{C} with the same efficiency, but human rPrP^{c} is slower. B. cBSE prions convert human and N-Bo-Hu-C chimeric rPrP^{C} with the same efficiency, while the

conversion of bovine rPrP^C is faster. C. sCJD prions convert bovine and N-Hu-Bo-C chimeric rPrP^C with the same efficiency, but human rPrP^C is faster. D. sCJD prions convert human and N-Bo-Hu-C chimeric rPrP^C with the same efficiency, while the conversion of bovine rPrP^C is slower. E. CWD prions convert bovine and N-Hu-Bo-C chimeric rPrP^C with the same efficiency, but conversion of human rPrP^C is faster. F. CWD prions convert human and N-Bo-Hu-C chimeric rPrP^C with the same efficiency, while the conversion of bovine rPrP^C is slower.

CWD prions convert human rPrP^C efficiently, regardless of amino terminal domain sequence.

Given the previous result, we alternatively hypothesized that human rPrP^C is susceptible to conversion by CWD prions independent of NTD sequence, as long as the NTD was present. We created the N-Bo-Hu-C chimera, which substitutes the bovine NTD for the human NTD, to investigate the importance of the NTD in the CWD species barrier. When we added cBSE prions to the N-Bo-Hu-C chimera, the conversion of the chimera was statistically indistinguishable from full-length human rPrP^C (Fig. 4.8B). When we added sCJD prions, the N-Bo-Hu-C chimera likewise was statistically indistinguishable from full-length human rPrP^C (Fig. 4.8D). Finally, when we added CWD prions, the chimera was statistically indistinguishable from full-length human rPrP^C (Fig. 4.8F). These results suggest that the presence of an amino terminal domain preserves the susceptibility of full length human rPrP^C to CWD prions, even if it does not have exactly the same sequence as the human NTD.

Discussion

The role of the PrP^C amino terminal domain (NTD, aa23-90) in the physiological role of PrP^C, disease progression and amyloidogenicity have been reported (352-354, 357-359, 367-369). However, the role of the NTD in trans-species transmission of prions has not been studied. Here, we used RT-QuIC to compare the conversion efficiency of white-tailed deer (WTD), bovine, bank vole or human PrP^C, with or without the NTD, in the presence of CWD, cBSE, sCJD or no prions.

We demonstrated that truncated (aa90-231) WTD, bovine, bank vole and human PrP^C spontaneously form amyloid faster than the full-length forms, which suggests that the NTD reduces the amyloidogenicity of PrP^C. However, the efficiency of conversion *in the presence of a prion seed* relies upon the compatibility of the prion seed with the substrate and upon the amyloidogenicity of the PrP^C

substrate. Truncated bovine and WTD rPrP^C formed amyloid faster than full-length rPrP^C upon addition of a seed, whereas truncated human and bank vole rPrP^C converted more slowly than full-length rPrP^C upon addition of a seed. This suggested that the NTD of human and bank vole may increase the compatibility of the seed and substrate in some way.

Next, we tested the effect of the NTD on the permissiveness of the rPrP^C to conversion by homologous and heterologous prions. cBSE, CWD and sCJD converted their native substrates more efficiently than non-native substrates, regardless of truncation. This suggested that a prion seed is able to recognize its host PrP^C with or without the NTD and that the NTD does not play an essential role in defining a PrP^C molecule as one species or another. We observed previously that human rPrP^C is susceptible to misfolding by CWD prions (93). Here, we demonstrated that CWD misfolded truncated human rPrP^C less efficiently than it misfolded full-length human rPrP^C, suggesting that the susceptibility of human rPrP^C to CWD prions may involve the NTD. The results are summarized in Table 4.2.

Table 4.2. Summary of results for NTD of various species' rPrP^c. See figures for more details.

Species PrP^C	**NTD role in permissiveness**	**NTD role in rate of misfolding**	**NTD required to recognize host**	**Chimera behaves like:**
Bank Vole	↑	↑	No	
Bovine	↔	↓	No	
Human	↑	↑	No	
White-tailed deer	↔	↓	No	
N-Hu-Bo-C				Bovine
N-Bo-Hu-C				Human
See Figure:	Fig. 4.5	Fig. 4.2	Fig. 4.5	Fig. 4.7

Chimeric PrP^C molecules are commonly used in prion research to focus on the region of the protein responsible for resistance to prion conversion (57, 64, 316, 370, 371). We were particularly interested in whether the NTD of human PrP^C could increase susceptibility to trans-species conversion by CWD prions, so we created a chimera with a human NTD substituted into bovine PrP^C (N-Hu-Bo-C) and a chimera with the bovine NTD substituted into human PrP^C (N-Bo-Hu-C). We hypothesized that the human NTD would increase promiscuity, so we tested the susceptibility of the N-Hu-Bo-C chimera to

seeded conversion. However, N-Hu-Bo-C was indistinguishable from bovine $rPrP^C$, whether homologous or non-homologous prions were used as seeds. We concluded that the human NTD alone did not confer additional susceptibility to conversion.

Alternatively, we hypothesized that the presence of *any* NTD to human substrate would have the effect of increasing the susceptibility of the chimera vs. the truncated $rPrP^C$. Indeed, we found that N-Bo-Hu-C had essentially the same permissiveness as full-length human $rPrP^C$ to conversion by human, cBSE and CWD prions. The importance of the NTD for human $rPrP^C$ susceptibility invokes transgenic mouse studies wherein truncation around amino acid 90 results in reduced attack rate and PrP^{Sc} accumulation (352, 353). It is possible that the human and bank vole PrP^C have a site in the globular domain that interacts with the NTD to facilitate seeded conversion, but not spontaneous conversion.

Together, the above data suggest that the PrP^C NTD alone does not control species barriers *in vitro,* but that interaction of the amino terminal domain with the rest of the protein may be involved in the susceptibility of human $rPrP^C$ to *in vitro* conversion by CWD prions. Multiple investigators have studied the role of specific regions of the PrP^C core and carboxy-terminal domain in prion disease species barriers. Reports have identified the β2-α2 loop and amino acids 165-175 as regions controlling trans-species transmission of prions, particularly of CWD prions to humans (255, 264). A favored interpretation of these data describes a steric zipper, wherein very few amino acid changes can severely disrupt the tertiary structure. Several polymorphisms between human and WTD PrP^C exist in this region, which may explain the apparent resistance of humans to CWD (56, 264). However, our data indicates that the variation in the β2-α2 loop does not prevent *in-vitro* conversion, which suggests that factors in addition to the PrP^C – PrP^{Sc} interactions we modeled *in vitro* must influence *in vivo* conversion.

Our empirical observation that unseeded conversion of truncated $rPrP^c$ was more efficient than full-length $rPrP^C$ made us wonder whether the NTD impeded conversion universally or in a species-specific manner, serving to protect against spontaneous misfolding or against trans-species infection. We hypothesized that the NTD may play a protective role in trans-species prion conversion, perhaps in addition to the β2-α2 loop. However, our data suggests that the NTD does not control trans-species prion

conversion, but that it may contribute to the promiscuity of human and bank vole $rPrP^{C}$. It is possible that the NTD, which is natively unfolded, has some interaction with other regions of the $rPrP^{C}$ or with the PrP^{Sc} seed. A recent report suggested a structural mechanism by which the NTD may interact with the globular domain (372). These observations suggest that full-length protein should be used in structural studies of human PrP^{C} and the mechanisms of its seeded or spontaneous conversion.

We found that human $rPrP^{C}$ can be readily converted to an amyloid state by CWD prions, and that the NTD facilitates this conversion. As there is little evidence for the susceptibility of humans to CWD, the biologic significance of our observation remains to be determined. However, the role of the NTD in this *in vitro* phenomenon may be important to the *in vivo* mechanism as well. RT-QuIC, transgenic mouse bioassay, and protein misfolding cyclic amplification (PMCA) measure different outcomes. This manuscript compares the efficiency of initial amyloid formation, while bioassay and PMCA reflect total accumulation of protease-resistant PrP^{Sc}, which may explain the difference in the apparent susceptibility of full-length human $rPrP^{C}$ in these models. The molecular underpinnings for species barriers and trans-species prion conversion remain a complex, important problem in prion biology. We propose that an interaction between the amino terminal domain and the globular domain facilitates *in vitro* susceptibility of human $rPrP^{C}$ to conversion by CWD prions. Such an interaction may be important when considering the susceptibility of humans to animal prion diseases.

CHAPTER 5: WHITE-TAILED DEER SALIVA CONTAINS INHIBITORS OF AMYLOID FORMATION IN RT-QUIC

Summary

Chronic wasting disease (CWD) is the prion disease of cervids, and involves the conversion of a normal protein, PrP^{C} to an abnormal conformation, PrP^{Sc}. PrP^{Sc} is autocatalytic and the conversion of PrP^{C} to PrP^{Sc} propagates. PrP^{C} is expressed throughout the deer, and PrP^{Sc} has been identified in many tissues and in excreta. CWD is unique in its facile horizontal transmission, which has resulted in a dramatic expansion of the geographic range and prevalence of CWD since its discovery in the 1980s. Infectious prions have been identified in saliva, and there have been several attempts to quantify PrP^{Sc} in saliva. The introduction of ultra-sensitive prion detection techniques like real-time, quaking-induced conversion (RT-QuIC) has made the detection of very low levels of prions possible.

However, detection of seeding activity in saliva with RT-QuIC is hampered by imperfect sensitivity and specificity, despite the development of several approaches to improve specificity and sensitivity. Here, we describe an RT-QuIC inhibitor in saliva, confirm that inhibition is not due to protease activity, and suggest that the inhibitor is a mucin protein. Recognition and characterization of RT-QuIC inhibitors in saliva and other biological samples is crucial to understand the frequency and magnitude of prion shedding in saliva and to understand CWD horizontal transmission.

Background

CWD has spread across much of the western United States since its identification in the 1980s (61, 271). It is clear that horizontal transmission is common in wild and captive cervid populations, but the mechanisms of transmission of CWD remain incompletely understood (135). As with any infectious (and potentially zoonotic) disease, it is crucial that we understand the routes of transmission of CWD. An understanding of the prevalence of prions in excreta would enable the calculation of R_0, which is essential for an explanation of the disease process and spread. The development of sensitive diagnostic tools has

increased our ability to detect prions, but the interpretation is more complex than yes-or-no. RT-QuIC does not have 100% sensitivity or 100% specificity, leaving the possibility for both false negatives and false positives (288). My colleagues have investigated the presence of prions and seeding activity in saliva from CWD(+) white-tailed deer for many years. We have confirmed that prions in saliva are infectious, and have made attempts to quantify prions in saliva and other excreta (123, 218, 230, 231, 288, 305). Through these studies, we have relied on negative controls to prevent misinterpretation of false positives and have suspected the presence of false negatives. Sample preparation with phosphotungstic acid precipitation (PTA) and iron-oxide magnetic extraction (IOME) increases the sensitivity of RT-QuIC in saliva samples (230, 288). Despite these additional steps, we have observed the pattern wherein saliva samples appear to be negative in RT-QuIC until diluted. The requirement for sample dilution to enable seeding caused us to hypothesize that an inhibitor of RT-QuIC was present in some saliva samples, an inhibitor which would cause us to underestimate the frequency or titer of seeding activity in saliva from CWD(+) deer.

There is evidence that RT-QuIC is susceptible to inhibition from non-prion components. Hoover, et al. observed that the highest concentrations of brain homogenate are inhibitory to amyloid formation in RT-QuIC and that the expected dilutional response does not commence until the brain homogenate has been diluted to approximately a 0.01% w/v homogenate. However, when polar lipids are removed from the brain homogenate with alcohol precipitation, the dilutional response is restored. The addition of polar lipids from brain inhibits the RT-QuIC reaction for other tissue types as well, confirming that polar brain lipids are a bona fide inhibitor of RT-QuIC (373). The other compelling evidence for inhibitors of the RT-QuIC reaction comes from the attempts to diagnose prions in blood. Several approaches have been described for detecting seeding activity in “inhibitor-laden” samples like whole blood and blood plasma (374, 375). For example, Byron Caughey’s group used immunoaffinity capture to trap prions from blood plasma, which were then subjected to a modified RT-QuIC protocol to facilitate detection. In the case of RT-QuIC inhibition by blood, no inhibitor(s) was identified (150).

Though inhibitors are problematic for detection by RT-QuIC, inhibition of amyloid formation has therapeutic potential. Several molecules have been used *in vitro* and *in vivo* to inhibit amyloid formation or prion propagation, with the goal of prion disease treatment. For example, doxycycline (a tetracycline antibiotic) decreased the amount of PrP^{Sc} in animal models, though it had no effect in a human clinical trial (376-378). Similarly, quinacrine, an anti-malarial compound, inhibited PrP^{Sc} propagation *in vitro* and in some animal models, but had no effect in a human clinical trial (198, 379-381). Others have explored potential inhibitors of amyloid propagation *in vitro*, but prion disease remains essentially untreatable (361, 382-384). Progress requires more compounds and a better understanding of the mechanisms by which prion propagation may be inhibited, both of which may be explored with high-throughput, *in vitro* assays like RT-QuIC (385).

We suspected that the RT-QuIC inhibitor in saliva was among the normal components of ruminant saliva. In ruminants generally, and fallow and roe deer (*Cervus dama dama*, *Capreolus capreolus*) in particular, saliva is basic (pH 8.2-8.6) and buffered, principally by Na^+, K^+, inorganic phosphate and Ca^{++} (386, 387). Mixed saliva (from all salivary gland tissue) contains 0.7-6.7mg/mL protein (386). There are several protein families in ruminant saliva. In mule deer (*Odocoileus hemionus hemionus*), saliva contains more proline-rich proteins than cattle and sheep, which are presumed to facilitate consumption of high levels of tannins (388). The most common protein family in saliva is the mucin family, which is comprised of complex glycoproteins that lend saliva its viscosity and provide lubrication (389). Mucins have cysteine-rich termini to facilitate disulfide bonds between and within monomers and serine/threonine-rich cores to facilitate the addition of O- and N-linked oligosaccharides, including sialic acids and acetylhexosamine (390).

Our observations from many years of experience with saliva from CWD(+) deer suggested that at least some samples contained an RT-QuIC inhibitor. The presence of an inhibitor would result in an underestimation of the frequency and/or titer of seeding activity in saliva, information that is crucial to understanding the spread of CWD. In these experiments, we confirmed the presence of an RT-QuIC inhibitor and provided evidence that the inhibitor is a protein, perhaps a member of the mucin family.

This work provides the basis for further optimization of the RT-QuIC assay and provides motivation to analyze results of excreta screens in a manner that accounts for false negatives (and false positives).

Methods

Western blot and Coomassie stain

We pooled replicate RT-QuIC wells and combined 20μL RT-QuIC product or saliva with 20μL 2X LSB/βME (Novagen) and boiled the samples for 5 minutes. We loaded 30μL each sample to a 12-well, 12% Bis-Tris, pre-cast, polyacrylamide gel (Novagen) and electrophoresed at 150V for one hour. For Coomassie stained gels, we added Coomassie stain (0.25%w/v Coomassie Brilliant Blue R250, 7.5% v/v glacial acetic acid, 50% v/v methanol) to the gel and rocked at room temperature (RT) for 2 hours, then removed the stain, rinsed the gel, and destained (7.5% v/v glacial acetic acid, 50% v/v methanol) for 2 hours at RT. For western blots, we transferred the proteins to polyvinylidene fluoride (PVDF) membranes for one hour at 80V on ice. We blocked the membranes in 5% non-fat dry milk, then exposed the membranes to anti-PrP antibody Bar224 (Cayman Chemicals) overnight at 4°C, followed by secondary antibody (goat anti-mouse IgG_{2a}-HRP (SeraCare)) for one hour at RT. We developed the western blots with Pierce ECL substrate (Thermo Scientific). For both western blots and Coomassie stained gels, we collected images with an ImageQuant LS.

Inhibitory saliva pools

We made a large pool of CWD(-) saliva to be used for the experiments in this study. The pool was comprised of 1mL baseline saliva samples (pre-inoculation) from each of the following deer: 1201, 1204, 1205, 1211, 1218. Data confirming the inhibitory nature of this pool is shown in Fig. 5.2A.

NaPTA treatment

We added fresh 7μL sodium phosphotungstic acid (final concentration: 0.33% NaPTA, 0.28% $MgCl_2$ w/v) to 100μL undiluted saliva. We shook the solution for 1 hour at 37°C and 1400 RPM, then

pelleted the proteins by centrifugation at 14,000g for 30 minutes. We resuspended the pellets in 10µL 0.1% SDS/PBS, then spiked 1µL 0.01% brain homogenate into 9µL the resuspended, NaPTA-treated saliva pellet.

PTA treatment

We added 4% fresh phosphotungstic acid (PTA) (Sigma) to 100µL undiluted saliva or 1% tonsil homogenate for a final concentration of 0.3%, then incubated the samples for 1 hour at 37°, shaking at 1700 RPM. We pelleted the proteins by centrifugation at 17,000g for 30 minutes, then resuspended the pellets in 10µL 0.1% SDS/PBS, then spiked 1µL 0.01% brain or tonsil homogenate into 9µL treated saliva pellet.

Iron-oxide bead treatment

We diluted saliva 1:5 in 0.1% SDS/PBS (100µL total) and added a final concentration of 0.00001% brain homogenate, plus 2µL iron-oxide beads (~9µm, Bangs Laboratory). We rocked the solution for 1 hour at RT, then used a magnetic particle separator to pellet the beads. We saved the supernatant and resuspended the beads in 0.1% SDS/PBS. To test whether the inhibitors in saliva bind the beads, we did not add brain before bead binding, but resuspended the beads in 0.001% brain homogenate after incubation with saliva. Therefore, the beads were exposed to the same amount of brain material in both scenarios.

Protease treatment

We treated saliva samples with proteinase K (PK, final concentration of 4µg/mL) at 45°C for 1 hour at 900 RPM. We added 10mM phenylmethylsulfonyl fluoride (PMSF) to each sample and boiled for 5 minutes to inactivate the PK. Next, we spiked 1µL 0.01% brain homogenate into 9µL treated saliva.

Protease inhibitor treatment

To test whether the proteases present in saliva were destroying the recombinant PrP^C ($rPrP^C$) upon which the RT-QuIC assay relies, we pre-incubated saliva with $rPrP^C$, with or without protease inhibitors. We substituted 1/3 the water in the RT-QuIC mastermix (1mM EDTA, 0.1mg/mL rPrP, 320mM NaCl, 10μM ThT, H_2O) with saliva (for a final concentration of 20% v/v). We added protease inhibitor cocktail (EDTA-free protease inhibitor cocktail, Thermo Scientific 78437) and incubated for 1hr, 2hr, 6hr or overnight at 42°C with one minute of shaking (500RPM) alternating with one minute of rest. We used these samples as the substrate for RT-QuIC or for electrophoresis, then western blot or Coomassie stain.

Mucin treatment

We made fresh mucin daily (25mg/mL bovine submaxillary mucin, Sigma; in 10mM HEPES buffer, pH 7.6) and diluted it in PBS or saliva electrolytes for final concentrations of 0.5mg/mL, 1.25mg/mL, 2.5mg/mL, 5.0mg/mL, 6.25mg/mL or 12.5mg/mL. The use of 10mM HEPES as a diluent for bovine submaxillary mucin was published previously (391).

NaLC treatment

We made fresh N-acetly-L-cysteine in water (NaLC, Sigma, 0.3M), then diluted it in saliva or PBS for final concentrations of 30μM, 15μM or 5μM. Concentrations were based on other *in vitro* experiments with NaLC (392).

Saliva electrolyte treatment

We created a solution with the electrolyte concentrations of ruminant saliva based on a 1948 report by McDougall (393). The solution composition is as follows: 117mM $NaHCO_3$, 26mM $Na_2HPO_4*12H_2O$, 8mM NaCl, 8mM KCl, 0.2mM $CaCl_2$ anhydrous, 0.3mM $MgCl_2$ anhydrous. We dissolved these salts in deionized water and filtered the solution. We added 2% SDS for a final concentration of 0.1% SDS and diluted brain homogenate into the SDS/electrolyte solution.

Saliva screen

To determine the frequency with which negative saliva samples contain inhibitors of RT-QuIC, we devised a screening protocol. First, we diluted positive brain to a final concentration of 0.01% or 0.001% in saliva and 0.01%SDS and tested for inhibition in triplicate in RT-QuIC. To test the dilutional response of the inhibitor, we added 0.001% positive brain in 30% saliva or 60% saliva, added SDS for a final concentration of 0.01%, and added the sample to triplicate wells in RT-QuIC.

RT-QuIC

We purified Syrian hamster $rPrP^C$ (codons 90-231) as previously described (325). We expressed the cDNA in *E. coli* BL21-Star cells overnight under the following inducing conditions: LB media, kanamycin and chloramphenicol, 20X NPS [0.5M $(NH_4)_2SO_4$, 1M KH_2PO_4, 1M Na_2HPO_4], 50X 5052 [0.5% glycerol, 0.05% glucose, 0.2% lactose], 1mM $MgSO_4$. We harvested inclusion bodies with lysozyme (0.25mg/mL), DNase (1µg/mL) and $MgCl_2$ (5mM) in 1X Bugbuster (Novagen) following the manufacturer's protocol (Novagen). We solubilized inclusion body pellets in 8M guanidine hydrochloride (GdnHCl) overnight, then bound the solubilized protein to Ni-agarose resin, rotating at room temperature for 45 minutes (GE Healthcare Life Sciences). We refolded the $rPrP^C$ with a gradient from 6M GdnHCl in 100mM Na_2HPO_4 and 10mM Tris to the same buffer with no GdnHCl on a GE FPLC (AktaPure, GE Healthcare Life Sciences). We eluted with a gradient from 0.0M to 0.5M imidazole and dialyzed the $rPrP^C$ in two changes of 20mM NaH_2PO_4 overnight, then stored at 4°C.

We added 10µg $rPrP^C$ to 10µM thioflavin T (ThT), 320mM NaCl, 1mM EDTA and 1X PBS in one well of a 96-well plate (Nunc black, optical-bottom, 96-well plates, ThermoScientific). Sample preparation was variable, depending on the treatment, and is described in the previous sections, but we always added 2µL of the sample to each well. We either prepared the sample in 0.1% SDS or added 2µL 0.1% SDS to the plate separately. For controls, we included brain (positive and negative) diluted into PBS and into inhibitory saliva on every plate. We used a BMG Fluostar Omega microplate reader to shake the plates for one minute (double orbital shaking at 700RPM), followed by one minute of rest, for 62.5 hours

at 42°C. The fluorescence was recorded every 15 minutes with a 450nm excitation wavelength, a 480nm emission wavelength, and a gain of 1700.

Results

Some saliva samples require dilution to enable seeding in RT-QuIC.

We have studied the presence of prions and seeding activity in saliva from CWD(+) white-tailed deer for many years. We previously confirmed that prions in saliva are infectious, and have quantified prions in saliva and other excreta (123, 218, 230, 231, 288, 305). In many of these studies, we used RT-QuIC to measure the seeding activity in saliva samples. Over years of experience testing saliva, we observed that some saliva samples were apparently negative, until they were diluted (some examples in Fig. 5.1A). We hypothesized that saliva contains an inhibitor of RT-QuIC, which impedes seeding when the inhibitor concentration is particularly high, the seeding activity is low, or some combination of both conditions.

We designed a number of experiments to confirm the presence of an RT-QuIC inhibitor and to attempt to identify the molecule. First, we used SDS-PAGE and Coomassie stain to compare the total protein content of saliva samples that either did or did not require dilution to enable RT-QuIC seeding (Fig. 5.1B). The saliva samples varied in their total protein content, based on the total intensity of each lane, and there were only a few apparent differences in the presence or absence of bands from the samples that require dilution for seeding. The bands that appear only in the samples that require dilution are indicated with arrows. The requirement for dilution of some samples, and the unclear results from the Coomassie stain prompted us to confirm the presence of an RT-QuIC inhibitor in saliva and to attempt to identify the molecule(s) responsible.

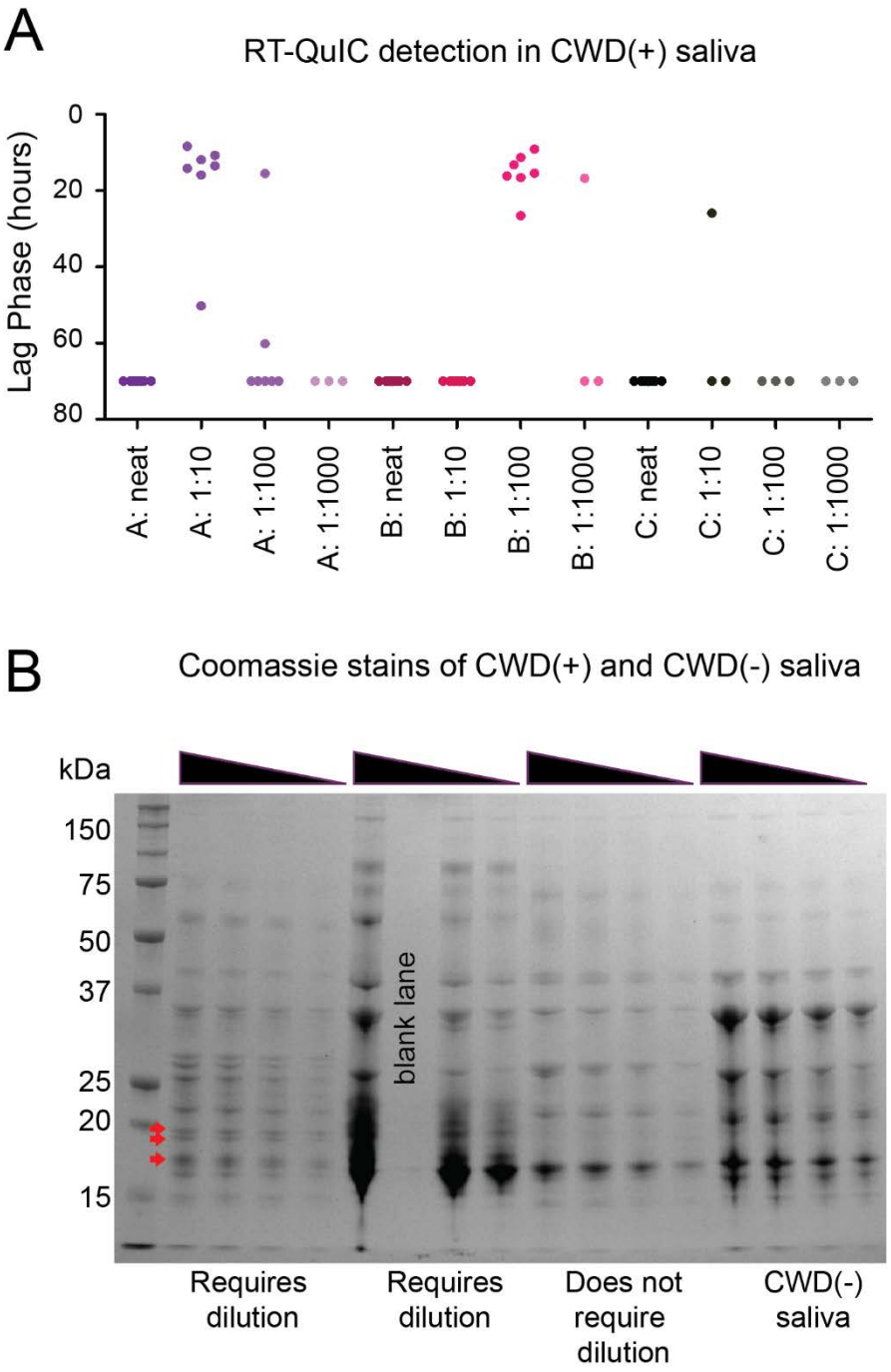

Figure 5.1. Some saliva samples must be diluted to enable seeding in RT-QuIC. A. Points indicate the lag phase for each replicate in RT-QuIC, which indicates the efficiency with which amyloid formation occurred. We show three examples of saliva samples that have detectable seeding activity upon dilution. (A=121, B=139, C=143) B. We analyzed the total protein content in four saliva samples by Commassie stain. Black arrows along the top of the image indicate dilution of the samples and labels on the bottom of the gel indicate which samples require dilution for RT-QuIC seeding. Red arrows indicate bands that appear only in samples that require dilution. Samples, from L-R, are 121, 142, 132, 137.

Saliva inhibits seeding activity in RT-QuIC

To test whether saliva has an inhibitor that hampers seeding in in RT-QuIC, we performed a series of spiking experiments. We created a pool of saliva from naïve deer that we used for all subsequent spiking and subtraction experiments. First, we diluted CWD(+) brain in neat saliva with SDS or in PBS with SDS, then tested the solution in RT-QuIC. All but the highest dilution of brain homogenate were completely inhibited by saliva, and the highest dilution had a decreased lag phase compared to the PBS/SDS control, indicating inhibition in this prion-laden sample (Fig. 5.2A). Next, we added 200ng CWD(+) brain to saliva diluted in PBS. There is a dilutional response; seeding activity is completely inhibited at 100% saliva (neat) and 60% saliva, severely delayed at 30% saliva and uninhibited at 0% saliva (Fig. 5.2B). Finally, we tested dilutions of CWD(-) brain in PBS/SDS or saliva/SDS to ensure that components of saliva do not cause spontaneous misfolding of $rPrP^{C}$ (Fig. 5.2C). We have observed that the addition of SDS is essential to the RT-QuIC system; without SDS, there is no seeding (unpublished). It is possible that SDS is less effective when added to saliva than when added to PBS, so we tested whether increased SDS concentrations could rescue the inhibition. However, increased SDS concentrations had no effect on inhibition from the saliva diluent (Fig. 5.2D).

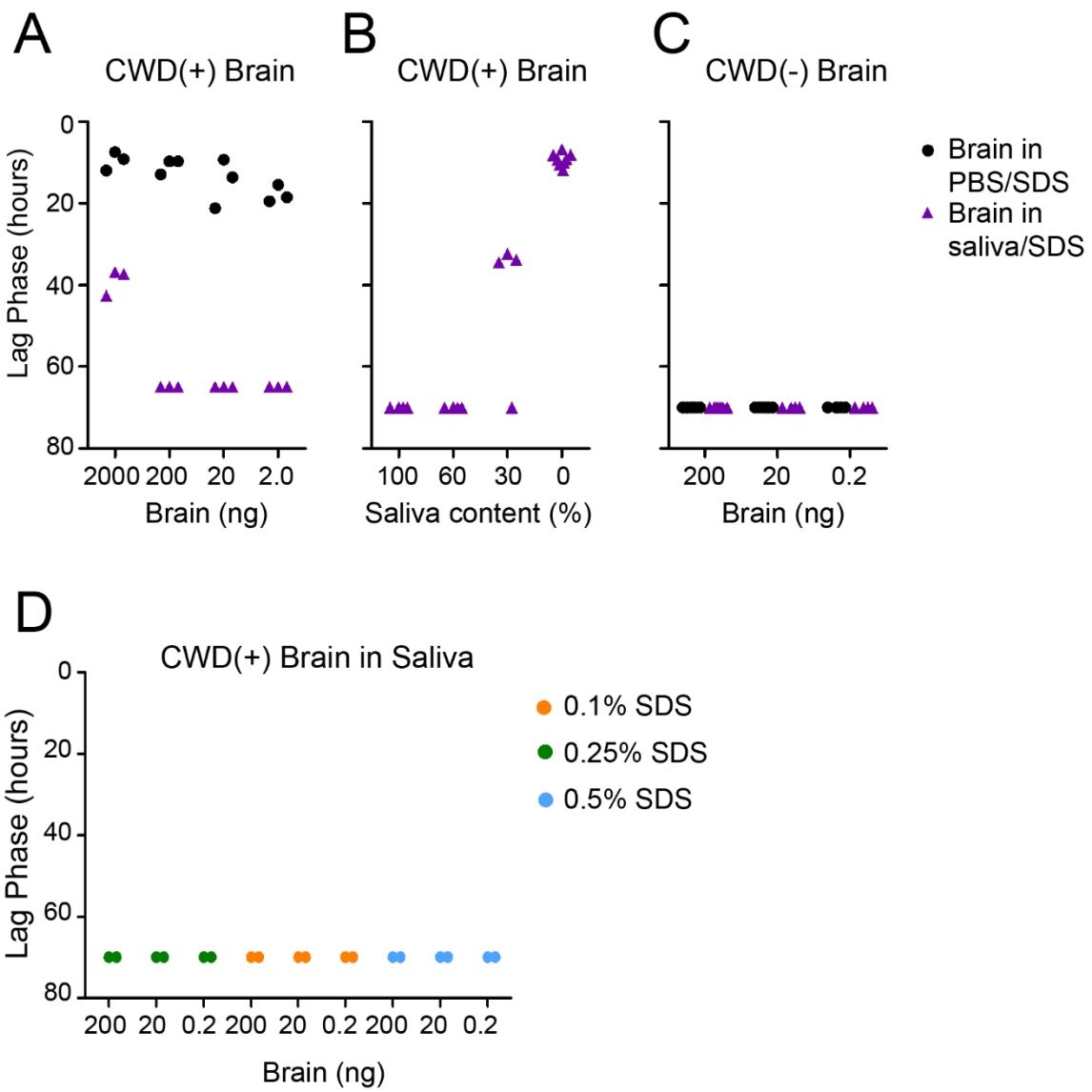

Figure 5.2. Saliva inhibits seeding activity in RT-QuIC. We tested the ability of saliva to inhibit seeding activity from CWD(+) brain homogenate. Points indicate the lag phase for each replicate in RT-QuIC. A. First, we diluted brain homogenate into neat saliva, then added 2µL of each dilution to the RT-QuIC assay. B. Next, we added 200ng brain homogenate to a series of saliva dilutions (100%, 60%, 30% and 0% saliva) and added 2µL of each sample to RT-QuIC. C. Finally, we diluted CWD(-) brain in saliva to ensure that saliva did not cause spontaneous conversion of $rPrP^C$ to amyloid. D. The RT-QuIC assay is very sensitive to changes in SDS concentration, and we have observed that low SDS concentrations or omission of SDS will prevent seeding. Therefore, we added extra SDS when we diluted brain in neat saliva to try to rescue the inhibition. The SDS concentration of the sample is indicated in the legend; the final concentration is 2% of the concentration indicated in the legend.

Inhibition is common among CWD(-) saliva samples.

We were curious how representative our inhibitory, negative saliva pool was for the larger population of negative saliva samples. We screened 39 negative saliva samples for their tendency to inhibit prion seeding activity from CWD(+) brain homogenate. Roughly 25% of the saliva samples completely inhibited (3/3 replicates) 200ng CWD(+) brain homogenate. That percentage increases to nearly 50% when we only added 20ng CWD(+) brain homogenate (Fig. 5.3A). We confirmed a dilutional response by diluting CWD(+) brain homogenate in 100% saliva, 60% saliva, 30% saliva and 0% saliva. More samples were completely inhibited (4/4 replicates) when the saliva concentration was higher, confirming a dilutional response (Fig. 5.3B). Even in samples that were not completely inhibited, it was common for the lag phase to be lower in the presence of increasing concentrations of saliva (Fig. 5.3C).

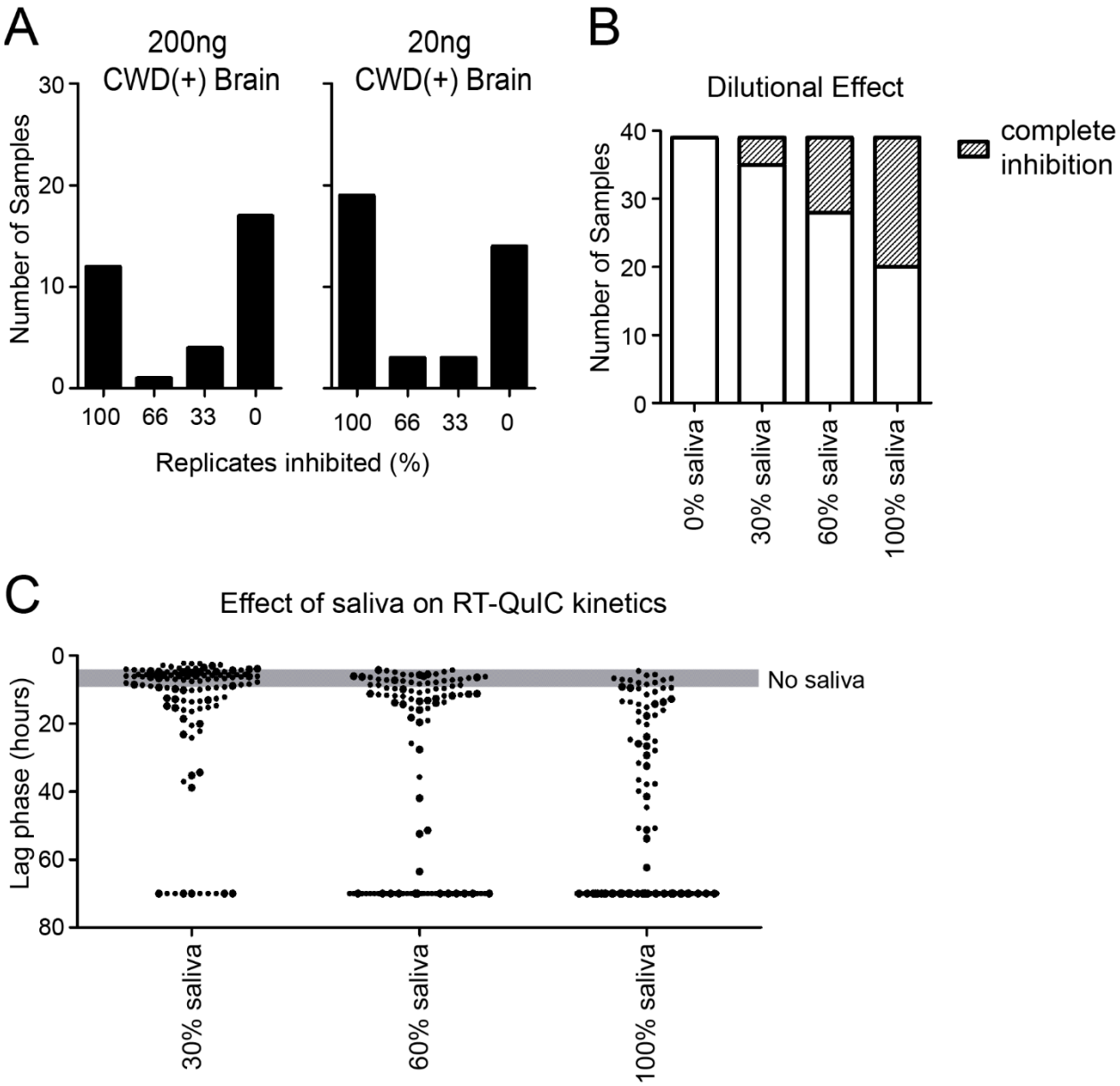

Figure 5.3. Inhibition is common among CWD(-) saliva samples. We tested 39 saliva samples from CWD(-) deer for their ability to inhibit prion seeding activity from brain homogenate in RT-QuIC. A. First, we tested the tendency of neat saliva to inhibit seeding from 200ng CWD(+) brain or 20ng CWD(+) brain. The number of saliva samples that inhibited 100%, 66%, 33% or 0% of the replicates are indicated by the bars. B. Next, we tested whether dilution of the saliva sample resulted in a dilutional response. Indeed, more samples were completely inhibitory (inhibited 4/4 replicates) as the percentage of saliva in the diluent increased. C. Not all samples prevented seeding entirely, but still had an inhibitory effect on the RT-QuIC lag phase. The gray shaded area represents the range of lag phases for 20ng CWD(+) brain with no saliva in the diluent. Each point represents the lag phase for an individual replicate for an individual saliva sample (3 replicates, 39 samples).

The inhibitor interferes with several RT-QuIC detection paradigms.

We have used several protocols to concentrate seeding activity in saliva and increase sensitivity in RT-QuIC. These include PTA precipitation and concentration of seeding activity with IOME (230, 231, 288, 305). Both treatments improved sensitivity, but our identification of an RT-QuIC inhibitor in saliva caused us to question whether the inhibitor may also be concentrated by these methods and continue to interfere with RT-QuIC sensitivity (230, 288). Therefore, we designed a series of experiments to test the behavior of the inhibitor in RT-QuIC following PTA precipitation, the related NaPTA precipitation, and IOME (Fig. 5.4, Table 5.1). Briefly, we detected inhibition when brain was combined with saliva, but detection was rescued by bead extraction. However, when we added iron-oxide beads to inhibitory, negative saliva, the beads and supernatant were inhibitory when brain was added after separation. This suggests that the RT-QuIC inhibitor binds the beads to some degree, though the presence of brain homogenate during incubation competes with the inhibitor binding. NaPTA and PTA treatment of brain homogenates does not result in seeding activity, so we switched to CWD(+) tonsil for PTA and NaPTA experiments. When we added CWD(+) tonsil to inhibitory, negative saliva, seeding activity was inhibited, but PTA treatment restored seeding activity to the pellet, although it was slightly delayed compared to PTA-treatment of tonsil without saliva. These data suggest that the RT-QuIC inhibitor is precipitated by PTA treatment, but perhaps the seeding activity in the concentrated sample can again be high enough to overcome inhibition. When we treated inhibitory, negative saliva with NaPTA, the pellet and supernatant were both inhibitory to spiked brain homogenate. Similarly, when we treated inhibitory, negative saliva with PTA, the pellet and supernatant were both inhibitory. The supernatant from a PTA-treated blank was also slightly inhibitory. The pellet is the target fraction that is traditionally used in RT-QuIC. Together, these data suggest that the RT-QuIC inhibitor is distributed to both the pellet and the supernatant in NaPTA and PTA.

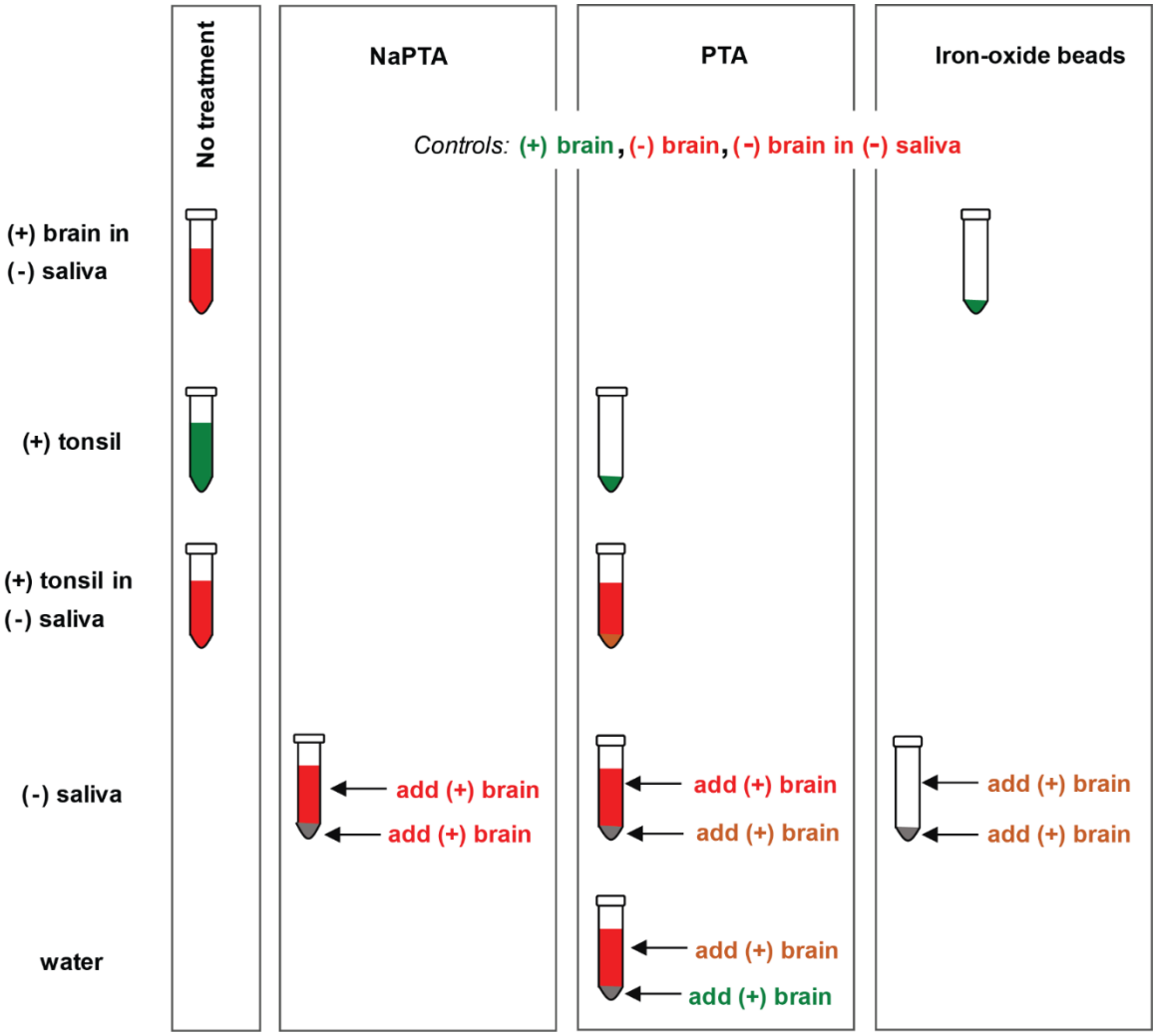

Figure 5.4. Experimental design to determine effects of saliva inhibitor on RT-QuIC detection methods. We have used several methods to enhance the detection of seeding activity in saliva with RT-QuIC, including PTA precipitation and iron-oxide beads. We applied each of these treatments to saliva, with or without brain homogenate (as outlined in the figure and in the methods section). Red fill or text indicates no RT-QuIC activity existed in this fraction, while green indicates full seeding activity and orange indicates partial inhibition. Detailed results are in Table 5.1.

Table 5.1. The saliva inhibitor interferes with several RT-QuIC detection paradigms. We often use ancillary concentration techniques to increase the detection of seeding activity in saliva (and other dilute) samples. We tested each technique (iron-oxide beads, NaPTA, PTA) with saliva spiked (or not) with brain homogenate. Summarized results are in Fig. 5.4, and the detailed results are described here. We assigned a value of 70 hours for replicates that never crossed the threshold. The median lag phase and % positive replicates were calculated from 8 replicates. The approach is described in detail in the methods section.

Sample description	Median lag phase	% Positive replicates
(+) brain (0.01%)	12.46	100%
(+) brain (0.001%)	11.04	100%
(+) brain (0.0001%)	11.93	100%
(-) brain (0.01%)	70.00	0%
(-) brain (0.001%)	70.00	0%
(-) brain (0.0001%)	70.00	0%
(-) brain (0.01%) in (-) saliva	70.00	0%
(-) brain (0.001%) in (-) saliva	70.00	0%
(-) brain (0.0001%) in (-) saliva	70.00	0%
(+) brain (0.01%) in (-) saliva	70.00	0%
(+) brain (0.001%) in (-) saliva	70.00	0%
(+) brain (0.0001%) in (-) saliva	70.00	0%
beads incubated with 20% (-) saliva and (+) brain	9.38	100%
(+) tonsil (0.1%)	10.33	100%
(+) tonsil (0.01%)	11.77	100%
(+) tonsil (0.001%)	49.49	100%
pellet from PTA-treated (+) tonsil	11.22	100%
(+) tonsil in saliva (0.1%)	70.00	0%
(+) tonsil in saliva (0.01%)	70.00	0%
(+) tonsil in saliva (0.001%)	70.00	0%
pellet from PTA-treated (+) tonsil in saliva	15.35	100%
supernatant from PTA-treated (+) tonsil in saliva	70.00	0%
(+) brain in pellet from NaPTA-treated (-) saliva	70.00	20%
(+) brain in supernatant from NaPTA-treated (-) saliva	70.00	0%
supernatant from NaPTA-treated (-) saliva	70.00	0%
(+) brain in pellet from PTA-treated (-) saliva	62.27	60%
(+) brain in supernatant from PTA-treated (-) saliva	70.00	0%
supernatant from PTA-treated (-) saliva	70.00	0%
(+) brain in beads incubated with 20% (-) saliva	59.84	50%
(+) brain in supernatant from beads incubated with 20% (-) saliva	58.97	75%
(+) brain in pellet from PTA-treated (-) blank	12.76	100%
(+) brain in supernatant from PTA-treated (-) blank	20.12	80%
supernatant from PTA-treated (-) blank	70.00	0%

Saliva contains proteases which degrade rPrP in RT-QuIC.

We hypothesized that the RT-QuIC inhibitor in saliva may function in one of two ways; first, it could damage one of the essential components of the RT-QuIC assay (like $rPrP^{C}$) or it could inhibit the

conversion of $rPrP^C$ to amyloid. To test whether saliva was impeding the RT-QuIC assay by degrading $rPrP^C$, we incubated saliva with $rPrP^C$ for one hour and assessed degradation by western blot (Fig. 5.5A). It was apparent that the addition of large concentrations of saliva (1/3 - 1/5 total volume) resulted in degradation of the $rPrP^C$, which suggested the presence of protease(s) in saliva. We used the same pre-incubated samples as the substrate in RT-QuIC and observed no amyloid formation upon the addition of CWD(+) brain (Fig. 5.5B).

We also performed RT-QuIC as we have in previous figures; we diluted brain homogenate into saliva and added 2μL of the solution to the RT-QuIC assay without saliva pre-incubation (this constitutes a final saliva concentration of approximately 2%). In this case, we also saw inhibition of amyloid formation, but without substantial degradation of the $rPrP^C$ (Fig. 5.5B). We suspected that the degradation of $rPrP^C$ was not responsible for the inhibition of the RT-QuIC assay by saliva, but we confirmed this hypothesis by treating saliva and $rPrP^C$ with a protease-inhibitor cocktail (PIC). We took samples of the solution periodically during an overnight incubation, then used the incubated samples as substrate for a 62.5 hour RT-QuIC assay. The addition of PIC dramatically reduced the degradation of $rPrP^C$ by saliva proteases, but seeding was not rescued (Fig. 5.5C). Therefore, we concluded that saliva does not inhibit RT-QuIC only by degrading the $rPrP^C$ substrate, and we proceeded to test other components of saliva that may constitute the RT-QuIC inhibitor.

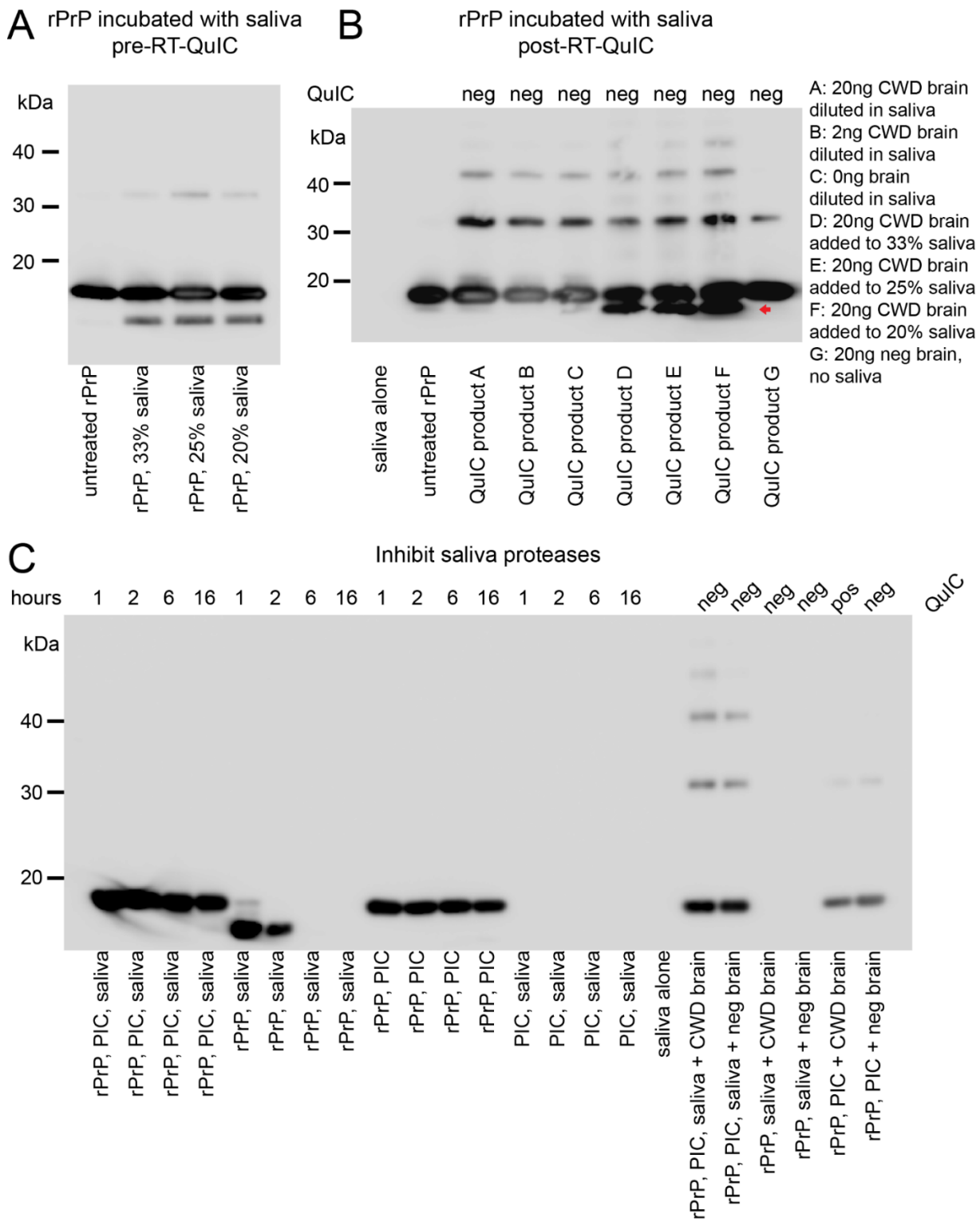

Figure 5.5. Saliva contains proteases, which degrade rPrP in RT-QuIC, but is not the only reaction inhibitor. A. To test the effect of saliva on the $rPrP^C$ in the RT-QuIC assay, we incubated $rPrP^C$ with saliva of various concentrations. When $rPrP^C$ was combined with a final saliva concentration of 33%, 25% or 20% for one hour at RT, there was a noticeable degradation product (indicated by red arrow on right). B. We subjected the same samples to RT-QuIC with positive or negative brain homogenate spikes or added brain diluted in saliva to RT-QuIC, then analyzed the QuIC products by western blot. C. We treated saliva (20%

v/v) and $rPrP^{C}$ (.1mg/mL) with a protease inhibitor cocktail (PIC) and collected samples periodically during an overnight incubation period. We then used the treated samples as substrate for RT-QuIC and compared pre- and post-RT-QuIC samples by western blot.

PK removes RT-QuIC inhibitor in CWD(-) saliva, but does not reliably rescue seeding in CWD(+) saliva samples.

Based on the tendency of the RT-QuIC inhibitor to end up in NaPTA and PTA pellets (Fig. 5.4, Table 5.1) and the appearance of extra bands in a Coomassie stain of neat saliva (Fig. 5.1B), we suspected that the inhibitor may be a protein. To remove PK-sensitive proteins, we treated inhibitory, negative saliva with several concentrations of PK. We observed noticeable changes in the total protein content of the samples between 1.0 and 5.0µg/mL PK (Fig. 5.6A). We tested the ability of PK-treated saliva to inhibit RT-QuIC (after PMSF treatment). At and above 1.0µg/mL PK, the inhibitory saliva pool was no longer inhibitory. We also PK-treated PBS and stopped the reaction with PMSF to 1) ensure that we were removing all PK activity and to 2) ensure that PMSF does not affect the reaction (Fig. 5.6B). We chose a concentration of 4µg/mL and compared PK-treated, heated (the PK protocol requires one hour at 45°C, followed by the addition of PMSF and boiling, so we included heating alone as a control for the PK treatment) and untreated saliva in their ability to inhibit RT-QuIC. PK-treatment, but not heat alone, rescued seeding in the RT-QuIC assay (Fig. 5.6C).

With the evidence that PK-treatment removed the RT-QuIC inhibitor in inhibitory, negative saliva and spiking experiments, we treated CWD(+) saliva with 4µg/mL PK and compared the seeding from the PK-treated sample to neat or diluted saliva (Fig. 5.6D). Interestingly, the PK treatment only rescued seeding in one of the three samples we tested. We suspect that the PrP^{Sc} in saliva may not be as PK-resistant as typical PrP^{Sc} and that we destroyed the seeding activity (and, presumably, the inhibitor) in the two samples that were not rescued. These data demonstrate one of our challenges in addressing detection in saliva: positive control saliva is hard to reliably identify and we are left using brain homogenate and spiking experiments. Together, these data suggest that the RT-QuIC inhibitor is a protein and that the PrP^{Sc} in saliva is protease-sensitive.

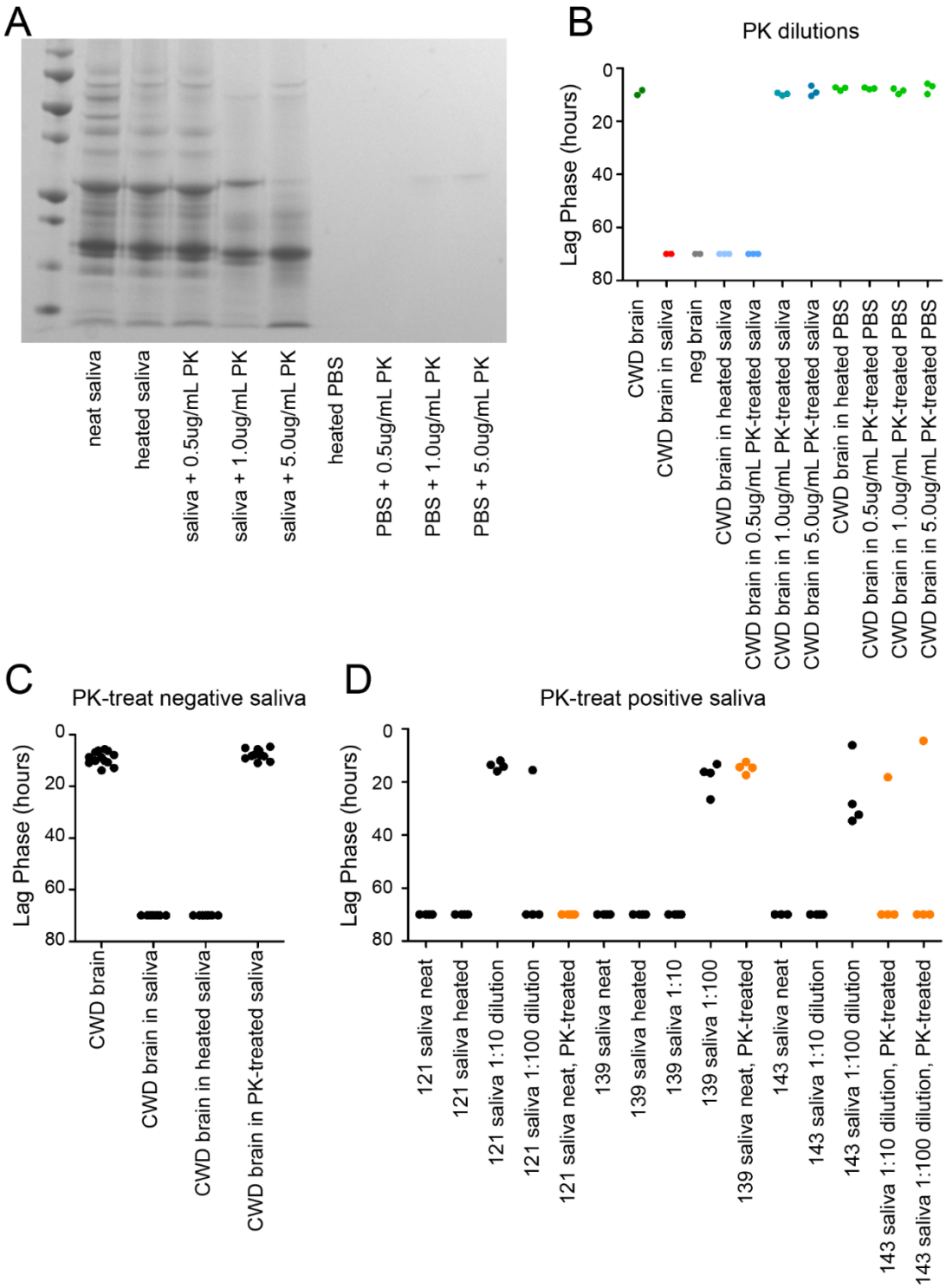

Figure 5.6. Protease treatment rescues seeding in spiked negative saliva, and in some positive saliva samples. To test whether the RT-QuIC inhibitor is a protein, we treated saliva samples with PK. A. First, we determined the effect of PK on the total protein profile in our inhibitory saliva pool. We treated saliva with a range of PK concentrations, stopped the PK with PMSF, and assessed the total protein content by Coomassie stain. B. We tested the effects of a range of PK concentrations on our inhibitory saliva by treating saliva with PK, stopping the reaction with PMSF, then adding 200ng CWD(+) brain homogenate and adding the solution to

RT-QuIC. Shades of blue indicate PK concentrations and green points indicate PK-treatment of a blank (to ensure that the PK is destroyed and does not degrade the $rPrP^C$ in the RT-QuIC assay.) Points indicate the lag phase for each replicate. C. We chose a concentration of 4µg/mL PK/sample and compared treatment with PK to heat alone (since there is a heat step in the PK protocol). Points indicate the lag phase for each replicate. 20ng brain are added to each sample. D. Finally, we tested the effect of PK on CWD(+) saliva samples that require dilution for seeding (and presumably contain the inhibitor). Orange points indicate the lag phase for PK-treated neat saliva, while black points indicate the lag phase for dilutions of untreated saliva.

Electrolytes in saliva are compatible with RT-QuIC.

The major components of saliva besides protein are electrolytes. We created a solution that mimics the electrolyte milieu of ruminant saliva and diluted brain homogenate into the solution instead of saliva (393). We did not observe inhibition from the electrolyte solution (Fig. 5.7A).

Mucin inhibits RT-QuIC assay.

The major protein component of saliva is the mucin family, a complex group of glycoproteins that provide the viscosity of saliva (394, 395). We compared several mucin concentrations (made from reconstituted bovine submaxillary mucin in 10mM HEPES), all of which are in the range of reported physiological concentrations, with PBS as a diluent for CWD(+) brain homogenate (394-397). We observed a dose-dependent inhibition of seeding activity in RT-QuIC upon the addition of increasing mucin concentrations, but not in our buffer-only controls (Fig. 5.7B,C). Interestingly, mucin inhibited the RT-QuIC assay at lower concentrations when combined with the electrolyte solution described previously (Fig. 5.7C).

We tested the ability of PK to relieve the inhibition caused by mucin. At low mucin concentrations, the heat step in the PK protocol (45°C for one hour, followed by PMSF and boiling) was sufficient to eliminate the inhibition from mucin (Fig. 5.7D). However, at 5mg/mL mucin, PK treatment removed the inhibition, but the heated control was still inhibited (Fig. 5.7D).

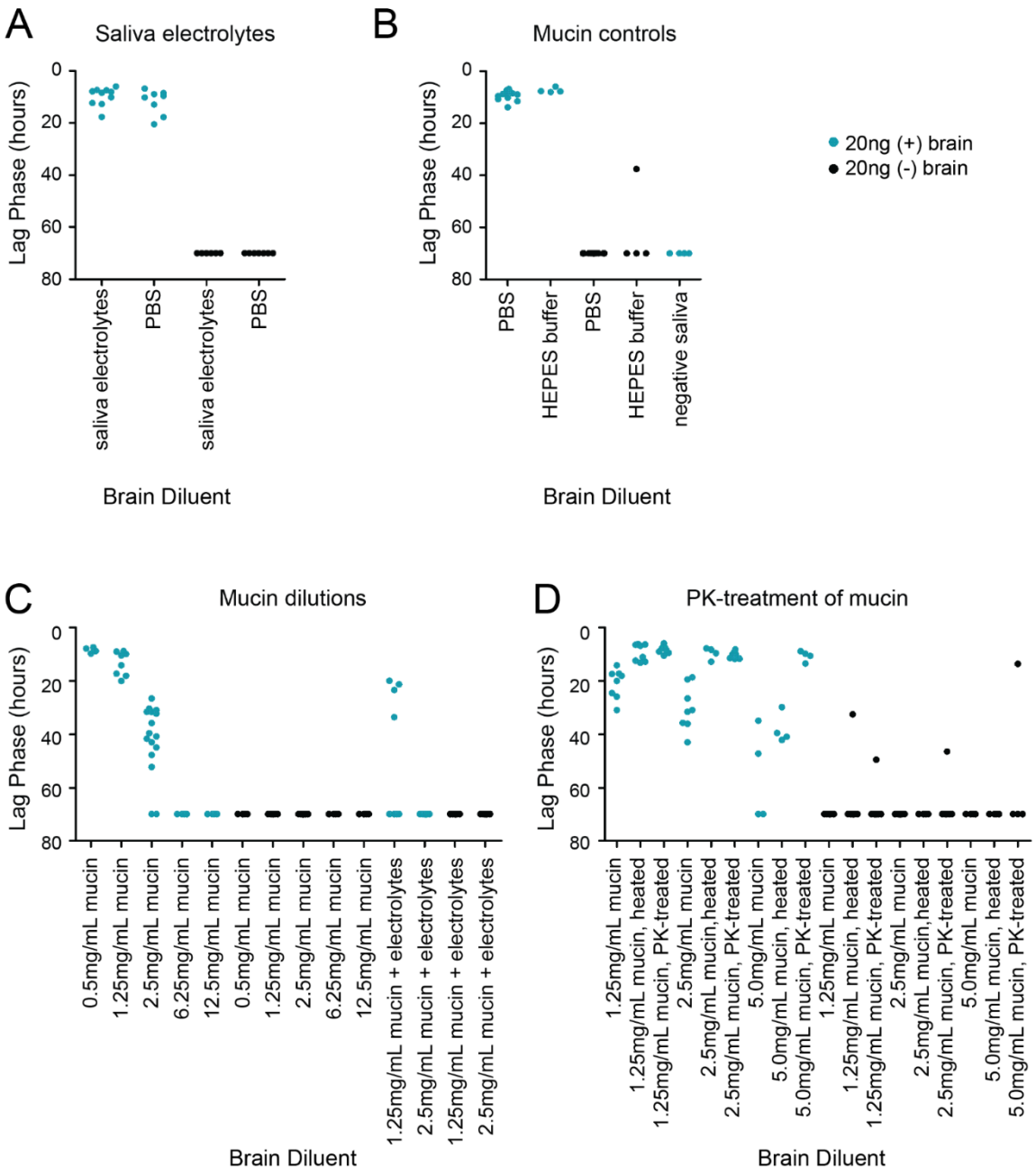

Figure 5.7. The electrolytes in saliva are compatible with RT-QuIC, but mucin is not. Points indicate the lag phase for each replicate. A. We confirmed that the electrolyte composition of saliva is compatible with RT-QuIC by diluting brain in a solution designed to mimic the electrolyte composition of saliva (393). B-C. We tested the inhibitory effects of mucin (purified bovine submaxillary mucin) in the RT-QuIC assay. There is a dose-dependent inhibition of seeding as mucin concentrations are increased (within the physiological range) (394-397). We compared the mucin treatments to buffer only (HEPES) and to PBS. D. We treated mucin-spiked PBS with PK and observe the effects of PK (but not heat) at 5mg/mL mucin.

N-acetyl-L-cysteine inconsistently relieves inhibition in negative saliva samples, but not in mucin-spiked PBS or CWD(+) saliva samples.

N-acetyl-L-cysteine (NaLC) is an antioxidant with a number of clinical applications in human medicine (398, 399). NaLC is classified as a mucolytic agent, and contains free sulfhydryl groups that hydrolyze the disulfide bonds that link mucin oligomers (399). NaLC hydrolyzes mucin *in vitro* (392), so we tested the effect of NaLC on our inhibitory saliva pool, on CWD(+) saliva and on mucin itself. Overall, the results were inconsistent (which appears to be the case for *in vivo* applications of NaLC as well (399)). 5mM NaLC did not relieve the inhibition of seeding activity from CWD(+) brain by inhibitory, negative saliva, but 15mM NaLC completely rescued seeding (Fig. 5.8A). However, the dilutional response was not evident when we treated the samples with 30mM NaLC (which only partially relieved inhibition) (Fig. 5.8A). Concentrations in this range were used in other *in vitro* models (392). We noticed that the blank (PBS) treated with 30mM NaLC had slightly delayed seeding relative to the blank treated with 15mM NaLC, so it's possible that NaLC inhibits the RT-QuIC reaction at higher concentrations.

Interestingly, there was more (and faster) spontaneous conversion when 30mM NaLC was added to saliva or PBS, and then used to dilute negative brain homogenate (Fig. 5.8B). It is clear that NaLC has off-target effects on the RT-QuIC assay. More importantly, NaLC did not rescue seeding in CWD(+) saliva samples that require dilution for seeding (Fig. 5.8A). We tested the impact of NaLC on mucin directly and observed that NaLC did not rescue inhibition by mucin at the concentrations we tested (Fig. 5.8B).

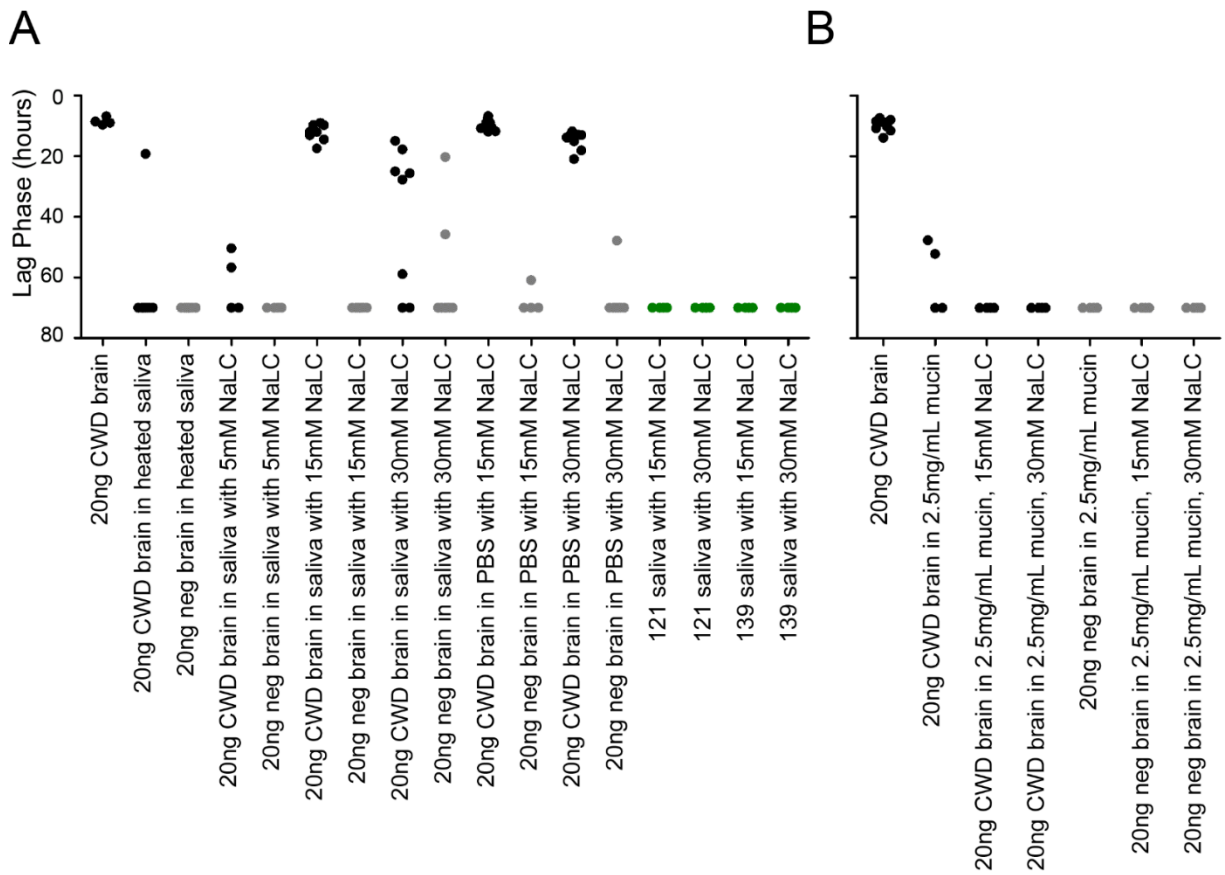

Figure 5.8. N-acetyl-L-cysteine inconsistently relieves inhibition in inhibitory, negative saliva samples, but not in mucin-spiked PBS or in CWD(+) samples. Points indicate the lag phase for each replicate. A. We treated inhibitory, negative saliva with NaLC, then added brain homogenate, or we treated CWD(+) saliva that requires dilution with NaLC. Positive brain homogenate is indicated by black points and negative is indicated by gray points. CWD(+) saliva samples are represented by green points. B. We treated various mucin concentrations with NaLC, then added CWD(+) (black points) or CWD(-) (gray points) brain homogenate and tested whether mucin was inhibitory after NaLC treatment.

Discussion

Detection of prions in excreta from CWD(+) cervids is an essential step for understanding horizontal transmission of CWD. Sensitive detection assays, including RT-QuIC, have made such investigations possible. However, we have suspected that RT-QuIC has imperfect sensitivity (ability to detect true positives) and specificity (ability to classify true negatives). In previous work, we have relied upon the inclusion of negative controls to improve our ability to identify false positives, but we have struggled to identify false negatives, even with sample preparation protocols that improve sensitivity (230, 288). We designed the experiments described in this chapter to confirm the presence of an RT-QuIC

inhibitor in saliva samples and to attempt to identify the inhibitor. This information will make it possible to optimize the RT-QuIC assay and improve our analyses of RT-QuIC results.

We confirmed the presence of an RT-QuIC inhibitor through dilution of positive saliva samples and through spiking of CWD(+) brain material into inhibitory, negative saliva samples (Fig. 5.1, 5.2, 5.3). We tested the most common sample preparation protocols that have been applied to saliva samples (PTA, IOME and NaPTA) and confirmed that none of these protocols eliminates the inhibitor problem entirely (Fig. 5.4, Table 5.1). We identified protease activity in saliva samples, but when we blocked that activity with a protease-inhibitor cocktail, the saliva samples remained inhibitory. Therefore, it is not protease activity that results in false negative detections (Fig. 5.5). Saliva has anti-viral activity against human immunodeficiency virus, which has also been demonstrated not to be due to protease activity (400).

We confirmed that the electrolyte milieu in saliva is not inhibitory, and proceeded to investigate the role of salivary proteins (Fig. 5.6, 5.7, 5.8). Addition of mucin to PBS inhibited the RT-QuIC reaction, which was rescued with PK treatment of the mucin, but not with N-acetyl-cysteine treatment (Fig. 5.7, 5.8). We expected NaLC to hydrolyze the mucin *in vitro*, but other literature suggests that the effectiveness of NaLC is not predictable (399). Treatment of inhibitory, negative saliva with PK reliably removed the RT-QuIC inhibitor, but treatment of CWD(+) saliva did not enable seeding (Fig. 5.6). The likely explanation for this outcome is that the seeding activity in saliva is PK-sensitive and that the same treatment that destroyed the inhibitor (4µg/mL PK, 45°C for 60 minutes) also destroyed the PrP^{Sc}.

RT-QuIC relies upon the tendency of PrP^{Sc} to induce the misfolding of PrP^{C}. The misfolding is then propagated and PrP^{Sc} aggregates in the form of amyloid. ThT intercalates in amyloid and its fluorescence spectrum shifts, which is detected by the fluorimeter. Therefore, lack of signal in RT-QuIC could indicate a lack of amyloid or a failure of ThT to intercalate, fluoresce and be detected. A lack of amyloid could be due to missing subunits (PrP^{C}) or a failure of amyloid propagation. We confirmed that the lack of signal that results from the addition of inhibitory saliva is not due to destruction of PrP^{C}. We assume that the lack of signal it is not due to a failure of ThT to fluoresce based on previous work in our lab and unaffected maximum fluorescence values (373). Therefore, we chose to describe the inhibition as

inhibition of seeding, suggesting that amyloid formation is inhibited. However, the efficacy of ThT in the presence of saliva should be confirmed.

These data are the first step toward 1) identification of the RT-QuIC inhibitor in saliva and 2) optimization of RT-QuIC for saliva testing. The frequency of inhibition among negative samples suggests that inhibition in saliva is common, the results from RT-QuIC analysis of saliva may be significantly affected, and that interpretation must account for the possibility of low sensitivity (Fig. 5.2). There are a number of experiments that should be pursued to improve seeding from saliva samples. It is worth considering the lipid content in saliva, which is low, but not absent. In brain samples, lipids inhibit RT-QuIC, and it would be interesting to test that possibility in saliva (373). However, the protocol recommended for brain samples is not compatible with saliva, because the saliva is simply washed away in the alcohol washes. Lipase treatment of saliva had no effect (data not shown), but interpretation of those results was complicated by the lack of an appropriate positive control for the lipase treatment. However, it is an important step in this systematic approach to eliminate lipids as the species responsible for inhibition.

The failure of PK treatment to rescue seeding in CWD(+) samples was disappointing, but not surprising. There exists anecdotal evidence that prions outside the brain may be more susceptible to PK than brain prions. It is likely that the PK treatment destroyed the seeding activity in the positive saliva samples. Therefore, PK treatment is not a viable pre-treatment to increase the seeding of RT-QuIC by saliva. However, the effectiveness of PK treatment on inhibitory, negative saliva suggests that the inhibitor is a protein, information that is useful for subsequent experiments. Treatment with glycosidases will remove the oligosaccharides from mucin, but will not affect the peptide (and, hypothetically, will not affect seeding activity). Together, these enzymes are referred to as “mucinase,” and the class includes glycosulfatases, sialidases and others (401). If mucin is indeed the RT-QuIC inhibitor, and if inhibition relies on the presence of mucin’s post-translational modifications and quaternary structure, mucinase treatment should relieve inhibition and leave seeding activity intact. A mucinase cocktail could be used as

a pre-treatment for saliva samples, or for samples that remain RT-QuIC-negative after PTA or IOME treatment. Finally, it would be interesting to assess the effects of mucin on prions other than PrP.

To identify the RT-QuIC inhibitor more specifically, inhibitory saliva could be separated by ion-exchange (or size-exclusion) chromatography, then the fractions could be tested with RT-QuIC to identify which contain the inhibitor. Inhibitory fractions could then be compared to non-inhibitory fractions by mass spectrometry (402). This approach would make identification of the protein possible, which could be followed by addition of the purified protein of interest to RT-QuIC to confirm its inhibitory character. Of course, the question that underlies all these experiments, and the justification for carrying them out, is whether this RT-QuIC inhibitor matters *in vivo.* There are bench-top approaches for increasing prion detection *in vitro* and modeling techniques to improve our inference from *in vitro* data, so the knowledge that there is an inhibitor may be sufficient for diagnostic needs (403).

However, if the inhibitor has a role *in vivo*, it is crucial to understand its nature and the mechanism by which it inhibits the RT-QuIC reaction. Despite the observation that treatment of prion diseases is difficult, it seems worthwhile to pursue identification of inhibitors of amyloid formation, for the chance that the molecule has therapeutic potential. Therefore, identification of the inhibitor should lead to *in vitro* experiments to test the molecule's ability to inhibit amyloid formation in other systems, like PMCA and cell culture. These experiments would provide a foundation for the treatment of prion-infected mice with the inhibitor. The likelihood that the RT-QuIC inhibitor in saliva has physiological activity is low, but the reward makes these experiments worthwhile.

CONCLUSIONS AND FUTURE DIRECTIONS

The horizontal transmissibility of CWD and its risk to humans remain important questions in prion disease research. Specifically, we were interested in factors that contribute to the reproductive number (R_0) of CWD and the role of protein-protein interactions in the host range of CWD, particularly the susceptibility of humans.

R_0 and the horizontal transmission of CWD

Conclusions

We demonstrated that PrP^C expression is common in the alimentary and lymphoid tissues of white-tailed deer, though expression is much lower in non-CNS tissues than in the brain. We confirmed that seeding activity is present in alimentary tissues before it is detectable in the brain, and that seeding activity is not detectable earliest in tissues with the highest PrP^C expression. Next, we considered the infectivity of prions found in lymph nodes, compared to those found in the brain. Prions in lymph nodes and brain were variable in *in vitro* assays; both seeded RT-QuIC, but lymph node prions were less consistently detectable using PK-treatment and western blot or PrP^{Sc}-specific ELISA. Importantly, brain and lymph node prions were infectious in cell culture. Finally, we scrutinized the detection of saliva prions with RT-QuIC, which we use to understand prion shedding in excreta. We confirmed that many saliva samples contain an inhibitor of RT-QuIC, which affects our interpretation of results, regardless of which sample preparation protocol we use. The RT-QuIC inhibitor is likely a protein, and may be a member of the mucin family. The presence of an inhibitor suggests that we have been underestimating the frequency (and perhaps the titer) of prion shedding in saliva.

Future directions

A. Seeding activity is common in the tissues of deer in the terminal stages of CWD, but we simplified our results by classifying tissues as positive or negative, with no attempt to rank the tissues by

their level of seeding activity. To better understand prion pathogenesis, it would be useful to rank tissues. NaPTA precipitation of tissues is necessary to limit spontaneous conversion for many of the tissues we studied, but it may also blunt differences in seeding activity, since it concentrates prions. A dilutional series of NaPTA pellets and analysis of the endpoint dilution might enable researchers to rank the tissues by seeding activity.

B. Traditionally, CWD diagnosis relies on recto-anal mucosal-associated lymphoid tissue (RAMALT) biopsy, followed by IHC, or IHC analysis of the brain of hunter-killed cervids (61). However, our detection of seeding activity in every tissue we tested suggests that many other tissues could be used for CWD diagnosis. Any tissue could be selected, then collected from hunter-killed cervids, and compared to the sensitivity and specificity of testing brain. It is possible that sensitivity would be increased with the use of a non-CNS tissue, since many tissues seem to have detectable seeding activity earlier than brain in the disease course. However, specificity must not be ignored, especially when alimentary tissues are used.

C. The propagation of seeding activity in alimentary tissues before the brain is surprising, considering the hypothesis that prions reach peripheral tissues by centrifugal spread from the brain. The mechanism for prion propagation in peripheral tissues has not been described. Immunohistochemistry of RT-QuIC positive, alimentary tissues may indicate whether the PrP^{Sc} is deposited in nervous tissue components of the alimentary tract (i.e. myenteric plexi) or if PrP^{Sc} is present in epithelial cells, where PrP^{C} is also expressed (or both). The local PrP^{C} population responsible for propagation may indicate differences among prions from different tissues. If prions are always formed from neuronal PrP^{C}, perhaps one would hypothesize that prions in the periphery are not different (in their biochemical features or infectivity). However, if prions propagate in non-neuronal cells, perhaps they are more likely to be different from CNS prions.

D. The use of CPCA to detect PrP^{Sc} from lymph nodes suggests that the assay may be useful for the detection of PrP^{Sc} in many non-brain tissues. We should take the opportunity to test infectivity *in vitro* for tissues from the alimentary tract, which contain substantial RT-QuIC seeding activity.

E. To understand the dilution-dependent delay we observed in prion propagation in the CPCA cells, one could spike a 0.1% brain homogenate into a 1% homogenate of brain or lymph node and use the spiked material to coat the plates. If high tissue concentrations are inhibitory, the cells exposed to the spiked samples will develop spots later in infection than 0.1% brain homogenate in PBS.

F. We observed differences in the behavior of LN and brain prions in 7-5 ELISA. As we discussed, 7-5 ELISA is specific for underglycosylated $PrP^{C/Sc}$. It is certainly possible that the recruitment of underglycosylated PrP^{C} to prions is not as extensive in the lymph nodes as it is in the brain, though we didn't observe a dramatic differences in glycosylation patterns by western blotting. A thorough analysis of the PrP^{C} or PrP^{Sc} glycoform ratios in brain vs. lymph node would clarify whether the starting material is dramatically different among tissues.

G. There are a number of experiments that can be pursued to complete the investigation of RT-QuIC inhibitors in saliva. First, lipids should be eliminated as the inhibitory species (lipase treatment). Next, substitution of mucinase for proteinase K would confirm whether the mucin family (specifically, their post-translational modifications) are responsible for the inhibition of RT-QuIC by saliva.

H. Chromatography, selection of inhibitory fractions from saliva, and mass spectrometry can be used to identify the proteinaceous inhibitor specifically. With the identification of the inhibitor, it would be possible to test its role in other *in vitro* assays (including PMCA and cell culture) and *in vivo.*

I. We have demonstrated for the first time that PrP^{Sc} in saliva is protease-sensitive. PrP^{Sc} in excreta and brain should be compared for other features as well (infectivity, etc.)

Host range of CWD and the risk to humans

Conclusions

We confirmed that PrP^{Sc} preferentially induces amyloid formation in the homologous $rPrP^{C}$ substrate in RT-QuIC. BSE maintained its preferential seeding of bovine $rPrP^{C}$ upon passage of BSE to felines, while CWD adapted to felines and seeded feline $rPrP^{C}$ more efficiently. Interestingly, CWD very

efficiently caused amyloid formation in human rPrP^{C}, suggesting that the species barrier preventing CWD infection of humans is not due to the compatibility of CWD PrP^{Sc} and human PrP^{C}.

We tested the role of the amino-terminus of PrP^{C} in *in vitro* amyloid formation and in the species barrier. We concluded that for bovine and white-tailed deer rPrP^{C}, the NTD hampered seeded amyloid formation, while the human and bank vole NTD improved seeded amyloid formation. The human rPrP^{C} was more susceptible to misfolding when an amino terminus was present, whether it had exactly the same primary sequence as the human NTD or not.

Future directions

A. In light of the recent description of prion strains that do not adapt upon transmission to a new species, it would be very interesting to test non-adaptive prions in both the enciphering and recipient rPrP^{C} species (92). We hypothesize that non-adaptive prions would always seed the enciphering host more efficiently than the new host (like BSE and FSE).

B. Our data suggests that there is an interaction of the NTD and the rest of the protein. A recent publication proposed an interaction of the NTD and a portion of the carboxy-terminal domain (the discontinuous epitope for the antibody POM1) (372). It would be interesting to alter the POM1 epitope in the human rPrP^{C} and assess whether alteration of that epitope removes the effect of the NTD on the species barrier between human rPrP^{C} and CWD prions.

Many years of prion research have described a novel class of pathogens, defined a mechanism by which information can be transferred by proteins alone, and established the zoonotic potential of prion diseases. Prion research continues to be preoccupied by the horizontal transmission of CWD and its risk to humans. We have explored the role of tissues outside the CNS in the horizontal transmission of CWD, and confirmed that these tissues play a role in generating, harboring and shedding prions. A prion disease species barrier could manifest in many ways, including immunological defenses, failure of trafficking from the periphery to the brain, or an incompatibility of donor and recipient PrP^{Sc}/PrP^{C}. We conclude that

PrP^{Sc} from CWD(+) deer is not incompatible with human $rPrP^{C}$ and that the apparent species barrier must result from another feature of the host-pathogen interaction.

REFERENCES

1. **Merriam Webster.** Merriam-Webster.com.
2. **The Lancet.** 2012. Zoonoses uncaged. The Lancet **380:**1882.
3. **Karesh WB, Dobson A, Lloyd-Smith JO, Lubroth J, Dixon MA, Bennett M, Aldrich S, Harrington T, Formenty P, Loh EH, Machalaba CC, Thomas MJ, Heymann DL.** 2012. Ecology of zoonoses: natural and unnatural histories. The Lancet **380:**1936-1945.
4. **Estrada-Pena A, Ostfeld RS, Peterson AT, Poulin R, de la Fuente J.** 2014. Effects of environmental change on zoonotic disease risk: an ecological primer. Trends Parasitol **30:**205-214.
5. **Asokan GV, Asokan V.** 2016. Bradford Hill's criteria, emerging zoonoses, and One Health. Journal of Epidemiology and Global Health **6:**125-129.
6. **Morse SS, Mazet JAK, Woolhouse M, Parrish CR, Carroll D, Karesh WB, Zambrana-Torrelio C, Lipkin WI, Daszak P.** 2012. Prediction and prevention of the next pandemic zoonosis. The Lancet **380:**1956-1965.
7. **Brown P, Will, R.G., Bradley, R., Asher, D.M., Detwiler, L.** 2001. Bovine spongiform encephalopathy and variant Creutzfeldt-Jakob disease: background, evolution and current concerns. Emerging Infectious Diseases **7:**6-16.
8. **Anderson RM, Donnelly CA, Ferguson NM, Woolhouse MEJ, Watt CJ, Udy HJ, MaWhinney S, Dunstan SP, Southwood TRE, Wilesmith JW, Ryan JBM, Hoinville LJ, Hillerton JE, Austin AR, Wells GAH.** 1996. Transmission dynamics and epidemiology of BSE in British cattle. Nature **382:**779-788.
9. **Bruce M, Chree A, McConnell I, Foster J, Pearson G, Fraser H.** 1994. Transmission of Bovine Spongiform Encephalopathy and Scrapie to Mice: Strain Variation and the Species Barrier. Philosophical Transactions of the Royal Society of London Series B: Biological Sciences **343:**405-411.
10. **Will RG, Ironside JW, Zeidler M, Estibeiro K, Cousens SN, Smith PG, Alperovitch A, Poser S, Pocchiari M, Hofman A.** 1996. A new variant of Creutzfeldt-Jakob disease in the UK. The Lancet **347:**921-925.
11. **Collinge J, Sidle KCL, Meads J, Ironside J, Hill AF.** 1996. Molecular analysis of prion strain variation and the aetiology of 'new variant' CJD. Nature **383:**685-690.
12. **Prusiner SB.** 1997. Prion diseases and the BSE crisis. Science **278**.
13. **Basler K, Oesch B, Scott M, Westaway D, Wälchli M, Groth DF, McKinley MP, Prusiner SB, Weissmann C.** 1986. Scrapie and cellular PrP isoforms are encoded by the same chromosomal gene. Cell **46:**417-428.
14. **Oesch B, Westaway D, Wälchli M, McKinley MP, Kent SBH, Aebersold R, Barry RA, Tempst P, Teplow DB, Hood LE, Prusiner SB, Weissmann C.** 1985. A cellular gene encodes scrapie PrP 27-30 protein. Cell **40:**735-746.
15. **Prusiner SB, Groth DF, Bolton DC, Kent SB, Hood LE.** 1984. Purification and structural studies of a major scrapie prion protein. Cell **38:**127-134.
16. **Prusiner S.** 1982. Novel proteinaceous infectious particles cause scrapie. Science **216:**136-144.
17. **Scott M, Foster D, Mirenda C, Serban D, Coufal F, Wälchli M, Torchia M, Groth D, Carlson G, DeArmond SJ, Westaway D, Prusiner SB.** 1989. Transgenic mice expressing hamster prion protein produce species-specific scrapie infectivity and amyloid plaques. Cell **59:**847-857.
18. **Hay B, Prusiner SB, Lingappa VR.** 1987. Evidence for secretory form of the cellular prion protein. Biochemistry **26:**8110-8115.
19. **Soto C.** 2011. Prion Hypothesis: The end of the Controversy? Trends in biochemical sciences **36:**151-158.

20. **Byrd AL, Segre JA.** 2016. Adapting Koch's postulates. Science **351:**224-226.
21. **Walker L, Levine H, Jucker M.** 2006. Koch's postulates and infectious proteins. Acta Neuropathologica **112:**1-4.
22. **Hope J, Ritchie L, Farquhar C, Somerville R, Hunter N.** 1989. Bovine spongiform encephalopathy: a scrapie-like disease of British cattle. Progess in Clinical and Biological Research **317:**659-667.
23. **Hope J, Reekie LJ, Hunter N, Multhaup G, Beyreuther K, White H, Scott AC, Stack MJ, Dawson M, Wells GA.** 1988. Fibrils from brains of cows with new cattle disease contain scrapie-associated protein. Nature **336:**390-392.
24. **Scott AC, Wells GA, Stack MJ, White H, Dawson M.** 1990. Bovine spongiform encephalopathy: detection and quantitation of fibrils, fibril protein (PrP) and vacuolation in brain. Veterinary Microbiology **23:**295-304.
25. **Bockman JM, Kingsbury DT, McKinley MP, Bendheim PE, Prusiner SB.** 1985. Creutzfeldt-Jakob disease prion proteins in human brains. New England Journal of Medicine **312:**73-78.
26. **Guiroy DC, Williams ES, Song KJ, Yanagihara R, Gajdusek DC.** 1993. Fibrils in brain of Rocky Mountain elk with chronic wasting disease contain scrapie amyloid. Acta Neuropathologica Communications **86:**77-80.
27. **Guiroy DC, Williams ES, Yanagihara R, Gajdusek DC.** 1991. Immunolocalization of scrapie amyloid (PrP27-30) in chronic wasting disease of Rocky Mountain elk and hybrids of captive mule deer and white-tailed deer. Neurosci Lett **126:**195-198.
28. **Prusiner SB, Barry RA, McKinley MP, Bellinger CG, Meyer RK, DeArmond SJ, Kingsbury DT.** 1985. Scrapie and Creutzfeldt-Jakob disease prions. Microbiological sciences **2:**33-39.
29. **Spraker TR, Miller MW, Williams ES, Getzy DM, Adrian WJ, Schoonveld GG, Spowart RA, O'Rourke KI, Miller JM, Merz PA.** 1997. Spongiform encephalopathy in free-ranging mule deer (Odocoileus hemionus), white-tailed deer (Odocoileus virginianus) and Rocky Mountain elk (Cervus elaphus nelsoni) in northcentral Colorado. Journal of Wildlife Disease **33:**1-6.
30. **DeArmond SJ, McKinley MP, Barry RA, Braunfeld MB, McColloch JR, Prusiner SB.** 1985. Identification of prion amyloid filaments in scrapie-infected brain. Cell **41:**221-235.
31. **Acevedo-Morantes C, Wille H.** 2014. The Structure of Human Prions: From Biology to Structural Models—Considerations and Pitfalls. Viruses **6:**3875-3892.
32. **Stahl N, Borchelt DR, Hsiao K, Prusiner SB.** 1987. Scrapie prion protein contains a phosphatidylinositol glycolipid. Cell **51:**229-240.
33. **Stahl N, Prusiner SB.** 1991. Prions and prion proteins. FASEB Journal **5:**2799-2807.
34. **Wille H, Bian W, McDonald M, Kendall A, Colby DW, Bloch L, Ollesch J, Borovinskly AL, Cohen FE, Prusiner SB, Stubbs G.** 2009. Natural and synthetic prion structure from X-ray fiber diffraction. Proceedings of the National Academy of Sciences **106**.
35. **Vázquez-Fernández E, Vos MR, Afanasyev P, Cebey L, Sevillano AM, Vidal E, Rosa I, Renault L, Ramos A, Peters PJ, Fernández JJ, van Heel M, Young HS, Requena JR, Wille H.** 2016. The Structural Architecture of an Infectious Mammalian Prion Using Electron Cryomicroscopy. PLoS Pathog **12:**e1005835.
36. **Ryan AM, Womack JE.** 1993. Somatic cell mapping of the bovine prion protein gene and restriction fragment length polymorphism studies in cattle and sheep. Animal Genetics **24:**23-26.
37. **Westaway D, Zuliani V, Cooper CM, Da Costa M, Neuman S, Jenny AL, Detwiler L, Prusiner SB.** 1994. Homozygosity for prion protein alleles encoding glutamine-171 renders sheep susceptible to natural scrapie. Genes and Development **8:**959-969.
38. **O'Rourke KI, Spraker TR, Hamburg LK, Besser TE, Brayton KA, Knowles DP.** 2004. Polymorphisms in the prion precursor functional gene but not the pseudogene are associated with susceptibility to chronic wasting disease in white-tailed deer. Journal of General Virology **85:**1339-1346.

39. **Brayton KA, O'Rourke KI, Lyda AK, Miller MW, Knowles DP.** 2004. A processed pseudogene contributes to apparent mule deer prion gene heterogeneity. Gene **326:**167-173.
40. **Pan K-M, Baldwin M, Nguyen J, Gasset M, Serban A, Groth D, Mehlhorn I, Huang Z, Fletterick RJ, Cohen FE.** 1993. Conversion of alpha-helices into beta-sheets features in the formation of the scrapie prion proteins. Proceedings of the National Academy of Sciences **90:**10962-10966.
41. **Nguyen JT, Inouye H, Baldwin MA, Fletterick RJ, Cohen FE, Prusiner SB, Kirschner DA.** 1995. X-ray diffraction of scrapie prion rods and PrP peptides. Journal of Molecular Biology **252:**412-422.
42. **Requena JR, Wille H.** 2014. The structure of the infectious prion protein: experimental data and molecular models. Prion **8:**60-66.
43. **Marshall KE, Hughson A, Vascellari S, Priola SA, Sakudo A, Onodera T, Baron GS.** 2016. PrP knockout cells expressing transmembrane PrP resist prion infection. Journal of Virology doi:10.1128/jvi.01686-16.
44. **Taraboulos A, Scott M, Semenov A, Avrahami D, Laszlo L, Prusiner SB.** 1995. Cholesterol depletion and modification of COOH-terminal targeting sequence of the prion protein inhibit formation of the scrapie isoform. The Journal of Cell Biology **129:**121-132.
45. **Aguilar-Calvo P, Xiao X, Bett C, Erana H, Soldau K, Castilla J, Nilsson KP, Surewicz WK, Sigurdson CJ.** 2017. Post-translational modifications in PrP expand the conformational diversity of prions in vivo. Scientific Reports **7:**43295.
46. **Chesebro B, Trifilo M, Race R, Meade-White K, Teng C, LaCasse R, Raymond L, Favara C, Baron G, Priola S, Caughey B, Masliah E, Oldstone M.** 2005. Anchorless prion protein results in infectious amyloid disease without clinical scrapie. Science **308:**1435-1439.
47. **Chesebro B, Race B, Meade-White K, Lacasse R, Race R, Klingeborn M, Striebel J, Dorward D, McGovern G, Jeffrey M.** 2010. Fatal transmissible amyloid encephalopathy: a new type of prion disease associated with lack of prion protein membrane anchoring. PLoS Pathogens **6:**e1000800.
48. **Stahl N, Baldwin MA, Teplow DB, Hood L, Gibson BW, Burlingame AL, Prusiner SB.** 1993. Structural studies of the scrapie prion protein using mass spectrometry and amino acid sequencing. Biochemistry **32:**1991-2002.
49. **Rudd PM, Merry AH, Wormald MR, Dwek RA.** 2002. Glycosylation and prion protein. Current Opinion in Structural Biology **12:**578-586.
50. **Nishina K, Deleault NR, Mahal S, Baskakov I, Luhrs T, Riek R.** 2006. The stoichiometry of host PrPC glycoforms modulates the efficiency of PrPSc formation in vitro. Biochemistry **45**.
51. **Katorcha E, Makarava N, Savtchenko R, D'Azzo A, Baskakov IV.** 2014. Sialylation of prion protein controls the rate of prion amplification, the cross-species barrier, the ratio of PrPSc glycoform and prion infectivity. PLoS Pathogens **10**.
52. **Katorcha E, Daus ML, Gonzalez-Montalban N, Makarava N, Lasch P, Beekes M, Baskakov IV.** 2016. Reversible off and on switching of prion infectivity via removing and reinstalling prion sialylation. Scientific Reports **6:**33119.
53. **Katorcha E, Makarava N, Savtchenko R, Baskakov IV.** 2015. Sialylation of the prion protein glycans controls prion replication rate and glycoform ratio. Scientific Reports **5:**16912.
54. **Srivastava S, Makarava N, Katorcha E, Savtchenko R, Brossmer R, Baskakov IV.** 2015. Post-conversion sialylation of prions in lymphoid tissues. Proceedings of the National Academy of Sciences **112:**E6654-E6662.
55. **Sigurdson CJ, Nilsson KP, Hornemann S, Manco G, Fernandez-Borges N, Schwarz P, Castilla J, Wuthrich K, Aguzzi A.** 2010. A molecular switch controls interspecies prion disease transmission in mice. Journal of Clinical Investigation **120:**2590-2599.
56. **Kurt TD, Sigurdson CJ.** 2016. Cross-species transmission of CWD prions. Prion doi:10.1080/19336896.2015.1118603**:**00-00.

57. **Scott M, Groth D, Foster D, Torchia M, Yang S-L, DeArmond SJ, Prusiner SB.** 1993. Propagation of prions with artificial properties in transgenic mice expressing chimeric PrP genes. Cell **73:**979-988.
58. **Moore RA, Vorberg I, Priola SA.** 2005. Species barriers in prion diseases - a brief review, p 187-202. *In* Peters CJ, Calisher CH (ed), Infectious Diseases from Nature: Mechanisms of Viral Emergence and Persistence. Springer, Vienna.
59. **Büeler H, Aguzzi A, Sailer A, Greiner RA, Autenried P, Aguet M, Weissmann C.** 1993. Mice devoid of PrP are resistant to scrapie. Cell **73:**1339-1347.
60. **Brandner S, Raeber A, Sailer A, Blättler T, Fischer M, Weissmann C, Aguzzi A.** 1996. Normal host prion protein (PrPC) is required for scrapie spread within the central nervous system. Proceedings of the National Academy of Sciences **93:**13148-13151.
61. **Haley NJ, Hoover EA.** 2015. Chronic Wasting Disease of Cervids: Current Knowledge and Future Perspectives. Annual Review of Animal Biosciences **3:**305-325.
62. **Kaneko K, Zulianello L, Scott M, Cooper CM, Wallace AC, James TL, Cohen FE, Prusiner SB.** 1997. Evidence for protein X binding to a discontinuous epitope on the cellular prion protein during scrapie prion propagation. Proceedings of the National Academy of Sciences **94:**10069-10074.
63. **Hachiya NS, Imagawa M, Kaneko K.** 2007. The possible role of protein X, a putative auxiliary factor in pathological prion replication, in regulating a physiological endoproteolytic cleavage of cellular prion protein. Medical Hypotheses **68:**670-673.
64. **Telling GC, Scott M, Mastrianni J, Gabizon R, Torchia M, Cohen FE, DeArmond SJ, Prusiner SB.** 1995. Prion propagation in mice expressing human and chimeric PrP transgenes implicates the interaction of cellular PrP with another protein. Cell **83:**79-90.
65. **Imberdis T, Harris DA.** 2015. Synthetic Prions Provide Clues for Understanding Prion Diseases. The American Journal of Pathology doi:http://dx.doi.org/10.1016/j.ajpath.2015.12.005.
66. **Legname G, Baskakov IV, Nguyen H-OB, Riesner D, Cohen FE, DeArmond SJ, Prusiner SB.** 2004. Synthetic Mammalian Prions. Science **305:**673-676.
67. **Legname G, Nguyen HO, Baskakov IV, Cohen FE, Dearmond SJ, Prusiner SB.** 2005. Strain-specified characteristics of mouse synthetic prions. Proceedings of the National Academy of Sciences **102:**2168-2173.
68. **Colby DW, Wain R, Baskakov IV, Legname G, Palmer CG, Nguyen HO, Lemus A, Cohen FE, DeArmond SJ, Prusiner SB.** 2010. Protease-sensitive synthetic prions. PLoS Pathogen **6:**e1000736.
69. **Colby DW, Giles K, Legname G, Wille H, Baskakov IV, DeArmond SJ, Prusiner SB.** 2009. Design and construction of diverse mammalian prion strains. Proceedings of the National Academy of Sciences **106**.
70. **Castilla J, Saá P, Hetz C, Soto C.** 2005. In Vitro Generation of Infectious Scrapie Prions. Cell **121:**195-206.
71. **Barria MA, Mukherjee A, Gonzalez-Romero D, Morales R, Soto C.** 2009. De novo generation of infectious prions in vitro produces a new disease phenotype. PLoS Pathogens **5:**e1000421.
72. **Zhang Z, Zhang Y, Wang F, Wang X, Xu Y, Yang H, Yu G, Yuan CG, Ma J.** 2013. De novo generation of infectious prions with bacterially expressed recombinant prion protein. FASEB Journal **27**.
73. **Makarava N, Kovacs GG, Bocharova OV, Savtchenko R, Alexeeva I, Budka H, Rohwer RG, Baskakov I.** 2010. Recombinant prion protein induces a new transmissible prion disease in wild type animals. Acta Neuropathologica **119**.
74. **Makarava N, Kovacs GG, Savtchenko R, Alexeeva I, Budka H, Rohwer RG, Baskakov I.** 2011. Genesis of mammalian prions: from non-infectious amyloid fibrils to a transmissible prion disease. PLoS Pathogens **7**.

75. **Makarava N, Kovacs GG, Savtchenko R, Alexeeva I, Ostapchenko VG, Budka H, Rohwer RG, Baskakov I.** 2012. A New Mechanism for Transmissible Prion Diseases. The Journal of Neuroscience **32**.
76. **Makarava N, Savtchenko R, Baskakov IV.** 2015. Two alternative pathways for generating transmissible prion disease de novo. Acta Neuropathologica Communications **3:**1-13.
77. **Makarava N, Baskakov IV.** 2012. Genesis of transmissible protein states via deformed templating. Prion **6**.
78. **Deleault NR, Lucassen RW, Supattapone S.** 2003. RNA molecules stimulate prion protein conversion. Nature **425:**717-720.
79. **Deleault NR, Geoghegan JC, Nishina K, Kascsak R, Williamson RA, Supattapone S.** 2005. Protease-resistant Prion Protein Amplification Reconstituted with Partially Purified Substrates and Synthetic Polyanions. Journal of Biological Chemistry **280:**26873-26879.
80. **Deleault NR, Kascsak R, Geoghegan JC, Supattapone S.** 2010. Species-Dependent Differences in Cofactor Utilization for Formation of the Protease-Resistant Prion Protein in Vitro. Biochemistry **49:**3928-3934.
81. **Deleault NR, Walsh DJ, Piro JR, Wang F, Wang X, Ma J, Rees JR, Supattapone S.** 2012. Cofactor molecules maintain infectious conformation and restrict strain properties in purified prions. Proceedings of the National Academy of Sciences **109:**E1938–E1946.
82. **Deleault NR, Piro JR, Walsh DJ, Wang F, Ma J, Geoghegan JC, Supattapone S.** 2012. Isolation of phosphatidylethanolamine as a solitary cofactor for prion formation in the absence of nucleic acids. Proceedings of the National Academy of Sciences **109:**8546-8551.
83. **Deleault NR, Harris BT, Rees JR, Supattapone S.** 2007. Formation of native prions from minimal components in vitro. Proceedings of the National Academy of Sciences **104:**9741-9746.
84. **Edgeworth JA, Gros N, Alden J, Joiner S, Wadsworth JD, Linehan J, Brandner S, Jackson GS, Weissmann C, Collinge J.** 2010. Spontaneous generation of mammalian prions. Proceedings of the National Academy of Sciences **107:**14402-14406.
85. **Mulcahy ER, Bessen RA.** 2004. Strain-specific kinetics of prion protein formation in vitro and in vivo. Journal of Biological Chemistry **279:**1643-1649.
86. **Crowell J, Hughson A, Caughey B, Bessen RA.** 2015. Host determinants of prion strain diversity independent of prion protein genotype. Journal of Virology doi:10.1128/jvi.01586-15.
87. **Bessen RA, Kocisko DA, Raymond GJ, Nandan S, Lansbury PT, Caughey B.** 1995. Non-genetic propagation of strain-specific properties of scrapie prion protein. Nature **375:**698-700.
88. **Bessen RA, Marsh RF.** 1994. Distinct PrP properties suggest the molecular basis of strain variation in transmissible mink encephalopathy. Journal of Virology **68:**7859-7868.
89. **Bessen RA, Marsh RF.** 1992. Biochemical and physical properties of the prion protein from two strains of the transmissible mink encephalopathy agent. Journal of Virology **66:**2096-2101.
90. **Bessen RA, Marsh RF.** 1992. Identification of two biologically distinct strains of transmissible mink encephalopathy in hamsters. Journal of General Virology **73 (Pt 2):**329-334.
91. **Almond J, Pattison J.** 1997. Human BSE. Nature **389:**437-438.
92. **Bian J, Khaychuk V, Angers RC, Fernandez-Borges N, Vidal E, Meyerett-Reid C, Kim S, Calvi CL, Bartz JC, Hoover EA, Agrimi U, Richt JA, Castilla J, Telling GC.** 2017. Prion replication without host adaptation during interspecies transmissions. Proceedings of the National Academy of Sciences doi:10.1073/pnas.1611891114.
93. **Davenport KA, Henderson DM, Mathiason CK, Hoover EA.** 2015. Insights into CWD and BSE species barriers using real-time conversion. Journal of Virology doi:10.1128/jvi.01439-15.
94. **Wickner RB.** 1994. [URE3] as an altered URE2 protein: evidence for a prion analog in Saccharomyces cerevisiae. Science **264:**566-569.
95. **Wickner RB, Shewmaker FP, Bateman DA, Edskes HK, Gorkovskiy A, Dayani Y, Bezsonov EE.** 2015. Yeast Prions: Structure, Biology, and Prion-Handling Systems. Microbiology and Molecular Biology Reviews **79:**1-17.

96. **Masison DC, Wickner RB.** 1995. Prion-inducing domain of yeast Ure2p and protease resistance of Ure2p in prion-containing cells. Science **270:**93-95.
97. **Wickner RB, Kelly AC.** 2015. Prions are affected by evolution at two levels. Cellular and Molecular Life Sciences doi:10.1007/s00018-015-2109-6**:**1-14.
98. **Coustou V, Deleu C, Saupe S, Begueret J.** 1997. The protein product of the het-s heterokaryon incompatibility gene of the fungus Podospora anserina behaves as a prion analog. Proceedings of the National Academy of Sciences **94:**9773-9778.
99. **Khan Mohammed R, Li L, Pérez-Sánchez C, Saraf A, Florens L, Slaughter Brian D, Unruh Jay R, Si K.** 2015. Amyloidogenic Oligomerization Transforms Drosophila Orb2 from a Translation Repressor to an Activator. Cell **163:**1468-1483.
100. **Majumdar A, Cesario WC, White-Grindley E, Jiang H, Ren F, Khan MR, Li L, Choi EM, Kannan K, Guo F, Unruh J, Slaughter B, Si K.** 2012. Critical role of amyloid-like oligomers of Drosophila Orb2 in the persistence of memory. Cell **148:**515-529.
101. **Cai X, Chen J, Xu H, Liu S, Jiang QX, Halfmann R, Chen ZJ.** 2014. Prion-like polymerization underlies signal transduction in antiviral immune defense and inflammasome activation. Cell **156:**1207-1222.
102. **Hou F, Sun L, Zheng H, Skaug B, Jiang QX, Chen ZJ.** 2011. MAVS forms functional prion-like aggregates to activate and propagate antiviral innate immune response. Cell **146:**448-461.
103. **Si K, Giustetto M, Etkin A, Hsu R, Janisiewicz AM, Miniaci MC, Kim JH, Zhu H, Kandel ER.** 2003. A neuronal isoform of CPEB regulates local protein synthesis and stabilizes synapse-specific long-term facilitation in aplysia. Cell **115:**893-904.
104. **Si K, Choi YB, White-Grindley E, Majumdar A, Kandel ER.** 2010. Aplysia CPEB can form prion-like multimers in sensory neurons that contribute to long-term facilitation. Cell **140:**421-435.
105. **Chakrabortee S, Kayatekin C, Newby GA, Mendillo ML, Lancaster A, Lindquist S.** 2016. Luminidependens (LD) is an Arabidopsis protein with prion behavior. Proceedings of the National Academy of Sciences doi:10.1073/pnas.1604478113.
106. **Yuan AH, Hochschild A.** 2017. A bacterial global regulator forms a prion. Science **355:**198-201.
107. **Chiesa R.** 2015. The Elusive Role of the Prion Protein and the Mechanism of Toxicity in Prion Disease. PLoS Pathogens **11:**e1004745.
108. **Walsh KP, Kuhn TB, Bamburg JR.** 2014. Cellular prion protein: a co-receptor mediating neuronal cofilin-actin rod formation induced by beta-amyloid and proinflammatory cytokines. Prion.
109. **Küffer A, Lakkaraju AKK, Mogha A, Petersen SC, Airich K, Doucerain C, Marpakwar R, Bakirci P, Senatore A, Monnard A, Schiavi C, Nuvolone M, Grosshans B, Hornemann S, Bassilana F, Monk KR, Aguzzi A.** 2016. The prion protein is an agonistic ligand of the G protein-coupled receptor Adgrg6. Nature **536:**464-468.
110. **Senatore A, Colleoni S, Verderio C, Restelli E, Morini R, Condliffe Steven B, Bertani I, Mantovani S, Canovi M, Micotti E, Forloni G, Dolphin Annette C, Matteoli M, Gobbi M, Chiesa R.** 2012. Mutant PrP Suppresses Glutamatergic Neurotransmission in Cerebellar Granule Neurons by Impairing Membrane Delivery of VGCC a2B-1 subunit. Neuron **74:**300-313.
111. **Khosravani H, Zhang Y, Tsutsui S, Hameed S, Altier C, Hamid J, Chen L, Villemaire M, Ali Z, Jirik FR, Zamponi GW.** 2008. Prion protein attenuates excitotoxicity by inhibiting NMDA receptors. The Journal of Cell Biology **181:**551-565.
112. **Mouillet-Richard S, Vilotte J-L.** 2015. Promiscuous functions of the prion protein family. Frontiers in Cell and Developmental Biology **3**.
113. **Aguzzi A, Lakkaraju AKK.** 2015. Cell Biology of Prions and Prionoids: A Status Report. Trends in Cell Biology doi:http://dx.doi.org/10.1016/j.tcb.2015.08.007.
114. **Wyatt J, Pearson G, Smerdon T, Gruffydd-Jones T, Wells G.** 1990. Spongiform encephalopathy in a cat. Vet Rec **126:**513.

115. **Wyatt J, Pearson G, Smerdon T, Gruffydd-Jones T, Wells G, Wilesmith J.** 1991. Naturally occurring scrapie-like spongiform encephalopathy in five domestic cats. Veterinary Record **129:**233-236.
116. **Grufiydd-Jones T, Galloway P, Pearson G.** 1992. Feline spongiform encephalopathy. Journal of Small Animal Practice **33:**471-476.
117. **Comoy EE, Mikol J, Ruchoux MM, Durand V, Luccantoni-Freire S, Dehen C, Correia E, Casalone C, Richt JA, Greenlee JJ, Torres JM, Brown P, Deslys JP.** 2013. Evaluation of the zoonotic potential of transmissible mink encephalopathy. Pathogens **2:**520-532.
118. **Collee JG, Bradley R.** 1997. BSE: a decade on--Part I. Lancet **349:**636-641.
119. **Plummer PJG.** 1946. Scrapie - A Disease of Sheep. Canadian Journal of Comparative Veterinary Science **10:**49-54.
120. **Arnold M, Ortiz-Pelaez A.** 2014. The evolution of the prevalence of classical scrapie in sheep in Great Britain using surveillance data between 2005 and 2012. Preventive Veterinary Medicine **117:**242-250.
121. **Department for Environment FaRA, Animal and Plant Health Agency, Veterinary and Science Policy Advice Team - International Disease Monitoring.** 2016. Cervid Spongiform Encephalopathy in Norway.
122. **Benestad SL, Mitchell G, Simmons M, Ytrehus B, Vikøren T.** 2016. First case of chronic wasting disease in Europe in a Norwegian free-ranging reindeer. Vet Res **47:**1-7.
123. **Mathiason CK, Powers JG, Dahmes SJ, Osborn DA, Miller KV, Warren RJ, Mason GL, Hays SA, Hayes-Klug J, Seelig DM, Wild MA, Wolfe LL, Spraker TR, Miller MW, Sigurdson CJ, Telling GC, Hoover EA.** 2006. Infectious prions in the saliva and blood of deer with chronic wasting disease. Science **314:**133-136.
124. **Haley NJ, Mathiason CK, Zabel MD, Telling GC, Hoover EA.** 2009. Detection of Sub-Clinical CWD Infection in Conventional Test-Negative Deer Long after Oral Exposure to Urine and Feces from CWD+ Deer. PLoS One **4:**e7990.
125. **Mathiason CK, Hays SA, Powers J, Hayes-Klug J, Langenberg J, Dahmes SJ, Osborn DA, Miller KV, Warren RJ, Mason GL, Hoover EA.** 2009. Infectious prions in pre-clinical deer and transmission of chronic wasting disease solely by environmental exposure. PLoS One **4:**e5916.
126. **Miller MW, Williams ES, Hobbs NT, Wolfe LL.** 2004. Environmental sources of prion transmission in mule deer. Emerging Infectious Diseases **10:**1003-1006.
127. **Krumm CE, Conner MM, Miller MW.** 2005. Relative vulnerability of chronic wasting disease infected mule deer to vehicle collisions. Journal of Wildlife Diseases **41:**503-511.
128. **Krumm CE, Conner MM, Hobbs NT, Hunter DO, Miller MW.** 2010. Mountain lions prey selectively on prion-infected mule deer. Biology Letters **6:**209-211.
129. **Foley AM, Hewitt DG, DeYoung CA, DeYoung RW, Schnupp MJ.** 2016. Modeled Impacts of Chronic Wasting Disease on White-Tailed Deer in a Semi-Arid Environment. PLoS One **11:**e0163592.
130. **Uehlinger FD, Johnston AC, Bollinger TK, Waldner CL.** 2016. Systematic review of management strategies to control chronic wasting disease in wild deer populations in North America. BMC veterinary research **12:**1-16.
131. **Gross JE, Miller MW.** 2001. Chronic Wasting Disease in Mule Deer: Disease Dynamics and Control. The Journal of Wildlife Management **65:**205-215.
132. **Miller MW, Williams ES, McCarty CW, Spraker TR, Kreeger TJ, Larsen CT, Thorne ET.** 2000. Epizootiology of chronic wasting disease in free-ranging cervids in Colorado and Wyoming. Journal of Wildlife Diseases **36:**676-690.
133. **Wasserberg G, Osnas EE, Rolley RE, Samuel MD.** 2009. Host culling as an adaptive management tool for chronic wasting disease in white-tailed deer: a modelling study. Journal of Applied Ecology **46:**457-466.

134. **Schauber EM, Woolf A.** 2003. Chronic Wasting Disease in Deer and Elk: A Critique of Current Models and Their Application. Wildlife Society Bulletin (1973-2006) **31:**610-616.
135. **Miller MW, Williams ES.** 2003. Prion disease: horizontal prion transmission in mule deer. Nature **425:**35-36.
136. **Monello RJ, Powers JG, Hobbs NT, Spraker TR, O'Rourke KI, Wild MA.** 2013. Efficacy of antemortem rectal biopsies to diagnose and estimate prevalence of chronic wasting disease in free-ranging cow elk (Cervus elaphus nelsoni). Journal of Wildlife Diseases **49:**270-278.
137. **Galloway N, Monello RJ, Brimeyer D, Hobbs NT.** 2017. Model forecasting of the impacts of CWD on the Jackson elk herd. National Parks Service, Biological Research Division,
138. **Selariu A, Powers JG, Nalls A, Brandhuber M, Mayfield A, Fullaway S, Wyckoff CA, Goldmann W, Zabel MM, Wild MA, Hoover EA, Mathiason CK.** 2015. In utero transmission and tissue distribution of chronic wasting disease-associated prions in free-ranging Rocky Mountain elk. Journal of General Virology **96:**3444-3455.
139. **Brown D.** 27 Oct 2000 2000. The 'recipe for disaster' that killed 80 and left a £5bn bill, p *In* The Telegraph. London, UK. http://www.telegraph.co.uk/news/uknews/1371964/The-recipe-for-disaster-that-killed-80-and-left-a-5bn-bill.html.
140. **Wells GA, Scott AC, Johnson CT, Gunning RF, Hancock RD, Jeffrey M, Dawson M, Bradley R.** 1987. A novel progressive spongiform encephalopathy in cattle. The Veterinary Record **121:**419-420.
141. **Collee JG, Bradley R.** 1997. BSE: a decade on--Part 2. Lancet **349:**715-721.
142. **Chazot G, Broussolle E, Lapras C, Blattler T, Aguzzi A, Kopp N.** 1996. New variant of Creutzfeldt-Jakob disease in a 26-year-old French man. Lancet **347:**1181.
143. **Will R.** 2003. Acquired prion disease: iatrogenic CJD, variant CJD, kuru. British Medical Bulletin **66:**255-265.
144. **Lasmézas CI, Fournier J-G, Nouvel V, Boe H, Marcé D, Lamoury F, Kopp N, Hauw J-J, Ironside J, Bruce M, Dormont D, Deslys J-P.** 2001. Adaptation of the bovine spongiform encephalopathy agent to primates and comparison with Creutzfeldt– Jakob disease: Implications for human health. Proceedings of the National Academy of Sciences **98:**4142-4147.
145. **Scott MR, Will R, Ironside J, Nguyen H-OB, Tremblay P, DeArmond SJ, Prusiner SB.** 1999. Compelling transgenetic evidence for transmission of bovine spongiform encephalopathy prions to humans. Proceedings of the National Academy of Sciences **96:**15137-15142.
146. **Bruce ME, Will R, Ironside J, McConnell I, Drummond D, Suttie A, McCardle L, Chree A, Hope J, Birkett C.** 1997. Transmissions to mice indicate that 'new variant'CJD is caused by the BSE agent. Nature **389:**498-501.
147. **Hill AF, Desbruslais M, Joiner S, Sidle KCL, Gowland I, Collinge J, Doey LJ, Lantos P.** 1997. The same prion strain causes vCJD and BSE. Nature **389:**448-450.
148. **Richt JA, Kunkle RA, Alt D, Nicholson EM, Hamir AN, Czub S, Kluge J, Davis AJ, Hall SM.** 2007. Identification and Characterization of two Bovine Spongiform Encephalopathy cases Diagnosed in the United States. Journal of Veterinary Diagnostic Investigation **19:**142-154.
149. **Notari S, Moleres FJ, Hunter SB, Belay ED, Schonberger LB, Cali I, Parchi P, Shieh W-J, Brown P, Zaki S, Zou W-Q, Gambetti P.** 2010. Multiorgan Detection and Characterization of Protease-Resistant Prion Protein in a Case of Variant CJD Examined in the United States. PLoS One **5:**e8765.
150. **Orrú CD, Wilham JM, Raymond LD, Kuhn F, Schroeder B, Raeber AJ, Caughey B.** 2011. Prion Disease Blood Test Using Immunoprecipitation and Improved Quaking-Induced Conversion. mBio **2**.
151. **Gill ON, Spencer Y, Richard-Loendt A, Kelly C, Dabaghian R, Boyes L, Linehan J, Simmons M, Webb P, Bellerby P, Andrews N, Hilton DA, Ironside JW, Beck J, Poulter M, Mead S, Brandner S.** 2013. Prevalent abnormal prion protein in human appendixes after bovine spongiform encephalopathy epizootic: large scale survey. Bmj **347:**f5675.

152. **Ironside JW, Bishop MT, Connolly K, Hegazy D, Lowrie S, Le Grice M, Ritchie DL, McCardle LM, Hilton DA.** 2006. Variant Creutzfeldt-Jakob disease: prion protein genotype analysis of positive appendix tissue samples from a retrospective prevalence study. Bmj **332:**1186-1188.
153. **Ironside JW, Hilton DA, Ghani A, Johnston NJ, Conyers L, McCardle LM, Best D.** 2000. Retrospective study of prion-protein accumulation in tonsil and appendix tissues. Lancet **355:**1693-1694.
154. **Kong Q.** 2013. Transgenic Mouse Models in Prion Transmission Studies, p 171-182 doi:10.1007/978-1-4614-5338-3_11.
155. **Wilson R, Plinston C, Hunter N, Casalone C, Corona C, Tagliavini F, Suardi S, Ruggerone M, Moda F, Graziano S, Sbriccoli M, Cardone F, Pocchiari M, Ingrosso L, Baron T, Richt J, Andreoletti O, Simmons M, Lockey R, Manson JC, Barron RM.** 2012. Chronic wasting disease and atypical forms of bovine spongiform encephalopathy and scrapie are not transmissible to mice expressing wild-type levels of human prion protein. Journal of General Virology **93:**1624-1629.
156. **Sigurdson CJ, Williams ES, Miller MW, Spraker TR, O'Rourke KI, Hoover EA.** 1999. Oral transmission and early lymphoid tropism of chronic wasting disease PrPres in mule deer fawns (Odocoileus hemionus). Journal of General Virology **80:**2757-2764.
157. **Sigurdson CJ, Spraker TR, Miller MW, Oesch B, Hoover EA.** 2001. PrPCWD in the myenteric plexus, vagosympathetic trunk and endocrine glands of deer with chronic wasting disease. Journal of General Virology **82:**2327-2334.
158. **Mediano DR, Sanz-Rubio D, Ranera B, Bolea R, Martín-Burriel I.** 2014. The Potential of Mesenchymal Stem Cell in Prion Research. Zoonoses and Public Health doi:10.1111/zph.12138**:**n/a-n/a.
159. **Clarke MC, Haig DA.** 1970. Evidence for the multiplication of scrapie agent in cell culture. Nature **225:**100-101.
160. **Schatzl HM, Laszlo L, Holtzman DM, Tatzelt J, DeArmond SJ, Weiner RI, Mobley WC, Prusiner SB.** 1997. A hypothalamic neuronal cell line persistently infected with scrapie prions exhibits apoptosis. Journal of Virology **71:**8821-8831.
161. **Race RE, Fadness LH, Chesebro B.** 1987. Characterization of scrapie infection in mouse neuroblastoma cells. Journal of General Virology **68 (Pt 5):**1391-1399.
162. **Butler DA, Scott MR, Bockman JM, Borchelt DR, Taraboulos A, Hsiao KK, Kingsbury DT, Prusiner SB.** 1988. Scrapie-infected murine neuroblastoma cells produce protease-resistant prion proteins. Journal of Virology **62:**1558-1564.
163. **Follet J, Lemaire-Vieille C, Blanquet-Grossard F, Podevin-Dimster V, Lehmann S, Chauvin JP, Decavel JP, Varea R, Grassi J, Fontes M, Cesbron JY.** 2002. PrP expression and replication by Schwann cells: implications in prion spreading. Journal of Virology **76:**2434-2439.
164. **Kikuchi Y, Kakeya T, Sakai A, Takatori K, Nakamura N, Matsuda H, Yamazaki T, Tanamoto K, Sawada J.** 2004. Propagation of a protease-resistant form of prion protein in long-term cultured human glioblastoma cell line T98G. Journal of General Virology **85:**3449-3457.
165. **Bian J, Napier D, Khaychuck V, Angers R, Graham C, Telling G.** 2010. Cell-Based Quantification of Chronic Wasting Disease Prions. Journal of Virology **84:**8322-8326.
166. **Vilette D, Andreoletti O, Archer F, Madelaine MF, Vilotte JL, Lehmann S, Laude H.** 2001. Ex vivo propagation of infectious sheep scrapie agent in heterologous epithelial cells expressing ovine prion protein. Proceedings of the National Academy of Sciences **98:**4055-4059.
167. **Milhavet O, Casanova D, Chevallier N, McKay RD, Lehmann S.** 2006. Neural stem cell model for prion propagation. Stem Cells **24:**2284-2291.
168. **Giri RK, Young R, Pitstick R, DeArmond SJ, Prusiner SB, Carlson GA.** 2006. Prion infection of mouse neurospheres. Proceedings of the National Academy of Sciences **103:**3875-3880.

169. **Herva ME, Relano-Gines A, Villa A, Torres JM.** 2010. Prion infection of differentiated neurospheres. J Neurosci Methods **188:**270-275.
170. **Hollister JR, Lee KS, Dorward DW, Baron GS.** 2015. Efficient Uptake and Dissemination of Scrapie Prion Protein by Astrocytes and Fibroblasts from Adult Hamster Brain. PLoS One **10:**e0115351.
171. **Iwamaru Y, Takenouchi T, Imamura M, Shimizu Y, Miyazawa K, Mohri S, Yokoyama T, Kitani H.** 2013. Prion Replication Elicits Cytopathic Changes in Differentiated Neurosphere Cultures. Journal of Virology **87:**8745-8755.
172. **Vorberg I, Raines A, Story B, Priola SA.** 2004. Susceptibility of common fibroblast cell lines to transmissible spongiform encephalopathy agents. Journal of Infectious Diseases **189:**431-439.
173. **Dlakic WM, Grigg E, Bessen RA.** 2007. Prion infection of muscle cells in vitro. Journal of Virology **81:**4615-4624.
174. **Archer F, Bachelin C, Andreoletti O, Besnard N, Perrot G, Langevin C, Le Dur A, Vilette D, Baron-Van Evercooren A, Vilotte JL, Laude H.** 2004. Cultured peripheral neuroglial cells are highly permissive to sheep prion infection. Journal of Virology **78:**482-490.
175. **Lawson VA, Vella LJ, Stewart JD, Sharples RA, Klemm H, Machalek DM, Masters CL, Cappai R, Collins SJ, Hill AF.** 2008. Mouse-adapted sporadic human Creutzfeldt-Jakob disease prions propagate in cell culture. The International Journal of Biochemistry & Cell Biology **40:**2793-2801.
176. **Bosque PJ, Prusiner SB.** 2000. Cultured Cell Sublines Highly Susceptible to Prion Infection. Journal of Virology **74:**4377-4386.
177. **Mahal SP, Baker CA, Demczyk CA, Smith EW, Julius C, Weissmann C.** 2007. Prion strain discrimination in cell culture: the cell panel assay. Proceedings of the National Academy of Sciences **104:**20908-20913.
178. **Bate C, Langeveld J, Williams A.** 2004. Manipulation of PrPres production in scrapie-infected neuroblastoma cells. Journal of Neuroscience Methods **138:**217-223.
179. **Marella M, Lehmann S, Grassi J, Chabry J.** 2002. Filipin prevents pathological prion protein accumulation by reducing endocytosis and inducing cellular PrP release. Journal of Biological Chemistry **277:**25457-25464.
180. **Turnbull S, Tabner BJ, Brown DR, Allsop D.** 2003. Quinacrine acts as an antioxidant and reduces the toxicity of the prion peptide PrP106-126. Neuroreport **14:**1743-1745.
181. **Sandberg MK, Wallen P, Wikstrom MA, Kristensson K.** 2004. Scrapie-infected GT1-1 cells show impaired function of voltage-gated N-type calcium channels (Ca(v) 2.2) which is ameliorated by quinacrine treatment. Neurobiology of Disease **15:**143-151.
182. **Yung L, Huang Y, Lessard P, Legname G, Lin ET, Baldwin M, Prusiner SB, Ryou C, Guglielmo BJ.** 2004. Pharmacokinetics of quinacrine in the treatment of prion disease. BMC Infectious Diseases **4:**53.
183. **Gayrard V, Picard-Hagen N, Viguie C, Laroute V, Andreoletti O, Toutain PL.** 2005. A possible pharmacological explanation for quinacrine failure to treat prion diseases: pharmacokinetic investigations in a ovine model of scrapie. British Journal of Pharmacology **144:**386-393.
184. **Nunziante M, Kehler C, Maas E, Kassack MU, Groschup M, Schatzl HM.** 2005. Charged bipolar suramin derivatives induce aggregation of the prion protein at the cell surface and inhibit PrPSc replication. Journal of Cell Science **118:**4959-4973.
185. **Kocisko DA, Engel AL, Harbuck K, Arnold KM, Olsen EA, Raymond LD, Vilette D, Caughey B.** 2005. Comparison of protease-resistant prion protein inhibitors in cell cultures infected with two strains of mouse and sheep scrapie. Neuroscience Letters **388:**106-111.
186. **Enari M, Flechsig E, Weissmann C.** 2001. Scrapie prion protein accumulation by scrapie-infected neuroblastoma cells abrogated by exposure to a prion protein antibody. Proceedings of the National Academy of Sciences **98:**9295-9299.

187. **Kim CL, Karino A, Ishiguro N, Shinagawa M, Sato M, Horiuchi M.** 2004. Cell-surface retention of PrPC by anti-PrP antibody prevents protease-resistant PrP formation. Journal of General Virology **85:**3473-3482.
188. **Perrier V, Solassol J, Crozet C, Frobert Y, Mourton-Gilles C, Grassi J, Lehmann S.** 2004. Anti-PrP antibodies block PrPSc replication in prion-infected cell cultures by accelerating PrPC degradation. Journal of Neurochemistry **89:**454-463.
189. **Oboznaya MB, Gilch S, Titova MA, Koroev DO, Volkova TD, Volpina OM, Schatzl HM.** 2007. Antibodies to a nonconjugated prion protein peptide 95-123 interfere with PrP(Sc) propagation in prion-infected cells. Cellular and Molecular Neurobiology **27:**271-284.
190. **Taraboulos A, Raeber AJ, Borchelt DR, Serban D, Prusiner SB.** 1992. Synthesis and trafficking of prion proteins in cultured cells. Molecular Biology of the Cell **3:**851-863.
191. **Nishida N, Harris DA, Vilette D, Laude H, Frobert Y, Grassi J, Casanova D, Milhavet O, Lehmann S.** 2000. Successful transmission of three mouse-adapted scrapie strains to murine neuroblastoma cell lines overexpressing wild-type mouse prion protein. Journal of Virology **74:**320-325.
192. **Atarashi R, Sim VL, Nishida N, Caughey B, Katamine S.** 2006. Prion strain-dependent differences in conversion of mutant prion proteins in cell culture. Journal of Virology **80:**7854-7862.
193. **Paquet S, Langevin C, Chapuis J, Jackson GS, Laude H, Vilette D.** 2007. Efficient dissemination of prions through preferential transmission to nearby cells. Journal of General Virology **88:**706-713.
194. **Ghaemmaghami S, Phuan PW, Perkins B, Ullman J, May BC, Cohen FE, Prusiner SB.** 2007. Cell division modulates prion accumulation in cultured cells. Proceedings of the National Academy of Sciences **104:**17971-17976.
195. **Aguzzi A.** 2008. Unraveling prion strains with cell biology and organic chemistry. Proceedings of the National Academy of Sciences **105:**11-12.
196. **Oelschlegel AM, Fallahi M, Ortiz-Umpierre S, Weissmann C.** 2012. The extended cell panel assay characterizes the relationship of prion strains RML, 79A, and 139A and reveals conversion of 139A to 79A-like prions in cell culture. Journal of Virology **86:**5297-5303.
197. **Klohn PC, Stoltze L, Flechsig E, Enari M, Weissmann C.** 2003. A quantitative, highly sensitive cell-based infectivity assay for mouse scrapie prions. Proceedings of the National Academy of Sciences **100:**11666-11671.
198. **Bian J, Kang H-E, Telling GC.** 2014. Quinacrine promotes replication and conformational mutation of chronic wasting disease prions. Proceedings of the National Academy of Sciences **111:**6028-6033.
199. **Arellano-Anaya ZE, Savistchenko J, Mathey J, Huor A, Lacroux C, Andreoletti O, Vilette D.** 2011. A simple, versatile and sensitive cell-based assay for prions from various species. PLoS One **6:**e20563.
200. **Rubenstein R, Kascsak RJ, Merz PA, Papini MC, Carp RI, Robakis NK, Wisniewski HM.** 1986. Detection of scrapie-associated fibril (SAF) proteins using anti-SAF antibody in non-purified tissue preparations. Journal of General Virology **67 (Pt 4):**671-681.
201. **Seelig DM, Mason GL, Telling GC, Hoover EA.** 2010. Pathogenesis of Chronic Wasting Disease in Cervidized Transgenic Mice. The American Journal of Pathology **176:**2785-2797.
202. **Kang H-E, Weng CC, Saijo E, Saylor V, Bian J, Kim S, Ramos L, Angers R, Langenfeld K, Khaychuk V, Calvi C, Bartz J, Hunter N, Telling GC.** 2012. Characterization of Conformation-dependent Prion Protein Epitopes. Journal of Biological Chemistry **287:**37219-37232.
203. **Saijo E, Hughson AG, Raymond GJ, Suzuki A, Horiuchi M, Caughey B.** 2016. PrPSc-Specific Antibody Reveals C-terminal Conformational Differences between Prion Strains. Journal of Virology doi:10.1128/jvi.00088-16.

204. **Haley NJ, Carver S, Hoon-Hanks L, Henderson DM, Davenport KA, Bunting E, Gray S, Trindle B, Galeota J, LeVan I, Dubovos T, Shelton P, Hoover EA.** 2014. Chronic wasting disease detection in the lymph nodes of free-ranging cervids by real time quaking-induced conversion. Journal of Clinical Microbiology doi:10.1128/jcm.01258-14.
205. **Pan T, Chang B, Wong P, Li C, Li R, Kang SC, Robinson JD, Thompsett AR, Tein P, Yin S, Barnard G, McConnell I, Brown DR, Wisniewski T, Sy MS.** 2005. An aggregation-specific enzyme-linked immunosorbent assay: detection of conformational differences between recombinant PrP protein dimers and PrP(Sc) aggregates. Journal of Virology **79:**12355-12364.
206. **Pan T, Li R, Wong BS, Kang SC, Ironside J, Sy MS.** 2005. Novel antibody-lectin enzyme-linked immunosorbent assay that distinguishes prion proteins in sporadic and variant cases of Creutzfeldt-Jakob disease. Journal of Clinical Microbiology **43:**1118-1126.
207. **Kang S-C, Li R, Wang C, Pan T, Liu T, Rubenstein R, Barnard G, Wong B-S, Sy M-S.** 2003. Guanidine hydrochloride extraction and detection of prion proteins in mouse and hamster prion diseases by ELISA. The Journal of Pathology **199:**534-541.
208. **Saborio GP, Permanne B, Soto C.** 2001. Sensitive detection of pathological prion protein by cyclic amplification of protein misfolding. Nature **411:**810-813.
209. **Castilla J, Saa P, Soto C.** 2005. Detection of prions in blood. Nature Medicine **11:**982-985.
210. **Atarashi R, Moore RA, Sim VL, Hughson AG, Dorward DW, Onwubiko HA, Priola SA, Caughey B.** 2007. Ultrasensitive detection of scrapie prion protein using seeded conversion of recombinant prion protein. Nature Methods **4:**645-650.
211. **Atarashi R, Wilham JM, Christensen L, Hughson AG, Moore RA, Johnson LM, Onwubiko HA, Priola SA, Caughey B.** 2008. Simplified ultrasensitive prion detection by recombinant PrP conversion with shaking. Nature Methods **5:**211-212.
212. **Wilham JM, Orru CD, Bessen RA, Atarashi R, Sano K, Race B, Meade-White KD, Taubner LM, Timmes A, Caughey B.** 2010. Rapid end-point quantitation of prion seeding activity with sensitivity comparable to bioassays. PLoS Pathogens **6:**e1001217.
213. **Hackl EV, Darkwah J, Smith G, Ermolina I.** 2015. Effect of acidic and basic pH on Thioflavin T absorbance and fluorescence. European Biophysics Journal **44:**249-261.
214. **Mathiason CK, Hayes-Klug J, Hays SA, Powers J, Osborn DA, Dahmes SJ, Miller KV, Warren RJ, Mason GL, Telling GC, Young AJ, Hoover EA.** 2010. B Cells and Platelets Harbor Prion Infectivity in the Blood of Deer Infected with Chronic Wasting Disease. Journal of Virology **84:**5097-5107.
215. **Denkers ND, Hayes-Klug J, Anderson KR, Seelig DM, Haley NJ, Dahmes SJ, Osborn DA, Miller KV, Warren RJ, Mathiason CK, Hoover EA.** 2013. Aerosol Transmission of Chronic Wasting Disease in White-Tailed Deer. Journal of Virology **87:**1890-1892.
216. **Spraker TR, Zink RR, Cummings BA, Sigurdson CJ, Miller MW, O'Rourle KI.** 2002. Distribution of Protease-resistant Prion Protein and Spongiform Encephalopathy in Free-ranging Mule Deer (Odocoileus hemionus) with Chronic Wasting Disease. Veterinary Pathology Online **39:**546-556.
217. **Angers RC, Browning SR, Seward TS, Sigurdson CJ, Miller MW, Hoover EA, Telling GC.** 2006. Prions in Skeletal Muscles of Deer with Chronic Wasting Disease. Science **311:**1117.
218. **Haley NJ, Mathiason CK, Carver S, Zabel M, Telling GC, Hoover EA.** 2011. Detection of Chronic Wasting Disease Prions in Salivary, Urinary, and Intestinal Tissues of Deer: Potential Mechanisms of Prion Shedding and Transmission. Journal of Virology **85:**6309-6318.
219. **Balachandran A, Harrington NP, Algire J, Soutyrine A, Spraker TR, Jeffrey M, González L, O'Rourke KI.** 2010. Experimental oral transmission of chronic wasting disease to red deer (Cervus elaphus elaphus): Early detection and late stage distribution of protease-resistant prion protein. The Canadian Veterinary Journal **51:**169-178.
220. **Fox KA, Jewell JE, Williams ES, Miller MW.** 2006. Patterns of PrPCWD accumulation during the course of chronic wasting disease infection in orally inoculated mule deer (Odocoileus hemionus). Journal of General Virology **87:**3451-3461.

221. **Jewell JE, Brown J, Kreeger T, Williams ES.** 2006. Prion protein in cardiac muscle of elk (Cervus elaphus nelsoni) and white-tailed deer (Odocoileus virginianus) infected with chronic wasting disease. Journal of General Virology **87:**3443-3450.
222. **Race B, Meade-White K, Race R, Chesebro B.** 2009. Prion Infectivity in Fat of Deer with Chronic Wasting Disease. Journal of Virology **83:**9608-9610.
223. **Nalls AV, McNulty E, Powers J, Seelig DM, Hoover C, Haley NJ, Hayes-Klug J, Anderson K, Stewart P, Goldmann W, Hoover EA, Mathiason CK.** 2013. Mother to offspring transmission of chronic wasting disease in reeves' muntjac deer. PLoS One **8:**e71844.
224. **Hoover CE, Davenport KA, Henderson DM, Denkers ND, Mathiason CK, Soto C, Zabel MD, Hoover EA.** 2017. Pathways of prion spread during early chronic wasting disease in deer. Journal of Virology doi:10.1128/JVI.00077-17.
225. **Stamp JT, Brotherston JG, Zlotnik I, Mackay JMK, Smith W.** 1959. Further studies on scrapie. Journal of Comparative Pathology **69:**268-280.
226. **Kimberlin RH, Walker CA.** 1988. Incubation Periods in Six Models of Intraperitoneally Injected Scrapie Depend Mainly on the Dynamics of Agent Replication within the Nervous System and Not the Lymphoreticular System. Journal of General Virology **69:**2953-2960.
227. **Kimberlin RH, Walker CA.** 1989. The role of the spleen in the neuroinvasion of scrapie in mice. Virus Research **12:**201-211.
228. **Race R, Jenny A, Sutton D.** 1998. Scrapie Infectivity and Proteinase K—Resistant Prion Protein in Sheep Placenta, Brain, Spleen, and Lymph Node: Implications for Transmission and Antemortem Diagnosis. Journal of Infectious Diseases **178:**949-953.
229. **Hoover CE, Davenport KA, Henderson DM, Pulscher LA, Mathiason CK, Zabel MD, Hoover EA.** 2016. Detection and Quantification of CWD Prions in Fixed Paraffin Embedded Tissues by Real-Time Quaking-Induced Conversion. Scientific Reports **6:**25098.
230. **Denkers ND, Henderson DM, Mathiason CK, Hoover EA.** 2016. Enhanced prion detection in biological samples by magnetic particle extraction and real-time quaking-induced conversion. Journal of General Virology doi:doi:10.1099/jgv.0.000515.
231. **Henderson DM, Denkers ND, Hoover CE, Garbino N, Mathiason CK, Hoover EA.** 2015. Longitudinal Detection of Prion Shedding in Saliva and Urine by CWD-Infected Deer by RT-QuIC. Journal of Virology doi:10.1128/jvi.01118-15.
232. **Marsh RF, Kincaid AE, Bessen RA, Bartz JC.** 2005. Interspecies transmission of chronic wasting disease prions to squirrel monkeys (Saimiri sciureus). Journal of Virology **79:**13794-13796.
233. **Race B, Meade-White KD, Miller MW, Barbian KD, Rubenstein R, LaFauci G, Cervenakova L, Favara C, Gardner D, Long D, Parnell M, Striebel J, Priola SA, Ward A, Williams ES, Race R, Chesebro B.** 2009. Susceptibilities of Nonhuman Primates to Chronic Wasting Disease. Emerging Infectious Diseases **15:**1366-1376.
234. **Hamir AN, Kunkle RA, Miller JM, Greenlee JJ, Richt JA.** 2006. Experimental Second Passage of Chronic Wasting Disease (CWDmule deer) Agent to Cattle. Journal of Comparative Pathology **134:**63-69.
235. **Hamir AN, Miller JM, Kunkle RA, Hall SM, Richt JA.** 2007. Susceptibility of Cattle to First-passage Intracerebral Inoculation with Chronic Wasting Disease Agent from White-tailed Deer. Veterinary Pathology Online **44:**487-493.
236. **Hamir AN, Kunkle RA, Cutlip RC, Miller JM, Williams ES, Richt JA.** 2006. Transmission of Chronic Wasting Disease of Mule Deer to Suffolk Sheep following Intracerebral Inoculation. Journal of Veterinary Diagnostic Investigation **18:**558-565.
237. **Mathiason CK, Nalls AV, Seelig DM, Kraft SL, Carnes K, Anderson KR, Hayes-Klug J, Hoover EA.** 2013. Susceptibility of domestic cats to chronic wasting disease. Journal of Virology **87:**1947-1956.
238. **Bartz JC, Marsh RF, McKenzie DI, Aiken JM.** 1998. The host range of chronic wasting disease is altered on passage in ferrets. Virology **251:**297-301.

239. **Foster JD, Parnham D, Chong A, Goldmann W, Hunter N.** 2001. Clinical signs, histopathology and genetics of experimental transmission of BSE and natural scrapie to sheep and goats. Veterinary Record **148:**165-171.
240. **Wells GA, Hawkins SA, Austin AR, Ryder SJ, Done SH, Green RB, Dexter I, Dawson M, Kimberlin RH.** 2003. Studies of the transmissibility of the agent of bovine spongiform encephalopathy to pigs. Journal of General Virology **84:**1021-1031.
241. **Lasmézas CI, Comoy E, Hawkins S, Herzog C, Mouthon F, Konold T, Auvré F, Correia E, Lescoutra-Etchegaray N, Salès N.** 2005. Risk of oral infection with bovine spongiform encephalopathy agent in primates. The Lancet **365:**781-783.
242. **Lasmezas CI, Deslys JP, Demaimay R, Adjou KT, Lamoury F, Dormont D, Robain O, Ironside J, Hauw JJ.** 1996. BSE transmission to macaques. Nature **381:**743-744.
243. **Dagleish MP, Martin S, Steele P, Finlayson J, Sisó S, Hamilton S, Chianini F, Reid HW, González L, Jeffrey M.** 2008. Experimental transmission of bovine spongiform encephalopathy to European red deer (Cervus elaphus elaphus). BMC veterinary research **4:**17.
244. **Dagleish MP, Martin S, Steele P, Finlayson J, Eaton SL, Sisó S, Stewart P, Fernández-Borges N, Hamilton S, Pang Y, Chianini F, Reid HW, Goldmann W, González L, Castilla J, Jeffrey M.** 2015. Susceptibility of European Red Deer (Cervus elaphus elaphus) to Alimentary Challenge with Bovine Spongiform Encephalopathy. PLoS One **10:**e0116094.
245. **Lezmi S, Bencsik A, Monks E, Petit T, Baron T.** 2003. First case of feline spongiform encephalopathy in a captive cheetah born in France: PrPsc analysis in various tissues revealed unexpected targeting of kidney and adrenal gland. Histochemistry and Cell Biology **119:**415-422.
246. **Pearson G, Gruffydd-Jones T, Wyatt J, Hope J, Chong A, Scott A, Dawson M, Wells G.** 1991. Feline spongiform encephalopathy. Veterinary Record **128:**532-532.
247. **Kirkwood J, Cunningham A.** 1994. Epidemiological observations on spongiform encephalopathies in captive wild animals in the British Isles. Veterinary Record **135:**296-303.
248. **Sigurdson C, J.** 2008. A prion disease of cervids: Chronic wasting disease. Vet Res **39:**41.
249. **Collinge J, Palmer MS, Sidle KCL, Hill AF, Gowland I, Meads J, Asante E, Bradley R, Doey LJ, Lantos PL.** 1995. Unaltered susceptibility to BSE in transgenic mice expressing human prion protein. Nature **378:**779-783.
250. **Wadsworth JDF, Asante EA, Desbruslais M, Linehan JM, Joiner S, Gowland I, Welch J, Stone L, Lloyd SE, Hill AF, Brandner S, Collinge J.** 2004. Human Prion Protein with Valine 129 Prevents Expression of Variant CJD Phenotype. Science **306:**1793-1796.
251. **Asante EA, Linehan JM, Desbruslais M, Joiner S, Gowland I, Wood AL, Welch J, Hill AF, Lloyd SE, Wadsworth JDF, Collinge J.** 2002. BSE prions propagate as either variant CJD-like or sporadic CJD-like prion strains in transgenic mice expressing human prion protein. The EMBO Journal **21:**6358-6366.
252. **Asante EA, Linehan JM, Gowland I, Joiner S, Fox K, Cooper S, Osiguwa O, Gorry M, Welch J, Houghton R, Desbruslais M, Brandner S, Wadsworth JDF, Collinge J.** 2006. Dissociation of pathological and molecular phenotype of variant Creutzfeldt–Jakob disease in transgenic human prion protein 129 heterozygous mice. Proceedings of the National Academy of Sciences **103:**10759-10764.
253. **Kong Q, Huang S, Zou W, Vanegas D, Wang M, Wu D, Yuan J, Zheng M, Bai H, Deng H, Chen K, Jenny AL, O'Rourke K, Belay ED, Schonberger LB, Petersen RB, Sy MS, Chen SG, Gambetti P.** 2005. Chronic wasting disease of elk: transmissibility to humans examined by transgenic mouse models. Journal of Neuroscience **25:**7944-7949.
254. **Sandberg MK, Al-Doujaily H, Sigurdson CJ, Glatzel M, O'Malley C, Powell C, Asante EA, Linehan JM, Brandner S, Wadsworth JD, Collinge J.** 2010. Chronic wasting disease prions are not transmissible to transgenic mice overexpressing human prion protein. Journal of General Virology **91:**2651-2657.

255. **Tamguney G, Giles K, Bouzamondo-Bernstein E, Bosque PJ, Miller MW, Safar J, DeArmond SJ, Prusiner SB.** 2006. Transmission of elk and deer prions to transgenic mice. Journal of Virology **80:**9104-9114.
256. **Anderson CA, Bosque P, Filley CM, Arciniegas DB, Kleinschmidt-Demasters BK, Pape WJ, Tyler KL.** 2007. Colorado surveillance program for chronic wasting disease transmission to humans: lessons from 2 highly suspicious but negative cases. Archives of Neurology **64:**439-441.
257. **Olszowy KM, Lavelle J, Rachfal K, Hempstead S, Drouin K, Darcy Ii JM, Reiber C, Garruto RM.** 2014. Six-year follow-up of a point-source exposure to CWD contaminated venison in an Upstate New York community: risk behaviours and health outcomes 2005–2011. Public Health doi:http://dx.doi.org/10.1016/j.puhe.2014.06.012.
258. **Mawhinney S, Pape WJ, Forster JE, Anderson CA, Bosque P, Miller MW.** 2006. Human prion disease and relative risk associated with chronic wasting disease. Emerging Infectious Diseases **12:**1527-1535.
259. **Waddell L, Greig J, Mascarenhas M, Otten A, Corrin T, Hierlihy K.** 2017. Current evidence on the transmissibility of chronic wasting disease prions to humans-A systematic review. Transboundary and Emerging Diseases doi:10.1111/tbed.12612.
260. **Belay ED, Gambetti P, Schonberger LB, Parchi P, Lyon DR, Capellari S, McQuiston JH, Bradley K, Dowdle G, Crutcher JM, Nichols CR.** 2001. Creutzfeldt-Jakob disease in unusually young patients who consumed venison. Archives of Neurology **58:**1673-1678.
261. **Sano K, Atarashi R, Ishibashi D, Nakagaki T, Satoh K, Nishida N.** 2014. Conformational Properties of Prion Strains Can Be Transmitted to Recombinant Prion Protein Fibrils in Real-Time Quaking-Induced Conversion. Journal of Virology **88:**11791-11801.
262. **Sano K, Atarashi R, Nishida N.** 2015. Structural conservation of prion strain specificities in recombinant prion protein fibrils in real-time quaking-induced conversion. Prion **9:**237-243.
263. **Bartz JC, Bessen RA, McKenzie D, Marsh RF, Aiken JM.** 2000. Adaptation and selection of prion protein strain conformations following interspecies transmission of transmissible mink encephalopathy. Journal of Virology **74:**5542-5547.
264. **Kurt TD, Jiang L, Fernández-Borges N, Bett C, Liu J, Yang T, Spraker TR, Castilla J, Eisenberg D, Kong Q, Sigurdson CJ.** 2015. Human prion protein sequence elements impede cross-species chronic wasting disease transmission. Journal of Clinical Investigation **125:**0-0.
265. **Piening N, Nonno R, Di Bari M, Walter S, Windl O, Agrimi U, Kretzschmar HA, Bertsch U.** 2006. Conversion Efficiency of Bank Vole Prion Protein in Vitro Is Determined by Residues 155 and 170, but Does Not Correlate with the High Susceptibility of Bank Voles to Sheep Scrapie in Vivo. Journal of Biological Chemistry **281:**9373-9384.
266. **Raymond GJ, Hope J, Kocisko DA, Priola SA, Raymond LD, Bossers A, Ironside J, Will RG, Chen SG, Petersen RB, Gambetti P, Rubenstein R, Smits MA, Lansbury PT, Caughey B.** 1997. Molecular assessment of the potential transmissibilities of BSE and scrapie to humans. Nature **388:**285-288.
267. **Barria MA, Telling GC, Gambetti P, Mastrianni JA, Soto C.** 2011. Generation of a New Form of Human PrPSc in Vitro by Interspecies Transmission from Cervid Prions. Journal of Biological Chemistry **286:**7490-7495.
268. **Barria MA, Balachandran A, Morita M, Kitamoto T, Barron R, Manson J, Knight R, Ironside JW, Head MW.** 2014. Molecular barriers to zoonotic transmission of prions. Emerging Infectious Diseases **20:**88.
269. **Luers L, Bannach O, Stöhr J, Wördehoff MM, Wolff M, Nagel-Steger L, Riesner D, Willbold D, Birkmann E.** 2013. Seeded Fibrillation as Molecular Basis of the Species Barrier in Human Prion Diseases. PLoS One **8:**e72623.
270. **Kurt TD, Telling GC, Zabel MD, Hoover EA.** 2009. Trans-species amplification of PrPCWD and correlation with rigid loop 170N. Virology **387:**235-243.
271. **Williams ES, Young S.** 1980. Chronic wasting disease of captive mule deer: a spongiform encephalopathy. Journal of Wildlife Diseases **16:**89-98.

272. **Mabbott NA, MacPherson GG.** 2006. Prions and their lethal journey to the brain. Nature Reviews Microbiology **4:**201-211.
273. **Kimberlin RH, Walker CA.** 1989. Pathogenesis of scrapie in mice after intragastric infection. Virus Research **12:**213-220.
274. **Kimberlin RH, Field HJ, Walker CA.** 1983. Pathogenesis of Mouse Scrapie: Evidence for Spread of Infection from Central to Peripheral Nervous System. Journal of General Virology **64:**713-716.
275. **Lemaire-Vieille C, Schulze T, Podevin-Dimster V, Follet J, Bailly Y, Blanquet-Grossard F, Decavel J-P, Heinen E, Cesbron J-Y.** 2000. Epithelial and endothelial expression of the green fluorescent protein reporter gene under the control of bovine prion protein (PrP) gene regulatory sequences in transgenic mice. Proceedings of the National Academy of Sciences **97:**5422-5427.
276. **Paltrinieri S, Comazzi S, Spagnolo V, Rondena M, Ponti W, Ceciliani F.** 2004. Bovine Doppel (Dpl) and Prion Protein (PrP) Expression on Lymphoid Tissue and Circulating Leukocytes. Journal of Histochemistry & Cytochemistry **52:**1639-1645.
277. **Tichopad A, Pfaffl MW, Didier A.** 2003. Tissue-specific expression pattern of bovine prion gene: quantification using real-time RT-PCR. Molecular and Cellular Probes **17:**5-10.
278. **Peralta OA, Eyestone WH.** 2009. Quantitative and qualitative analysis of cellular prion protein (PrPC) expression in bovine somatic tissues. Prion **3:**161-170.
279. **Garcia-Crespo D, Juste RA, Hurtado A.** 2005. Selection of ovine housekeeping genes for normalisation by real-time RT-PCR; analysis of PrPgene expression and genetic susceptibility to scrapie. BMC veterinary research **1:**1-8.
280. **Horiuchi M, Yamazaki N, Ikeda T, Ishiguro N, Shinagawa M.** 1995. A cellular form of prion protein (PrPC) exists in many non-neuronal tissues of sheep. Journal of General Virology **76:**2583-2587.
281. **Bosque PJ, Ryou C, Telling G, Peretz D, Legname G, DeArmond SJ, Prusiner SB.** 2002. Prions in skeletal muscle. Proceedings of the National Academy of Sciences **99:**3812-3817.
282. **Ford MJ, Burton LJ, Morris RJ, Hall SM.** 2002. Selective expression of prion protein in peripheral tissues of the adult mouse. Neuroscience **113:**177-192.
283. **Ning Z-Y, Zhao D-M, Yang J-M, Cui Y-L, Meng L-P, Wu C-D, Liu H-X.** 2005. Quantification of prion gene expression in brain and peripheral organs of golden hamster by real-time RT-PCR. Animal Biotechnology **16:**55-65.
284. **Fournier JG, Escaig-Haye F, Billette de Villemeur T, Robain O, Lasmézas IC, Deslys J-P, Dormont D, Brown P.** 1998. Distribution and submicroscopic immunogold localization of cellular prion protein (PrPc) in extracerebral tissues. Cell and Tissue Research **292:**77-84.
285. **Clouse MD, Shikiya RA, Bartz JC, Kincaid AE.** 2015. Nasal Associated Lymphoid Tissue of the Syrian Golden Hamster Expresses High Levels of PrP^C. PLoS One **10:**e0117935.
286. **Stewart P, Campbell L, Skogtvedt S, Griffin KA, Arnemo JM, Tryland M, Girling S, Miller MW, Tranulis MA, Goldmann W.** 2012. Genetic Predictions of Prion Disease Susceptibility in Carnivore Species Based on Variability of the Prion Gene Coding Region. PLoS One **7:**e50623.
287. **Williamson RA, Peretz D, Pinilla C, Ball H, Bastidas RB, Rozenshteyn R, Houghten RA, Prusiner SB, Burton DR.** 1998. Mapping the prion protein using recombinant antibodies. Journal of Virology **72:**9413-9418.
288. **Henderson DM, Manca M, Haley NJ, Denkers ND, Nalls AV, Mathiason CK, Caughey B, Hoover EA.** 2013. Rapid Antemortem Detection of CWD Prions in Deer Saliva. PLoS One **8:**e74377.
289. **Donaldson DS, Kobayashi A, Ohno H, Yagita H, Williams IR, Mabbott NA.** 2012. M cell-depletion blocks oral prion disease pathogenesis. Mucosal Immunol **5:**216-225.
290. **Glaysher BR, Mabbott NA.** 2007. Role of the GALT in Scrapie Agent Neuroinvasion from the Intestine. The Journal of Immunology **178:**3757-3766.

291. **Prinz M, Huber G, Macpherson AJS, Heppner FL, Glatzel M, Eugster H-P, Wagner N, Aguzzi A.** 2003. Oral Prion Infection Requires Normal Numbers of Peyer's Patches but Not of Enteric Lymphocytes. The American Journal of Pathology **162:**1103-1111.
292. **Morel E, Fouquet S, Strup-Perrot C, Thievend CP, Petit C, Loew D, Faussat A-M, Yvernault L, Pinçon-Raymond M, Chambaz J, Rousset M, Thenet S, Clair C.** 2008. The Cellular Prion Protein PrPc Is Involved in the Proliferation of Epithelial Cells and in the Distribution of Junction-Associated Proteins. PLoS One **3:**e3000.
293. **Morel E, Fouquet S, Chateau D, Yvernault L, Frobert Y, Pinçon-Raymond M, Chambaz J, Pillot T, Rousset M.** 2004. The Cellular Prion Protein PrPc Is Expressed in Human Enterocytes in Cell-Cell Junctional Domains. Journal of Biological Chemistry **279:**1499-1505.
294. **Michel B, Meyerett-Reid C, Johnson T, Ferguson A, Wyckoff C, Pulford B, Bender H, Avery A, Telling G, Dow S, Zabel MD.** 2012. Incunabular Immunological Events in Prion Trafficking. Scientific Reports **2:**440.
295. **Heggebø R, Press CM, Gunnes G, González L, Jeffrey M.** 2002. Distribution and accumulation of PrP in gut-associated and peripheral lymphoid tissue of scrapie-affected Suffolk sheep. Journal of General Virology **83:**479-489.
296. **Andréoletti O, Berthon P, Marc D, Sarradin P, Grosclaude J, van Keulen L, Schelcher F, Elsen J-M, Lantier F.** 2000. Early accumulation of PrPSc in gut-associated lymphoid and nervous tissues of susceptible sheep from a Romanov flock with natural scrapie. Journal of General Virology **81:**3115-3126.
297. **van Keulen LJ, Schreuder BE, Meloen RH, Mooij-Harkes G, Vromans ME, Langeveld JP.** 1996. Immunohistochemical detection of prion protein in lymphoid tissues of sheep with natural scrapie. Journal of Clinical Microbiology **34:**1228-1231.
298. **Kimberlin RH, Walker CA.** 1979. Pathogenesis of mouse scrapie: Dynamics of agent replication in spleen, spinal cord and brain after infection by different routes. Journal of Comparative Pathology **89:**551-562.
299. **Race R, Oldstone M, Chesebro B.** 2000. Entry versus Blockade of Brain Infection following Oral or Intraperitoneal Scrapie Administration: Role of Prion Protein Expression in Peripheral Nerves and Spleen. Journal of Virology **74:**828-833.
300. **Thomzig A, Schulz-Schaeffer W, Kratzel C, Mai J, Beekes M.** 2004. Preclinical deposition of pathological prion protein PrPSc in muscles of hamsters orally exposed to scrapie. Journal of Clinical Investigation **113:**1465-1472.
301. **Kimberlin RH, Hall SM, Walker CA.** 1983. Pathogenesis of mouse scrapie: Evidence for direct neural spread of infection to the CNS after injection of sciatic nerve. Journal of the Neurological Sciences **61:**315-325.
302. **Urayama A, Concha-Marambio L, Khan U, Bravo-Alegria J, Kharat V, Soto C.** 2016. Prions efficiently cross the intestinal barrier after oral administration: Study of the bioavailability, and cellular and tissue distribution in vivo. Scientific Reports **6:**32338.
303. **Van Keulen LJM, Vromans MEW, Van Zijderveld FG.** 2002. Early and late pathogenesis of natural scrapie infection in sheep. APMIS **110:**23-32.
304. **Cheng YC, Hannaoui S, John TR, Dudas S, Czub S, Gilch S.** 2016. Early and Non-Invasive Detection of Chronic Wasting Disease Prions in Elk Feces by Real-Time Quaking Induced Conversion. PLoS One **11:**e0166187.
305. **Henderson DM, Davenport KA, Haley NJ, Denkers ND, Mathiason CK, Hoover EA.** 2014. Quantitative Assessment of Prion Infectivity in Tissues and Body Fluids by RT-QuIC. Journal of General Virology doi:10.1099/vir.0.069906-0.
306. **Haley NJ, Seelig DM, Zabel MD, Telling GC, Hoover EA.** 2009. Detection of CWD Prions in Urine and Saliva of Deer by Transgenic Mouse Bioassay. PLoS One **4:**e4848.
307. **Johnson RT.** 2005. Prion diseases. The Lancet Neurology **4:**635-642.

308. **van Keulen LJM, Schreuder BEC, Vromans MEW, Langeveld JPM, Smits MA.** 1999. Scrapie-associated Prion Protein in the Gastro-intestinal Tract of Sheep with Natural Scrapie. Journal of Comparative Pathology **121:**55-63.
309. **Jeffrey M, Begara-McGorum I, Clark S, Martin S, Clark J, Chaplin M, González L.** 2002. Occurrence and Distribution of Infection-specific PrP in Tissues of Clinical Scrapie Cases and Cull Sheep from Scrapie-affected Farms in Shetland. Journal of Comparative Pathology **127:**264-273.
310. **Jeffrey M, Martin S, Thomson JR, Dingwall WS, Begara-McGorum I, González L.** 2001. Onset and Distribution of Tissue PrP Accumulation in Scrapie-affected Suffolk Sheep as Demonstrated by Sequential Necropsies and Tonsillar Biopsies. Journal of Comparative Pathology **125:**48-57.
311. **Thomzig A, Schulz-Schaeffer W, Wrede A, Wemheuer W, Brenig B, Kratzel C, Lemmer K, Beekes M.** 2007. Accumulation of Pathological Prion Protein PrPSc in the Skin of Animals with Experimental and Natural Scrapie. PLoS Pathogens **3:**e66.
312. **Race B, Meade-White K, Oldstone MBA, Race R, Chesebro B.** 2008. Detection of Prion Infectivity in Fat Tissues of Scrapie-Infected Mice. PLoS Pathogens **4:**e1000232.
313. **Di Bari MA, Chianini F, Vaccari G, Esposito E, Conte M, Eaton SL, Hamilton S, Finlayson J, Steele PJ, Dagleish MP, Reid HW, Bruce M, Jeffrey M, Agrimi U, Nonno R.** 2008. The bank vole (Myodes glareolus) as a sensitive bioassay for sheep scrapie. Journal of General Virology **89:**2975-2985.
314. **Nonno R, Bari MAD, Cardone F, Vaccari G, Fazzi P, Dell'Omo G, Cartoni C, Ingrosso L, Boyle A, Galeno R, Sbriccoli M, Lipp H-P, Bruce M, Pocchiari M, Agrimi U.** 2006. Efficient Transmission and Characterization of Creutzfeldt Jakob Disease Strains in Bank Voles. PLoS Pathogens **2:**e12.
315. **Pattison IH, Millson GC.** 1961. Experimental Transmission of Scrapie To Goats and Sheep By the Oral Route. Journal of Comparative Pathology and Therapeutics **71:**171-176.
316. **Telling GC, Scott M, Hsiao KK, Foster D, Yang SL, Torchia M, Sidle KC, Collinge J, DeArmond SJ, Prusiner SB.** 1994. Transmission of Creutzfeldt-Jakob disease from humans to transgenic mice expressing chimeric human-mouse prion protein. Proceedings of the National Academy of Sciences **91:**9936-9940.
317. **Saá P, Yakovleva O, de Castro J, Vasilyeva I, De Paoli SH, Simak J, Cervenakova L.** 2014. First Demonstration of Transmissible Spongiform Encephalopathy-associated Prion Protein (PrPTSE) in Extracellular Vesicles from Plasma of Mice Infected with Mouse-adapted Variant Creutzfeldt-Jakob Disease by in Vitro Amplification. Journal of Biological Chemistry **289:**29247-29260.
318. **Rubenstein R, Deng H, Race R, Ju W, Scalici C, Papini M, Rubenstein A, Kascsak R, Carp R.** 1994. Scrapie strain infection in vitro induces changes in neuronal cells. Molecular Neurobiology **8:**129-138.
319. **Rubenstein R, Deng H, Scalici CL, Papini MC.** 1991. Alterations in neurotransmitter-related enzyme activity in scrapie-infected PC12 cells. Journal of General Virology **72 (Pt 6):**1279-1285.
320. **Rubenstein R, Carp RI, Callahan SM.** 1984. In vitro replication of scrapie agent in a neuronal model: infection of PC12 cells. Journal of General Virology **65 (Pt 12):**2191-2198.
321. **Courageot MP, Daude N, Nonno R, Paquet S, Di Bari MA, Le Dur A, Chapuis J, Hill AF, Agrimi U, Laude H, Vilette D.** 2008. A cell line infectible by prion strains from different species. Journal of General Virology **89:**341-347.
322. **Haley NJ, Van de Motter A, Carver S, Henderson D, Davenport K, Seelig DM, Mathiason C, Hoover E.** 2013. Prion-Seeding Activity in Cerebrospinal Fluid of Deer with Chronic Wasting Disease. PLoS One **8:**e81488.
323. **Haley NJ, Siepker C, Walter WD, Thomsen BV, Greenlee JJ, Lehmkuhl AD, Richt JA.** 2016. Antemortem detection of chronic wasting disease prions in nasal brush collections and

rectal biopsies from white-tailed deer by real time quaking-induced conversion. Journal of Clinical Microbiology doi:10.1128/jcm.02699-15.

324. **Davenport KA, Christensen JR, Bian J, Young M, Gallegos J, Calvi CL, Kim S, Balachandran A, Hoover EA, Telling GC.** 2017. Infectious prions are present in the lymphoid system of cervids with chronic wasting disease, Manuscript in preparation.
325. **Davenport KA, Henderson DM, Mathiason CK, Hoover EA.** 2016. Assessment of the PrPc Amino-Terminal Domain in Prion Species Barriers. Journal of Virology **90:**10752-10761.
326. **Silveira JR, Raymond GJ, Hughson AG, Race RE, Sim VL, Hayes SF, Caughey B.** 2005. The most infectious prion protein particles. Nature **437:**257-261.
327. **Balkema-Buschmann A, Eiden M, Hoffmann C, Kaatz M, Ziegler U, Keller M, Groschup MH.** 2011. BSE infectivity in the absence of detectable PrP(Sc) accumulation in the tongue and nasal mucosa of terminally diseased cattle. Journal of General Virology **92:**467-476.
328. **Hoffmann C, Eiden M, Kaatz M, Keller M, Ziegler U, Rogers R, Hills B, Balkema-Buschmann A, van Keulen L, Jacobs JG, Groschup MH.** 2011. BSE infectivity in jejunum, ileum and ileocaecal junction of incubating cattle. Veterinary Research **42:**21.
329. **Balkema-Buschmann A, Fast C, Kaatz M, Eiden M, Ziegler U, McIntyre L, Keller M, Hills B, Groschup MH.** 2011. Pathogenesis of classical and atypical BSE in cattle. Preventative Veterinary Medicine **102:**112-117.
330. **Wells GA, Spiropoulos J, Hawkins SA, Ryder SJ.** 2005. Pathogenesis of experimental bovine spongiform encephalopathy: preclinical infectivity in tonsil and observations on the distribution of lingual tonsil in slaughtered cattle. Veterinary Record **156:**401-407.
331. **Cutlip RC, Miller JM, Race RE, Jenny AL, Katz JB, Lehmkuhl HD, DeBey BM, Robinson MM.** 1994. Intracerebral Transmission of Scrapie to Cattle. The Journal of Infectious Diseases **169:**814-820.
332. **Haley N, Siepker C, Greenlee J, Richt J.** 2016. Limited amplification of chronic wasting disease prions in the peripheral tissues of intracerebrally inoculated cattle. Journal of General Virology doi:doi:10.1099/jgv.0.000438.
333. **Béringue V, Herzog L, Jaumain E, Reine F, Sibille P, Le Dur A, Vilotte J-L, Laude H.** 2012. Facilitated Cross-Species Transmission of Prions in Extraneural Tissue. Science **335:**472-475.
334. **Angers RC, Kang H-E, Napier D, Browning S, Seward T, Mathiason C, Balachandran A, McKenzie D, Castilla J, Soto C, Jewell J, Graham C, Hoover EA, Telling GC.** 2010. Prion Strain Mutation Determined by Prion Protein Conformational Compatibility and Primary Structure. Science **328:**1154-1158.
335. **van Rheede T, Smolenaars MMW, Madsen O, de Jong WW.** 2003. Molecular Evolution of the Mammalian Prion Protein. Molecular Biology and Evolution **20:**111-121.
336. **Sigurdson C, Miller MW.** 2003. Other animal prion diseases. British Medical Bulletin **66:**199-212.
337. **Hamir AN, Kunkle RA, Cutlip RC, Miller JM, O'Rourke KI, Williams ES, Miller MW, Stack MJ, Chaplin MJ, Richt JA.** 2005. Experimental Transmission of Chronic Wasting Disease Agent from Mule Deer to Cattle by the Intracerebral Route. Journal of Veterinary Diagnostic Investigation **17:**276-281.
338. **Kong Q, Huang S, Zou W, Vanegas D, Wang M, Wu D, Yuan J, Zheng M, Bai H, Deng H, Chen K, Jenny AL, O'Rourke K, Belay ED, Schonberger LB, Petersen RB, Sy MS, Chen SG, Gambetti P.** 2005. Chronic wasting disease of elk: transmissibility to humans examined by transgenic mouse models. J Neurosci **25:**7944-7949.
339. **Sandberg MK, Al-Doujaily H, Sigurdson CJ, Glatzel M, O'Malley C, Powell C, Asante EA, Linehan JM, Brandner S, Wadsworth JD, Collinge J.** 2010. Chronic wasting disease prions are not transmissible to transgenic mice overexpressing human prion protein. J Gen Virol **91:**2651-2657.

340. **Kurt TD, Jiang L, Fernández-Borges N, Bett C, Liu J, Yang T, Spraker TR, Castilla J, Eisenberg D, Kong Q, Sigurdson CJ.** 2015. Human prion protein sequence elements impede cross-species chronic wasting disease transmission. J Clin Invest **125:**0-0.
341. **Tamgüney G, Miller MW, Giles K, Lemus A, Glidden DV, DeArmond SJ, Prusiner SB.** 2009. Transmission of scrapie and sheep-passaged bovine spongiform encephalopathy prions to transgenic mice expressing elk prion protein. Journal of General Virology **90:**1035-1047.
342. **Raymond GJ, Bossers A, Raymond LD, O'Rourke KI, McHolland LE, Bryant PK, Miller MW, Williams ES, Smits M, Caughey B.** 2000. Evidence of a molecular barrier limiting susceptibility of humans, cattle and sheep to chronic wasting disease. The EMBO Journal **19:**4425-4430.
343. **Jones M, Wight D, Barron R, Jeffrey M, Manson J, Prowse C, Ironside JW, Head MW.** 2009. Molecular Model of Prion Transmission to Humans. Emerging Infectious Diseases **15:**2013-2016.
344. **Torres J-M, Espinosa J-C, Aguilar-Calvo P, Herva M-E, Relaño-Ginés A, Villa-Diaz A, Morales M, Parra B, Alamillo E, Brun A, Castilla J, Molina S, Hawkins SAC, Andreoletti O.** 2014. Elements Modulating the Prion Species Barrier and Its Passage Consequences. PLoS One **9:**e89722.
345. **Bruce M, Chree A, McConnell I, Foster J, Pearson G, Fraser H.** 1994. Transmission of Bovine Spongiform Encephalopathy and Scrapie to Mice: Strain Variation and the Species Barrier, vol 343.
346. **Orrú CD, Favole A, Corona C, Mazza M, Manca M, Groveman BR, Hughson AG, Acutis PL, Caramelli M, Zanusso G, Casalone C, Caughey B.** 2015. Detection and Discrimination of Classical and Atypical L-type Bovine Spongiform Encephalopathy by Real-Time Quaking-Induced Conversion. Journal of Clinical Microbiology doi:10.1128/jcm.02906-14.
347. **Wells GAH, McGill IS.** 1992. Recently described scrapie-like encephalopathies of animals: case definitions. Research in Veterinary Science **53:**1-10.
348. **Di Bari MA, Nonno R, Castilla J, D'Agostino C, Pirisinu L, Riccardi G, Conte M, Richt J, Kunkle R, Langeveld J, Vaccari G, Agrimi U.** 2013. Chronic Wasting Disease in Bank Voles: Characterisation of the Shortest Incubation Time Model for Prion Diseases. PLoS Pathog **9:**e1003219.
349. **Hamir AN, Cutlip RC, Miller JM, Williams ES, Stack MJ, Miller MW, O'Rourke KI, Chaplin MJ.** 2001. Preliminary Findings on the Experimental Transmission of Chronic Wasting Disease Agent of Mule Deer to Cattle. Journal of Veterinary Diagnostic Investigation **13:**91-96.
350. **Houston F, Foster JD, Chong A, Hunter N, Bostock CJ.** 2000. Transmission of BSE by blood transfusion in sheep. The Lancet **356:**999-1000.
351. **Shmerling D, Hegyi I, Fischer M, Blättler T, Brandner S, Götz J, Rülicke T, Flechsig E, Cozzio A, von Mering C, Hangartner C, Aguzzi A, Weissmann C.** 1998. Expression of Amino-Terminally Truncated PrP in the Mouse Leading to Ataxia and Specific Cerebellar Lesions. Cell **93:**203-214.
352. **Uchiyama K, Miyata H, Yano M, Yamaguchi Y, Imamura M, Muramatsu N, Das NR, Chida J, Hara H, Sakaguchi S.** 2014. Mouse-Hamster Chimeric Prion Protein (PrP) Devoid of N-Terminal Residues 23-88 Restores Susceptibility to 22L Prions, but Not to RML Prions in PrP-Knockout Mice. PLoS One **9:**e109737.
353. **Flechsig E, Shmerling D, Hegyi I, Raeber AJ, Fischer M, Cozzio A, von Mering C, Aguzzi A, Weissmann C.** 2000. Prion Protein Devoid of the Octapeptide Repeat Region Restores Susceptibility to Scrapie in PrP Knockout Mice. Neuron **27:**399-408.
354. **Supattapone S, Muramoto T, Legname G, Mehlhorn I, Cohen FE, DeArmond SJ, Prusiner SB, Scott MR.** 2001. Identification of Two Prion Protein Regions That Modify Scrapie Incubation Time. Journal of Virology **75:**1408-1413.
355. **Supattapone S, Bosque P, Muramoto T, Wille H, Aagaard C, Peretz D, Nguyen H-OB, Heinrich C, Torchia M, Safar J, Cohen FE, DeArmond SJ, Prusiner SB, Scott M.** 1999.

Prion Protein of 106 Residues Creates an Artificial Transmission Barrier for Prion Replication in Transgenic Mice. Cell **96:**869-878.
356. **Lawson VA, Priola SA, Meade-White K, Lawton M, Chesebro B.** 2004. Flexible N-terminal region of prion protein influences conformation of protease resistant prion protein isoforms associated with cross-species scrapie infection in vivo and in vitro. Journal of Biological Chemistry **279**.
357. **Surewicz WK, Jones EM, Apetri AC.** 2006. The Emerging Principles of Mammalian Prion Propagation and Transmissibility Barriers: Insight from Studies in Vitro. Accounts of Chemical Research **39:**654-662.
358. **Swietnicki W, Petersen R, Gambetti P, Surewicz WK.** 1997. pH-dependent Stability and Conformation of the Recombinant Human Prion Protein PrP(90–231). Journal of Biological Chemistry **272:**27517-27520.
359. **Frankenfield KN, Powers ET, Kelly JW.** 2005. Influence of the N-terminal domain on the aggregation properties of the prion protein. Protein Science **14:**2154-2166.
360. **Slapšak U, Salzano G, Amin L, Abskharon RNN, Ilc G, Zupančič B, Biljan I, Plavec J, Giachin G, Legname G.** 2016. The N-terminus of the Prion Protein Mediates Functional Interactions with NCAM Fibronectin Domain. Journal of Biological Chemistry doi:10.1074/jbc.M116.743435.
361. **Hamanaka T, Nishizawa K, Sakasegawa Y, Oguma A, Teruya K, Kurahashi H, Hara H, Sakaguchi S, Doh-ura K.** 2017. Melanin or melanin-like substance interacts with the N-terminal portion of prion protein and inhibits abnormal prion protein formation in prion-infected cells. Journal of Virology doi:10.1128/jvi.01862-16.
362. **Weissmann C.** 1996. Molecular biology of transmissible spongiform encephalopathies. FEBS Letters **389:**3-11.
363. **Guillot-Sestier M-V, Sunyach C, Druon C, Scarzello S, Checler F.** 2009. The α-Secretase-derived N-terminal Product of Cellular Prion, N1, Displays Neuroprotective Function in Vitro and in Vivo. Journal of Biological Chemistry **284:**35973-35986.
364. **Orru CD, Caughey B.** 2011. Prion seeded conversion and amplification assays. Top Curr Chem **305:**121-133.
365. **Orrú CD, Groveman BR, Raymond LD, Hughson AG, Nonno R, Zou W, Ghetti B, Gambetti P, Caughey B.** 2015. Bank Vole Prion Protein As an Apparently Universal Substrate for RT-QuIC-Based Detection and Discrimination of Prion Strains. PLoS Pathogens **11:**e1004983.
366. **Nonno R, Bari MAD, Cardone F, Vaccari G, Fazzi P, Dell'Omo G, Cartoni C, Ingrosso L, Boyle A, Galeno R, Sbriccoli M, Lipp H-P, Bruce M, Pocchiari M, Agrimi U.** 2006. Efficient Transmission and Characterization of Creutzfeldt–Jakob Disease Strains in Bank Voles. PLoS Pathog **2:**e12.
367. **Radovanovic I, Braun N, Giger OT, Mertz K, Miele G, Prinz M, Navarro B, Aguzzi A.** 2005. Truncated Prion Protein and Doppel Are Myelinotoxic in the Absence of Oligodendrocytic PrPC. The Journal of Neuroscience **25:**4879-4888.
368. **Jones EM, Surewicz K, Surewicz WK.** 2006. Role of N-terminal familial mutations in prion protein fibrillization and prion amyloid propagation in vitro. Journal of Biological Chemistry **281:**8190-8196.
369. **Jones EM, Surewicz WK.** 2005. Fibril Conformation as the Basis of Species- and Strain-Dependent Seeding Specificity of Mammalian Prion Amyloids. Cell **121:**63-72.
370. **Yokoyama T, Masujin K, Iwamaru Y, Imamura M, Mohri S.** 2009. Alteration of the biological and biochemical characteristics of bovine spongiform encephalopathy prions during interspecies transmission in transgenic mice models. Journal of General Virology **90:**261-268.
371. **Scott MR, Safar J, Telling G, Nguyen O, Groth D, Torchia M, Koehler R, Tremblay P, Walther D, Cohen FE, DeArmond SJ, Prusiner SB.** 1997. Identification of a prion protein

epitope modulating transmission of bovine spongiform encephalopathy prions to transgenic mice. Proceedings of the National Academy of Sciences **94:**14279-14284.

372. **Evans Eric GB, Pushie MJ, Markham Kate A, Lee H-W, Millhauser Glenn L.** Interaction between Prion Protein's Copper-Bound Octarepeat Domain and a Charged C-Terminal Pocket Suggests a Mechanism for N-Terminal Regulation. Structure doi:http://dx.doi.org/10.1016/j.str.2016.04.017.
373. **Hoover CE, Davenport KA, Henderson DM, Zabel MD, Hoover EA.** 2017. Endogenous brain lipids inhibit prion amyloid formation in vitro. Journal of Virology doi:10.1128/jvi.02162-16.
374. **Orru CD, Wilham JM, Vascellari S, Hughson AG, Caughey B.** 2012. New generation QuIC assays for prion seeding activity. Prion **6:**147-152.
375. **Abdel-Haq H.** 2014. Factors intrinsic and extrinsic to blood hamper the development of a routine blood test for human prion diseases. Journal of General Virology doi:10.1099/vir.0.070979-0.
376. **De Luigi A, Colombo L, Diomede L, Capobianco R, Mangieri M, Miccolo C, Limido L, Forloni G, Tagliavini F, Salmona M.** 2008. The efficacy of tetracyclines in peripheral and intracerebral prion infection. PLoS One **3:**e1888.
377. **Forloni G, Iussich S, Awan T, Colombo L, Angeretti N, Girola L, Bertani I, Poli G, Caramelli M, Grazia Bruzzone M, Farina L, Limido L, Rossi G, Giaccone G, Ironside JW, Bugiani O, Salmona M, Tagliavini F.** 2002. Tetracyclines affect prion infectivity. Proceedings of the National Academy of Sciences **99:**10849-10854.
378. **Haik S, Marcon G, Mallet A, Tettamanti M, Welaratne A, Giaccone G, Azimi S, Pietrini V, Fabreguettes JR, Imperiale D, Cesaro P, Buffa C, Aucan C, Lucca U, Peckeu L, Suardi S, Tranchant C, Zerr I, Houillier C, Redaelli V, Vespignani H, Campanella A, Sellal F, Krasnianski A, Seilhean D, Heinemann U, Sedel F, Canovi M, Gobbi M, Di Fede G, Laplanche JL, Pocchiari M, Salmona M, Forloni G, Brandel JP, Tagliavini F.** 2014. Doxycycline in Creutzfeldt-Jakob disease: a phase 2, randomised, double-blind, placebo-controlled trial. Lancet Neurol **13:**150-158.
379. **Doh-Ura K, Iwaki T, Caughey B.** 2000. Lysosomotropic agents and cysteine protease inhibitors inhibit scrapie-associated prion protein accumulation. Journal of Virology **74:**4894-4897.
380. **Collinge J, Gorham M, Hudson F, Kennedy A, Keogh G, Pal S, Rossor M, Rudge P, Siddique D, Spyer M, Thomas D, Walker S, Webb T, Wroe S, Darbyshire J.** 2009. Safety and efficacy of quinacrine in human prion disease (PRION-1 study): a patient-preference trial. The Lancet Neurology **8:**334-344.
381. **Korth C, May BC, Cohen FE, Prusiner SB.** 2001. Acridine and phenothiazine derivatives as pharmacotherapeutics for prion disease. Proc Natl Acad Sci U S A **98:**9836-9841.
382. **Risse E, Nicoll AJ, Taylor WA, Wright D, Badoni M, Yang X, Farrow MA, Collinge J.** 2015. Identification of a compound which disrupts binding of amyloid-beta to the prion protein using a novel fluorescence-based assay. Journal of Biological Chemistry doi:10.1074/jbc.M115.637124.
383. **Suenaga M, Hiramoto Y, Matsunaga Y.** 2013. Vitamin D 2 interacts with Human PrP (c) (90-231) and breaks PrP (c) oligomerization in vitro. Prion **7**.
384. **Cortez LM, Campeau J, Norman G, Kalayil M, Van der Merwe J, McKenzie D, Sim VL.** 2015. Bile acids reduce prion conversion, reduce neuronal loss, and prolong male survival in models of prion disease. Journal of Virology doi:10.1128/jvi.01165-15.
385. **Yamasaki T, Suzuki A, Hasebe R, Horiuchi M.** 2014. Comparison of the Anti-Prion Mechanism of Four Different Anti-Prion Compounds, Anti-PrP Monoclonal Antibody 44B1, Pentosan Polysulfate, Chlorpromazine, and U18666A, in Prion-Infected Mouse Neuroblastoma Cells. PLoS One **9:**e106516.
386. **Fickel J, Göritz F, Joest AB, Hildebrandt T, Hofmann RR, Breves G.** 1998. Analysis of parotid and mixed saliva in Roe deer (Capreolus capreolus L.). Journal of Comparative Physiology B **168:**257-264.
387. **Kay RNB.** 1960. The rate of flow and composition of various salivary secretions in sheep and calves. The Journal of Physiology **150:**515-537.

388. **Austin PJ, Suchar LA, Robbins CT, Hagerman AE.** 1989. Tannin-binding proteins in saliva of deer and their absence in saliva of sheep and cattle. Journal of Chemical Ecology **15:**1335-1347.
389. **Anonymous.** !!! INVALID CITATION !!! {Bartley, 1961 #1237;Park, 2007 #1583;Tettamanti, 1968 #1238}.
390. **Tettamanti G, Pigman W.** 1968. Purification and characterization of bovine and ovine submaxillary mucins. Archives of Biochemistry and Biophysics **124:**41-50.
391. **Brayshaw DJ, Berry M, McMaster TJ.** 2003. Optimisation of sample preparation methods for air imaging of ocular mucins by AFM. Ultramicroscopy **97:**289-296.
392. **Cao X, Muskhelishvili L, Latendresse J, Richter P, Heflich RH.** 2017. Evaluating the Toxicity of Cigarette Whole Smoke Solutions in an Air-liquid-interface Human in vitro Airway Tissue Model. Toxicological Sciences doi:10.1093/toxsci/kfw239.
393. **McDougall EI.** 1948. Studies on ruminant saliva. 1. The composition and output of sheep's saliva. Biochemical Journal **43:**99-109.
394. **Ionta FQ, Mendonca FL, de Oliveira GC, de Alencar CR, Honorio HM, Magalhaes AC, Rios D.** 2014. In vitro assessment of artificial saliva formulations on initial enamel erosion remineralization. Journal of Dentistry **42:**175-179.
395. **Langstroth GO, McRae DR, Stavraky GW.** 1938. The Secretion of Protein Material in the Parasympathetic Submaxillary Saliva. Proceedings of the Royal Society of London Series B, Biological Sciences **125:**335-347.
396. **Bartley EE, Yadava IS.** 1961. Bloat in Cattle. IV. the Role of Bovine Saliva, Plant Mucilages, and Animal Mucins1. Journal of Animal Science **20:**648-653.
397. **Park MS, Chung JW, Kim YK, Chung SC, Kho HS.** 2007. Viscosity and wettability of animal mucin solutions and human saliva. Oral Diseases **13:**181-186.
398. **Amini A, Masoumi-Moghaddam S, Ehteda A, Liauw W, Morris DL.** 2015. Depletion of mucin in mucin-producing human gastrointestinal carcinoma: Results from in vitro and in vivo studies with bromelain and N-acetylcysteine. Oncotarget **6:**33329-33344.
399. **Rubin BK.** 2007. Mucolytics, expectorants, and mucokinetic medications. Respiratory Care **52:**859-865.
400. **Kennedy S, Davis C, Abrams WR, Billings PC, Nagashunmugam T, Friedman H, Malamud D.** 1998. Submandibular salivary proteases: lack of a role in anti-HIV activity. Journal of Dental Research **77:**1515-1519.
401. **Roberton AM, Wiggins R, Horner PJ, Greenwood R, Crowley T, Fernandes A, Berry M, Corfield AP.** 2005. A Novel Bacterial Mucinase, Glycosulfatase, Is Associated with Bacterial Vaginosis. Journal of Clinical Microbiology **43:**5504-5508.
402. **Al-Soud WA, Jönsson LJ, Rådström P.** 2000. Identification and Characterization of Immunoglobulin G in Blood as a Major Inhibitor of Diagnostic PCR. Journal of Clinical Microbiology **38:**345-350.
403. **Davenport KA, Brost B, Mosher BA.** 2017. Non-random shedding of prions in saliva of deer with chronic wasting disease, Manuscript in preparation.